



**HAL**  
open science

# Sulphonamido-phosphorus nickel complexes for the selective oligomerisation of olefins - Exploring dissymmetric ligands and supramolecular strategies

Pierre Boulens

► **To cite this version:**

Pierre Boulens. Sulphonamido-phosphorus nickel complexes for the selective oligomerisation of olefins - Exploring dissymmetric ligands and supramolecular strategies. *Catalysis*. Ecole normale supérieure de lyon - ENS LYON; Universiteit van Amsterdam, 2014. English. NNT: 2014ENSL0973. tel-01418978

**HAL Id: tel-01418978**

**<https://theses.hal.science/tel-01418978>**

Submitted on 18 Dec 2016

**HAL** is a multi-disciplinary open access archive for the deposit and dissemination of scientific research documents, whether they are published or not. The documents may come from teaching and research institutions in France or abroad, or from public or private research centers.

L'archive ouverte pluridisciplinaire **HAL**, est destinée au dépôt et à la diffusion de documents scientifiques de niveau recherche, publiés ou non, émanant des établissements d'enseignement et de recherche français ou étrangers, des laboratoires publics ou privés.

# THÈSE

en vue de l'obtention du grade de

**Docteur de l'Université de Lyon, délivré par l'École Normale Supérieure de Lyon**

**En cotutelle avec l'Université d'Amsterdam (UvA)**

**Discipline : Chimie**

**Laboratoires** HomKat (HIMS), Université d'Amsterdam, Pays-Bas  
Catalyse moléculaire, IFPEN, Solaize, France

**École Doctorale** de Chimie de Lyon

présentée et soutenue publiquement le 17 décembre 2014

par Monsieur Pierre BOULENS

---

**Sulphonamido-Phosphorus Nickel Complexes for the Selective Oligomerisation of Olefins, Exploring Dissymmetric Ligands and Supramolecular Strategies**

---

Directeur de thèse : Mme. Hélène OLIVIER-BOURBIGOU

Devant la commission d'examen formée de :

M. Pierre-Alain BREUIL (Examinateur)

M. Bas de BRUIN (Rapporteur)

M. Kees C.J. ELSEVIER (Examinateur)

Mme Hélène OLIVIER-BOURBIGOU (Directeur)

M. Frédéric PATUREAU (Rapporteur)

Mme Alessandra QUADRELLI (Examinateur)

M. Joost REEK (Co-tuteur)

M. Sander WOUTERSEN (Examinateur)

*The research described in this dissertation has been financially supported by IFP Energies Nouvelles, France and was in collaboration with the University of Amsterdam (UvA). The thesis lasted 3 years, according to French regulations and time was equally shared between the HOMKat group, HIMS institute, Universiteit van Amsterdam and the research facility of IFP Energies nouvelles in Solaize, France.*

## TABLE OF CONTENTS

<b>Chapter 1</b>	Oligomerisation of Olefins by Nickel Complexes and Supramolecular Concepts of Homogeneous Catalysis: General introduction	1
<b>Chapter 2</b>	Synthesis of Sulphonamido-based Phosphorus Ligands and their Coordination to Nickel	59
<b>Chapter 3</b>	Iminobisphosphines to (non-) Symmetrical Di(phosphino)amine Ligands: Metal-induced Synthesis of Diphosphorus Nickel and Chromium Complexes and Application in Olefin Oligomerisation Reactions	87
<b>Chapter 4</b>	Self-Assembled Organometallic Nickel Complexes as Catalysts for Selective Oligomerisation of Ethylene	115
<b>Chapter 5</b>	Zwitterionic and Nickel Hydride Complexes based on METAMORPhos Ligand: a Parameter Study on their Formation	133
<b>Chapter 6</b>	Zwitterionic and Nickel Hydride Complexes: Reactivity for Ethylene Oligomerisation	179
<b>Appendix</b>		209
<b>Summary</b>		217
<b>Résumé</b>		223
<b>Samenvatting</b>		229
<b>Acknowledgements</b>		235





## ABBREVIATIONS

%	percent
°C	degree Celsius
μ	micro
1-C <sub>4</sub>	1-butene
1-C <sub>6</sub>	1-hexene
1-C <sub>8</sub>	1-octene
<sup>1</sup> H{ <sup>31</sup> P}	phosphorus decoupled proton
2,3-DMB	2,3-dimethylbutenes
2-C <sub>4</sub>	2-butene
<sup>31</sup> P{ <sup>1</sup> H}	proton decoupled phosphorus
Å	angstrom
acac	acetylacetonate
anal.	analysed
Ar	aryl
Binol	1,1'-bi-2-naphtyl
C <sub>2</sub> H <sub>4</sub>	ethylene
C <sub>6</sub> D <sub>6</sub>	deuterated benzene
CCDC	Cambridge Crystallographic Data Centre
CDCl <sub>3</sub>	deuterated chloroform
CD <sub>2</sub> Cl <sub>2</sub>	deuterated dichloromethane
C <sub>n</sub> <sup>+</sup>	oligomers greater than n
COD	cyclooctadiene
CSTR	Continuous stirred-tank reactor
Cy	cyclohexyl
DCM	dichloromethane
DEAC	diethylaluminium chloride
DEAD	diethylazodicarboxylate
DMB	dimethylbutenes
DME	1,2-dimethoxyethane
DPCyE	1,2-bis(dicyclohexylphosphino)ethane
DPiPrE	1,2-bis(diisopropylphosphino)ethane
DPPE	1,2-bis(diphenylphosphino)ethane
DTA	Differential thermal analysis
E2B1	1-butene-2-ethyl (ethyl-2-butene-1)
EADC	ethylaluminium dichloride
EASC	ethylaluminium sesquichloride

<b>EDG</b>	electron donating group
<b>EPR</b>	electron paramagnetic resonance
<b>eq.</b>	equivalent
<b>Et</b>	ethyl
<b><i>et al.</i></b>	<i>et alii</i>
<b>Et<sub>2</sub>O</b>	diethylether
<b>EWG</b>	electron withdrawing group
<b>exp.</b>	experimental
<b>g</b>	gram
<b>h</b>	hour
<b>H-bond</b>	hydrogen-bond
<b>HDPE</b>	high density polyethylene
<b>HEX</b>	hexenes
<b>HMDS</b>	hexamethyldisilazane
<b>Hz</b>	Hertz
<b><i>i</i>Pr</b>	isopropyl
<b>isol.</b>	isolated
<b><i>J</i></b>	coupling constant
<b>K</b>	Kelvin
<b>K<sub>a</sub></b>	Acidity constant
<b>K<sub>SF</sub></b>	Schulz-Flory constant
<b>L</b>	ligand
<b>LAO</b>	linear alpha olefins
<b>LLDPE</b>	linear low density polyethylene
<b>M</b>	molarity (mol/L)
<b>M3P1</b>	methyl-3-pentene-1
<b>M3P2</b>	methyl-3-pentene-1
<b>MAO</b>	methylaluminoxane
<b>Me</b>	methyl
<b>min.</b>	minute
<b>mL</b>	milliliter
<b>MMAO</b>	modified MAO
<b>mmol</b>	millimol
<b>M<sub>w</sub></b>	molecular weight
<b><i>n</i>Bu</b>	<i>n</i> -butyl
<b><i>n</i>C<sub>5</sub></b>	<i>n</i> -pentane
<b>NEt<sub>3</sub></b>	triethylamine
<b><sup>"</sup><i>J</i><sub><i>xy</i></sub></b>	coupling constant
<b>nm</b>	nanometer
<b>NMR</b>	nuclear magnetic resonance

<b>NPP</b>	iminobisphosphine
<b>obsd.</b>	observed
<b>OEt<sub>2</sub></b>	diethyl ether
<b>oligo.</b>	oligomers
<b><i>o</i>-tolyl</b>	ortho-tolyl
<b>PE</b>	polyethylene
<b>Ph</b>	phenyl
<b>PhCl</b>	chlorobenzene
<b><i>p</i>K<sub>a</sub></b>	- log <sub>10</sub> (K <sub>a</sub> )
<b><i>P</i><sub>n</sub></b>	polymer chain with n carbons
<b>PNP</b>	diphosphinamine
<b>ppm</b>	parts-per-million
<b>Prod.</b>	productivity
<b>PVC</b>	polyvinylchloride
<b>quat.</b>	quaternary
<b>R</b>	any carbon containing group
<b>®</b>	registered trademark
<b>Ref.</b>	reference (complex)
<b>RT</b>	room temperature
<b>s</b>	second
<b>SHOP</b>	Shell Higher Olefin Process
<b>SPS</b>	solvent purification system
<b><i>t</i>Bu</b>	tert-butyl
<b>th.</b>	theoretical
<b>THF</b>	tetrahydrofuran
<b>™</b>	trademark (unregistered)
<b>TMSCl</b>	trimethylsilyl chloride
<b>TOF</b>	turnover frequency
<b>tol-<i>d</i><sub>8</sub></b>	deuterated toluene
<b>TON</b>	turnover number
<b>vs.</b>	versus
<b>wt%</b>	weight percent
<b>ZW</b>	zwitterionic
<b>δ</b>	chemical shift
<b><math>\nu_{CO}</math></b>	IR carbonyl frequency (cm <sup>-1</sup> )

*Pressure is expressed in this thesis as absolute pressure with 0 bar corresponding to perfect vacuum and 1 bar corresponding to approximately one atmosphere.*



# Chapter 1

---

## **Oligomerisation of Olefins by Nickel Complexes and Supramolecular Concepts in Homogeneous Catalysis: General Introduction**

---

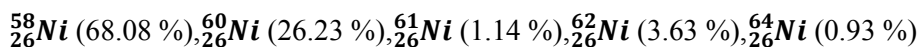
# 1 Nickel oligomerisation

## 1.1 History and general considerations about nickel in organometallic chemistry <sup>[1-3]</sup>

Nickel has been used by humanity for thousands of years. The oldest known examples of the employment of nickel come from Syria where bronze artefacts with high nickel contents from around 3500 BC have been found. In China, old manuscripts mention the common use of nickel (as “white silver”) between 1800 and 1500 BC. In the 16<sup>th</sup> century, miners in the region of Sachsen (Germany) tried to recover copper from a “reddish” ore (they called Kupfernicker), which contained only nickel and arsenic. They did not know that they were about to discover one of the metals which today is of high importance in industrial catalysis. A century later, Cronstedt, a Swedish mineralogist, isolated this metal and named it nickel. J.B. Richter determined its physical properties much later. Nickel is now extracted from ores such as nickelliferous limonite: (Fe,Ni)O(OH), garnierite: (Ni, Mg)<sub>3</sub>Si<sub>2</sub>O<sub>5</sub>(OH)<sub>4</sub> and pentlandite: (Ni, Fe)<sub>9</sub>S<sub>8</sub>.

### 1.1.1 Electronic and atomic properties

Nickel is a late and first row transition metal with symbol Ni and atomic number 28. It has two electronic configurations very similar in energy: [Ar]: 4s<sup>2</sup> 3d<sup>8</sup> and [Ar]: 4s<sup>1</sup> 3d<sup>9</sup> (the first one is generally admitted as the ground state). Nickel is commonly encountered in nature as Ni (II) compounds, but valencies -1, 0 +1, +3 and +4 also exist. The highest coordination number for Ni (0) is 5 (ten electrons required to reach the stable electronic [Kr] structure) and 6 for Ni<sup>2+</sup>. Nickel has five natural isotopes that are represented below with their natural isotopic abundance.



### 1.1.2 Geometries

Three main geometries (based on the valence-bond-theory) are relevant to explain the spatial organisation of nickel complexes: square planar, tetrahedral and octahedral. Besides these geometries trigonal planar, trigonal bipyramidal, trigonal prismatic, square pyramidal and pentagonal bipyramidal have been described.

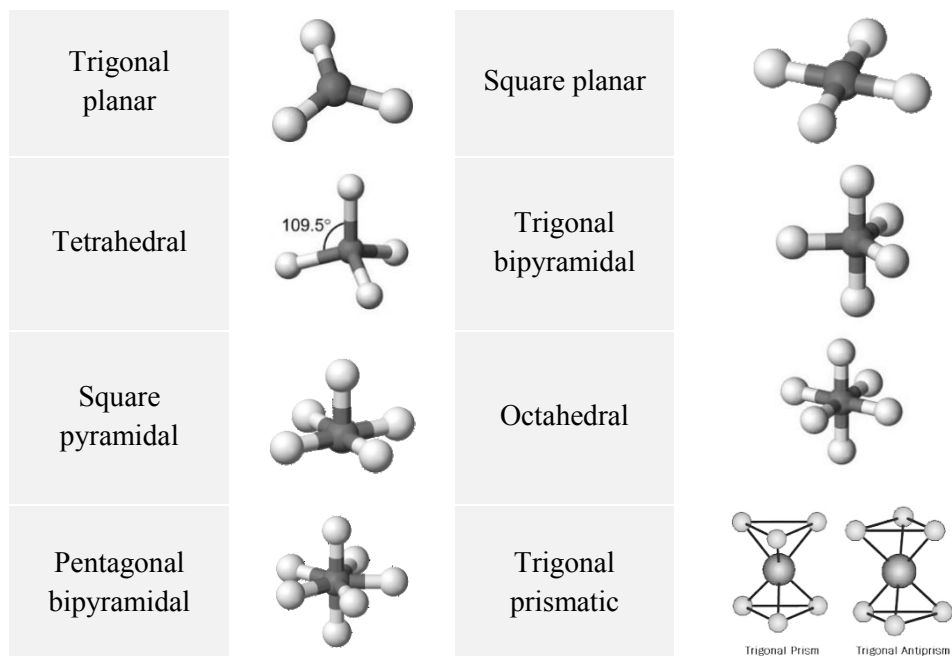


**Figure 1.** The different geometries adopted by nickel complexes.

The geometry of nickel complexes is strongly related to the oxidation number of the metal as shown in Table 1. For a given coordination number and oxidation state, several geometries are sometimes possible.

**Table 1.** Geometry of some Ni complexes as a function of the oxidation state and the coordination number (from Greenwood *et al.*)<sup>[2]</sup>

Oxidation state	Coordination number					Geometry	Complex
	3	4	5	6	7		
-1		+				-	$[\text{Ni}_2(\text{CO})_6]^{2-}$
0	+					Planar	$[\text{Ni}\{\text{P}(\text{OC}_6\text{H}_4\text{-2-Me})_3\}_3]$
		+				Tetrahedral	$[\text{Ni}(\text{CO})_4]$
1	+					Trigonal planar	$[\text{Ni}(\text{NPh}_2)_3]^-$
		+				Tetrahedral	$[\text{NiBr}(\text{PPh}_3)_3]$
		+				Tetrahedral	$[\text{NiCl}_4]^{2-}$
			+			Square planar	$[\text{Ni}(\text{CN})_4]^{2-}$
2			+			Trigonal pyramidal	$[\text{Ni}(\text{PPhMe}_2)_3(\text{CN})_2]$
			+			Square pyramidal	$[\text{Ni}(\text{CN})_5]^{3-}$
				+		Octahedral	$[\text{Ni}(\text{H}_2\text{O})_6]^{2+}$
					+	Trigonal prismatic	$\text{NiAs}^{(a)}$
3				+		Pentagonal bipyramidal	$[\text{Ni}(\text{dapbH})_2(\text{H}_2\text{O})_2]^{2+(b)}$
			+			Trigonal bipyramidal	$[\text{NiBr}_3(\text{PET}_3)_2]$
				+		Octahedral	$[\text{NiF}_6]^{3-}$
4				+		Octahedral	$[\text{NiF}_6]^{2-}$

<sup>(a)</sup> Nickeline :  $P6_3/mmc$  <sup>(b)</sup> dapbH, 2,6-diacetylpyridinebis(benzoic acid hydrazone).



Nickel (II) complexes that have 4 coordinated ligands lead either to square planar or to tetrahedral geometries (conformational isomerism). Indeed, both *sec*-alkylsalicylaldiminato derivatives and the complex  $[\text{NiBr}_2(\text{PEtPh}_2)_2]$  display an equilibrium between square planar and tetrahedral geometries in non-coordinating solvents. Solvents molecules such as water or bases can also coordinate to metallic centres and change the geometry of the complex. Two molecules of solvent can coordinate to square planar complexes increasing the coordination number up to 6 and leading to octahedral complexes.

A common observation is that reddish and yellowish nickel complexes have a square planar geometry whereas blue and green complexes have any other possible geometry. Square planar complexes are also diamagnetic and observable by NMR whereas paramagnetic complexes generally give rise to broad and undefined signals when using this spectroscopic technique.

## 1.2 Production of olefins by oligomerisation reactions

### 1.2.1 General market considerations

Ethylene and propylene are important raw materials in petrochemistry. The market for these first generation olefins is, and should remain in the nearby future, in constant growth (Table 2).<sup>[4-6]</sup>

**Table 2.** World demand for alpha-olefins in million tons and estimations for 2035.

	2011	2035
Ethylene	123	273
Propylene	81	217

Ethylene is a product that is particularly demanded. Indeed, 30% of the products manufactured by the petrochemical industries use ethylene in the process. The United States has the highest production capacity of ethylene with 28 Mt/y in 2011. This production relies on catalytic cracking and vapocacking processes in refineries that convert higher hydrocarbons into ethylene and propylene. More recently, biorefineries aim to produce “bio-ethylene” by dehydration of bio-ethanol. Most of ethylene and propylene produced worldwide is used for the plastics industry. In 2008, 58 % of the global ethylene production was used for HDPE, LLDPE and LDPE whereas 64 % of all propylene was used for polypropylene production.

The higher olefins ( $>\text{C}_3$ ) market, especially  $\alpha$ -linear-olefins, is also in constant growth. The demand for LAO (Linear Alpha Olefins) has been increasing to reach

5.1 Mt per year in 2011. Most of these olefins are used as co-monomers in the plastics industry for the production of HDPE and LLDPE (Table 3).<sup>[7-9]</sup>

**Table 3.** Demand of LAO in 2011 in the industry and importance of the plastics industry (LLDPE, HDPE).

Demand 2011 (%)	1-butene	1-hexene	1-octene
LLDPE	78	59	73
HDPE	14	32	2
Other	8	9	25

Besides being used in the production of polymers, linear alpha olefins are the starting material for surfactants, lubricants and other chemicals (Table 4). Several routes are used to produce LAO: Fisher-Tropsch synthesis and catalytic cracking and /or paraffin dehydrogenation, olefin metathesis, ethylene oligomerisation and dehydration of alcohols.<sup>[10,11]</sup> Growth estimations based on the demand for 1-butene (AAGR 2006-2015: 5.2%) and 1-hexene (AAGR 2006-2015: 4.7%) confirm that these short olefins remain key-intermediates for the industry.

**Table 4.** Different uses of alpha-olefins in industry depending on their chain length.

Chain length:									Applications	
$C_4$	$C_6$	$C_8$	$C_{10}$	$C_{12}$	$C_{14}$	$C_{16}$	$C_{18}$	$C_{20}$		
■									HDPE, LLDPE	
	■								PVC/plasticisers	
		■							Lubricants	
			■						Herbicides, plastics	
				■					Acids, detergents, alcohols	
					■					Surfactants
						■			Lubricant additives	
							■		Preservatives	
								■		Antistatics

### 1.2.2 Ethylene oligomerisation processes

Two types of oligomerisation processes produce alpha olefins: processes *on purpose* and *full range*. Processes on purpose target a defined linear alpha olefin (1- $C_4$  or 1- $C_6$  or/and 1- $C_8$ ) while full range processes target a broad mixture of linear alpha olefins (from  $C_4$  to  $C_{22}$  for instance) that generally follows a geometric distribution of products.

### 1.2.2.1 Full range processes: mixture of linear alpha olefins

One of the initial processes to manufacture mixtures of LAO was the Ziegler (Alfen) process (now replaced) using aluminium for chain growth. After the observation that nickel salts could modify the outcome of  $\text{AlR}_3$ -catalysed “growth reaction” (Aufbaureaktion) of ethylene<sup>[12,13]</sup>, this metal was also used as a catalyst to produce mixtures of LAO. Several processes that produce mixtures of LAO are presented in Table 5<sup>[10,11,14,15]</sup>

**Table 5.** Characteristics of processes affording linear alpha-olefins not selectively.

Process	«Catalyst»	T (°C)	P (bar)	Product distribution	$\alpha$ -selectivity
CP Chem	$\text{AlEt}_3$	180	230	15% $\text{C}_4^=$ 70% $\text{C}_6^=-\text{C}_{18}^=$ 15% $\text{C}_{20}^=-\text{C}_{40}^=$	<i>Schulz-Flory</i> (94-98%)
Ineos (Ethyl)	$\text{AlEt}_3/\text{AlR}_3$ (3 steps)	160-275	135-270	15% $\text{C}_4^=$	<i>Poisson</i> (63-97%)
		80-100	100-200	83% $\text{C}_6^=-\text{C}_{18}^=$	
		245-300	7-20	2% $\text{C}_{20}^=-\text{C}_{40}^=$	
SHOP	$\text{Ni(P,O)}$	80-140	70-140	11% $\text{C}_4^=$ 82% $\text{C}_6^=-\text{C}_{18}^=$ 7% $\text{C}_{20}^=-\text{C}_{40}^=$	<i>Schulz-Flory</i> 96-98%

The first two processes (Chevron-Phillips Chemicals and Ineos) are based on chain growth on aluminium. They are operated under very high pressure. The Chevron-Phillips Chemicals process uses  $\text{AlEt}_3$  as catalyst. The chain growth on aluminium (by insertion of ethylene into the Al-C bond) and transfer ( $\text{R}_2\text{Al-CH}_2\text{-CH}_2\text{-R}' + \text{H}_2\text{C}=\text{CH}_2 \rightarrow \text{R}_2\text{Al-CH}_2\text{-CH}_3 + \text{R}'\text{-CH}=\text{CH}_2$ ) are performed in the same reactor. The Ethyl process (currently employed by INEOS) is performed in two reactors with different temperatures and pressures. In the first reactor, short alkyl-aluminium species are formed and longer chains are formed in the second reactor. The product formed in this second reactor reacts in a third step with light products from the first reactor (trans-alkylation). The olefins produced follow a statistical Poisson distribution of products.

SHOP (Shell Higher Olefin Process) uses a nickel catalyst prepared *in situ* from a nickel(II) species associated with a P,O bidentate ligand (Figure 2) by a reduction with sodium borohydride.<sup>[16]</sup> After the first oligomerisation step, the olefins are readily separated from the catalyst thanks to a biphasic process. The SHOP process is designed to produce mainly  $\text{C}_{12}\text{-C}_{18}$  olefins. This fraction is first isolated while the

lighter and heavier fractions are subsequently isomerised to internal olefins that are engaged in a metathesis step leading to the desired olefins.

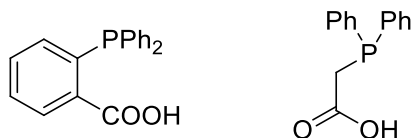


**Figure 2.** Examples of SHOP ligands used for the *in situ* formation of the catalytically active nickel complex in combination with a nickel salt and NaBH<sub>4</sub>.

There is currently a growing interest in short linear alpha-olefins. Several processes affording such distributions are commercialised. IFPEN developed the AlphaSelect process, based on a zirconium catalyst that produces  $\alpha$ -olefins from 1-butene to 1-decene (selectivity > 93%).<sup>[15,17,18]</sup> Sabic-Linde developed the Alpha-Sablin process that is currently in the demonstration phase. Idemitsu produces 55000 tons/year of C<sub>4</sub><sup>=</sup>-C<sub>18</sub><sup>=</sup>  $\alpha$ -linear olefins with the Idemitsu-Linealene process in Japan.<sup>[12,17,19]</sup>

### 1.2.2.2 On purpose processes: one olefin is produced

Four commercialised processes are selective towards the production of a single olefin. The main characteristics are outlined in Table 6.<sup>[11,20-22]</sup>

**Table 6.** Characteristics of processes affording linear alpha-olefins selectively.

Process	Temperature	« Catalytic system »	Products	$\alpha$ -selectivity
AlphaButol® (Axens)	45-55°C	Ti <sup>IV</sup> , AlR <sub>3</sub> , L	>90% C <sub>4</sub> <sup>=</sup> < 10% C <sub>6</sub> <sup>=</sup>	> 99% for C <sub>4</sub> <sup>=</sup>
AlphaPlus® 1- Hexene (CP Chem)	?	Cr <sup>III</sup> , AlEt <sub>3</sub> , L	1% C <sub>4</sub> <sup>=</sup> 93% C <sub>6</sub> <sup>=</sup> 6% C <sub>10</sub> <sup>=</sup>	> 99% for C <sub>6</sub> <sup>=</sup>
AlphaHexol™ (Axens)	120-140°C	Cr <sup>III</sup> , AlR <sub>3</sub> , L	>83% C <sub>6</sub> <sup>=</sup>	> 99% for C <sub>6</sub> <sup>=</sup>
Sasol	50-60°C	Cr <sup>III</sup> , MMAO, L	30% C <sub>6</sub> <sup>=</sup> 60% C <sub>8</sub> <sup>=</sup>	> 99% (in C <sub>8</sub> <sup>=</sup> )

These four processes target different LAOs: 1-butene, 1-hexene or 1-octene. AlphaButol® process, licensed by Axens targets selective ethylene dimerisation with a titanium catalyst activated by alkylaluminium.<sup>[15]</sup> Currently, more than 30 industrial plants use this technology to produce 1-butene which is massively used as a comonomer for the synthesis of branched polyethylene (HDPE, LLDPE).<sup>[23]</sup>

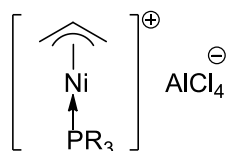
The AlphaPlus® 1-hexene process, currently employed by Chevron Phillips Chemicals produces 1-hexene by trimerisation of ethylene. The catalyst is a chromium alkanoate complexed by a pyrrolyle ligand and activated by triethylaluminium.<sup>[24]</sup> The first plant utilising this technology was set up in Qatar in 2003. Two other plants are in construction in Saudi Arabia and in Texas.

IFPEN discovered in 1998 a new catalytic system, able to trimerise ethylene into 1-hexene with a high selectivity, based on chromium and proprietary ligands. This process has been in commercial use as the AlphaHexol™ process currently employed by Axens since 2010.<sup>[25,26]</sup>

Sasol, discovered a new catalytic system for the tri- and tetramerisation of ethylene, based on a chromium diphosphinamine (*i*PrN(PPh<sub>2</sub>)<sub>2</sub>) catalyst and methylaluminumoxane as cocatalyst. A plant is now in construction on Sasol's site in Louisiana to produce 100 kt/year of 1-hexene and 1-octene.<sup>[27,28]</sup>

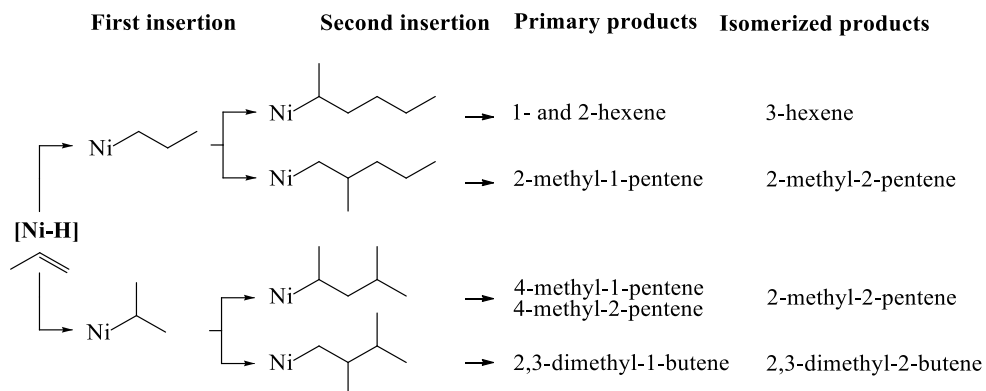
### 1.2.3 Propylene oligomerisation processes

The oligomerisation of propylene catalysed by a nickel compound and an alkylaluminium chloride derivative was first described in a 1955 patent by Lyons *et al.*<sup>[29]</sup> In 1966, the group of Wilke gave crucial impetus to this reaction by using a “well-defined” organometallic nickel complex: a cationic  $\eta^3$ -allylnickel complex **1**.<sup>[30]</sup> By this approach, they confirmed the reaction mechanism but also underlined the control by tertiary phosphines on the selectivity of the oligomers formed. Complex **1** is only soluble in chlorinated hydrocarbons. Many other systems based on nickel catalyse the dimerisation reaction and have been described in publications and patents.



**1**

The oligomerisation of propylene consists of the consecutive addition of two or more molecules of propylene to the active species (Ni-H and Ni-C complexes) with subsequent chain elimination (or chain transfer) to regenerate the catalyst and give the oligomer. The formation of olefin dimers predominate in the reaction products due to a high rate of beta-hydrogen elimination. The reaction pathways leading to the formation of all possible propylene dimers is presented in Scheme 1.



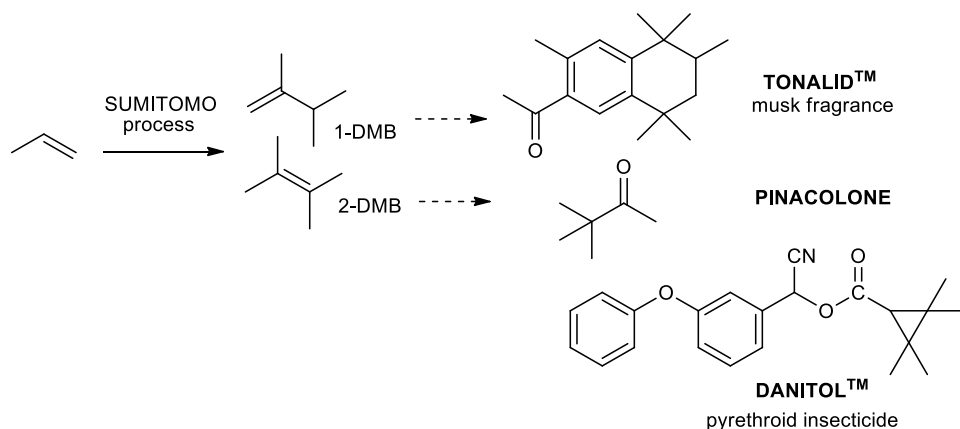
**Scheme 1.** Reaction pathways for propylene dimerisation by nickel complexes.

Trimers and tetramers, found in smaller proportions, form both by a parallel growing chain reaction and by consecutive reactions of dimers with monomer (co-dimerisation) as seen in Scheme 2. The selectivity in dimers at high conversion (> 80 %) strongly depends on the type of reactor used i.e., batch and plug-flow open systems, or semi-batch and one stage well-mixed open systems. Although the type of reactor has no effect on the parallel growing chain reaction it has a strong influence on the consecutive reaction (co-dimerisation).









**Scheme 3.** Selective dimerisation of propylene to dimethylbutenes (DMB) and uses of DMB for the synthesis of fine-products or intermediates.

Selective dimerisation of propylene to 2,3-dimethylbutenes (DMBs) is currently operated by Sumitomo and BP Chemicals.<sup>[32]</sup> In the Sumitomo process, very high selectivity for DMBs (up to 85 %) are obtained at 20-50°C thanks to a sophisticated, highly efficient Ziegler type catalyst system (ten times more efficient than those of conventional catalysts) and by using toluene as a solvent. Isomerisation of 2,3-dimethyl-1-butene (DMB-1) into 2,3-dimethyl-2-butene (DMB-2) takes place directly in the dimerisation reactor in the presence of an acidic component (a chlorinated phenol) coming from the catalyst formula. DMB-2 is easily extracted from the mixture by distillation. The BP Chemicals process operates without any solvent at lower temperature and the catalyst composition is simpler but gives DMB-1 as the main product. DMB-2 is obtained by subsequent isomerisation on an acidic resin catalyst. Many studies have been made on these Ni-phosphine catalytic systems to improve the activity and the selectivity, not only by varying the phosphine ligand, but also by varying the additives. Immobilisation of nickel-based catalysts on a solid support has also been reported.<sup>[36]</sup> On top of this, fluorinated biphasic systems have been also applied to facilitate the separation of the catalyst from the reaction products, e.g. by modifying nickel  $\beta$ -diketonate complexes with a long perfluorinated alkyl chain. However, the polar character of the Ni active species was not favourable to the non-polar fluorinated layer.<sup>[37]</sup>

## 1.3 Activation of nickel complexes for olefin oligomerisation

### 1.3.1 General considerations

Cationic nickel (II) hydride complexes have been proposed as being the active catalysts for olefin oligomerisation or polymerisation.<sup>[38]</sup> The stability of these very reactive species is, however, limited and makes nickel (II) hydride complexes very

difficult to handle. To circumvent this problem, a common practice consists of starting from a precatalyst (stable nickel complex). Nickel precatalysts are divided in two groups: single components catalysts that lead to the catalytically active species without activator and the others that require an activator (see Figure 4).

Catalytic systems working with an activator are evaluated in catalysis with an *in situ* approach. The reaction between the precatalyst and the activator to generate the active species takes place in the reactor. Although this approach is often considered as a “black box” (the active species that forms is not well defined and parallel reactions may happen), it is preferred in the industry for the robustness of the components and a facile synthetic access.

In contrast, single component catalysts are well defined catalysts that are organometallic nickel complexes (having a Ni-H or a Ni-C bond). They activate readily under an atmosphere of ethylene to give the active catalytic species. Since these single component catalysts work by themselves, they offer the possibility to understand the catalytic elementary steps by using *in situ* or *in operando* high-pressure NMR or IR spectroscopy. These type of single component catalysts is however less robust than catalytic systems working with an activator.

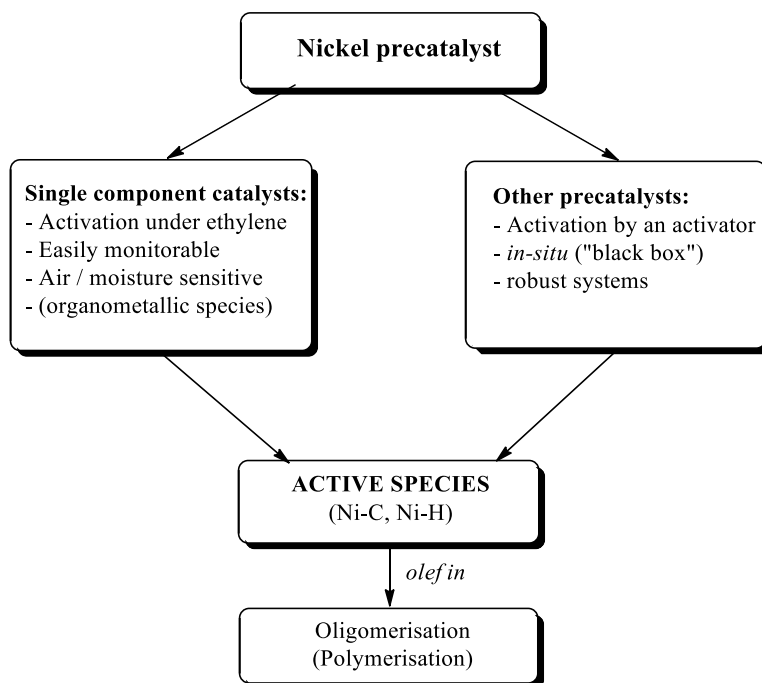


**Figure 4.** Activation of nickel precatalysts: single component catalysts (generally organometallic species) are directly active in ethylene oligomerisation while other precatalysts need an activation step by using a co-catalyst (also called activator).

Several nickel complexes that have been described in ethylene oligomerisation (single-component catalysts and precatalyst / activator systems) are presented in this Chapter with their synthetic pathway and their activation mode. The aim of this part is to understand which type of activation is needed for a given nickel complex and its impact on activity and selectivity. As oligomerisation and polymerisation are closely related reactions, some polymerisation systems are also included. Indeed, a simple change of solvent (toluene to heptane) may turn a system for oligomerisation into one for polymerisation.<sup>[39]</sup>

### 1.3.2 Aryl nickel complexes

Aryl-nickel complexes are organometallic compounds that are easily isolable. Most of them crystallise easily and adopt a square planar fashion giving diamagnetic complexes, observable by NMR spectroscopy.<sup>[40–42]</sup> These complexes are activated under an ethylene atmosphere (40-50 bars of ethylene) and heating is generally required. Some aryl-nickel complexes used in ethylene oligomerisation (or polymerisation) are presented in Figure 5.

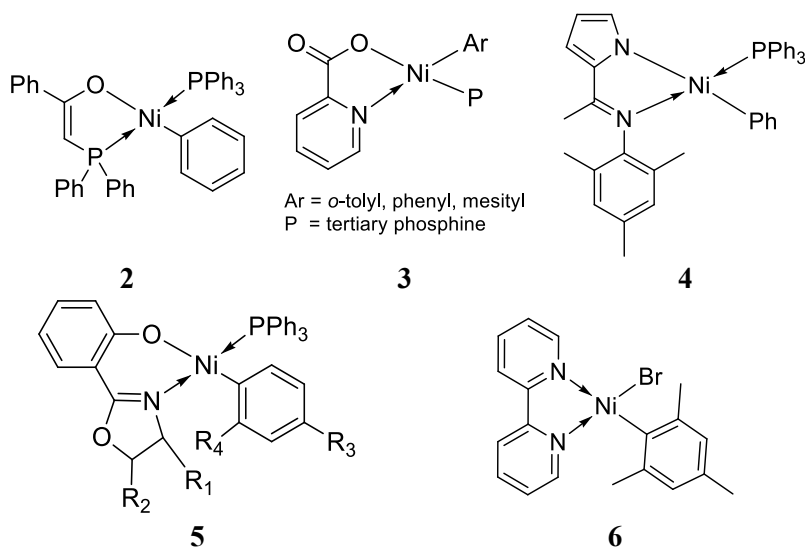
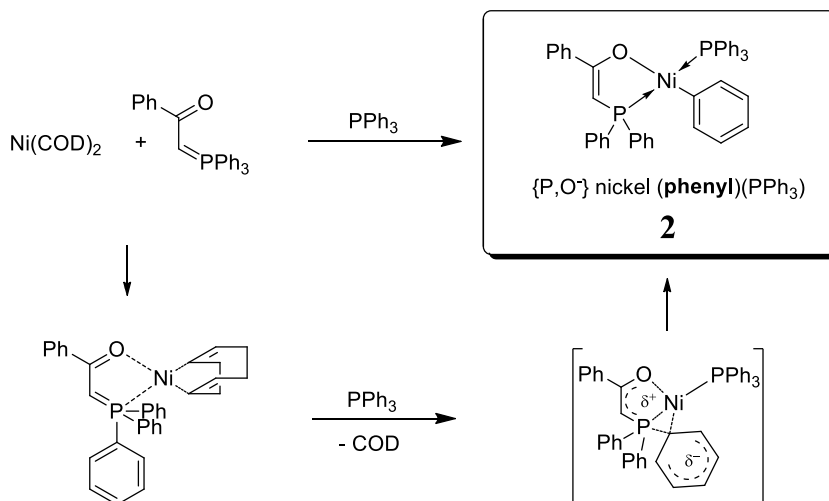


**Figure 5.** Selected examples of nickel-aryl complexes described for ethylene oligomerisation.

Several synthetic pathways lead to the formation of aryl-nickel complexes. On the track of SHOP process, Keim's group discovered that the reaction of the phosphorus ylide (benzoylmethylene)triphenylphosphorane ( $\text{Ph}_3\text{P}=\text{C}(\text{H})-\text{C}(=\text{O})\text{Ph}$ ) with  $\text{Ni}(\text{COD})_2$  and in the presence of a coordinating phosphine led to the nickel aryl complex **2**. The mechanism of this reaction is most likely an oxidative addition on the P-Ph bond followed by a rearrangement (Scheme 4). Aryl-nickel complexes may

also be formed by reaction of the precursor phenylnickelbromide bis(triphenylphosphine) with a base or reducing agents.<sup>[43–48]</sup>



**Scheme 4.** Synthesis of SHOP catalyst from a phosphorus ylide,  $\text{Ni}(\text{COD})_2$  and  $\text{PR}_3$  with the synthetic rearrangement proposed by Keim *et al.*<sup>[39]</sup>

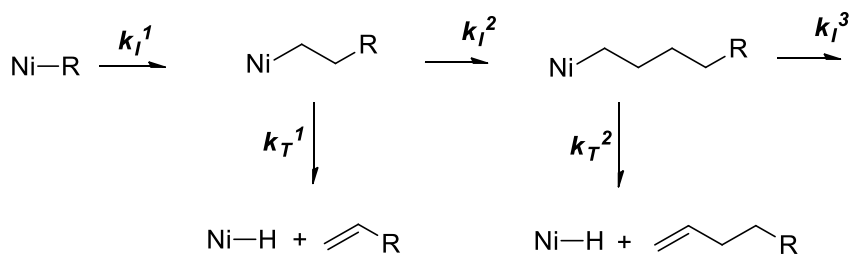
Nickel complex **2**, with a PO chelate is the showcase example of the SHOP catalyst.<sup>[39,40]</sup> This complex is activated under 50 bar of ethylene pressure at 50°C and a small induction time is required before ethylene uptake starts. In toluene, this complex produces olefins of which 99% are linear and 98% are alpha-olefins with activity of 1 000  $\text{g}_{\text{C}_2\text{H}_4}/(\text{g}_{\text{Ni}}\cdot\text{h})$ . Using hexanes instead of toluene leads only to linear polyethylene (PE) highlighting the importance of the solvent for the selectivity of the reaction.<sup>[49,50]</sup>

Nickel-aryl complexes with NO chelates received significantly less attention than those based on PO chelates. Cavell's group described NO-chelated nickel-aryl complexes of general formula **3** (see Figure 5) which under mild conditions (80°C, 40 bars), also affords oligomers with linearity above 84% and alpha linear products above 51%.<sup>[51]</sup> By using an iminopyrrole chelate, Gomes *et al.* synthesised a NN-chelated nickel-aryl complex **4** (see Figure 5) which under 2 bars of ethylene pressure and between 20 and 50°C gave only liquid oligomers.<sup>[52]</sup> These three examples show that aryl-nickel complexes are directly active and that oligomerisation activity does not appear to depend on a specific chelate since PO, NO and NN based complexes are active catalysts.

Whereas the above mentioned complexes are single component catalysts that are directly active under ethylene, these complexes have been sometimes evaluated in catalysis in combination with alkylaluminiums. Zhao *et al.*, for example combined

ligand **5** (of Figure 5) with MAO or  $\text{AlEt}_3$  producing very short oligomers  $\text{C}_4 - \text{C}_8$ , with a system significantly more active (up to  $550 \text{ kg}_{\text{oligomers}}/(\text{g}_{\text{Ni-h}})$ ) than SHOP catalyst **2**.<sup>[53]</sup> Aryl-nickel bromide complex **6** (of Figure 5), activated by 300 eq. or MAO, also displays high activity but low alpha-selectivity.<sup>[54]</sup> The presence of labile moieties (phosphines) or a vacant site at proximity of the aryl group seems to be an important requirement to observe catalytic activity for aryl-nickel complexes.

When aryl-nickel complexes are brought into contact with ethylene at a suitably high temperature for activation to occur, styrene is released.<sup>[40,41,55-59]</sup> This observation supports the ethylene insertion into the nickel-phenyl bond and the formation of a potentially active nickel-hydride by  $\beta$ -H elimination (or a nickel-ethyl by chain transfer). For systems  $\text{NiBrRL}_2$ , one or more insertions of ethylene may occur before the generation of the hydride (Scheme 5).<sup>[48]</sup> Multiple insertions of ethylene in the Ni-R bond appear for highly substituted R groups ( $2,4,6\text{-Me}_3\text{-C}_6\text{H}_2$ ,  $\text{C}_6\text{Cl}_5$ ) in the presence of a monodentate phosphine ( $\text{PPh}_3$ ,  $\text{PMe}_2\text{Ph}$ ,  $\text{P}(\text{CH}_2\text{-Ph})_3$ ), in that case  $k_I^2 > k_T^1$  and  $k_I^3 > k_T^2$ .



**Scheme 5.** Activation of aryl-nickel complexes of type  $[\text{NiBrRL}_2]$  compounds under ethylene. There may be several consecutive insertions of ethylene in the Ni-Ar bond.

### 1.3.3 Allyl and cyclopentadienyl nickel complexes

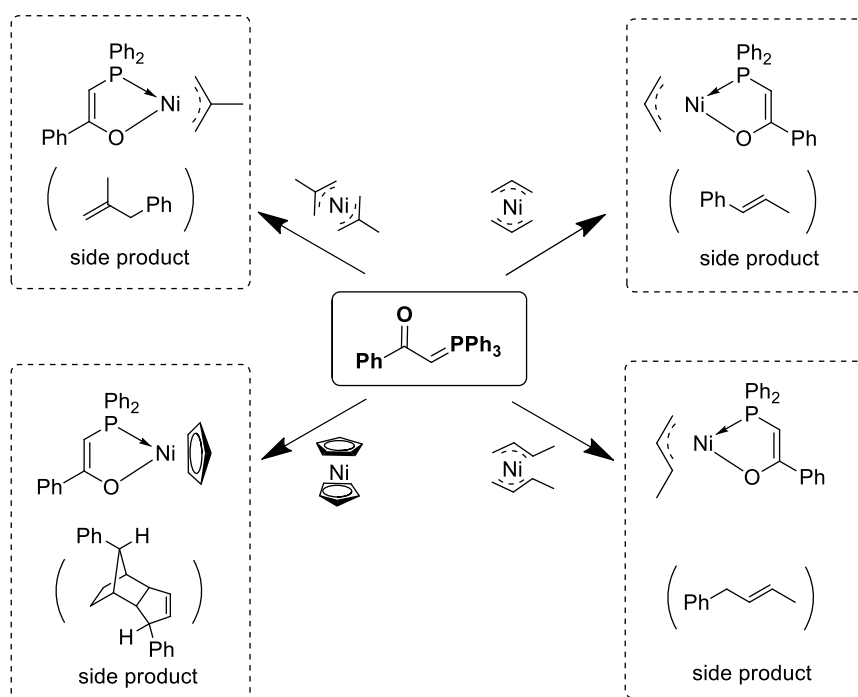
Allylic nickel complexes have appeared in the pioneering work of Wilke in 1966 on nickel chemistry.<sup>[30,60]</sup> Similarly to nickel-aryl complexes, allyl-nickel complexes are activated thermally *in situ* under an ethylene atmosphere.

#### 1.3.3.1 Preparation of $\eta^3$ and $\eta^5$ bound nickel complexes

The chemistry of Ni-allyl complexes and their synthetic access was particularly developed by the group of Bogdanovic.<sup>[61]</sup> Bis-( $\pi$ -allyl) nickel compounds  $[(\text{allyl})_2\text{Ni}]$  are synthesised from  $\text{NiBr}_2$  and two equivalents of the corresponding  $\pi$ -allyl Grignard reagent. Nickel (II) allyl precursors of formula  $[(\text{allyl})\text{Ni}(\text{halide})]_2$  are readily prepared by the reaction of a nickel(0) precursor (e.g.  $\text{Ni}(\text{COD})_2$  or  $\text{Ni}(\text{CO})_4$ )

with the corresponding allyl halide or hydration of  $[(\text{allyl})_2\text{Ni}]$  with anhydrous hydrogen halide.<sup>[30]</sup> They are now commercially available.

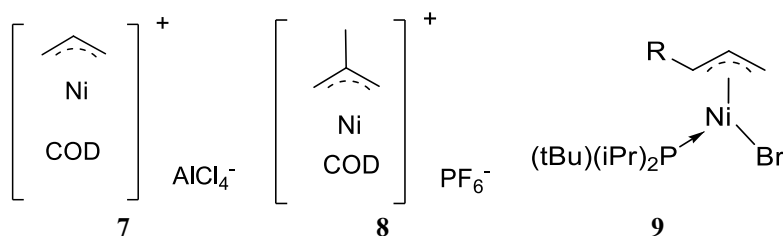
Cationic complexes of type  $[(\text{allyl})\text{NiL}_2]^+\text{B}^-$  are formed by abstraction of the halide from  $[(\text{allyl})\text{Ni}(\text{halide})]_2$ . This operation is generally performed with thallium salts ( $\text{TlBF}_4$ ,  $\text{TlOEt}$ ,  $\text{TlPF}_6$ ,  $\text{TlSbF}_6$ ,  $\text{TlBAR}_4^{\text{F}}$ , silver and sodium salts have also been reported) in the presence of two equivalents of a monodentate ligand L or one equivalent of a bidentate ligand  $\text{L}_2$ .<sup>[43,62]</sup> Based on the showcase example of SHOP nickel-aryl complex **2**, the group of Keim prepared in 1986, PO-chelated nickel allyl complexes by reacting (benzoylmethylene) triphenylphosphorane with bis allylnickel (II) precursors (Scheme 6).<sup>[40]</sup> In this synthesis there is no change in the oxidation state of the nickel between the precursor and the final PO-chelated complex and organic side products containing the allyl fragment substituted by a phenyl group (from the  $\text{PPh}_3$ ) are observed. Similar complexes may be synthesized using phosphine ligand of general formula  $\text{Ph}_2\text{P}-(\text{CH}_2)_n-\text{COOH}$  and bis allylnickel (II).<sup>[67]</sup>



**Scheme 6.** Preparation of  $\eta^3$  and  $\eta^5$  allylnickel complexes by Keim *et al.* starting from Ni(II) bis allyl precursors and (benzoylmethylene) triphenylphosphorane (the side product observed for the nickellacyclopentane results from the Diels-Alder condensation of two monomers).

### 1.3.3.2 Activation of allyl nickel halide complexes

Allyl nickel halide dimer precursors of general formula  $[(\text{allyl})\text{NiX}]_2$  are not directly active for ethylene oligomerisation. An activation step consisting of halide abstraction is required for the formation of a cationic nickel complex and the creation of a vacant site. The halide atoms from the dimer can be abstracted by a Lewis acid such as an aluminium halide or alkylaluminiums to form (non-isolable) active complexes *in situ* of formula  $(\text{allyl})\text{Ni}^+(\text{AlR}_n\text{X}_{3-n})^-$  with a vacant site which serves for ethylene coordination. Performing the abstraction in the presence of chelating agents lead to stable and isolable complexes (see **7** with COD as chelating agent).<sup>[63]</sup> The halogen atom may alternatively be replaced by non-coordinating anions such as  $\text{BF}_4^-$  or  $\text{PF}_6^-$  by anion exchange (see above).<sup>[64]</sup> The resulting cationic nickel complexes with a vacant site are active in oligomerisation (25°C, 10 bars, up to 2 000  $\text{g}_{\text{oligo}}/(\text{g}_{\text{Ni}}\cdot\text{h})$  for **8**) producing a mixture of ethylene dimers and short oligomers. The dimer fraction consists mainly of 2-butenes and the trimer fraction of 3-methylpentene and 2-methylpentene as well as a minor amount of n-hexenes.



Phosphine ligands have the ability to break the dimer structure of  $[(\text{allyl})\text{NiX}]_2$  to give two stable monomers  $(\text{allyl})\text{NiX}(\text{PR}_3)$  where the vacant site is occupied by the phosphine (such as **9**). Halide abstraction from this monomer (with  $\text{AlCl}_3$ ,  $\text{AlBr}_3$  or chloroalkylaluminium) gives “phosphine-modified catalysts” that are isolable. The phosphine ligand has a pronounced influence on both activity and selectivity of the complex as is clear from Table 7.<sup>[60,65]</sup> Nickel catalysts with a sterically demanding phosphine, such as tricyclohexylphosphine, produce mainly 2,3-dimethyl-1-butene in the propylene oligomerisation. Related complexes with a less sterically demanding phosphine will lead to *n*-hexenes and methylpentenes (2,3-dimethyl-1-butene is only a side product).

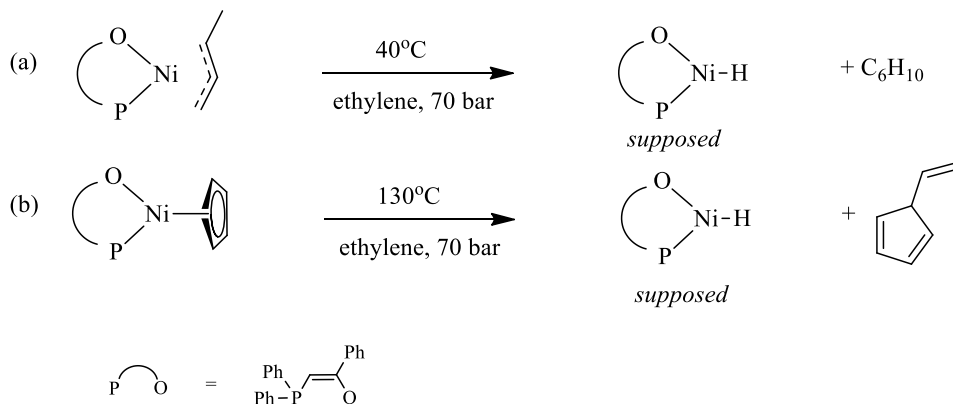
**Table 7.** Influence of the phosphine ligand on propylene oligomerisation for “phosphine modified catalysts”:  $[(\pi\text{-allylnickelchloride}) + \text{phosphine} + \text{AlCl}_3]$  at  $-20^\circ\text{C}$ , 1 bar, (from Bogdanovic *et al.*).<sup>[63]</sup>

Phosphine	hexenes (%)	methyl-pentenes (%)	2,3-dimethylbutenes
PPh <sub>3</sub>	21.6	73.9	4.5
PPh <sub>2</sub> (CH <sub>2</sub> Ph)	19.2	75.5	5.1
Ph <sub>2</sub> P-(CH <sub>2</sub> ) <sub>3</sub> -PPh <sub>2</sub>	20.	73.3	6.6
Ph <sub>2</sub> P-CH <sub>2</sub> -PPh <sub>2</sub>	12.2	83.0	4.7
PMe <sub>3</sub>	9.9	80.3	9.8
PPh <sub>2</sub> (iPr)	14.4	73.0	12.6
PEt <sub>3</sub>	9.2	69.7	21.1
P( <i>n</i> Bu) <sub>3</sub>	7.1	69.6	23.3
P(CH <sub>2</sub> Ph) <sub>3</sub>	6.7	63.6	29.2
P(NEt <sub>2</sub> ) <sub>3</sub>	5.5	51.4	43.0
PCy <sub>3</sub>	3.3	37.9	58.8
P( <i>i</i> Pr) <sub>3</sub>	1.8	30.3	67.9
PMe( <sup>t</sup> Bu) <sub>2</sub>	1.2	24.5	74.0
PPh( <sup>t</sup> Bu) <sub>2</sub>	0.6	22.3	77.0
P( <i>i</i> Pr)( <sup>t</sup> Bu) <sub>2</sub>	0.6	70.1	29.1

### 1.3.3.3 Activation of allyl and cyclopentadienyl nickel complexes

The activation of allyl and cyclopentadienyl nickel complexes with a vacant site (that may be chelated) is realised under an ethylene atmosphere. The mechanism is similar to nickel aryl complexes, according to the observation of by-products. Indeed, the formation of a product containing C<sub>allyl</sub> + 2 carbon atoms (see Scheme 7) suggests that ethylene inserts in the Ni-C bond of the allyl with subsequent  $\beta$ -H elimination or chain transfer to ethylene. The observation of this organic fragment is likely to result from the joint formation of the active species: a nickel-hydride (or ethyl) complex. The activation temperature of this class of complexes differs with the nature of the allyl group as seen in Scheme 7. The activation of the allyl complex (a) is realised at  $40^\circ\text{C}$  whereas the complex with a cyclopentadienyl group (b) is activated at  $130^\circ\text{C}$  (both under 70 bars of ethylene pressure).<sup>[66]</sup>

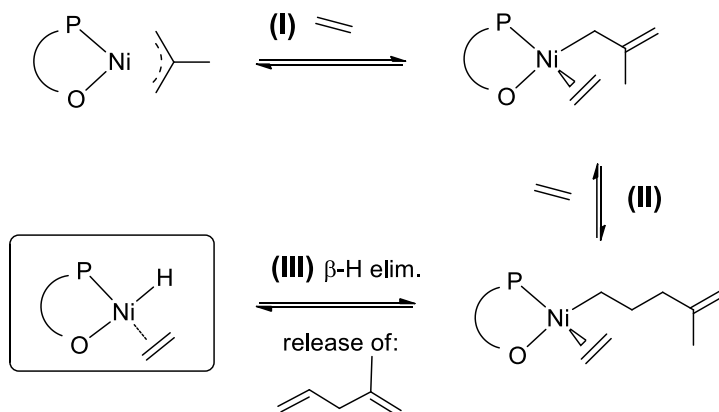




**Scheme 7.** Activation of SHOP-type P,O complexes bearing  $\eta^3$  or  $\eta^5$  moieties by insertion of ethylene in the Ni-allyl bond with subsequent cleavage of a vinyl-allyl group (here the  $\beta$ -H elimination pathway is considered).

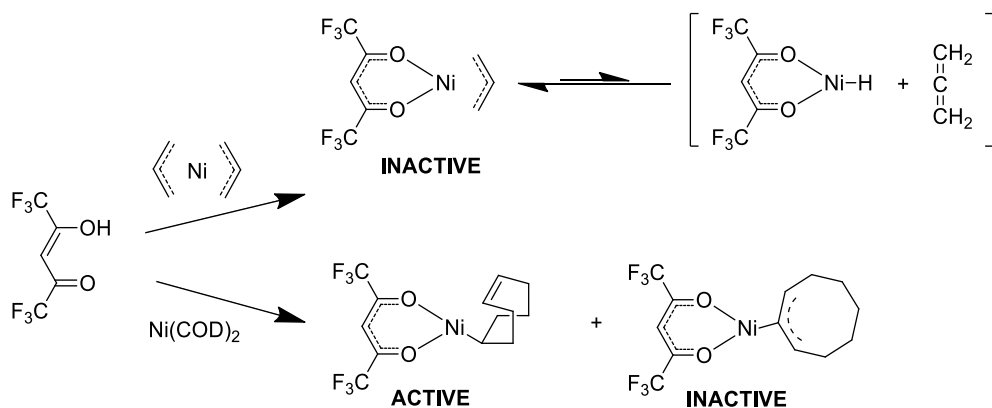
The activation temperature is also dependant on the chelate part. Starting from a phosphanylphenolate ligand for instance, the corresponding nickel *Cp* complex has to be activated at 190°C (as indicated by the loss of cyclopentadiene fragment observed by DTA) in order for the polymerisation of ethylene to commence.<sup>[50]</sup>

Methallyl complexes are also activated under ethylene pressure at different temperatures. The structure of the by-product (leaving group) gives insight in the formation of the active species, presumably a nickel hydride according to Keim *et al.* (Scheme 8).<sup>[67]</sup>



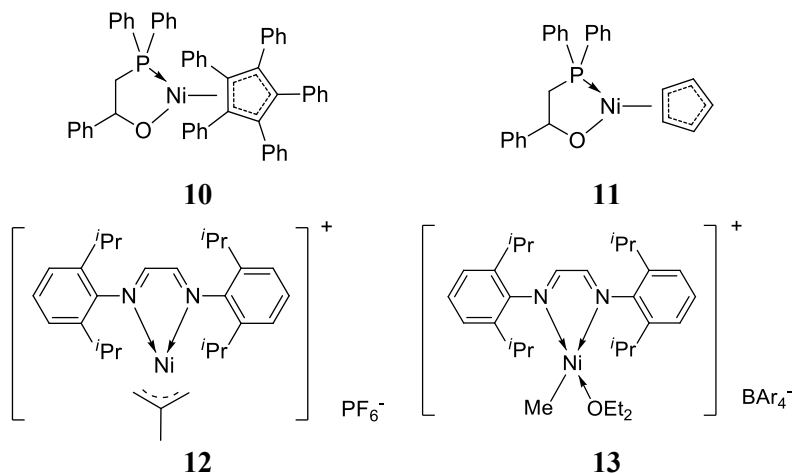
**Scheme 8.** Suggested mechanism for the activation of nickel-allyl complexes with insertion of ethylene and release of an dienyl compound and a nickel hydride. **(I)**: ethylene coordination to nickel, **(II)** migratory insertion of ethylene in the Ni-C<sub>allyl</sub> bond and coordination of another ethylene molecule, **(III)**  $\beta$ -H elimination and release of the nickel hydride complex and the diene compound (PO = Ph<sub>2</sub>P-(CH<sub>2</sub>)<sub>n</sub>-C(=O)O)

The activation of the simplest allylnickel  $\eta^3$ -propenyl nickel complex was reported to be more difficult than the other allylic analogues. Interestingly the  $\eta^3$ -propenyl nickel complexes in Scheme 9 (top) is inactive, whereas the same ligand reacted with  $\text{Ni}(\text{COD})_2$  gives two isomers. One is an excellent catalyst for 1-butene dimerisation and ethylene oligomerisation, the other  $\eta^3$ -octenyl is inactive.<sup>[66]</sup> Keim suggested that  $\eta^3$ -propenyl nickel complex is in equilibrium with the system propylallene / nickel hydride and that, due to the high reactivity of this allene, the equilibrium is pushed towards the  $\eta^3$ -propenyl nickel complex. This supposition is in contrast with other systems that lead first to ethylene insertion and then elimination.



**Scheme 9.** Reactivity of  $\eta^3$ -propenyl nickel complexes vs.  $\text{Ni}(\text{COD})$  complexes in olefins oligomerisation (from Keim *et al.*).

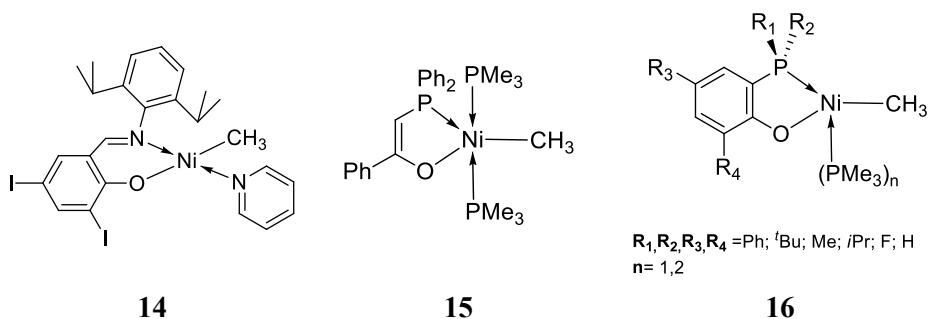
To bypass the drastic operating conditions relative to the activation of the  $\text{Ni-Cp}$  complexes (high temperature, 70 bar)<sup>[66]</sup>, Matt *et al.* used successfully a stoichiometric amount of  $\text{NaBH}_4$  and activated complexes **10** and **11** *in situ* under reduced ethylene pressure (< 40 bars).<sup>[68]</sup> Complex **10** +  $\text{NaBH}_4$  gave linear  $\alpha$ -olefins with a selectivity of 98% whereas **11** +  $\text{NaBH}_4$ , under the same reaction conditions led to high proportions of polyethylene ( $M_n = 479$ ). They interpret this striking difference by the greater ability of **11** to form a Ni-H bond due to the competition between the leaving groups and ethylene insertion.



The elevated pressure and temperature conditions required to activate allyl nickel complexes reveal that the allyl fragment has a strong binding affinity for nickel which in turns lowers the reactivity towards oligomerisation/polymerisation. Based on the same NN ligand and in similar conditions ( $0^{\circ}\text{C}$  and 1 bar), the methallyl-nickel complex **12** is inactive whereas complex **13**, the original Brookhart Ni-Me catalyst system is highly active (activity estimated to  $34\,000\text{ g}_{\text{C}_2\text{H}_4}/(\text{g}_{\text{Ni}}\cdot\text{h})$ ). This difference may also come from other parameters such as the presence of  $\text{Et}_2\text{O}$ .<sup>[69,70]</sup>

### 1.3.4 Alkyl nickel complexes

Alkyl-nickel complexes are generally air and moisture sensitive complexes that are difficult to handle. The addition of bidentate ligands has been reported to stabilise these systems. Nickel-alkyl species are organometallic complexes that and they should not require any co-catalyst to perform olefin oligomerisation.



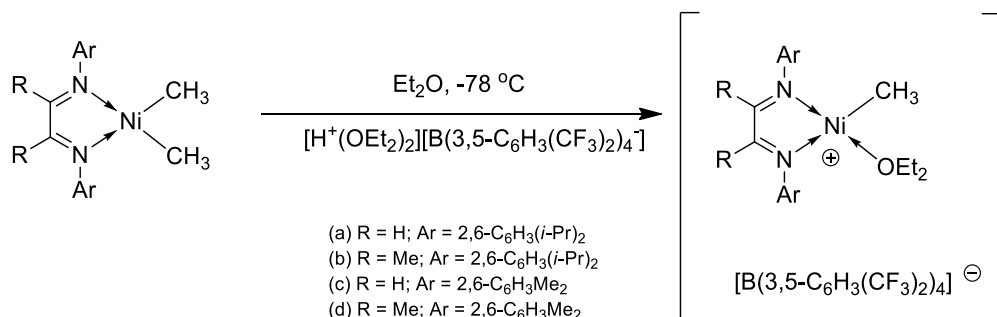
Bauers and Mecking isolated and characterised compound **14** by mixing salicylaldimine ligand and pyridine with one equivalent of  $[(\text{tmeda})\text{Ni}(\text{CH}_3)_2]$ .<sup>[71]</sup> When this complex was brought under an ethylene atmosphere in a water based

medium, polymer was formed with a moderate activity of  $600 \text{ g}_{\text{C}_2\text{H}_4}/(\text{g}_{\text{Ni}}\cdot\text{h})$ . The analogue complex bearing a phenyl group instead of  $-\text{CH}_3$  and a  $\text{PPh}_3$  adduct exhibits in the presence of a phosphine scavenger  $[\text{Rh}(\text{CH}_2=\text{CH}_2)_2(\text{acac})]$  the same reactivity.

Similarly to SHOP-type catalysts, Klabunde and Ittel reported the synthesis of the five coordinated (P,O) methyl-nickel complex **15** (18 valence electrons) that was active for ethylene polymerisation in toluene without an induction period, showing that ethylene insertion in the Ni-methyl bond is quick in this complex.<sup>[59]</sup> The corresponding phosphanylphenolato nickel complexes of general structure **16** were synthesised and characterised (NMR, IR, element analysis, nickel precursor:  $[\text{NiMe}(\text{PMe}_3)(\mu\text{-MeO})_2]$ ) and these yielded ethylene oligomers with a large distribution of products (Schulz Flory,  $\text{C}_4\text{-C}_{50}$ ).<sup>[72]</sup> Complexes bearing two  $(\text{PMe}_3)$  tend to give a narrower olefin distribution.

Interestingly most of Ni-Me complexes tend to oligomerise ethylene into long chain olefins. The use of nickel complexes with longer alkyl chains (ethyl, propyl, butyl...) was not reported in the literature. This may be explained by the fact that alkyl chains with more than 2 carbons lead to potential agostic interactions between the proton in beta position of the nickel and the nickel atom, which leads to the equilibrium nickel-alkyl / nickel hydride + olefin.<sup>[73,74]</sup>

Dimethyl nickel complexes were not reported as being active in ethylene oligomerisation. Brookhart and co-workers showed that such complexes could, however, be activated by methyl abstraction (see Scheme 10).<sup>[70]</sup> Strong acids such as  $[\text{H}(\text{OEt})^+]_2[\text{BAr}_4^-]$  protonate the  $[(\alpha\text{-diimine})\text{Ni}(\text{Me})_2]$  complex resulting in the loss of methane and formation of the monomethyl nickel complex with a diethyl ether adduct. These complexes produce high molecular weight polymer when using ethylene, propylene or 1-hexene as monomers.



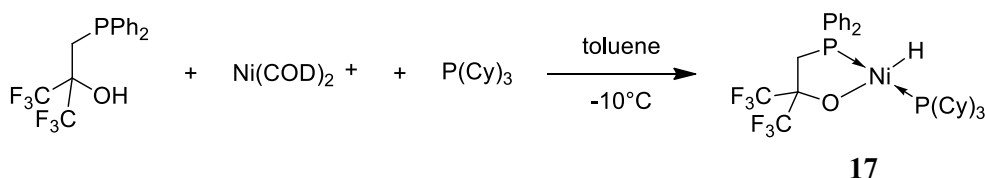
**Scheme 10.** Activation of a Ni-dimethyl complex by protonation of a methyl group by a Brønsted acid.

### 1.3.5 Nickel hydrides and related complexes

#### 1.3.5.1 Oxidative addition on zerovalent nickel

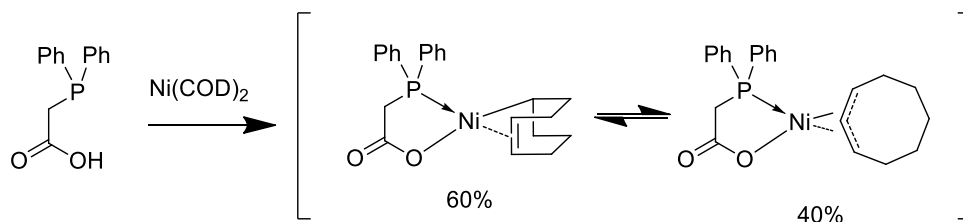
Nickel hydride is regarded as being the active species in ethylene oligomerisation. It forms by  $\beta$ -H elimination starting from e.g. conventional nickel aryl or nickel allyl complexes. Nickel hydrides can also be prepared by reacting zerovalent nickel with protic species. Ni(COD)<sub>2</sub> for instance, reacts with ligands bearing a Brønsted acid moiety, presumably by oxidative addition.

By mixing Ni(COD)<sub>2</sub> with a phosphanyl alcohol *in situ*, Keim and co-workers observed the formation of a hydride signal in <sup>1</sup>H NMR but this very reactive system could not be isolated. The same system reacted in the presence of ethylene to form LAO with a broad Schulz-Flory distribution (C<sub>4</sub>-C<sub>30</sub>) and a good activity (2 400 g<sub>C<sub>2</sub>H<sub>4</sub></sub>/(g<sub>Ni</sub>·h)). The addition of PCy<sub>3</sub> to this system blocked the catalytic activity but allowed to trap and characterise a nickel hydride **17** (Scheme 11). In the presence of ethylene, **17** reacted to form a Ni-ethyl species.<sup>[38]</sup> These observations likely support the mechanism of degenerate polymerisation proposed by Cossee and Arlmann, based on the nickel-hydride active species.<sup>[75-77]</sup>



**Scheme 11.** Formation of a (P,O) chelated nickel hydride complex, by oxidative addition of a phosphanylalcohol in Ni(COD)<sub>2</sub> in presence of PCy<sub>3</sub>. This type of complex (without PCy<sub>3</sub>) is considered as the active species for the oligomerisation of olefins.

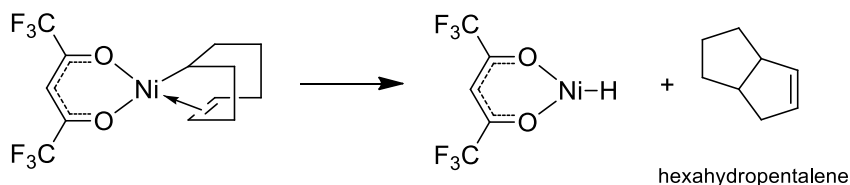
Ni(COD)<sub>2</sub> reacts also with Phosphinocarboxylic acid but no hydride was detected by NMR. A mixture of two (P,O) chelated nickel complexes appeared instead in which the nickel is attached to a cyclooctene ring (see Figure 12). This cycle with 8 carbons likely comes from the 1,5-cyclooctadiene of the nickel precursor. The presence of only one insaturation (double bond) in the complexes suggest that a nickel hydride complex formed (upon mixing the the acid and the Ni(COD)<sub>2</sub>) that instantly reacts with one of the cyclooctadiene double bond to give an -enyl or -allyl nickel complex. The resulting nickel complex mixture presented Scheme 12 is moderately active in ethylene oligomerisation ( $\pm$  2 000 g<sub>C<sub>2</sub>H<sub>4</sub></sub>/(g<sub>Ni</sub>·h)), affording a mixture of linear alpha olefins (C<sub>4</sub>-C<sub>24</sub>,  $\alpha$ % > 99%, linearity > 99%).<sup>[78]</sup> This work was completed recently: the structure of the complex was confirmed by MS, IR, <sup>1</sup>H, <sup>13</sup>C and <sup>31</sup>P NMR.<sup>[79]</sup>



**Scheme 12.** Reaction of diphosphinomethylcarboxylic acid with  $\text{Ni}(\text{COD})_2$  forming two types of PO-chelated allyl-nickel complexes.

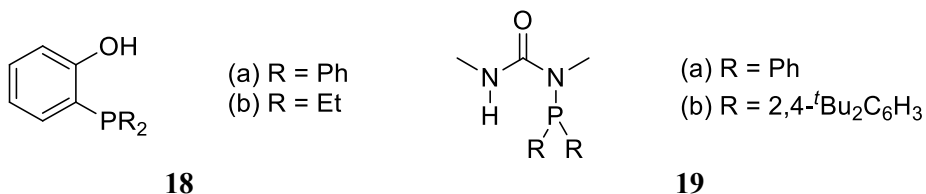
The equilibrium depicted in Scheme 12 between a 4-enylnickel and a  $^3\eta$ -allyl nickel might be the result of an isomerisation reaction due to a Ni-H species. Interestingly, changing the PO chelate to an (O,O) chelate led to the formation of the same two isomers which did not present any equilibrium between each other and could be isolated.<sup>[80]</sup> The first one (4-enylnickel) is an excellent catalyst for 1-butene oligomerisation while the other ( $^3\eta$ -allyl nickel) is inactive.<sup>[39,49,78,81]</sup>

In the course of the catalytic reaction with the 4-enylnickel complex, the group of Keim observed the formation of hexahydropentalene.<sup>[80]</sup> This molecule suggests the formation of the active Ni-hydride from the 4-enylnickel (Scheme 13). In contrast, they explained that the other isomer was inactive because it was unable to release a Ni-H by elimination of hexahydropentalene.



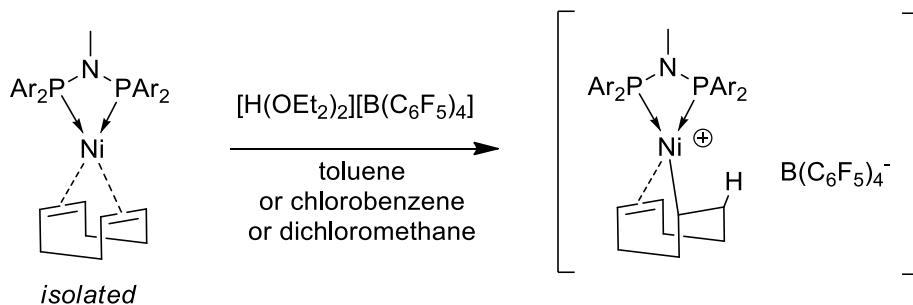
**Scheme 13.** Formation of Ni-H starting from  $\text{Ni}(\text{COD})_2$ .

Phosphanylphenols, which are stronger Brønsted acids than phosphanylalcohols also react with  $\text{Ni}(\text{COD})_2$ .<sup>[50,82]</sup> The reaction of **18(a)** with  $\text{Ni}(\text{COD})_2$  gives a system which reacts with ethylene and forms linear polymer and a small amount of linear oligomers. In contrast, **18(b)** under the same conditions shows less activity (3.5% conversion) but lead to short oligomers ( $\text{C}_4$  68%,  $\text{C}_6$  24%,  $\text{C}_8^+$  8%). The basicity and the steric bulk of the phosphine are certainly responsible for this behaviour.



Oxidative addition was also reported for N-H bonds (such as Phosphanyl ureas **19** or carbamylmethylphosphines).<sup>[49,83]</sup> Under ethylene pressure, the system **19(a)** + Ni(COD)<sub>2</sub> produces a high content of LAO (75% α-C<sub>4</sub><sup>−</sup>, 10 % C<sub>6</sub><sup>−</sup>, 5% C<sub>8</sub><sup>−</sup>, activity= 2 900 g<sub>C<sub>2</sub>H<sub>4</sub></sub>/(g<sub>Ni</sub>.h)). In comparison, the system **19(b)** + Ni(COD)<sub>2</sub> is more active (7 200 g<sub>C<sub>2</sub>H<sub>4</sub></sub>/(g<sub>Ni</sub>.h)) affording mainly *n*-hexenes of which 65% are branched. A change in the phosphine substitution induces major changes in catalysis.

When the chelating ligand is not acidic, the addition of a strong Brønsted acids (e.g. [H(OEt)<sub>2</sub>][B(C<sub>6</sub>F<sub>5</sub>)<sub>4</sub>]) leads to similar protonation of nickel. Carpentier *et al.* reported precatalysts of the type (PNP)Ni<sup>0</sup>(cod) which, once activated by [H(OEt)<sub>2</sub>][B(C<sub>6</sub>F<sub>5</sub>)<sub>4</sub>], polymerise at room temperature ethylene into low molecular weight, moderately branched, polyethylene.<sup>[84]</sup> NMR studies and ESI-MS data show that protonation occurs at the cyclooctadiene moiety affording a cationic nickel-allyl species. They postulate the structure (PNP)Ni(codH)<sup>+</sup> presented in Scheme 14.

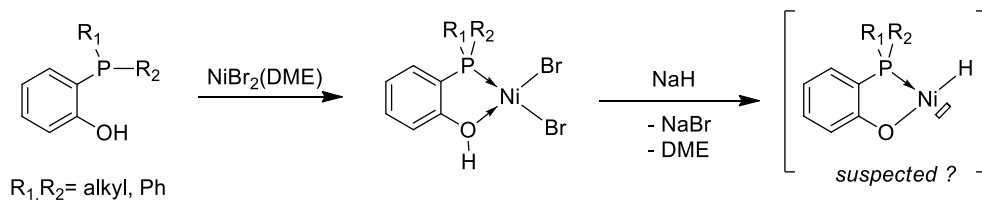


**Scheme 14.** Protonation of a Ni<sup>(0)</sup>PNP(COD) complex by [H(OEt)<sub>2</sub>][B(C<sub>6</sub>F<sub>5</sub>)<sub>4</sub>].

### 1.3.5.2 In situ hydride formation

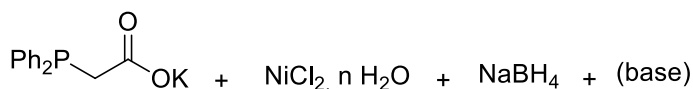
Nickel hydride has been postulated to be the active species for ethylene oligomerisation reaction. As this class of compounds is very reactive and the corresponding complexes are not very stable, Heinicke *et al.* attempted to form a PO chelated nickel hydride complex *in situ* similar to **17** by using a mixture of NiBr<sub>2</sub>(DME), NaH and an *ortho*-phosphanylphenol.<sup>[82]</sup> This mixture, together with gaseous ethylene led to linear polyethylene with low catalytic activity and poor selectivity (compared to activation with Ni(COD)<sub>2</sub>: see **18(a)**). This suggests that a nickel-hydride complex forms according to Scheme 15. Besides, an increase in the

phosphine basicity of the ligand (e.g. 2-dialkylphosphanylphenols) led to complex inactivity (compared to the Ni(COD)<sub>2</sub> analogues).



**Scheme 15.** *In situ* generation of nickel-hydride complexes by using a mixture of phosphanylphenol, NiBr<sub>2</sub>(DME) and sodium hydride.

The use of sodium borohydride has also been reported to activate a mixture of potassium phosphinoacetate and NiCl<sub>2</sub> (Scheme 16).<sup>[85,86]</sup> The mixture has activity similar to the systems presented above [phosphinoacetic acid + Ni(COD)<sub>2</sub>] and certainly forms a nickel-hydride intermediate. This reaction has been extensively studied and is the heart of the industrial SHOP process.

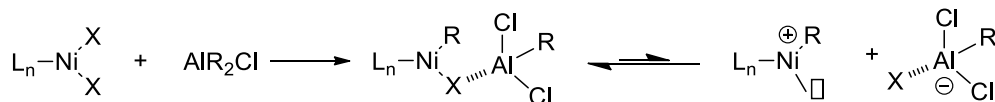


**Scheme 16.** Typical composition of the catalytic mixture used in the SHOP process.

### 1.3.6 Di-halide nickel complexes

Nickel halides complexes are among the easiest accessible and stable nickel compounds. They are generally obtained by mixing one or two equivalents of ligand with NiBr<sub>2</sub>(DME) or other nickel precursors.

In order to become catalysts for ethylene oligomerisation, nickel di-halide complexes require an activation step with an aluminium activator that abstracts the halide and acts as an alkylating agent (Scheme 17). In this case, the nature of the anion greatly influences the activity of the catalytic system.



**Scheme 17.** Activation of a Ni dihalide complexes by chlorodialkylaluminium: general mechanism.

The co-catalysts used are generally chloroalkylaluminium compounds and since the 1990s also aluminoxanes. Alkyl aluminium activators are avoided because they reduce complexes to Ni(0) species which are not active in oligomerisation.<sup>[87,88]</sup>



The ability of chloroalkylaluminiums to activate nickel di-halide complexes is related to their Lewis acidity (potential to abstract Cl) but also their alkylation potential. Only a small number of chloroalkylaluminiums are used in practice, with a variable Cl/Al ratio. De Souza *et al.* observed that the activity of a complex was proportional to the Lewis acidity of the co-catalyst (see Figure 6).<sup>[89]</sup> Interestingly,  $\text{AlCl}_3$ , which has the most pronounced Lewis acid character despite having no alkylation potential, would be the best halide abstractor. Although this candidate is not soluble in organic media, its properties were investigated in combination with ionic liquids at IFPEN for the activation of nickel methallyl nickel chloride dimer.<sup>[33]</sup>

	$\text{AlEt}_3$	DEAC	EASC	EADC	$\text{AlCl}_3$
Ratio Cl/Al	0	1	1.5	2	3
Lewis acidity	—————→				
Activity	—————→				

**Figure 6.** Some commonly used chloroalkylaluminium for nickel complexes activation ranked by increasing Lewis acidity and activity in the transformation (correlation proposed by De Souza *et al.*)<sup>[89]</sup>.

In industry, the Dimersol process (1977) uses the more Lewis acidic reagent EADC to activate  $\text{NiX}_2$  whereas the Phillips process uses it to activate  $\text{NiX}_2\text{L}_2$  ( $\text{L} = \text{P}(n\text{Bu})_3$ ). In this process ethylene selectively converts into 2-butene.

The use of aluminoxanes has started relatively recently and originates from the polymerisation research on group IV transition metals. In the late '90, BP and DuPont (Gibson, Brookhart and co-workers) developed bis-imino ligands (known as Versipol®). The related nickel complex **20**, activated by 100 eq. of MMAO (modified MAO) gave linear olefins with a broad Schulz Flory distribution (activity: 57 000  $\text{g}_{\text{C}_2\text{H}_4}/(\text{g}_{\text{Ni}}\cdot\text{h})$ ,  $\alpha$ -selectivity: 94% with possibility to reach 110 000  $\text{g}_{\text{C}_2\text{H}_4}/(\text{g}_{\text{Ni}}\cdot\text{h})$  with an  $\alpha$ -selectivity of 80%).<sup>[70,90,91]</sup>

Although MAO significantly reduces isomerisation, a large excess of this activator is generally required ( $\text{Al/Ni} > 100$  and 1000 in some cases) and activation by MAO generally shows a significantly diminished activity in comparison with chloroalkylaluminium activators. The reaction of MAO and its analogues with nickel halide complexes leads to the formation of bulky counter ions that prevent ligand migration from nickel to aluminium. The proposed structures of MAO vary between one-dimensional linear chain, two-dimensional structures, three-dimensional clusters, cyclic and cage structures (Figure 7).<sup>[92]</sup> The MAO structure cannot be directly elucidated because of different equilibria between the conformers. MAO is produced by partial hydrolysis of trimethylaluminium (TMA) and so the commercial product always holds a small quantity of residual TMA (around 5%).

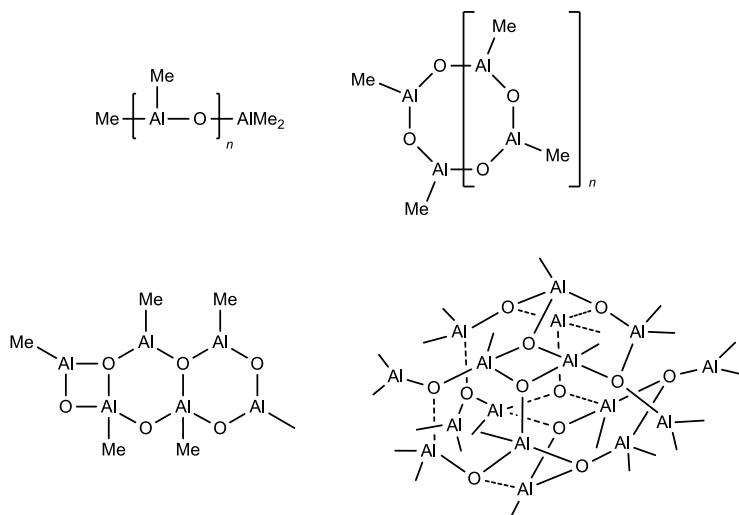
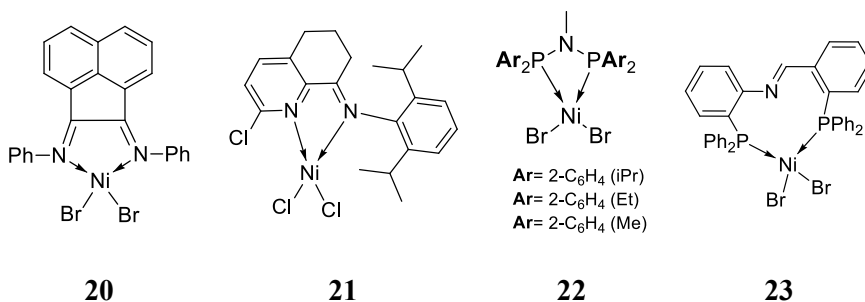


**Figure 7.** Suggested structure for methylaluminoxane (from Sinn *et al.*<sup>[92]</sup>).

Due to the easy synthesis of  $\text{NiCl}_2$  chelated complexes, many groups have been working on the synthesis of bidentate or tridentate ligands combining oxygen, nitrogen, sulphur or phosphorus.<sup>[7,93]</sup> Based on this work, Sun *et al.* extended the scope to several other (N,N) complexes of type imino-pyridinyl. They found that complex **21**, after activation with 400 eq. of EASC is highly active as an ethylene oligomerisation catalyst (150 000  $\text{g}_{\text{C}_2\text{H}_4}/(\text{g}_{\text{Ni}}\cdot\text{h})$ ) producing short  $\alpha$ -olefins ( $\text{C}_4\text{-C}_6$ ,  $\alpha\text{-C}_4/\text{C}_4 > 99\%$ ).<sup>[94-96]</sup> In the same way, many bidentate and tridentate ligands (**22**, **23**) have been developed and were found to be active in ethylene oligomerisation.<sup>[93]</sup>



In industry, nickel halides are replaced by nickel(2-ethylhexanoate) (also called nickel octoate) with a similar activation procedure (alkylaluminium or aluminoxanes). This nickel precursor with long alkyl chains is very soluble in aliphatic solvents, including olefin feeds, and is therefore preferred for continuous oligomerisation processes.

## 1.4 Mechanistic considerations

### 1.4.1 Nickel hydrides and the degenerated polymerisation mechanism

Thanks to a careful observation of several precatalyst side products (**Figure 8**), Ni-H or Ni-C based complexes have been identified as the active species for olefins oligomerisation.

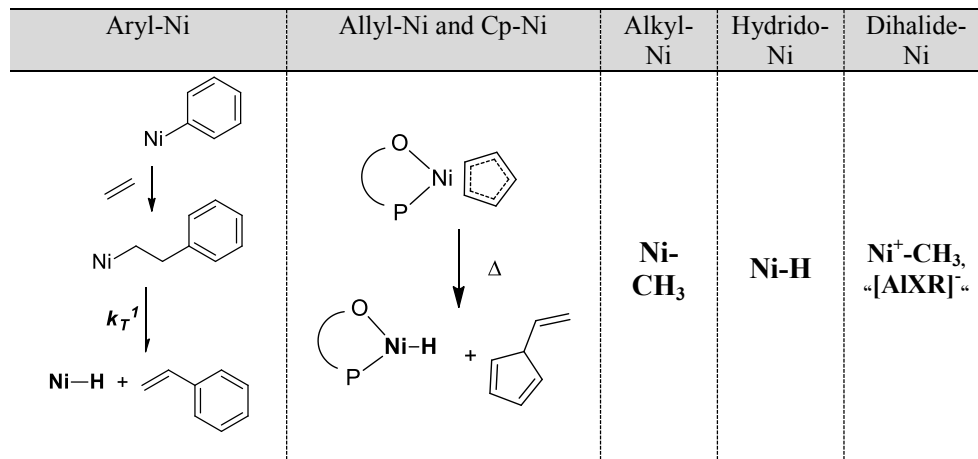


**Figure 8.** Activation of different families of Ni precatalysts

Nickel (II) hydride species are generally considered as the active species coming from the degenerate polymerisation mechanism. This mechanism, presented in Figure 9, consists of the successive insertion of ethylene in the metal-hydride (**I**) or metal-alkyl bond (**II** and **III**). Linear  $\alpha$ -olefins are subsequently released by  $\beta$ -H elimination of the metal-alkyl intermediate (**IV**). The isomerisation process is responsible for internal and/or branched olefins.

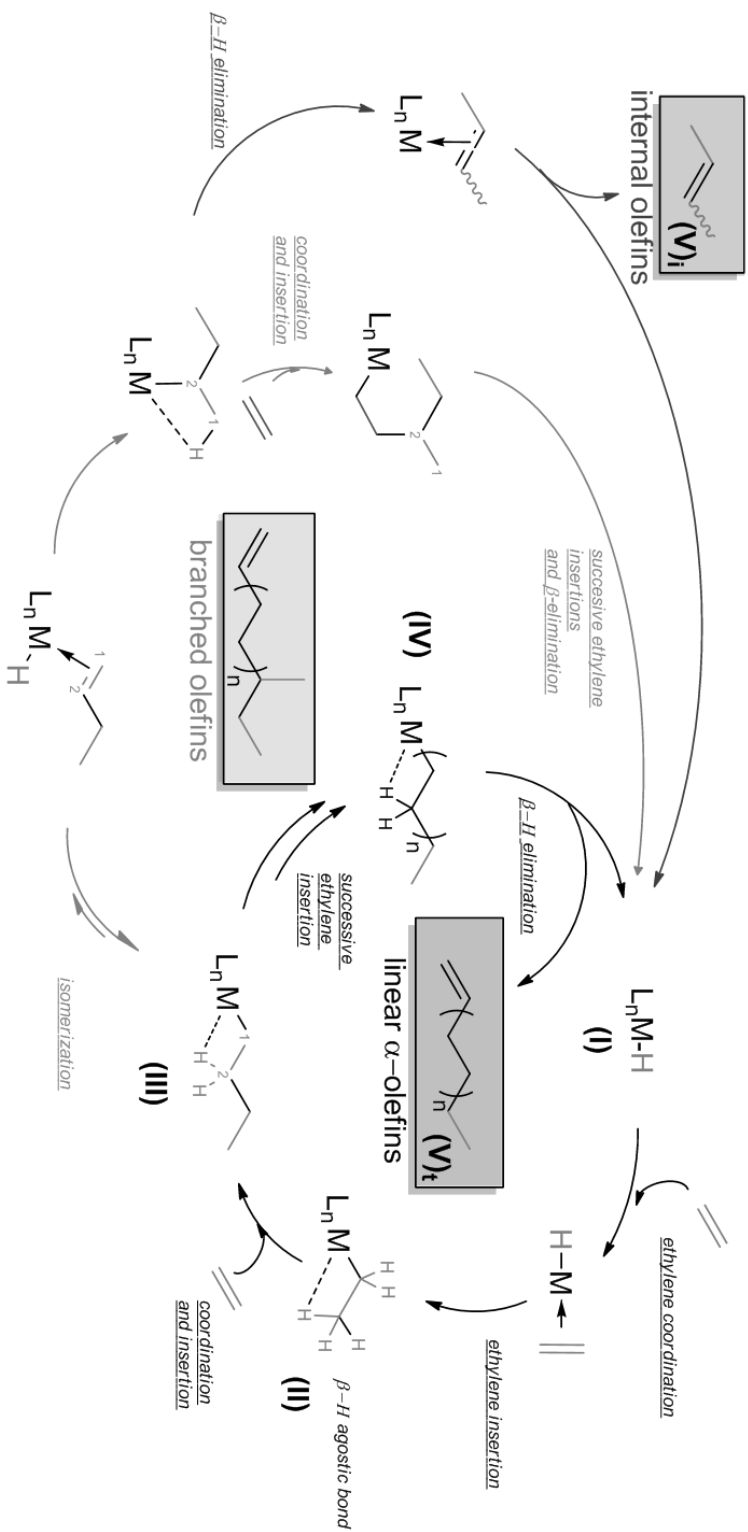


**Figure 9.** Postulated mechanism for degenerated polymerisation including isomerisation and co-dimerisation pathways.

The distribution of olefins in this mechanism relies on two parameters: the propagation and termination constants (resp.  $k_p$  and  $k_t$ ). If the ratio  $k_p/k_t = 1$ , the system will produce olefins following a broad Schulz-Flory distribution.<sup>[97]</sup> For  $k_p/k_t \ll 1$ , the system will afford short olefins (1-butene, 1-hexene, 1-octene) as shown in Figure 10. This distribution is modelled by the Schulz Flory constant,<sup>[10]</sup>  $K_{SF}$  (also called growing factor), calculated from the oligomers product distribution (% weight) determined from GC and averaged on the  $C_8$ - $C_{18}$  oligomers. The general formula for the calculation of  $K_{SF}$  is given by eq. 1, in which  $p$  corresponds to the number of monomer units (for ethylene  $p = \text{number of carbons} / 2$ , for propylene  $p = \text{number of carbons} / 3$ ) and  $Cte$  is a constant.

$$\log\left(\frac{\%weight\ of\ p}{p}\right) = (\log K_{SF\ p})(p - 1) + Cte \quad \text{eq. 1}$$

In practice, the determination of the  $K_{SF(p)}$  constant at the degree  $p$  is calculated between  $p$  and the consecutive oligomer  $p+1$  and the previous equation is simplified as seen in eq. 2.

$$K_{SF(p)} = \left(\frac{\%weight\ C_{p+1}}{\%weight\ C_p}\right) \cdot \left(\frac{p}{p+1}\right) \quad \text{eq. 2}$$

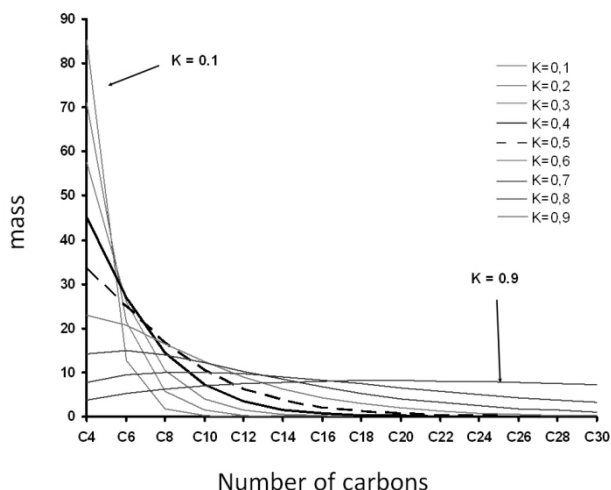


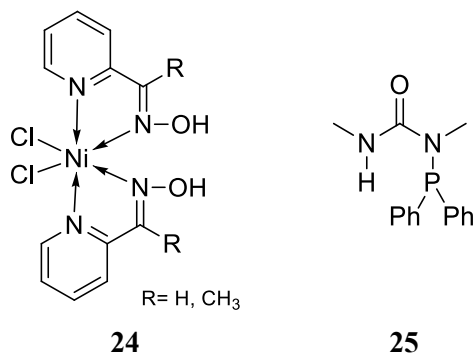
**Figure 10.** Schulz-Flory olefin distribution

This geometric oligomer distribution has been applied to describe many nickel-based oligomerisation systems. It fitted particularly well with SHOP-type complexes that

produced exclusively LAO, thus enabling the determination of a good structure-selectivity relationship.<sup>[98,99]</sup>

### 1.4.2 Towards other mechanisms

Although the most frequently encountered mechanism for ethylene oligomerisation by nickel is the degenerate polymerisation described by Cossee and Arlman, certain systems show exceptional selectivity for one LAO and in particular 1-butene. Mukherjee *et al.* reported a nickel oxime complex **24**, which in combination with by EADC, produces 77 % ethylene dimers comprising 99.5% of 1-butene.<sup>[100]</sup> As another example, the phosphanyl-urea ligand system **25** + Ni(COD)<sub>2</sub> is reported to afford 75% butenes of which 1-butene is predominant.<sup>[83]</sup>



High contents of 1-butene for nickel catalysts are surprising considering a degenerate polymerisation mechanism, which usually gives rise to a geometric mixture of long oligomers (Schulz-Flory). This hints at other oligomerisation mechanisms at work, such as metallacyclic pathways.

Early transition metals such as titanium or chromium oligomerise ethylene with a very high selectivity towards a single LAO. This ability lies in the possibility of a concerted coupling mechanism (Figure 11).<sup>[101]</sup> In this approach, two molecules of ethylene coordinate to the metal in a coplanar fashion. Oxidative coupling of this system leads to a metallacyclopentane. Depending on its stability, this intermediate evolves according to two pathways:

- the metallacyclopentane is stable and an extra molecule of ethylene coordinates, inserts and forms a metallacycloheptane,
- the metallacyclopentane is unstable and releases a molecule of 1-butene by intramolecular hydrogen transfer.

During the catalytic loop the metal is oxidised and reduced between a valence state of  $n$  and  $n+2$ .

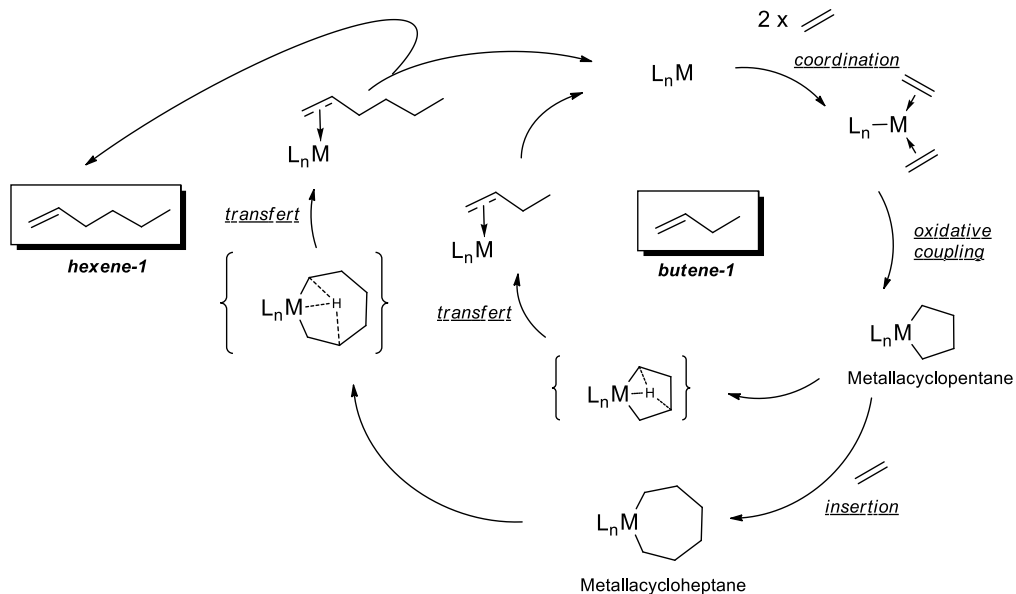


**Figure 11.** Mechanism of concerted coupling: affords one olefin selectively.

These observations lead to the important question if this concerted coupling mechanism applies to nickel oligomerisation. Although metallacycles are common in chromium and titanium chemistry, literature examples of nickellacycles are extremely scarce. The only example is from Grubbs *et al.* who managed to synthetically create a nickellacyclopentane stable at low temperature. Depending on the type of phosphine attached to the metal, the elimination step triggered by increasing the temperature leads to the formation of cyclobutane, ethylene or 1-butene. The presence of ethylene in the degradation products could indicate that the reverse reaction (oxidative coupling) is possible<sup>[102,103]</sup>

This example shows that nickellacyclopentane may be stable (at low temperature), however oxidative coupling of ethylene to Ni(0) and formation of a nickellacyclopentane has not been reported so far. The work of Grubbs was later supported by a DFT investigation showing that ethylene could in theory oxidatively couple to a nickel(0)bisphosphine complex (Figure 31).<sup>[104]</sup> The pathway calculated in Figure 12 suggests that two molecules of ethylene coordinate around the metallic centre ( $M_2$ ). When a third free molecule of ethylene is added, energy is required to reach the transition state ( $TS_1$ ) in which the extra molecule is in weak anti-interaction with coordinated ethylene to subsequently form a new C-C bond ( $M_3$ ). A rotation

along the newly created C-C bond lowers the energy ( $M_4$ ) putting the two radicals in proximity. In this situation the two electrons couple to form the new Ni-C bond (metallacycle  $M_5$ ) and release the coordinating ethylene.

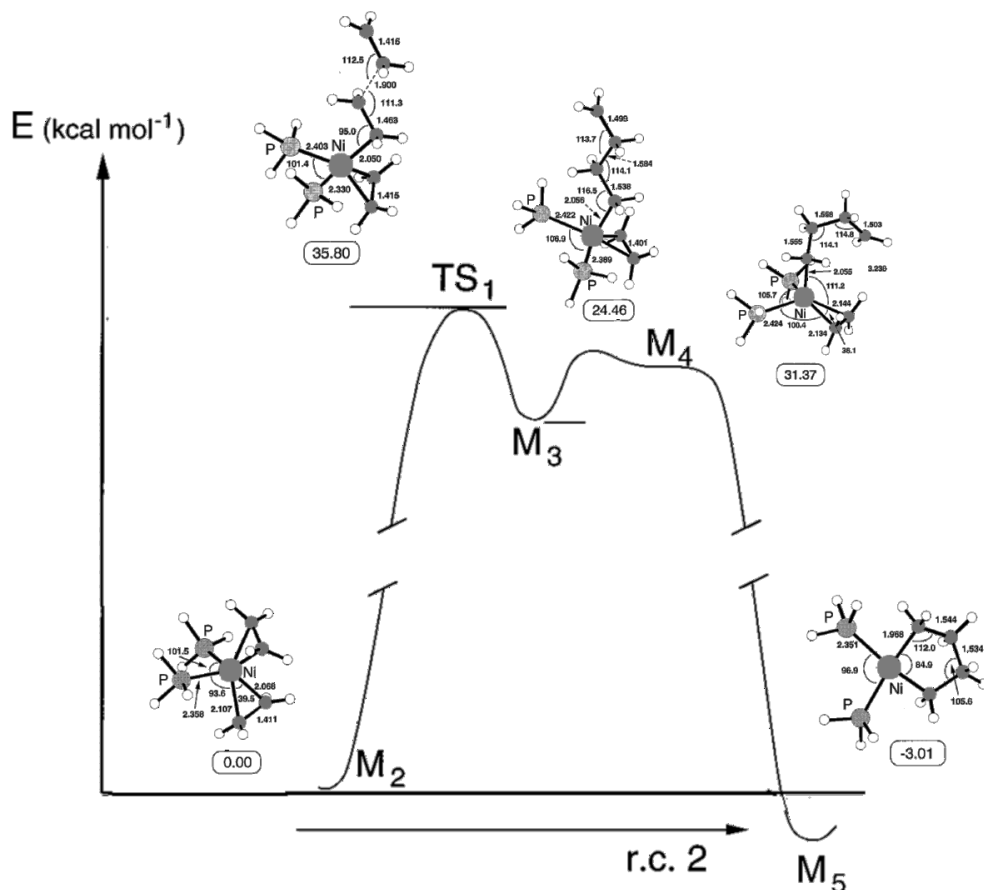


**Figure 12.** Energy profile describing the attack of an ethylene molecule on the  $M_2$  complex; r.c. 2: reaction coordinates leading to the formation of the  $M_5$  biradical; the formation of a nickelacyclopentane is energetically favoured (extracted from Bernardi *et al.*<sup>[104]</sup>).

These studies suggest that a metallacyclic pathway could take place with nickel catalyst forming 1-butene. Furthermore, this leads to the question if higher olefins (such as 1-hexene or 1-octene) are reachable by this pathway.

Recently Alt *et al.* showed the possibility of activating a nickel dihalide complex in the absence of any alkylating agent. The metal species in the presence of a weak Lewis acid and dissolved in chloroaluminate buffered ionic liquids yielded under an ethylene atmosphere alpha-olefins with high selectivity. The absence of an alkylating agent or the presence of a group with the ability to generate an hydride species contradicts the degenerate polymerisation mechanism and opens the way to a

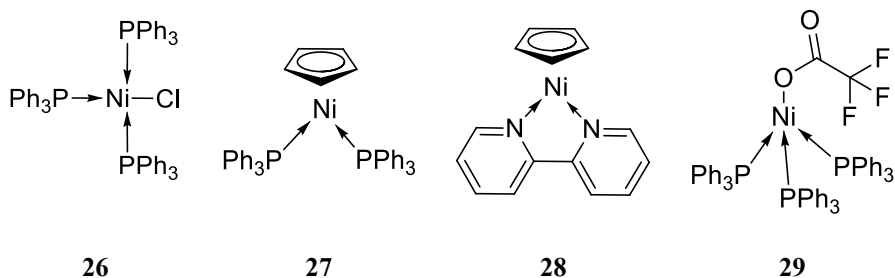


possible concerted coupling mechanism or a new pathways.<sup>[105–107]</sup> The reduction of Ni(II) to the unusual oxidative state Ni(I) would be a natural consequence of this pathway.

### 1.4.3 The potential of Ni(I)

While nickel (II) and nickel (0) complexes are widely reported in the literature, less is known about the oxidative states (I) and (III). Some studies in heterogeneous catalysis by Che *et al.* have demonstrated the potential of Ni(I) immobilised on silica for ethylene oligomerisation without generating nickel hydride or nickel alkyl intermediates.<sup>[108]</sup> Compounds of Ni(I) are paramagnetic and their observation relies exclusively on EPR, elemental analysis, mass spectroscopy or single crystal diffraction. Due to this unusual oxidative state, Ni(I) can accommodate a greater number of coordinating ligands. Olivier *et al.* showed that a coordination number up to five was possible (when immobilised on silica) which renders a metallacyclic pathway possible to account for the formation of 1-butene.<sup>[109]</sup> A catalytic pathway involving Ni(I), however, is not generally accepted. Go *et al.* suggested that the activity of Ni(I) relies on a disproportionation leading to Ni(0) and Ni(II).<sup>[110]</sup>

Some complexes of Ni(I) can be isolated and thus their catalytic ethylene oligomerisation activity can be investigated. Bogdanovic reported that complex **26** in presence of  $\text{AlCl}_3$  or  $\text{BF}_3 \cdot \text{OEt}_2$  is moderately active.<sup>[63,110]</sup>



Complexes of monovalent nickel are obtained by the reduction of  $(\text{PR}_3)_2\text{NiX}_2$  complexes using sodium sand,<sup>[111]</sup> zinc,<sup>[112]</sup> or sodium borohydride.<sup>[113]</sup> Other procedures mention a comproportionation pathway that leads to Ni(I) species by reacting a cationic nickel (II) species with a phosphine nickel (0) complex (comproportionation:  $\text{Ni(II)} + \text{Ni(0)} \rightarrow \text{Ni(I)}$ ).<sup>[114]</sup> Bigorgne *et al.* reported a way to form nickel (I) hydride complexes upon the reaction of triisopropylaluminium with  $\text{Ni}(\text{acac})_2$  in the presence of triethylphosphine.<sup>[115]</sup> This species may be formed first by alkylation followed by  $\beta$ -H elimination.

The group of Saraev also devoted a lot of attention to Ni(I) complexes and studied them by EPR spectroscopy. They isolated and characterised complexes **27** and **28**.<sup>[116]</sup> Furthermore, in addition to the well-known formation of the metal hydride, when strong Brønsted acids oxidatively adds to zerovalent nickel, they observed by EPR the formation of Ni(I) complex **29**, which is active in ethylene oligomerisation. They claim that Ni(II) hydrides are not active in oligomerisation but that they rearrange (comproportionation) in presence of Ni(0) to the potentially active Ni (I) species.<sup>[117–119]</sup>

Similar species are formed with the system  $(\text{PPh}_3)_4\text{Ni} / \text{BF}_3\text{-OEt}_2$ . The cationic system forms  $(\text{PPh}_3)_3\text{NiBF}_4$  which upon phosphine decoordination leads to catalytically active  $(\text{PPh}_3)_2\text{Ni}(\text{OEt}_2)\text{BF}_4$ . In contact with ethylene, oligomerisation starts, the bis ethylene intermediate  $(\text{PPh}_3)\text{Ni}(\text{C}_2\text{H}_4)_2\text{BF}_4$  forms but quickly disappears towards a species not visible in EPR. This compound is considered to be the active oligomerisation species and may be either a dimer or an oxidised / reduced version of  $(\text{PPh}_3)\text{Ni}(\text{C}_2\text{H}_4)_2\text{BF}_4$ .<sup>[120]</sup> However, more experimental data is required to claim the role of Ni(I) in ethylene oligomerisation reactions.

## 2 Major families of catalysts

A nickel based (pre)catalyst used in catalytic ethylene can consist in a wide variety of different ligands around the metallic centre. These ligands have a profound influence on the activity and the selectivity of the oligomerisation reaction. In order to rationalise the ligands effects, Keim *et al.* suggested an analysis of the ligands (based on the SHOP-complexes) by fragmentation of the complex in a chelate part and an organo part (see Figure 13).<sup>[121]</sup>

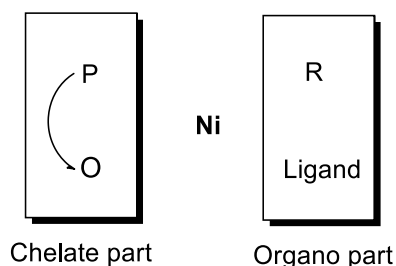
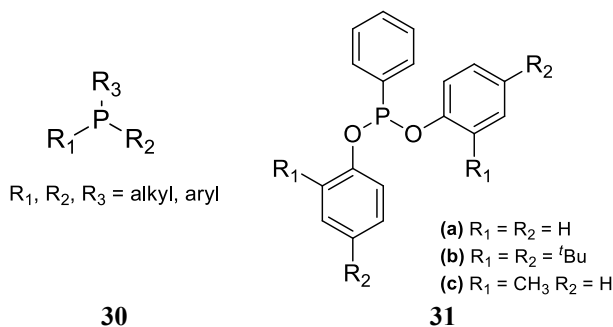


**Figure 13.** Fragmentation of a typical SHOP catalysts by Keim *et al.* into functional groups. The chelate part and the organo part both have an influence on the activity and selectivity.

Many studies have focussed on the role of the chelate part. This fragment, which remains bonded to the metal during the course of the reaction, is supposed to have a greater influence on the outcome and selectivity than the organo part.<sup>[67,122,123]</sup> A great

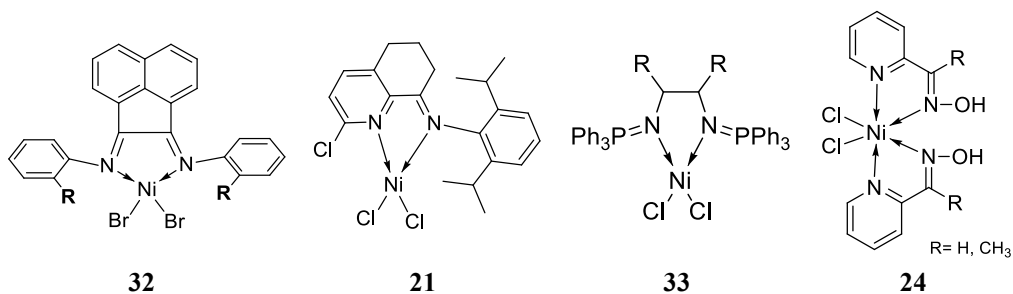
deal of ligands have been synthesised and chelated to the nickel centre in order to control the reactivity and the selectivity of the oligomerisation reaction. Some commonly employed ligand classes are discussed below.

## 2.1 Monodentate ligands



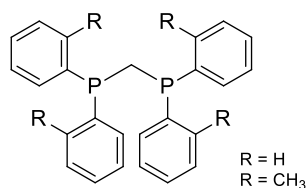
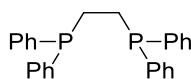
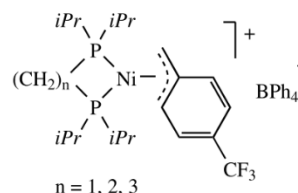
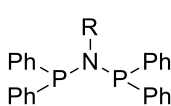
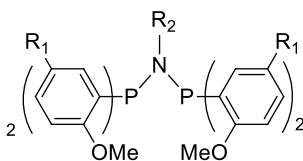
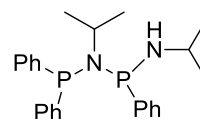
In early work on nickel catalysed oligomerisation, monodentate ligands were the most widely used. Monodentate neutral ligands resulting in neutral or cationic nickel (II) complexes have an influence on the outcome of the reaction. Noticeable examples of “phosphine modified catalysts” using phosphine ligands **30** were developed by Wilke *et al.* for propylene dimerisation (see 1.3.3.2.)<sup>[60]</sup> Besides phosphines, monodentate phosphites **31** were also used by the Mitsubishi Chemical Corporation for the Ni-catalysed dimerisation of *trans*-2-butene.<sup>[124]</sup>

## 2.2 Bidentate ligands



Bidentate ligands offer the possibility to combine hard donor atoms (such as nitrogen, oxygen) with soft donor atoms (such as phosphorus, sulphur). The most common class of bidentate ligands are the  $\alpha$ -diimines (N,N) introduced by Brookhart (**32**).<sup>[70,90,91,125]</sup> It is noteworthy that nickel  $\alpha$ -diimines complexes can be used both for the polymerisation and the oligomerisation of ethylene. If **R** is a bulky group the system produces polyethylene whereas oligomers are formed in the absence of steric hindrance. The group of Sun developed ligands based on the same “ $\alpha$ -diimines”

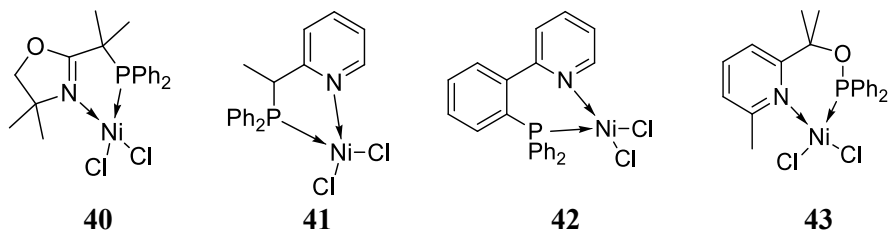
backbone (**21**).<sup>[126]</sup> Variations on this template include the 1,2-diiminophosphoranes based nickel complexes (**33**) leading to active systems in ethylene oligomerisation.<sup>[127]</sup> Those complexes show a tetrahedral geometry around nickel and are therefore paramagnetic. The activity is generally high, especially for the Sun system (167 000 g<sub>C<sub>2</sub>H<sub>4</sub></sub>/(g<sub>Ni</sub>.h)). They produce, under an ethylene atmosphere, a short (C<sub>4</sub>-C<sub>6</sub>) to broad distribution of oligomers (C<sub>4</sub>-C<sub>30</sub>) with a high content of LAO. Mukherjee *et al.* reported nickel oxime complexes **24**, which is the association of two (N,N) bidentate ligands described before.

**34****35****36****37****38****39**

Diphosphines (**P,P**) present some similarities to  $\alpha$ -diimines (**N,N**), however, they give generally less active complexes (by a factor 10). The diarylphosphinomethane ligand **34** in combination with by Ni(COD)<sub>2</sub> and BAr<sup>F</sup> produces a broad distribution of oligomers when the ligand is not very bulky (R= H or CH<sub>3</sub>). For more bulky groups (*iPr*, CF<sub>3</sub>), polymer is produced.<sup>[128]</sup> Bianchini *et al.* showed that DPPE (diphenylphosphinoethane) **35** is active and they optimised the structure to a phosphine tetrasubstituted cyclobutane analogue, that give complexes with higher activity and robustness.<sup>[129]</sup> Campora *et al.* found that the length of the backbone and therefore the bite angle in **36** is in direct correlation with the  $\beta$ -hydrogen elimination and the switch between polymerisation and oligomerisation. With the number **n** of methylene increasing, the activity decreases and low molecular weight polyethylene is formed for n=1 and n=2, while n=3 produces oligomers.<sup>[130]</sup> (PNP) ligands with consecutive donor atoms enter in the (**P,P**) category because, according to crystal structures, the nitrogen does not have the ability to coordinate. The group of Wu synthesised (PNP) Ni(II) complexes (based on **37**) which, activated by MAO or DEAC, produces dimers and trimers with moderate activity (10 200 g<sub>C<sub>2</sub>H<sub>4</sub></sub>/(g<sub>Ni</sub>.h)).<sup>[131]</sup>

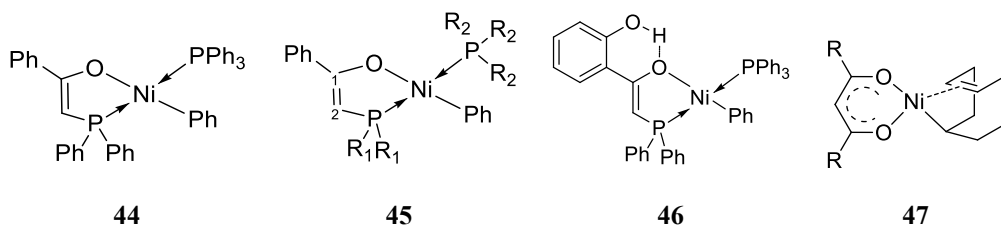
Such systems were also reported as polymerisation catalysts by the groups of Carpentier (38) and Rosenthal (39).<sup>[40]</sup>

Mixed (P,N) ligands combine a soft and hard donor atom. Modification of the steric bulk attached to the phosphine or the nitrogen influences the coordination chemistry and the catalysis. A large number of this type of complexes has been described.<sup>[93,132]</sup>



Complexes **40-43** activated by MAO (400 or 800 eq.) or by EADC oligomerise ethylene into olefins with low molecular weight (C<sub>4</sub>-C<sub>8</sub>) and high activities (up to 23 500 g<sub>C<sub>2</sub>H<sub>4</sub></sub>/(g<sub>Ni</sub>·h) (EADC)) are obtained in the same range as diphosphines (P,P).<sup>[93]</sup> The LAO content is not very high (even with MAO), probably because of isomerisation. Kamer *et al.* synthesised various pyridylphosphine analogues and found that increasing the bite angle leads to a higher activity but also more pronounced isomerisation.<sup>[133]</sup>

Mixed (P,O-) ligands were extensively studied by Keim *et al.* as they are currently used industrially by SHELL to produce LAO with a broad Schulz-Flory type product distribution. A square planar geometry seems to be a prerequisite for good activity and selectivity of these catalysts.<sup>[67]</sup> Much research effort has been directed towards the elucidation of the structure activity pattern of catalyst **44**.<sup>[98,99]</sup>

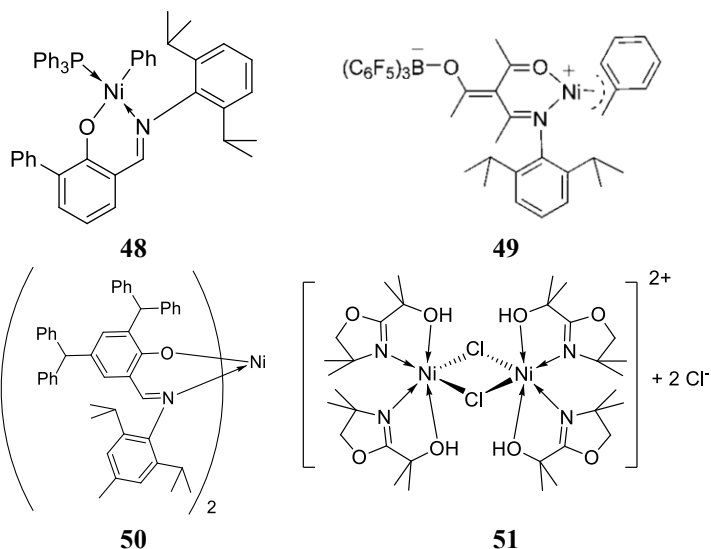


The properties of these catalysts depend strongly on the donor properties of the P and O atoms, which are ruled by the C<sub>1</sub> and C<sub>2</sub> substitution (complex **45**). Strong withdrawing groups on C<sub>1</sub> particularly favour the formation of shorter oligomers by lengthening the O-Ni-C(Ph) bonds and therefore increasing the rate of termination step.<sup>[56]</sup> Mercier *et al.* showed in **46** that artificially lowering the electron density on the oxygen by means of an intramolecular hydrogen bond results in formation of LAO of lower molecular weight.<sup>[58]</sup> Other factors such as the basicity and the steric

hindrance of the phosphines  $\mathbf{P(R_2)_3}$  or  $\mathbf{P(R_1)_2}$  in **44** affect the activity (inactive to active) or the formation of polymer. These effects are generally interdependent and related to the backbone.<sup>[59,122,123]</sup> Matt *et al.* studied and reviewed these systems in depth.<sup>[98,99]</sup>

Keim *et al.* also studied the  $(\mathbf{O,O})$  ligands and particularly the acetylacetonate fragment (which is also an electron delocalised ring system based on 6 atoms).<sup>[80,134]</sup> The allylic COD complexes depicted as **47** were studied in 1-butene dimerisation; they produce dimers with a good selectivity only if R is a  $\text{CF}_3$ . Acetylacetonate nickel itself is inactive.<sup>[66,80]</sup>

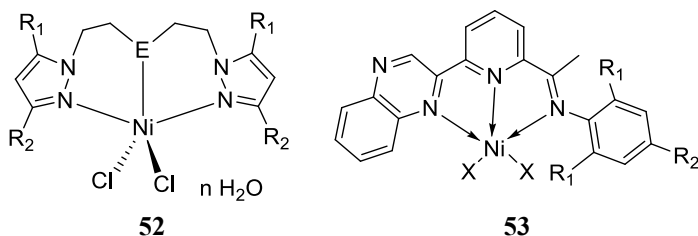
$(\mathbf{N,O-})$  ligands have been extensively investigated.<sup>[135]</sup> One major breakthrough is the discovery of salicylaldimine-based nickel(II) complexes (such as **48**) by the group of Grubbs that perform ethylene polymerisation without co-catalyst with activities up to 51 000  $\text{g}_{\text{PE}}/(\text{g}_{\text{Ni.h}})$  under very mild conditions.<sup>[136]</sup> By modifying the chelate backbone, the group of Bazan found that system **49**, with 2 eq. of  $\text{B}(\text{C}_6\text{F}_5)_3$ , is able to produce internal olefins with very high activity 93 000  $\text{g}_{\text{C}_2\text{H}_4}/(\text{g}_{\text{Ni.h}})$ .<sup>[137]</sup> Other modifications on Grubbs original catalyst led to bis NO chelate-type **50**, which, activated by EASC, dimerises ethylene into butenes with activities up to 49 000  $\text{g}_{\text{C}_2\text{H}_4}/(\text{g}_{\text{Ni.h}})$ .<sup>[138]</sup>



Catalyst **51** developed by Braunstein *et al* has a bimetallic structure *via* bridging Cl with hexacoordinated nickel. Activated by 6 eq. of EADC it produces mostly 1-butene with an activity of 83 000  $\text{g}_{\text{C}_2\text{H}_4}/(\text{g}_{\text{Ni.h}})$ .<sup>[139,140]</sup>

## 2.3 Tridentate ligands

Tridentate ligands have also been used with the potential advantage of offering an even wider diversity of nickel based catalysts. One strategy consists of introducing an additional donor group on bidentate ligands. Tridentate ligands favour new types of geometries with a coordination number of 5 (trigonal pyramidal, square pyramidal).



Carpentier *et al.* developed nickel tridentates **52** with different central atoms (NNN, NON, NSN). Activated by MAO, the catalytic systems oligomerise ethylene with very high activities ( $60\,000 \text{ g}_{\text{C}_2\text{H}_4}/(\text{g}_{\text{Ni}}\cdot\text{h})$ ) producing exclusively butenes of which 87% is 1-butene. NSN complexes are more active than NNN or NON complexes but they also produce larger amounts of internal olefins.<sup>[141]</sup> 2-quinoxaliny-6-iminopyridines-based nickel complexes, reported by the group of Sun and activated by EADC, gave dimers and trimers with high activity ( $32\,000 \text{ g}_{\text{C}_2\text{H}_4}/(\text{g}_{\text{Ni}}\cdot\text{h})$ ).<sup>[142]</sup> Tetradentates have not been used in the field of nickel oligomerisation.

## 3 Supramolecular catalysis

### 3.1 From Nature to supramolecular catalysis

Enzymes are maybe the most beautiful example of the supramolecular catalysts in Nature. They are linear assemblies of aminoacids (primary structure) that fold by weak interactions to adopt a three dimensional structure containing an active site (secondary and tertiary structures). In the course of the catalytic reaction, there is a molecular recognition between the substrate and the enzyme's active site leading to very quick and selective chemical transformations.

The key to the high activity and selectivity is the geometry of the binding pocket in which the substrate is accommodated by host-guest interactions. This complementarity has been a source of inspiration for chemists who created different techniques at the molecular level to confine molecules in space (e.g. cages and capsules as in Figure 14) leading to higher selectivity compared to traditional non-confined systems.<sup>[143–151]</sup> More recently, based on a molecular recognition and the use

of co-factors, the ligand that is binding to the metal also pre-organises polar substrates inside the cavity, leading to highly selective transformations (DIMPhos as an example in Figure 15)<sup>[152–154]</sup>

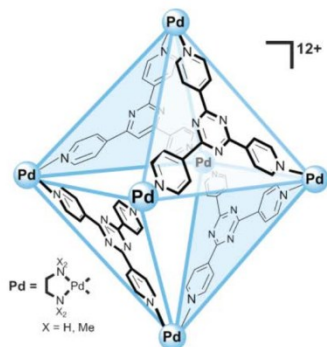


**Figure 14.** Octahedral  $M_6L_4$  cage developed by the group of Fujita<sup>[150,151]</sup> used in the Diels-Alders condensation<sup>[155]</sup> or olefins photodimerisation<sup>[156]</sup> (from Reek *et al.*)<sup>[143]</sup>

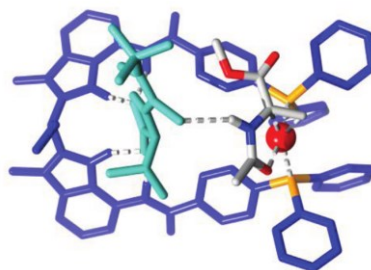


**Figure 15.** Molecular modeling of DIMPhos (dark blue) accommodating a co-factor (light blue) and Methyl 2-acetamidoacrylate from Dydio *et al.*<sup>[152]</sup>

Supramolecular catalysis was introduced as a new approach to design catalysts and in particular, creating supramolecular bidentate ligands.<sup>[157–159]</sup> Indeed, starting from two monodentate ligands, it is possible to create a supramolecular bidentate assembly as depicted in Figure 16. This system with a flexible weak interaction in its backbone differs from traditional bidentate ligands having a rigid backbone such as BINAP, DIOP, DIPAMP, JOSIPHOS or XANTPHOS among others. Moreover, the synthesis of diphosphine ligands, which was long and tedious, is achieved more simply just by mixing two monophosphine building blocks.

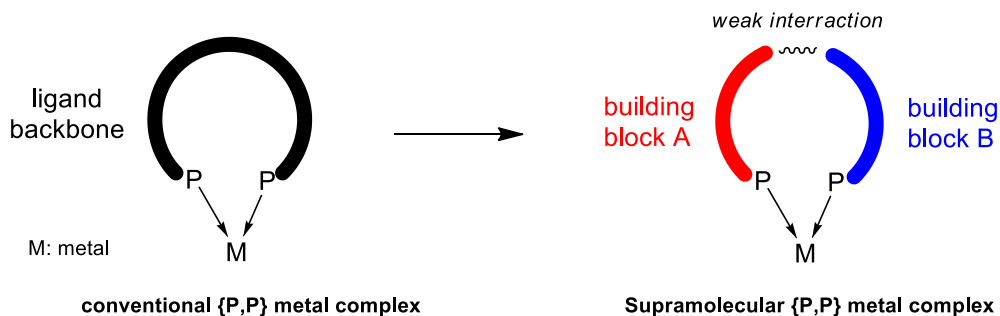


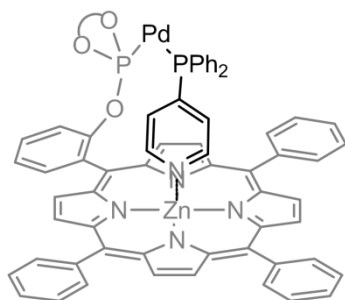
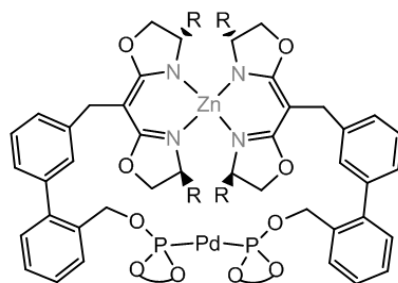
**Figure 16.** From conventional to supramolecular bidentate ligands and associated complexes



In the rest of this Chapter, we will focus on bidentate supramolecular ligands and we will explore the different type of supramolecular interactions used to pre-organise the different building blocks.

### 3.2 Ligand metal interaction

In traditional catalysis metals are the active site. In supramolecular chemistry they are also used for the assembly process. Generally, the metal is anchored to one building block and does not interact with the active (P,P) binding site. From this principle, Reek *et al.* developed SUPRAPhos **54**, a new bidentate supramolecular assembly of a Zn-porphyrin functionalised by a phosphorus atom and a pyridine-phosphine. The weak interaction takes place between the Zn atom (from the porphyrin) and the pyridine moiety.<sup>[160]</sup> The selective formation of this assembly lies in a stronger affinity of the Zn-porphyrins for N atoms than for phosphorus. On the same principle Takacs *et al.* reported the Pd complex **55** performing allylic amination with good yields and selectivity.<sup>[161]</sup>

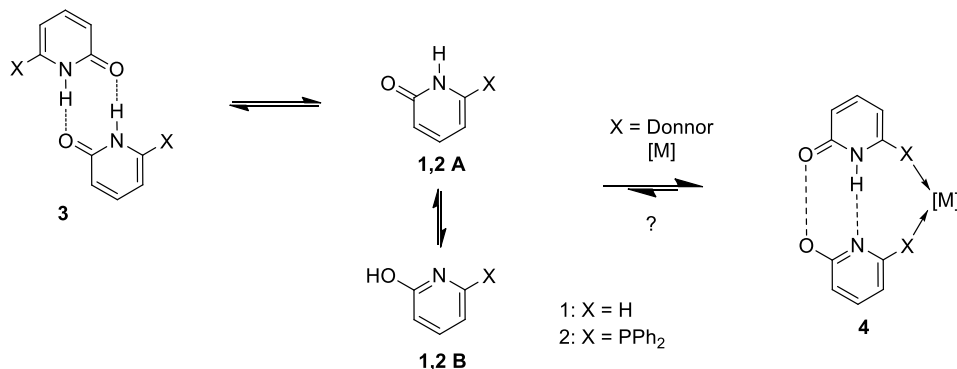
**54****55**

The power of this approach has been demonstrated by the preparation of a library of 20 building blocks based on the porphyrins and 20 building blocks with a pyridyl, leading to a library of 400 supramolecular bidentate ligands. Preparation and screening different catalysts is therefore much easier and faster than with traditional catalysts.<sup>[162–164]</sup> Metal ligand interaction are also used to create tree dimensional cages in which the substrate is encapsulated and reacts with unprecedented yield and selectivity.<sup>[143]</sup>

### 3.3 Hydrogen bond interaction

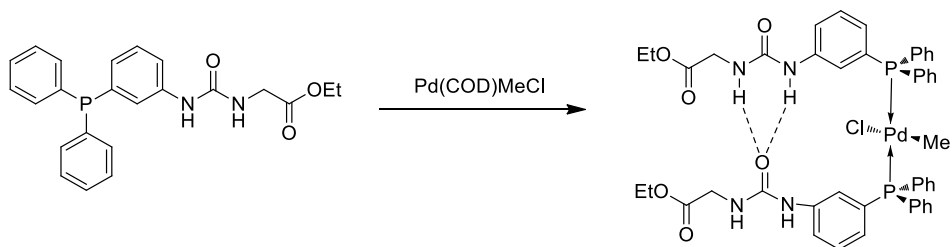
Hydrogen bonding is a powerful tool for the construction of bidentate P,P ligands. The use of H-bond in catalysis was initiated by B. Breit *et al.* who developed complementary ligands based on DNA bases pairs Adenine-Thymine such as 6-

diphenylphosphanyl-2-pyridone (6-DPPON, see Scheme 18), which in the presence of a metal rearrange to form two hydrogen bonds.<sup>[165]</sup> This chemistry requires most of the time the use of non-coordinating and aprotic solvents to favour H-bonds between the constituents.



**Scheme 18.** The two tautomeric forms of the 6-diphenylphosphanyl-2-pyridone (6-DPPON) and metal-induced rearrangement to a diposphine supramolecular complex. The weak interaction consists of two hydrogen bonds: OH...O and NH...N which resembles DNA complementary bases (adenine-thymine, cytosine-guanine)

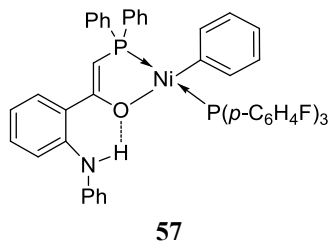
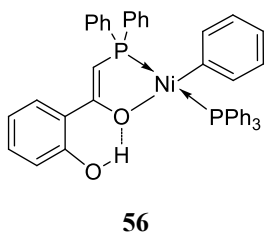
This work has been extended to new classes of donor/ acceptor ligands and libraries of ligands have been generated and studied in hydroformylation and hydrogenation of alkenes.<sup>[166,167]</sup> Some of these assemblies are even stable in protic conditions.<sup>[168]</sup> Interestingly, nickel ( $\text{Ni}(\text{COD})_2$ ) has been used in these systems to perform alkene hydrocyanation.<sup>[169]</sup> On the same strategy, the group of Reek developed UREAPhos ligands that give rhodium complexes that are active and selective in asymmetric hydrogenation.<sup>[170–173]</sup> These systems are based on a hydrogen-bond interaction between the carbonyl of the urea (H acceptor) and the two NH of the urea (H-donors) as seen in Scheme 19.



**Scheme 19.** Synthesis of UREAPhos Pd complex by using the complementarity between two urea moieties.

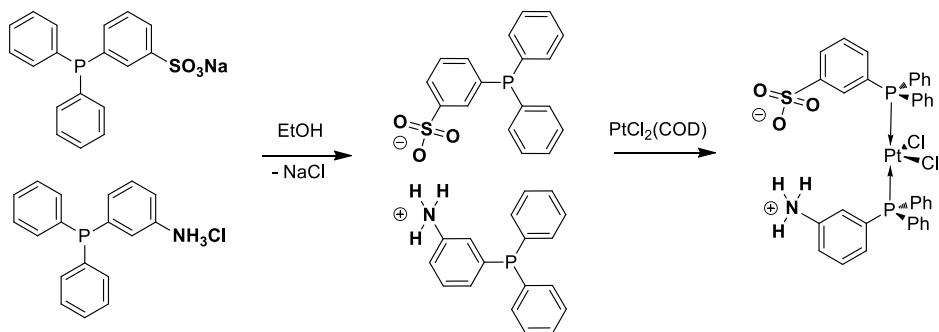
The same group developed the METAMORPhos ligand which exists in two different tautomeric forms, which will be discussed further in detail in this thesis.

The hydrogen bond, which is a structure element in a supramolecular approach, was also reported in the domain of nickel-catalysed ethylene oligomerisation. Mercier *et al.*, based on SHOP catalysts, developed systems that lower the electron-density at the nickel in **56** and **57**, by means of an intramolecular H-bond. This results in a shift of the olefin distribution towards shorter linear alpha olefins.<sup>[42,174]</sup>



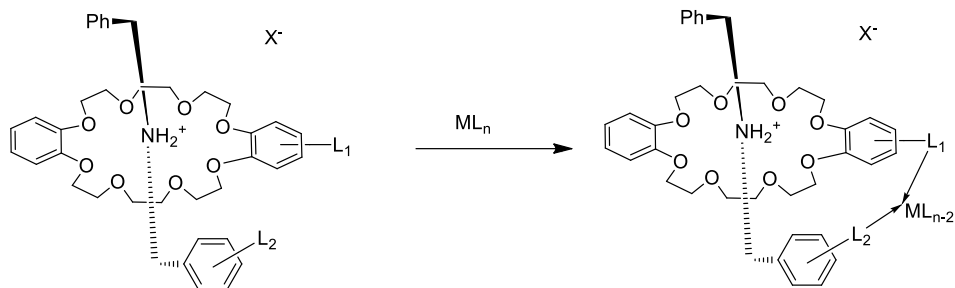
### 3.4 Ionic interaction

Ionic interactions are used as a tool to join two ligand building blocks in a supramolecular way. The most common strategy consists of the creation of an ion pair. For example monosulphonated triphenylphosphine sodium salt and 3-(diphenylphosphanyl)anilide hydrochloride are reported to react together (Scheme 20) with  $[\text{PtCl}_2(\text{COD})]$  to form a supramolecular complex.<sup>[175,176]</sup>



**Scheme 20.** Creation of an ionic interaction between a sodium sulphonate and an amine hydrochloride moieties resulting in a bidentate diphosphine ligand.

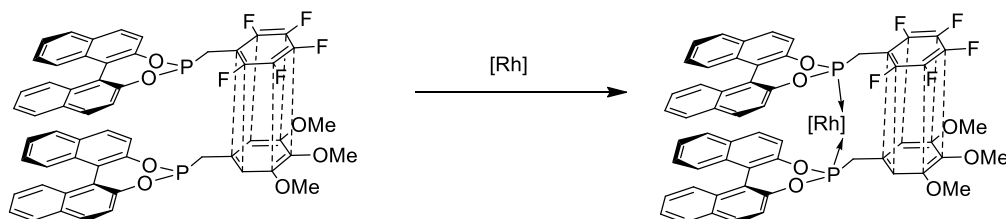
Based on the extensive work in the area of rotaxanes, a bidentate (or tridentate) supramolecular ligand (Scheme 21) was based on two molecules that are interlocked. These complexes were also used in asymmetric hydrogenation with rhodium.<sup>[177,178]</sup>



**Scheme 21.** Interlocked moieties that form a metallic supramolecular assembly (from Hattori *et al.*).<sup>[177]</sup>

### 3.5 Pi stacking interaction

Pi-Pi interactions have also been used to assemble two ligand building blocks. This type of electronic interaction relies on dipole-dipole interactions (Van der Waals) between an electron-rich motif (anthracene, anisoles), and an electron-deficient substituent (2,4,7-trinitrofluorene-9-one, pentafluorobenzene). The previous motifs have been substituted by phosphorus donor groups which can coordinate to metals (Scheme 22).<sup>[179,180]</sup> However, there is no proof that such type of interaction is sufficiently strong to have effects in catalysis.



**Scheme 22.** Pi-Pi interaction between an electron rich and electron poor group.

## 4 Aim and outline of the thesis

Linear alpha olefins are of significant importance in the chemical and petrochemical industry and they represent a constantly growing market. Several processes have been developed leading to high selectivity in LAO formation, but a central issue still needs to be addressed at both academic and industrial levels: the control of the chain length and therefore the development of catalytic systems that are able to produce selectively 1-butene, 1-hexene, 1-octene.

One of the limitations encountered with most catalysts is the Schulz-Flory distribution obtained that highlight the limited selectivity that can be obtained for the different “light” products LAO (C<sub>4</sub>-C<sub>6</sub>) which are the most demanded on the market.

However, a more limited number of catalysts were successfully used to induce selective dimerisation. Nickel catalysts were not much reported for selective oligomerisation of ethylene. Among bidentate ligands, two types of chelates have emerged: PO anionic ligands such as used in the SHOP process or the N,N diimine ligands, both being very robust and transposable to industrial scale or pilot plants. Substituting these non-selective systems to selective ones represent a strong challenge.

By using a supramolecular strategy we aimed to construct supramolecular bidentate complexes by the assembly of two monodentate ligands connected by a hydrogen bond, as shown in Figure 17. Although this approach has been successfully used for transition metals such as Rh, Pd and Pt, research on nickel is limited to one example *in situ* that described the application of these complexes to the hydrocyanation of alkenes.<sup>[181]</sup>

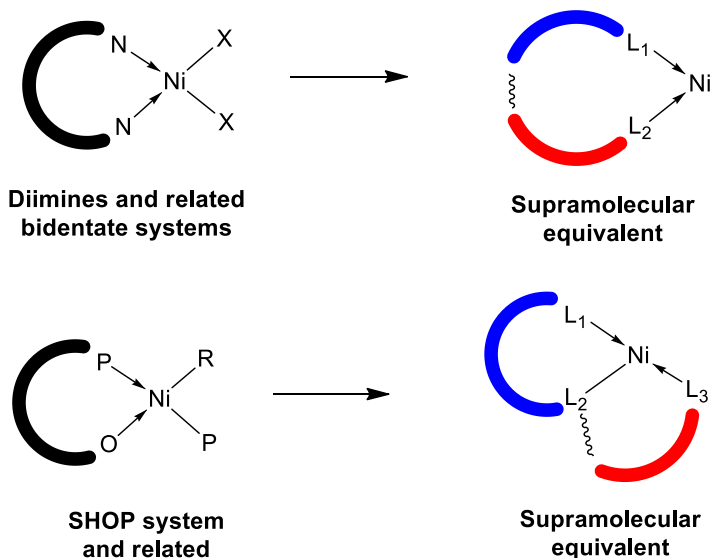


**Figure 17.** Nickel oligomerisation precatalysts and their possible supramolecular equivalents. The wavy bond indicates a supramolecular interaction.

Recently, Reek's group reported a supramolecular rhodium complex (Figure 18, bottom right) bearing two METAMORPhos ligands in close interaction by means of a hydrogen bond. Besides being supramolecular, this complex has a particular chelation mode (PO anionic ligand + phosphine), which is similar to the structure of the SHOP nickel catalyst used industrially for olefin production (Figure 18, top left). We therefore expected that the combination of METAMORPhos ligands with nickel complexes would form active systems for olefin oligomerisation.

We hypothesised that the presence of a hydrogen bond in PO-chelated nickel complexes would lower the electron density of the coordinating O of the PO chelate and would, in the case of nickel complexes, favour the  $\beta$ -elimination step over the propagation leading to shorter carbon chains (C<sub>4</sub>-C<sub>8</sub>). In a nickel system based on METAMORPhos ligands, the strength of the intermolecular hydrogen bond and thus the electron density on the oxygen atom can easily be tuned by modifying one or both ligands (see work of Mercier *et al.* and Figure 18, top right).<sup>[42,58,174]</sup>

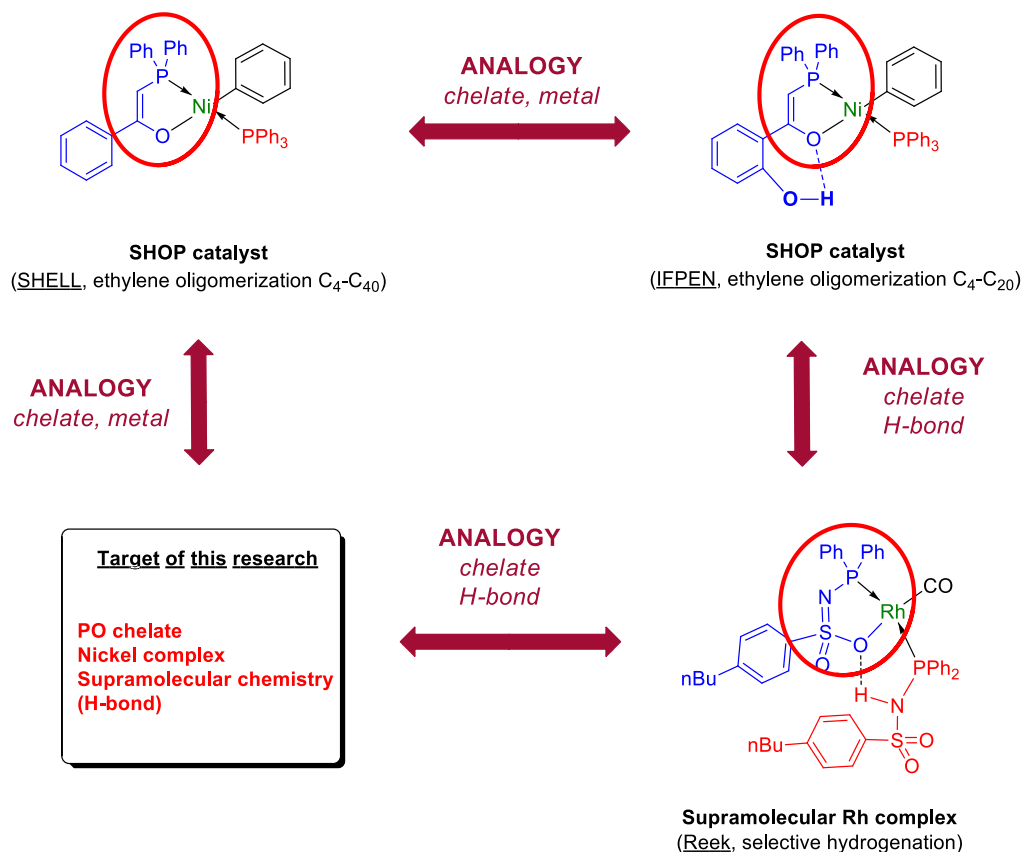


**Figure 18.** Analogy between a supramolecular Rh complex and SHOP Ni catalyst.

Apart from the hydrogen bond, SHOP type catalysts are tuneable by substituents at different positions offering a wide diversity of complexes for employment in catalytic reactions. Heinicke *et al.*<sup>[123]</sup> reported that increasing the basicity of the labile PR<sub>3</sub> phosphine (and consequently its ability to coordinate to the metal) leads to shorter  $\alpha$ -olefins, and a decrease of the activity. They explained this observation by a potential competition between ethylene and the phosphine. The substrate coordination is suggested to favour the propagation and the chain growth, while the

phosphine coordination would favour the  $\beta$ -elimination step and the chain termination. Matt *et al.*<sup>[98]</sup> also proposed that the chain termination involves a  $\beta$ -hydrogen transfer to the coordinated olefin of an 18-electron species. Additionally, the extra ligand is necessary to avoid deactivation of the catalyst by disproportionation, leading to the formation of the inactive bis(PO) chelate.

The positive effect expected using the aminophosphine ligands is the use of the dynamic character of supramolecular assemblies. As mentioned above the distribution in LAO is related to the coordination ability of the phosphine. With the additional hydrogen bond interaction between the phosphorus ligand and the chelate, being in the range of 2-10 kcal/mol, we put forward the hypothesis that the presence of this hydrogen bond strengthens the coordination ability of the additional ligand favouring the formation of short oligomers.

This concept of pre-organised supramolecular assemblies can be extended to discover new classes of ligands. Several ligands formed by cheap and versatile building blocks such as phosphinamide, hydroxyphosphine, aminopyridine or amidopyridine can be used for this purpose.

In this thesis we explore in Chapter 2 the synthesis of a library of phosphorus ligands with H-acceptor and H-donor moieties and in particular the synthesis of amidophosphines and sulphonamide phosphorus ligands (METAMORPhos). Several METAMORPhos ligands that exist as a mixture of tautomers (PH or NH), with diverse electronic and steric properties have been isolated and characterised by NMR. We also report how the tautomeric equilibrium is influenced by the substituents on the nitrogen and the phosphorus atoms. A side “self-condensation” reaction was identified, that converts METAMORPhos ligands into iminobisphosphines (bis-addition product). The rate of this transformation could be reduced and even suppressed by choosing suitable substituents on the phosphorus. Some nickel complexes of these ligands have been studied by NMR and X-Ray diffraction.

In Chapter 3, we employ iminobisphosphines, which serendipitously formed as by-product, and were used as ligands. We could prepare symmetrical and non-symmetrical ligands of general formula  $R^1-N=P(R^2)_2-P(R^3)_2$  with good yields. In the presence of  $NiBr_2(DME)$  the ligands rearranged to PNP complexes of general formula  $(R^2)_2P-NR_1-P(R^3)_2, NiX_2$ . This rearrangement is likely due to the P-P bond cleavage caused by the  $NiBr_2(DME)$ . The complexes were evaluated in ethylene oligomerisation activated by MAO. They display a high productivity, and an unusual product distribution of butenes along with oligomers ( $C_6$  and  $C_{8+}$ ). The complexes also possess a good activity for propylene oligomerisation producing mainly dimers

and more specifically 2,3-dimethylbutenes when basic phosphines were used. Moreover the rearrangement was applied to chromium ethylene oligomerisation aiming to feature the PNP ligands developed by Sasol.

In Chapter 4 we report the synthesis and detailed characterisation of stable zwitterionic nickel complexes supported by supramolecular bidentate ligands based on sulphonamido-phosphorus and aminophosphine ligands. This novel class of complexes appears to be highly active and selective as catalysts for ethylene oligomerisation with up to 84 wt.% of 1-butene. This high selectivity for short linear alpha olefins is interesting considering the change in the market demand towards such products. *In situ* NMR experiments under ethylene pressure show the rearrangement of these structures to the proposed monoanionic P,O-P nickel complex as the resting state, a stable supramolecular pincer complex that could explain the specific properties displayed by the catalyst.

In Chapter 5 we identified that the electron density on the aminophosphine is the determining factor leading to the formation of stable nickel zwitterionic cationic heterocomplexes. The introduction of more conventional unsubstituted phosphines in the place of aminophosphines indicates that there is a threshold in the phosphine basicity above which complex formation occurs. Moreover there is a steric control in complex formation: phosphines with limited steric bulk lead to the formation of zwitterionic complexes whereas bulky phosphines lead to *trans*-(PO,P) nickel hydride complexes. A mechanism to account for the formation of both related complexes is proposed.

In Chapter 6, the catalytic performances of zwitterionic cationic nickel complexes and nickel hydride complexes were evaluated in the ethylene oligomerisation reaction. Both systems are active, either producing selectively 1-butene or a distribution of higher molecular weight oligomers. According to ethylene high-pressure NMR experiments, cationic zwitterionic and nickel hydride complexes both react under ethylene leading to the same proposed active species. The catalytic activity and selectivity of the nickel complexes were correlated to the electronic parameters of the complexes allowing fine-tuning of the catalytic system.

## 5 References

- [1] W. M. Haynes, D. R. Lide, *CRC Handbook of Chemistry and Physics, 93rd Edition*, Taylor & Francis, **2012**.
- [2] N. N. Greenwood, A. Earnshaw, in *Chem. Elem.* (Ed.: Elsevier), **1980**, pp. 1144–1172.
- [3] K. Lascelles, L. G. Morgan, D. Nicholls, in *Ullmann's Encycl. Ind. Chem.*, Wiley-VCH Verlag GmbH & Co. KGaA, **2000**.



- [4] D. N. Nakamura, *Oil Gas J.* **2007**, July 16th, 46.
- [5] *Oil Gas J.* **2008**, July 28th, 46.
- [6] W. R. True, *Oil Gas J.* **2011**, April 7th.
- [7] S. D. Ittel, L. K. Johnson, M. Brookhart, *Chem. Rev.* **2000**, *100*, 1169–204.
- [8] J. Gromada, J.-F. Carpentier, A. Mortreux, *Coord. Chem. Rev.* **2004**, 397–410.
- [9] B. Cornils, W. A. Herrmann, in *Appl. Homog. Catal. with Organomet. Compd.*, Wiley-VCH Verlag GmbH, **2008**, pp. 213–385.
- [10] G. R. Lappin, in *Alpha Olefin. Appl. Handb.* (Eds.: G.R. Lappin, J.D. Sauer), **1992**, pp. 35–61.
- [11] A. M. Al-Jarallah, J. A. Anabtawi, M. A. Siddiqui, A. M. Aitani, A. W. Al-Sa'doun, *Catal. Today* **1992**, *14*, 1–124.
- [12] K. Ziegler, H. G. Gellert, E. Holzkamp, G. Wilke, *Brennst. -Chem* **1954**, *35*, 321.
- [13] K. Ziegler, *Brennst. -Chem* **1952**, *35*, 193.
- [14] in *Hydrocarb. Process.*, Gulf Publishing Company Ed., Houston, TX, **2010**, p. 147.
- [15] A. Forestière, H. Olivier-Bourbigou, L. Saussine, *Oil Gas Sci. Technol.* **2009**, *64*, 649–667.
- [16] P. W. N. M. van Leeuwen, in *Homog. Catal. Underst. Art.*, Dordrecht, **2004**, pp. 175–190.
- [17] Y. Chauvin, D. Commereuc, F. Hugues, H. Olivier-Bourbigou, L. Saussine, *Catalysts for the Production of Light Alpha Olefins by Oligomerization of Ethylene*, **1996**, U.S. Patent US5496783.
- [18] D. Commereuc, Y. Glaize, F. Hugues, L. Saussine, *Method of Production of Improved Purity Light Alpha Olefins by Oligomerisation of Ethylene*, **1998**, U.S. Patent US5811619A.
- [19] G. Moussali, H. Bölt, P. M. Fritz, P. E. Matkovskii, P. S. Chekry, V. N. Melnikov, *No Title*, **1995**, U.S. Patent DE4338416C1.
- [20] N. Le Quan, D. Cruyepelink, D. Commereuc, Y. Chauvin, G. Léger, *Process for the Synthesis of Butene-1 by Dimerisation of Ethylene*, **1986**, U.S. Patent EP0135441B1.
- [21] W. K. Reagan, J. W. Freeman, B. K. Conroy, T. M. Pettijohn, E. A. Benham, *Process for the Preparation of a Catalyst for Olefin Polymerization*, **2001**, U.S. Patent EP0608447B1.
- [22] J. Freeman, T. Pettijohn, W. Reagan, *Process of Trimerizing and Oligomerizing Olefins Using Chromium Compounds*, **1996**, U.S. Patent US5523507.
- [23] H. Olivier-Bourbigou, A. Forestière, L. Saussine, L. Magna, F. Favre, F. Hugues, *Oil Gas- Eur. Mag.* **2010**, *36*, 97–102.
- [24] R. Whyman, *Piet W. N. M. Van Leeuwen. Homogeneous Catalysis—understanding the Art.*, John Wiley & Sons, Ltd., Dordrecht, **2004**.
- [25] D. Commereuc, S. Drochon, L. Saussine, *Catalytic Composition and Process for the Oligomerisation of Ethylene, to Primarily 1-Hexene*, **2003**, U.S. Patent EP1110930B1.
- [26] D. Commereuc, S. Drochon, L. Saussine, *Catalytic Composition and Process for Oligomerising Ethylene in Particular to 1-Butene And/or 1-Hexene*, **2000**, U.S. Patent US006031145A.
- [27] J. T. Dixon, D. H. Morgan, H. Maumela, P. Nongodlwana, J. A. Willemse, *Two Stage Activation of Oligomerisation Catalyst and Oligomerization of Olefinic Compounds in the Presence of an Oligomerisation Catalyst so Activated*, **2008**, U.S. Patent WO2008/146215 A1.
- [28] A. Bollmann, K. Blann, J. T. Dixon, F. M. Hess, E. Killian, H. Maumela, D. S. McGuinness, D. H. Morgan, A. Neveling, S. Otto, et al., *J. Am. Chem. Soc.* **2004**, *126*, 14712–14713.
- [29] G. Nowlin, G. Burnie, H. D. Lyons, *Process and Catalyst for Polymerization of Olefins*, **1961**, U.S. Patent US 2969408 A.

- [30] G. Wilke, B. Bogdanovic, P. Hardt, P. Heimbach, W. Keim, M. Kröner, W. Oberkirch, K. Tanaka, E. Steinrücke, D. Walter, et al., *Angew. Chem., Int. Ed.* **1966**, *5*, 151–266.
- [31] M. Uchino, Y. Chauvin, G. Lefebvre, *C. R. Acad. Sc. Paris* **1967**, *265/2*, 103–106.
- [32] H. Sato, H. Tojima, K. Ikimi, *J. Mol. Catal. A* **1999**, *144*, 285–293.
- [33] Y. Chauvin, B. Gilbert, I. Guibard, *J. Chem. Soc., Chem. Commun.* **1990**, 1715–1716.
- [34] Y. Chauvin, S. Einloft, H. Olivier Bourbigou, *Ind. Eng. Chem. Res.* **1995**, *34*, 1149–1155.
- [35] B. Gilbert, H. Olivier-Bourbigou, F. Favre, *Oil Gas Sci. Technol.* **2007**, *62*, 745–759.
- [36] C. Carlini, M. Marchionna, A. M. Raspolli Galletti, G. Sbrana, *Appl. Catal. A* **2001**, *206*, 1–12.
- [37] C. Carlini, M. Marchionna, A. Raspolli Galletti, *J. Mol. Catal. A* **2001**, *169*, 79–88.
- [38] U. Müller, W. Keim, C. Krüger, P. Betz, *Angew. Chem., Int. Ed.* **1989**, *28*, 1011–1013.
- [39] W. Keim, F. H. Kowaldt, R. Goddard, C. Krüger, *Angew. Chem., Int. Ed.* **1978**, *17*, 466–467.
- [40] W. Keim, A. Behr, B. Gruber, B. Hoffmann, F. H. Kowaldt, U. Kürschner, B. Limbacher, F. P. Sistic, *Organometallics* **1986**, *5*, 2356–2359.
- [41] K. Alexander Ostoja Starzewski, L. Born, *Organometallics* **1992**, *11*, 2701–2704.
- [42] P. Braunstein, Y. Chauvin, S. Mercier, L. Saussine, A. De Cian, J. Fischer, *Chem. Commun.* **1994**, *332*, 2203.
- [43] S. Mecking, *Coord. Chem. Rev.* **2000**, *203*, 325–351.
- [44] B. J. Chatt, B. L. Shaw, *J. Chem. Soc.* **1960**, 1718–1729.
- [45] M. Wada, K. Oguro, Y. Kawasaki, *J. Organomet. Chem.* **1979**, *178*, 261–271.
- [46] J. M. Coronas, G. Muller, M. Rocamora, C. Miravittles, X. Solans, *J. Chem. Soc., Dalt. Trans.* **1985**, 2333–2341.
- [47] M. Hidai, T. Kashiwagi, T. Ikeuchi, Y. Uchida, *J. Organomet. Chem.* **1971**, *30*, 279–282.
- [48] R. Ma Ceder, J. Cubillo, G. Muller, M. Rocamora, J. Sales, *J. Organomet. Chem.* **1992**, *429*, 391–401.
- [49] R. S. Bauer, H. Chung, P. W. Glockner, W. Keim, *Ethylene Oligomerization*, **1972**, U.S. Patent US3644563.
- [50] J. Heinicke, M. Koesling, R. Brüll, W. Keim, H. Pritzkow, *Eur. J. Inorg. Chem.* **2000**, *2000*, 299–305.
- [51] S. Y. Desjardins, K. J. Cavell, H. Jin, B. W. Skelton, A. H. White, *J. Organomet. Chem.* **1996**, *515*, 233–243.
- [52] R. M. Bellabarba, P. T. Gomes, S. I. Pascu, *Dalt. Trans.* **2003**, *2*, 4431–4436.
- [53] W. Zhao, Y. Qian, J. Huang, J. Duan, *J. Organomet. Chem.* **2004**, *689*, 2614–2623.
- [54] D. G. Yakhvarov, D. I. Tazeev, O. G. Sinyashin, G. Giambastiani, C. Bianchini, A. M. Segarra, P. Lönnecke, E. Hey-Hawkins, *Polyhedron* **2006**, *25*, 1607–1612.
- [55] P. Braunstein, J. Pietsch, Y. Chauvin, A. DeCian, J. Fischer, *J. Organomet. Chem.* **1997**, 387–393.
- [56] J. Pietsch, P. Braunstein, Y. Chauvin, *New J. Chem.* **1998**, *22*, 467–472.
- [57] D. V. Gutsulyak, A. L. Gott, W. E. Piers, M. Parvez, *Organometallics* **2013**, *32*, 3363–3370.
- [58] P. Braunstein, J. Pietsch, Y. Chauvin, S. Mercier, L. Saussine, A. DeCian, J. Fischer, *Dalt. Trans.* **1996**, 3571–3574.
- [59] U. Klabunde, S. D. Ittel, *J. Mol. Catal.* **1987**, *41*, 123–134.
- [60] G. Wilke, *Angew. Chem., Int. Ed.* **1988**, *27*, 185–206.

- [61] U. Birkenstock, H. Bönnermann, B. Bogdanovic, D. Walter, G. Wilke, in *Homog. Catal.*, The American Chemical Society, **1974**, pp. 13–250.
- [62] M. Bonnet, F. Dahan, A. Ecke, W. Keim, R. P. Schulz, I. Tkatchenko, *Chem. Commun.* **1994**, 055, 615–616.
- [63] B. Bogdanovic, *Adv. Organomet. Chem.* **1979**, 17, 105–140.
- [64] R. Pardy, I. Tkatchenko, *Chem. Commun.* **1981**, 49–50.
- [65] B. Bogdanovic, B. Henc, H. Karmann, *Ind. Eng. Chem. Res.* **1963**, 62, 34–44.
- [66] W. Keim, *New J. Chem.* **1987**, 11, 531–534.
- [67] W. Keim, R.-P. Schulz, *J. Mol. Catal.* **1994**, 92, 21–33.
- [68] D. Matt, M. Huhn, J. Fischer, A. De Cian, W. Kläui, I. Tkatchenko, M. C. Bonnet, *Dalt. Trans.* **1993**, 1173–1778.
- [69] R. F. De Souza, R. S. Mauler, L. C. Simon, F. F. Nunes, D. V. S. Vescia, A. Cavagnoli, *Macromol. Rapid Commun.* **1997**, 18, 795–800.
- [70] L. K. Johnson, C. M. Killian, M. Brookhart, *J. Am. Chem. Soc.* **1995**, 117, 6414–6415.
- [71] F. M. Bauers, S. Mecking, *Macromolecules* **2001**, 34, 1165–1171.
- [72] J. Heinicke, M. He, A. Dal, H.-F. Klein, O. Hetche, W. Keim, U. Flörke, H.-J. Haupt, *Eur. J. Inorg. Chem* **2000**, 2000, 431–440.
- [73] E. Kogut, A. Zeller, T. H. Warren, T. Strassner, *J. Am. Chem. Soc.* **2004**, 126, 11984–11994.
- [74] H. L. Wiencko, E. Kogut, T. H. Warren, *Inorganica Chim. Acta* **2003**, 345, 199–208.
- [75] P. Cossee, *J. Catal.* **1964**, 38, 80–88.
- [76] J. Arlman, P. Cossee, *J. Catal.* **1964**, 104, 99–104.
- [77] J. Arlman, *J. Catal.* **1964**, 98, 89–98.
- [78] M. Peuckert, W. Keim, *Organometallics* **1983**, 2, 594–597.
- [79] H. Luo, D. Li, *Appl. Organomet. Chem.* **2000**, 389–393.
- [80] W. Keim, B. Hoffmann, R. Lodewick, M. Peuckert, G. Schmitt, J. Fleischhauer, U. Meier, *J. Mol. Catal.* **1979**, 6, 79–97.
- [81] S. R. Bauer, H. Chung, P. Glockner, W. Keim, H. van Zwet, *Ethylene Polymerization*, **1972**, U.S. Patent US3635937.
- [82] J. Heinicke, M. Köhler, N. Peulecke, M. He, M. K. Kindermann, W. Keim, G. Fink, *Chem. Eur. J.* **2003**, 9, 6093–107.
- [83] O. Kühl, P. Lobitz, N. Peulecke, *Phosphorus, Sulfur, Silicon Relat. Elem.* **2011**, 37–41.
- [84] L. Lavanant, A.-S. Rodrigues, E. Kirillov, J.-F. Carpentier, R. F. Jordan, *Organometallics* **2008**, 27, 2107–2117.
- [85] R. F. Mason, *Alpha-Olefin Production*, **1972**, U.S. Patent US3686351.
- [86] E. F. Lutz, P. A. Gautier, *Ethylene Oligomerization Process Carried out in a Diol-Based Solvent Containing Monohydric Alcohol or Water*, **1989**, U.S. Patent EP0177999.
- [87] W. M. Alley, I. K. Hamdemir, Q. Wang, A. I. Frenkel, L. Li, J. C. Yang, L. D. Menard, R. G. Nuzzo, S. Ozkar, K. Yih, et al., *Langmuir* **2011**, 27, 6279–6294.
- [88] F. Peruch, H. Cramail, A. Deffieux, *Macromolecules* **1999**, 32, 7977–7983.
- [89] C. G. de Souza, R. F. de Souza, K. Bernardo-Gusmão, *Appl. Catal. A Gen.* **2007**, 325, 87–90.
- [90] C. M. Killian, L. K. Johnson, M. Brookhart, *Organometallics* **1997**, 16, 2005–2007.
- [91] S. A. Svejda, M. Brookhart, *Organometallics* **1999**, 18, 65–74.

- [92] H. Sinn, W. Kaminsky, H.-J. Vollmer, R. Woldt, *Angew. Chem., Int. Ed.* **1980**, 390–392.
- [93] F. Speiser, P. Braunstein, L. Saussine, *Acc. Chem. Res.* **2005**, *38*, 784–793.
- [94] J. Yu, X. Hu, Y. Zeng, L. Zhang, C. Ni, X. Hao, W.-H. Sun, *New J. Chem.* **2011**, *35*, 178.
- [95] S. Jie, D. Zhang, T. Zhang, W.-H. Sun, J. Chen, Q. Ren, D. Liu, G. Zheng, W. Chen, *J. Organomet. Chem.* **2005**, *690*, 1739–1749.
- [96] X. Tang, W.-H. Sun, T. Gao, J. Hou, J. Chen, W. Chen, *J. Organomet. Chem.* **2005**, *690*, 1570–1580.
- [97] P. J. Flory, *J. Am. Chem. Soc.* **1936**, *58*, 1877–1885.
- [98] P. Kuhn, D. Sémeril, D. Matt, M. J. Chetcuti, P. Lutz, *Dalt. Trans.* **2007**, 515–528.
- [99] P. Kuhn, D. Sémeril, C. Jeunesse, D. Matt, M. Neuburger, A. Mota, *Chem. Eur. J.* **2006**, *12*, 5210–5219.
- [100] S. Mukherjee, B. A. Patel, S. Bhaduri, *Organometallics* **2009**, 3074–3078.
- [101] J. T. Dixon, M. J. Green, F. M. Hess, D. H. Morgan, *J. Organomet. Chem.* **2004**, *689*, 3641–3668.
- [102] R. H. Grubbs, A. Miyashita, M. I. M. Liu, P. L. Burk, *J. Am. Chem. Soc.* **1977**, *99*, 3863–3864.
- [103] R. H. Grubbs, A. Miyashita, *J. Am. Chem. Soc.* **1978**, *100*, 7416–7418.
- [104] F. Bernardi, A. Bottoni, I. Rossi, *J. Am. Chem. Soc.* **1998**, *7863*, 7770–7775.
- [105] M. Dötterl, H. G. Alt, *ChemCatChem* **2011**, *3*, 1799–1804.
- [106] M. Dötterl, P. Thoma, H. G. Alt, *Adv. Synth. Catal.* **2012**, *354*, 389–398.
- [107] M. Dötterl, H. G. Alt, *ChemCatChem* **2012**, *4*, 370–378.
- [108] L. Bonneviot, D. Olivier, M. Che, *EP Pat.* 0,089,895 **1983**.
- [109] F. X. Cai, C. Lepetit, M. Kermarec, D. Olivier, *J. Mol. Catal. A* **1987**, *43*, 93–116.
- [110] H. Go, M. Akihisa, *Chem. Ind.* **1967**, *22*, 921–922.
- [111] M. Aresta, C. Nobile, A. Sacco, *Inorganica Chim. Acta* **1975**, *12*, 167–178.
- [112] H. Kenai, *Chem. Commun.* **1972**, 203–204.
- [113] B. Corain, M. Bressan, P. Rigo, A. Turco, *Chem. Commun.* **1968**, 509–510.
- [114] V. V. Saraev, P. B. Kraikivskii, D. A. Matveev, A. S. Kuzakov, A. I. Vil’ms, A. A. Fedonina, *Russ. J. Coord. Chem.* **2008**, *34*, 438–442.
- [115] S. C. Srivastava, M. Bigorgne, *J. Organomet. Chem.* **1969**, *18*, 30–32.
- [116] V. Saraev, P. Kraikivskii, S. N. Zelinskii, A. I. Vil’ms, D. A. Matveev, A. Y. Yunda, A. A. Fedonina, K. Lammertsma, *Russ. J. Coord. Chem.* **2006**, *32*, 397–401.
- [117] V. V. Saraev, P. B. Kraikivskii, D. a. Matveev, S. N. Zelinskii, K. Lammertsma, *Inorganica Chim. Acta* **2006**, *359*, 2314–2320.
- [118] R. Beck, M. Shoshani, J. Krasinkiewicz, J. A. Hatnean, S. A. Johnson, *Dalton Trans.* **2013**, *42*, 1461–75.
- [119] S. J. Schofer, M. W. Day, L. M. Henling, J. A. Labinger, J. E. Bercaw, *J. Am. Chem. Soc.* **2006**, *25*, 2743–2749.
- [120] V. Saraev, P. Kraikivskii, V. V. Annenkov, S. N. Zelinskii, D. A. Matveev, A. I. Vilms, E. N. Danilovtseva, K. Lammertsma, *Arkivoc* **2005**, *2005*, 44–52.
- [121] W. Keim, *Angew. Chem., Int. Ed.* **1990**, *29*, 235–244.
- [122] K. Hirose, W. Keim, *J. Mol. Catal.* **1992**, *1992*, 271–276.
- [123] J. Heinicke, M. Köhler, N. Peulecke, W. Keim, *J. Catal.* **2004**, *225*, 16–23.

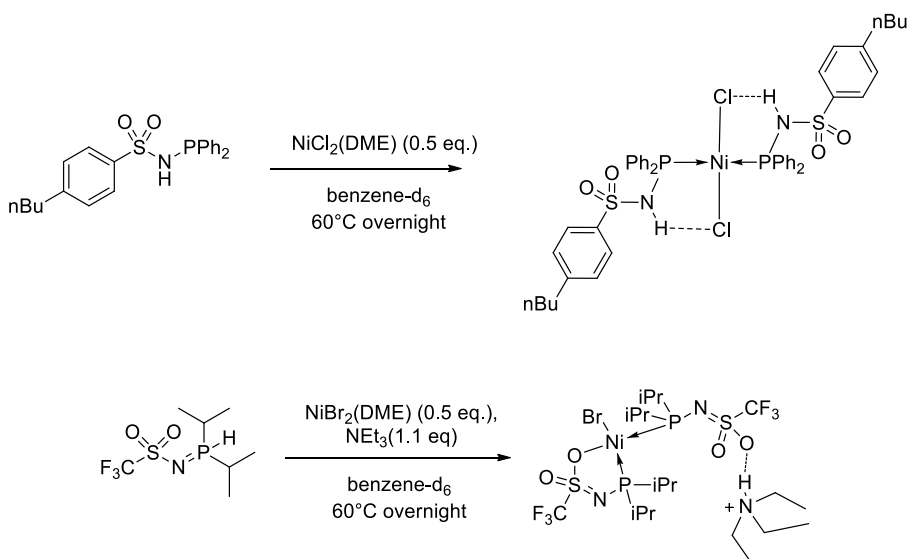
- [124] Y. Kawaragi, Y. Nalajima, *Dimerization of Olefins*, **1996**, U.S. Patent JP09268132 A2.
- [125] L. K. Johnson, S. Mecking, M. Brookhart, *J. Am. Chem. Soc.* **1996**, 267–268.
- [126] X. Hou, T. Liang, W.-H. Sun, C. Redshaw, X. Chen, *J. Org. Chem.* **2012**, 708–709, 98–105.
- [127] M. Sauthier, F. Leca, R. Fernando de Souza, K. Bernardo-Gusmão, L. F. Trevisan Queiroz, L. Toupet, R. Réau, *New J. Chem.* **2002**, 26, 630–635.
- [128] J. N. L. Dennett, A. L. Gillon, K. Heslop, D. J. Hyett, J. S. Fleming, C. E. Lloyd-Jones, A. G. Orpen, P. G. Pringle, D. F. Wass, J. N. Scutt, et al., *Organometallics* **2004**, 23, 6077–6079.
- [129] C. Bianchini, L. Gonsalvi, W. Oberhauser, D. Sémeril, P. Brüggeller, R. Gutmann, *Dalt. Trans.* **2003**, 3869–3875.
- [130] I. Albers, E. Álvarez, J. Cámpora, C. M. Maya, P. Palma, L. J. Sánchez, E. Passaglia, *J. Organomet. Chem.* **2004**, 689, 833–839.
- [131] K. Song, H. Gao, F. Liu, J. Pan, L. Guo, S. Zai, Q. Wu, *Eur. J. Inorg. Chem.* **2009**, 2009, 3016–3024.
- [132] Z. Guan, W. Marshall, *Organometallics* **2002**, 3580–3586.
- [133] J. Flapper, H. Kooijman, M. Lutz, A. L. Spek, P. W. N. M. van Leeuwen, C. J. Elsevier, P. C. J. Kamer, *Organometallics* **2009**, 1180–1192.
- [134] W. Keim, *J. Mol. Catal.* **1989**, 52, 19–25.
- [135] A. Kermagoret, P. Braunstein, *Dalt. Trans.* **2008**, 33, 822–831.
- [136] T. R. Younkin, *Science (80- )*. **2000**, 287, 460–462.
- [137] Y. Chen, G. Wu, G. C. Bazan, *Angew. Chem., Int. Ed.* **2005**, 44, 1108–1112.
- [138] Z. Zhou, X. Hao, C. Redshaw, L. Chen, W.-H. Sun, *Catal. Sci. Technol.* **2012**, 2, 1340–1345.
- [139] A. Kermagoret, P. Braunstein, *Dalt. Trans.* **2008**, 32, 1564–1573.
- [140] F. Speiser, P. Braunstein, L. Saussine, R. Welter, *Inorg. Chem.* **2004**, 43, 1649–1658.
- [141] N. Ajellal, M. C. a. Kuhn, A. D. G. Boff, M. Hörner, C. M. Thomas, J.-F. Carpentier, O. L. Casagrande, *Organometallics* **2006**, 25, 1213–1216.
- [142] S. Adewuyi, G. Li, S. Zhang, W. Wang, P. Hao, W.-H. Sun, N. Tang, J. Yi, *J. Organomet. Chem.* **2007**, 692, 3532–3541.
- [143] T. S. Koblenz, J. Wassenaar, J. N. H. Reek, *Chem. Soc. Rev.* **2008**, 37, 247–262.
- [144] J. Patriceon, F. Hapiot, M. Canipelle, S. Menuel, E. Monflier, *Organometallics* **2010**, 29, 6668–6674.
- [145] F. Hapiot, S. Tilloy, E. Monflier, *Chem. Rev.* **2006**, 106, 767–781.
- [146] C. Machut, J. Patriceon, S. Tilloy, H. Bricout, F. Hapiot, E. Monflier, *Angew. Chem., Int. Ed.* **2007**, 46, 3040–3042.
- [147] M. Raynal, P. Ballester, A. Vidal-Ferran, P. W. N. M. van Leeuwen, *Chem. Soc. Rev.* **2014**, 43, 1660–1733.
- [148] V. F. Slagt, P. C. J. Kamer, P. W. N. M. van Leeuwen, J. N. H. Reek, *J. Am. Chem. Soc.* **2004**, 126, 1526–36.
- [149] M. D. Pluth, R. G. Bergman, K. N. Raymond, *Science (80- )*. **2007**, 316, 85–8.
- [150] M. Fujita, K. Umemoto, M. Yoshizawa, N. Fujita, T. Kusukawa, K. Biradha, *Chem. Commun.* **2001**, 509–518.
- [151] M. Fujita, M. Tominaga, A. Hori, B. Therrien, *Acc. Chem. Res.* **2005**, 38, 369–378.
- [152] P. Dydio, C. Rubay, T. Gadzikwa, M. Lutz, J. N. H. Reek, *J. Am. Chem. Soc.* **2011**, 133, 17176–17179.

- [153] P. Dydio, R. J. Detz, B. de Bruin, J. N. H. Reek, *J. Am. Chem. Soc.* **2014**, *136*, 8418–8429.
- [154] P. Dydio, R. J. Detz, J. N. H. Reek, *J. Am. Chem. Soc.* **2013**, *135*, 10817–10828.
- [155] M. Yoshizawa, M. Tamura, M. Fujita, *Science (80-. )*. **2006**, *312*, 251–254.
- [156] M. Yoshizawa, Y. Takeyama, T. Kusakawa, M. Fujita, *Angew. Chem., Int. Ed.* **2002**, 1347–1349.
- [157] A. J. Sandee, J. N. H. Reek, *Dalton Trans.* **2006**, 3385–91.
- [158] J. Meeuwissen, J. N. H. Reek, *Nat. Chem.* **2010**, *2*, 615–621.
- [159] B. Breit, W. Seiche, *Angew. Chem., Int. Ed.* **2005**, *44*, 1640–3.
- [160] J. N. H. Reek, M. Röder, P. E. Goudriaan, P. C. J. Kamer, P. W. N. M. van Leeuwen, V. F. Slagt, *Organometallics* **2004**, *126*, 4505–4516.
- [161] J. M. Takacs, D. Reddy Sahadeva, S. A. Moteki, D. Wu, H. Palencia, *J. Am. Chem. Soc.* **2004**, *126*, 4494–4495.
- [162] J. N. H. Reek, M. Röder, P. E. Goudriaan, P. C. J. Kamer, P. W. N. M. van Leeuwen, V. F. Slagt, *J. Organomet. Chem.* **2005**, *690*, 4505–4516.
- [163] X.-B. Jiang, L. Lefort, P. E. Goudriaan, A. H. M. de Vries, P. W. N. M. van Leeuwen, J. G. de Vries, J. N. H. Reek, *Angew. Chem., Int. Ed.* **2006**, *45*, 1223–1227.
- [164] P. E. Goudriaan, X.-B. Jang, M. Kuil, R. Lemmens, P. W. N. M. Van Leeuwen, J. N. H. Reek, *Eur. J. Org. Chem.* **2008**, *2008*, 6079–6092.
- [165] B. Breit, W. Seiche, *J. Am. Chem. Soc.* **2003**, *125*, 6608–6609.
- [166] B. Breit, W. Seiche, *Pure Appl. Chem* **2006**, *78*, 249–256.
- [167] B. Breit, M. Weis, C. Waloch, W. Seiche, *J. Am. Chem. Soc.* **2006**, *128*, 4188–4189.
- [168] C. Waloch, J. Wieland, M. Keller, B. Breit, *Angew. Chem., Int. Ed.* **2007**, *46*, 3037–3039.
- [169] M. de Greef, B. Breit, *Angew. Chem., Int. Ed.* **2009**, *48*, 551–554.
- [170] A. J. Sandee, A. M. van der Burg, J. N. H. Reek, *Chem. Commun.* **2007**, *2*, 864–866.
- [171] L. K. Knight, Z. Freixa, P. W. N. M. Van Leeuwen, J. N. H. Reek, *Organometallics* **2006**, *25*, 954–960.
- [172] J. Meeuwissen, M. Kuil, A. M. van der Burg, A. J. Sandee, J. N. H. Reek, *Chem. Eur. J.* **2009**, *15*, 10272–10279.
- [173] J. Meeuwissen, R. J. Detz, A. J. Sandee, B. de Bruin, M. A. Siegler, A. L. Spek, J. N. H. Reek, *Eur. J. Inorg. Chem.* **2010**, *2010*, 2992–2997.
- [174] P. Braunstein, Y. Chauvin, S. Mercier, L. Saussine, *C. R. Chim.* **2005**, *8*, 31–38.
- [175] H. Gulyás, J. Benet-Buchholz, E. C. Escudero-Adan, Z. Freixa, P. W. N. M. Van Leeuwen, *Chem. Eur. J.* **2007**, *13*, 3424–3430.
- [176] L. Pignataro, B. Lynikaite, J. Cvengroš, M. Marchini, U. Piarulli, C. Gennari, *Eur. J. Org. Chem.* **2009**, *2009*, 2539–2547.
- [177] G. Hattori, T. Hori, Y. Miyake, Y. Nishibayashi, *J. Am. Chem. Soc.* **2007**, *129*, 12930–12931.
- [178] Y. Li, Y. Feng, Y.-M. He, F. Chen, J. Pan, Q.-H. Fan, *Tetrahedron Lett.* **2008**, *49*, 2878–2881.
- [179] B. Lynikaite, U. Piarulli, C. Gennari, J. Cvengros, *Tetrahedron Lett.* **2008**, *49*, 755–759.
- [180] O. Chuzel, C. Magnier-Bouvier, E. Schulz, *Tetrahedron: Asymmetry* **2008**, *19*, 1010–1019.
- [181] B. Breit, W. Seiche, *Angew. Chem., Int. Ed.* **2005**, *44*, 1640–1643.



# Chapter 2

## Synthesis of Sulphonamido-Based Phosphorus Ligands and their Coordination to Nickel

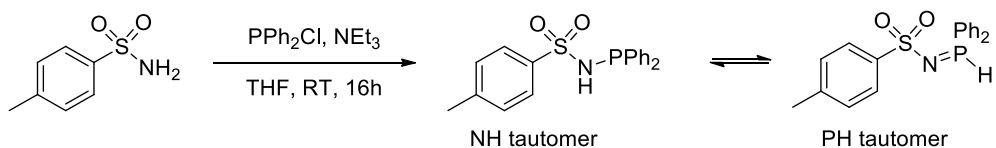




# 1 Introduction

The access to a diverse set of functionalised phosphorus ligands is of prime interest in the field of homogeneous catalysis as they allow the generation of easily tunable coordination complexes through self-assembly *via* the functional groups or by formation of chelate coordination complexes. Recently, sulphonamido based phosphorus compounds were introduced as a new class of ligands.<sup>[1]</sup> This ligand motif can coordinate by a number of different manners around the metal centre, (i.e. monodentate (P),<sup>[1-3]</sup> bidentate (P,O),<sup>[1,3-5]</sup> in neutral (PO)<sup>[3,5]</sup> or in anionic fashion (PO<sup>-</sup>, PN<sup>-</sup>)<sup>[1,3-7]</sup> to a single metal or bridging between metal centres<sup>[6,7]</sup> giving access to diverse set of complexes with only few ligands. The coordination behaviour of these ligands was notably described with Rh, Ir, Ru and besides, it was successfully used to construct supramolecular systems through hydrogen bonding.<sup>[3,4]</sup> Sulphonamido phosphorus-based ligands, known as METAMORPhos, exist in two tautomeric forms: a NH form with trivalent phosphorus and a PH form with pentavalent phosphorus as shown in Scheme 1.<sup>[1,8]</sup>

The synthesis of METAMORPhos ligands involves the mono addition of a chlorophosphine on a sulphonamide in the presence of a base (Scheme 1). It is a nucleophilic substitution reaction in which the sulphonamide attacks the chlorophosphine and releases a chlorine atom (leaving group) to form HCl, which is captured by the base (NEt<sub>3</sub>). The synthesis is generally performed in THF or diethyl ether to separate the triethylammonium salt from the organic compounds.



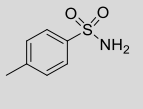
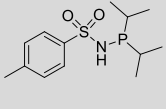
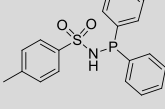
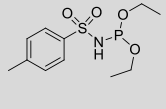
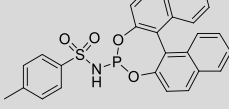
**Scheme 1.** Synthesis of METAMORPhos ligands from a sulphonamide and a chlorophosphine with NEt<sub>3</sub>.

Sulphonamides are weak acids with pKa values around 10 (see Table 1 and experimental part) and their acidity may be modulated by the introduction of electron withdrawing groups at the sulphur as -CF<sub>3</sub> (pKa = 6.4). Introducing electron withdrawing phosphine groups, such as P(1,1'-bi(2-naphtol)) (P(Binol)) to the METAMORPhos structures, results in an increase of overall acidity shifting the pKa from 9.2 to 3.8 (Table 2).

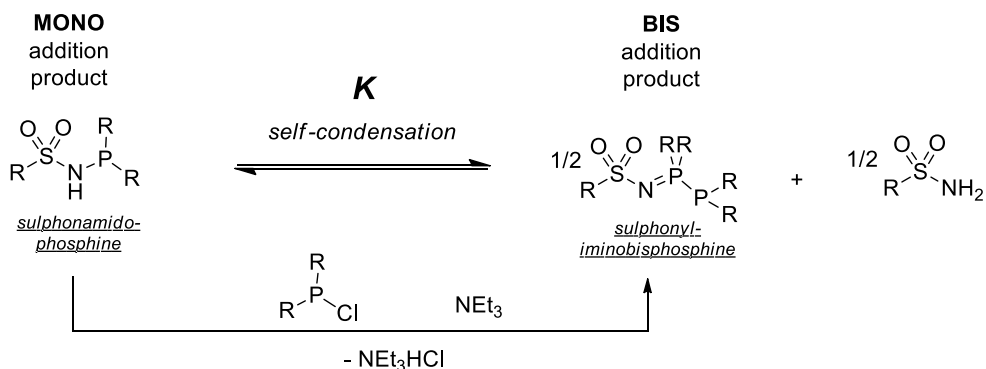
**Table 1.** Calculated pKa values of common sulphonamides R-SO<sub>2</sub>-NH<sub>2</sub> (first acidity) –from SciFinder.

R=	Ph	4-Me-Ph	4-nBu-Ph	4-MeO-Ph	4-Br-Ph	Me	CF <sub>3</sub>
pKa	10.1±0.1	10.2±0.1	10.2±0.2	10.3±0.1	9.9±0.1	10.9±0.6	6.4±0.6

**Table 2.** Calculated pKa values of some phosphorus N-substituted sulphonamides (METAMORPhos) – from SciFinder.

				
10.2±0.1	9.2±0.4	6.8±0.4	6.1±0.4	3.8±0.2

The decrease of pKa of mono-substituted sulphonamides is expected to lead to competitive formation of mono- and bis-addition of chlorophosphine on the sulphonamide when triethylamine is used as base during the reaction ( $pK_a = 10.6 \pm 0.2$ ). Initial studies by Reek and co-workers already indicated that the bis-addition product can form in this reaction, as a side or as the main product.<sup>[4]</sup> This competitive addition had also been previously reported by the group of Foss *et al.* who studied the reaction of primary alkylamines and tosylamide with chlorophosphines.<sup>[9]</sup> They suggested that the competitive addition was in fact the result of two independent reactions as depicted in Scheme 2. The first reaction involves the bis-addition of chlorophosphine on the mono-substituted product, in line with increased nucleophilicity of the mono-addition product (Table 2). The second reaction is a disproportionation equilibrium (“self-condensation”), that is an equilibrium between the mono-addition product and the bis-addition product plus sulphonamide. The same group also established that tosylamides stabilise the bis-addition product under the iminobisphosphines ( $-N=P-P$ ).<sup>[10]</sup>


**Scheme 2.** Side reactions affecting sulphonamido-phosphines: bis addition and self-condensation equilibrium.

In this Chapter we describe the reinvestigation of the synthesis of METAMORPhos ligands by a comprehensive study of the reaction between sulphonamides and chlorophosphines. Based on phosphorus NMR, the formation of METAMORPhos and the by-products was established from the crude mixtures. Also it was possible to

determine the state of the tautomeric equilibrium in solution between the NH and the PH forms. The results from the condensation reactions (mono or di-substitution products, PH or NH tautomers) allowed the identification of the drivers that account for by-product formation but also the relative stability of the tautomeric forms of the ligands. Preliminary coordination studies of METAMORPhos with nickel(II) precursors revealed several possible coordination modes. The reactivity of sulphonamido-phosphine ligands was also transposed to Ni(0) with the aim to generate organometallic nickel species. For this purpose, sulphonyl-iminophosphoranes were introduced as promising pre-ligands for the formation of PO-chelated organometallic nickel complexes.

## 2 Synthesis and characterisation of tautomeric ligands

The reaction between several sulphonamides and chlorophosphines was explored (Scheme 1), using in all reactions triethylamine as a base. The course of the reaction (products formation) was monitored by unlocked  $^{31}\text{P}$  NMR.<sup>[11–13]</sup> This non-destructive technique is a precious asset to get information on the composition of the mixture. From these experiments the change in ratio between the PCl signal (indicative chemical shifts in Table 3) and that of the products was established and used as a measure for the reaction progress.

**Table 3.** Indicative  $^{31}\text{P}$  chemical shifts for some common chlorophosphines.

	$\text{PPh}_2\text{Cl}$	$\text{P}(i\text{Pr})_2\text{Cl}$	$\text{P}(t\text{Bu})_2\text{Cl}$	$\text{P}(o\text{-tolyl})_2\text{Cl}$	$\text{P}(\text{Binol})\text{Cl}$	$\text{PEt}_2\text{Cl}$	$\text{PCy}_2\text{Cl}$
$\delta(\text{ppm})$	81	133	146	67	179	118	128

Recording unlocked  $^{31}\text{P}\{^1\text{H}\}$  and  $^{31}\text{P}$  NMR allowed to discriminate systems leading to mono-addition, bis-addition or a combination of both. Unlocked NMR easily evidences the tautomer equilibrium PH/NH since the two tautomers display distinct chemical shifts in  $^{31}\text{P}\{^1\text{H}\}$  NMR where they appear as singlets.<sup>[11]</sup> Both tautomers can be distinguished by proton-coupled phosphorus NMR ( $^{31}\text{P}$  NMR) as shown in Figure 1. The PH tautomer has a covalent bond between the phosphorus and the proton leading to large  $^1J_{\text{PH}}$  coupling (around 490 Hz) in the phosphorus NMR spectrum. The coupling for the NH tautomer is much smaller (ca. 7 Hz). Similarly, the tautomers also appear distinctly in the  $^1\text{H}$  NMR spectra as two independent signals. In a phosphorus-decoupled proton NMR ( $^1\text{H}\{^{31}\text{P}\}$  NMR), both tautomers appear as singlets while in phosphorus-coupled proton NMR ( $^1\text{H}$  NMR) the PH proton appears as a doublet with a large coupling identical to that observed in  $^{31}\text{P}$  NMR. The NH proton splits also but with a much smaller constant. In these NMR experiments, iminobisphosphines, the bis-addition products, were also identified as two doublets

exhibiting  $^1J_{PP}$  couplings around 350 Hz. A quick and comprehensive mixture analysis based on  $^{31}\text{P}\{^1\text{H}\}$  NMR,  $^{31}\text{P}$  NMR and  $^1\text{H}$  analyses is displayed in Table 4.

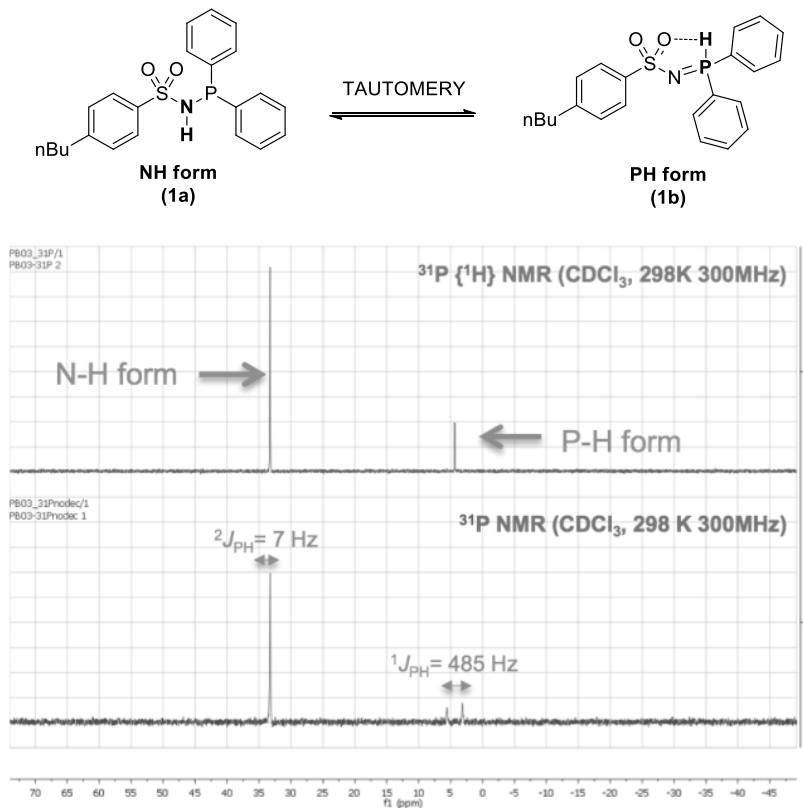


**Figure 1.** Tautomeric equilibrium of METAMORPhos ligand and corresponding pattern in  $^{31}\text{P}$  NMR.

**Table 4.** Determination grid based on NMR for products stemming from chlorophosphine and sulphonamides in presence of  $\text{NEt}_3$ .

		$^{31}\text{P}\{^1\text{H}\}$	$^{31}\text{P}$	$^1\text{H}\{^{31}\text{P}\}$	$^1\text{H}$
<b>MONO</b>	N-H form	singlet	doublet ( $^2J_{PH}$ ca. 7 Hz)	singlet	singlet
	P-H form	singlet	doublet ( $^1J_{PH}$ ca. 480 Hz)	singlet	doublet ( $J_{HP}$ ca. 480 Hz)
<b>BIS (by-product)</b>		2 doublets	2 doublets	no acidic proton	

The reaction involved the dropwise addition of chlorophosphine (1 eq.) to a mixture of sulphonamide (1 eq.) with excess of triethylamine (2.6 eq.) in THF at room temperature. Almost all condensation reactions leading to **1-20** were quick as all the starting material (according to the disappearance of the chlorophosphine) had reacted after 10 minutes at room temperature. Yet, the use of phenyl sulphonamide to form

ligands **6** and **13** resulted in low conversion. The very bulky di-tert-butylchlorophosphine took much longer to react with sulphonamides (**15** and **17**) and refluxing the mixture was necessary to obtain full conversion.

The qualitative results at full conversion based on unlocked NMR, are presented in Table 5. Under the applied reaction conditions (see Footnote Table 5), ligands **1** and **2** containing the electron withdrawing and bulky P(Binol) resulted both in selective formation of METAMORPhos. Carrying out the condensation reaction with diphenylchlorophosphine led to the partial formation of iminobisphosphine by-product along with ligands **3-7** (bis-addition product < 50%). However, increasing the steric bulk from phenyl to *o*-tolyl led to selective formation of the mono-addition product **8**. Switching to alkyl phosphines with low steric bulk -P(Et)<sub>2</sub> (Entries **9** and **10**) resulted both in the formation of the bis-addition product (quantitative for **10**). In contrast, the products **11-14** with the more bulky -P(*i*Pr)<sub>2</sub> were obtained with the bis-addition side-product in much smaller quantity (< 10%). The even bulkier -PCy<sub>2</sub> and -P(*t*Bu)<sub>2</sub> resulted in selective formation of the sulphonamidophosphine **15-20**.

The pKa values described in Table 2 show that all the METAMORPhos ligands, regardless of the ligand substituents, have pKa values lower than the sulphonamide. This suggests that whatever the substituents is at the phosphorus, the formation of the bis addition product is favoured. This suggests also that the discrimination between mono or bis addition only relies on the steric hindrance at the phosphorus. The more bulky ligands all resulted in cleaner reactions, suggesting that the side reaction to form the iminobisphosphine is suppressed by steric hindrance at the phosphorus, in line with the observations of groups of Rossknecht<sup>[14]</sup> and Foss.<sup>[9]</sup>

Since the scope of available METAMORPhos ligands is limited to very bulky analogues we sought to optimise the reaction conditions to facilitate the extension of the ligand synthesis to less bulky ligand, including diphenylphosphine-based METAMORPhos. For this purpose, the challenging reaction of CH<sub>3</sub>-SO<sub>2</sub>-NH<sub>2</sub> and PPh<sub>2</sub>Cl that produced equimolar ratio of mono- and bis-addition product (Entry 7) was selected. Increasing the reaction temperature to 60°C led to the same product ratio obtained at RT while performing the experiment at -80°C led first to exclusive iminobisphosphine formation which subsequently equilibrated to the usual mixture obtained at room temperature (ratio mono:bis = 1:1, K = 1). Changing the base ratio (2.6 eq. or 1.0 eq.) did not have impact on the product ratio. Finally, the best results were obtained with butyl-lithium (BuLi) and particularly with in 1:1 combination with TMEDA followed by the addition of the chlorophosphine. This protocol, gave selectively the mono-addition product (peak at 35 ppm) according to the unlocked <sup>31</sup>P NMR of the reaction mixture. However, the product could not be isolated as it

rearranged quickly to the iminobisphosphine upon standing. This rapid rearrangement complies with the self-condensation equilibrium, as described by Foss *et al.*, which also means that the formation of bis-addition product is independent on the mode of preparation.

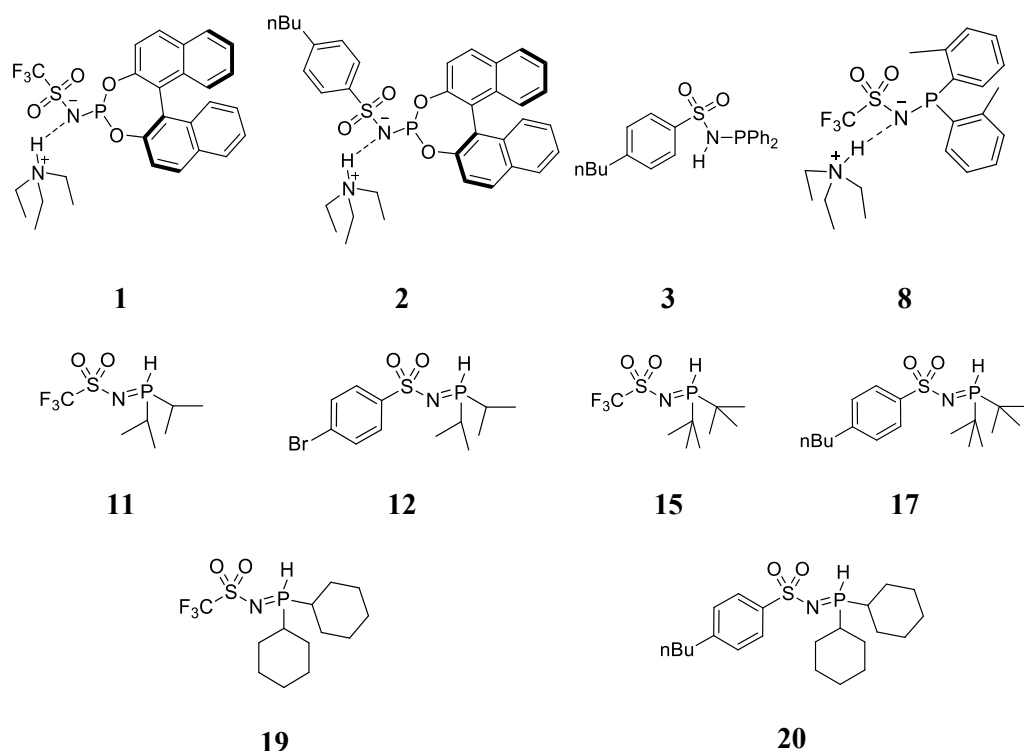
**Table 5.** Condensation of chlorophosphines or chlorophosphites with sulphonamides.

Ligand	Chlorophosphine	Sulphonamide	Product crude	Tautomer <i>in situ</i>	Tautomer isolated
1	P(Binol)Cl	F <sub>3</sub> C-SO <sub>2</sub> NH <sub>2</sub>	mono	NH--NEt <sub>3</sub>	NH--NEt <sub>3</sub>
2	P(Binol)Cl	4- <i>n</i> Bu-Ph-SO <sub>2</sub> NH <sub>2</sub>	mono	NH--NEt <sub>3</sub>	NH--NEt <sub>3</sub>
3	PPh <sub>2</sub> Cl	4- <i>n</i> Bu-Ph-SO <sub>2</sub> NH <sub>2</sub>	mono, bis	NH	NH, PH
4	PPh <sub>2</sub> Cl	F <sub>3</sub> C-SO <sub>2</sub> NH <sub>2</sub>	mono, bis	NH	-
5	PPh <sub>2</sub> Cl	4-Br-Ph-SO <sub>2</sub> NH <sub>2</sub>	bis	-	-
6	PPh <sub>2</sub> Cl	Ph-SO <sub>2</sub> NH <sub>2</sub>	mono, bis	NH	-
7	PPh <sub>2</sub> Cl	H <sub>3</sub> C-SO <sub>2</sub> NH <sub>2</sub>	mono, bis	NH	-
8	P( <i>o</i> -tolyl) <sub>2</sub> Cl	F <sub>3</sub> C-SO <sub>2</sub> NH <sub>2</sub>	mono	NH--NEt <sub>3</sub>	NH--NEt <sub>3</sub>
9	P(Et) <sub>2</sub> Cl	F <sub>3</sub> C-SO <sub>2</sub> NH <sub>2</sub>	mono, bis	NH	-
10	P(Et) <sub>2</sub> Cl	4- <i>n</i> Bu-Ph-SO <sub>2</sub> NH <sub>2</sub>	bis	-	-
11	P( <i>i</i> Pr) <sub>2</sub> Cl	F <sub>3</sub> C-SO <sub>2</sub> NH <sub>2</sub>	mono	(no <sup>1</sup> J <sub>PH</sub> )	PH
12	P( <i>i</i> Pr) <sub>2</sub> Cl	4-Br-Ph-SO <sub>2</sub> NH <sub>2</sub>	mono, bis	PH, NH	PH
13	P( <i>i</i> Pr) <sub>2</sub> Cl	Ph-SO <sub>2</sub> NH <sub>2</sub>	mono, bis	PH	-
14	P( <i>i</i> Pr) <sub>2</sub> Cl	4-MeO-Ph-SO <sub>2</sub> NH <sub>2</sub>	mono, bis	PH	-
15	P( <i>t</i> Bu) <sub>2</sub> Cl	F <sub>3</sub> C-SO <sub>2</sub> NH <sub>2</sub>	mono	(no <sup>1</sup> J <sub>PH</sub> )	PH
16	P( <i>t</i> Bu) <sub>2</sub> Cl	Ph-SO <sub>2</sub> NH <sub>2</sub>	(mono)	PH	-
17	P( <i>t</i> Bu) <sub>2</sub> Cl	4- <i>n</i> Bu-Ph-SO <sub>2</sub> NH <sub>2</sub>	mono	PH	PH
18	P( <i>t</i> Bu) <sub>2</sub> Cl	4-MeO-Ph-SO <sub>2</sub> NH <sub>2</sub>	mono, bis	PH	-
19	PCy <sub>2</sub> Cl	F <sub>3</sub> C-SO <sub>2</sub> NH <sub>2</sub>	mono	PH	PH
20	PCy <sub>2</sub> Cl	4- <i>n</i> Bu-Ph-SO <sub>2</sub> NH <sub>2</sub>	mono	PH	PH

General conditions: Sulphonamide (10 mmol, 1eq.) and triethylamine (26 mmol, 2.6 eq.) dissolved in THF (20 mL), and then chlorophosphine (10 mmol, 1 eq.) is added dropwise to the mixture at RT under vigorous stirring. Reaction time was 16 h, unless completion was noted after unlocked <sup>31</sup>P NMR after 10 min.

Product purification from the crude mixture by chromatography column was not effective due to the self-condensation equilibrium, and also the similar polarity of

some of the components and their sensitivity on basic alumina complicated such purification procedure. Selective precipitation was nonetheless effective to purify crude mixtures containing no more than 30 % iminobisphosphines such as **3** or **12** (DCM / nC<sub>5</sub> or THF / nC<sub>5</sub> 1:3). Finally, ligands with sufficient steric bulk at the phosphorus (**1**, **2**, **8**, **11**, **15**, **17**, **19** and **20**) were easily isolated as pure powders with moderate to excellent yields (up to 92%) on the gram scale. Isolated products are presented in Scheme 3 with their predominant tautomer that was present in solution (from CDCl<sub>3</sub>, C<sub>6</sub>D<sub>6</sub> or CD<sub>2</sub>Cl<sub>2</sub>). The structures of ligands **8** and **11** were confirmed by X-ray diffraction. In the solid state ligand **8** forms a ion pair with triethylamine as shown in Figure 2 (N4--H241 2.063 Å) and a weak interaction with the oxygen of the sulphonamide (O2--H241 2.989 Å). In the solid state, ligand **11** is in the PH tautomeric form, with a short PN bond (1.619 Å). This ligand establishes intermolecular hydrogen bond with another moiety as shown in Figure 3 (O--H bond, 2.477 Å).



**Scheme 3.** Isolated METAMORPhos ligands with predominant tautomer observed in apolar and aprotic organic solvents

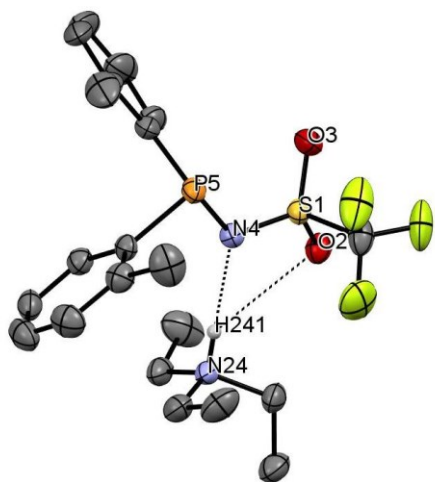


**Figure 2.** ORTEP plot (50% probability displacement ellipsoids) of ligand **8**. Hydrogen atoms have been omitted for clarity (except for  $\text{NEt}_3\text{H}^+$  moiety). Selected bond lengths (Å) and angles ( $^\circ$ ): S1-O2 1.438 (2); S1-O3 1.434 (2); S1-N4 1.541 (2); N4-P5 1.728 (2); S1-N4-P5 117.85 (14); [ion pair geometry: N24-H241 0.893; N4--H241 2.063; O2--H241 2.989; N24-H241-N4 174.51; N24-H241-O2 121.23].

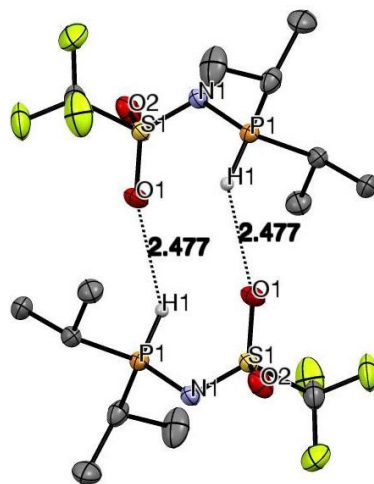


**Figure 3.** ORTEP plot (50% probability displacement ellipsoids) of ligand **11**. Hydrogen atoms have been omitted for clarity (except for PH moiety). Selected bond lengths (Å) and angles ( $^\circ$ ): S1-O1 1.4402(9); S1-O2 1.4316(9); S1-N1 1.5471(9); N1-P1 1.6193(9); P1-H1 1.305(15); S1-N1-P1 124.19(6). [H-bond geometry: P1-H1 1.305(1); H1-O1 2.477(1); P1-O1 3.5799(9); P1-H1-O1 140.4(9)].

The different isolated METAMORPhos ligands displayed in Scheme 3 exhibit different tautomeric ratio's in solution. Ligand **1**, with bulky and electron withdrawing Binol moiety, led to exclusive formation of the NH tautomer and formed an ion pair with triethylamine. By keeping the substitution at S identical ( $-\text{CF}_3$ ) but increasing the donating ability of the phosphorus gave ligand **8** (tolyl) that was also in the NH- $\text{NEt}_3$  tautomer. Going from aryl to alkyl phosphines such as  $-\text{P}(i\text{Pr})_2$ ,  $-\text{P}(t\text{Bu})_2$  or  $-\text{PCy}_2$  (in **11**, **15** or **19**), shifted the tautomer from NH to the PH form. Interestingly, ligand **3** displayed both the NH and the PH tautomer in equilibrium. Again, introducing bulkiness and electron donating property on the phosphino group shifted the equilibrium to the PH tautomer (from **3** to **17** or to **20**). Changing the sulphonamide substituent with the same phosphine moiety (from **1** to **2**, **11** to **12**, **15** to **17** or **19** to **20**) had no visible impact on the tautomer formed, which was always PH. This strongly suggests that the main driver of the tautomeric equilibrium are the electronic properties of the phosphine. METAMORPhos under the NH form are favoured by phosphines substituted by electron withdrawing groups while METAMORPhos under the PH are stabilised by electron donating phosphines, as alkyl phosphines.



As we anticipated to observe tautomeric behaviour similar to METAMORPhos ligands, we prepared four amidophosphines of general formula  $R^1\text{-CO-NH-P}(R^2)_2$  with diverse electronic properties introduced either *via* the carbonyl ( $R^1$ ) or at the phosphorus ( $R^2$ ) (Scheme 4).<sup>[15]</sup> Amidophosphines **21-24** gave rise to three tautomers: NH, OH and PH; NH being the most commonly represented in the literature.<sup>[16]</sup> Amidophosphine **21** with electron withdrawing groups  $R^1 = \text{Ph}$  lead preferentially to the NH form (**21**), while amidophosphines with electron donating groups ( $R^1 = \text{CH}_3$ ) favour the OH tautomer, which is still in equilibrium with the NH tautomer for ligands **22** and **23**. The OH tautomer was never observed so far for METAMORPhos. Also increasing the donating ability of the phosphine from **22** to **23** led to an increase of this OH tautomer (from 32 % to 77%). The tautomer equilibrium is shifted more towards the PH form as for **24** when  $R^1$  and  $R^2$  are electron withdrawing and donating groups, respectively. METAMORPhos ligands **3** (NH/PH) and **11** (PH), display higher proportion of the PH tautomer compared to the analogous amidophosphines **21** (NH) and **24** (NH/PH) as shown in Scheme 4. This shift towards the PH tautomer is also driven by a higher electron withdrawing influence of the sulphonyl group compared to the carbonyl group which certainly also accounts for the absence of the OH tautomer within METAMORPhos.

	<b>NH</b>	NH: 100 % (CD <sub>2</sub> Cl <sub>2</sub> )	<b>21</b>
	<b>NH/OH</b>	NH: 68 % (CD <sub>2</sub> Cl <sub>2</sub> )	<b>22</b>
	<b>NH/OH</b>	NH: 23% (C <sub>6</sub> D <sub>6</sub> )	<b>23</b>
	<b>NH/PH</b>	NH: 69 % (CD <sub>2</sub> Cl <sub>2</sub> )	<b>24</b>
	<b>NH/PH</b>	NH: 86 % (CD <sub>2</sub> Cl <sub>2</sub> )	<b>3</b>
	<b>PH</b>	PH: 100 % (C <sub>6</sub> D <sub>6</sub> )	<b>11</b>

**Scheme 4.** Four amidophosphines and two METAMORPhos ligands with diverse electronic contributions and their corresponding tautomeric forms.

Besides being affected by the electronic properties of the substituents at P and S, the tautomer equilibrium within METAMORPhos is influenced by the presence of a base or by hydrogen bond acceptor moieties, similar to that reported for secondary

phosphine oxides.<sup>[17]</sup> Indeed, there is a difference between the tautomeric ratio from the crude reaction mixture compared to that of the isolated product as can be seen in Table 5, which substantiates the influence of triethylamine. The base, present in excess in the reaction mixtures shifts the equilibrium from the PH to the NH as is observed for ligands **3** and **12**.

Since the PH and NH tautomers for METAMORPhos originate all from the delocalised P-N-S-O fragment we expected that they would display a pKa in a close range that would be detectable by a single NMR titration of METAMORPhos by a base (Figures 4 and 5). Triethylamine was chosen as a weak base to ensure that it would not deprotonate the ligand. Upon increasing the base concentration in a CDCl<sub>3</sub> solution of ligand **11**, the PH doublet in <sup>1</sup>H NMR became broader and its intensity decreased (Figure 4).

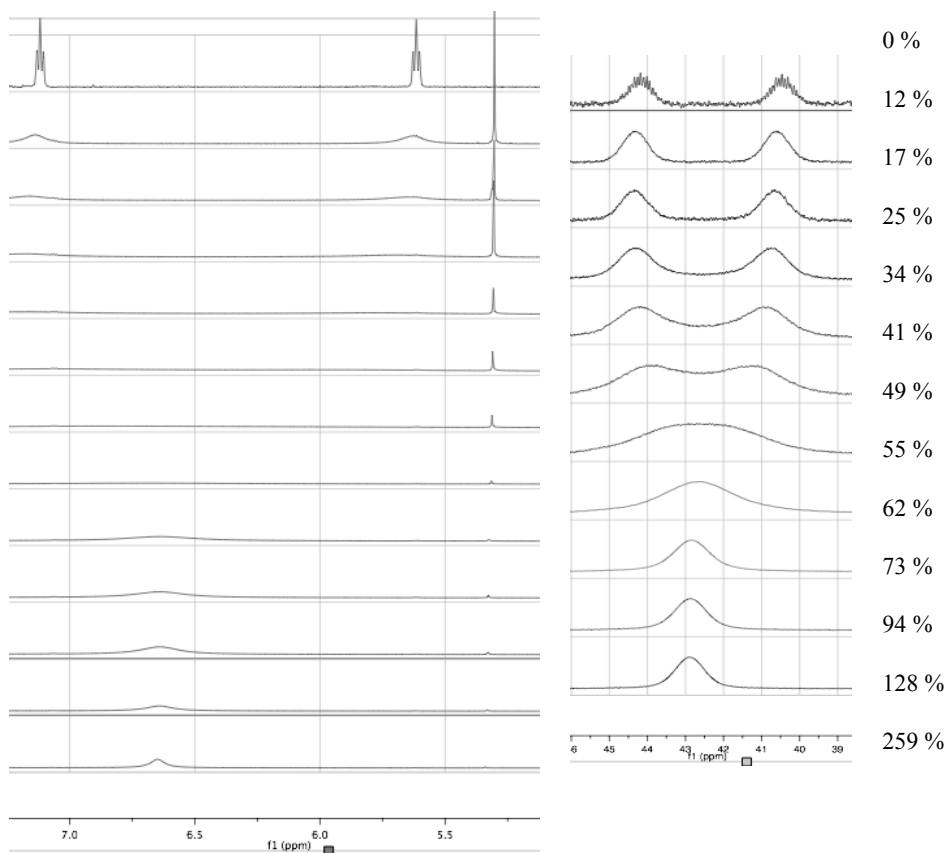


**Figure 4.** Titration of ligand **11** by NEt<sub>3</sub> – <sup>1</sup>H NMR study (CDCl<sub>3</sub>, relative intensity and chemical shifts corrected on the basis of *iPr* signals with no NEt<sub>3</sub> in CDCl<sub>3</sub>, initial ligand concentration= 0.1 M).

**Figure 5.** Titration of ligand **11** by NEt<sub>3</sub> – <sup>31</sup>P NMR study (CDCl<sub>3</sub>).Initial, ligand concentration: 0.1 M.

A new sharp peak progressively formed at  $\delta(\text{CDCl}_3)$ : 5.28 ppm which was maximal around 20 mol% of triethylamine and decreased upon further increasing the  $\text{NEt}_3$  concentration. Finally when the base concentration increased above 62% a very broad peak around  $\delta(\text{CDCl}_3)$ : 6.80 ppm appeared, which was the major product even at the highest  $\text{NEt}_3$  concentration (260 mol%). There was no trace of triethylammonium proton in the 8-10 ppm range, which suggests that this is more an interaction than a full deprotonation. In parallel to the proton spectrum, the PH signals in  $^{31}\text{P}$  NMR became broader with triethylamine increasing and merged into one central peak around 50 mol% of  $\text{NEt}_3$  (Figure 5). This suggests that triethylamine shifted the original tautomer equilibrium, for which the main form is PH, in favour of other tautomers. However, the proximity between the original doublet and final singlet in  $^{31}\text{P}$  NMR is surprising considering the chemical shift difference observed for other ligands between the NH and the PH tautomer (for **3**:  $^{31}\text{P}$  NMR ( $\text{C}_6\text{D}_6$ ): NH tautomer at  $\delta = 32.75$  ppm; PH tautomer at  $\delta = 2.82$  ppm). It is likely that the phosphorus remains pentavalent in presence of triethylamine but that the interatomic distance P-H was increased by formation of a hydrogen bond as proposed in Figure 6.

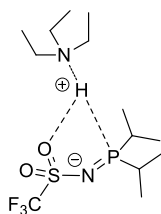


**Figure 6.** Possible interaction with triethylamine and METAMORPhos ligand **11**.

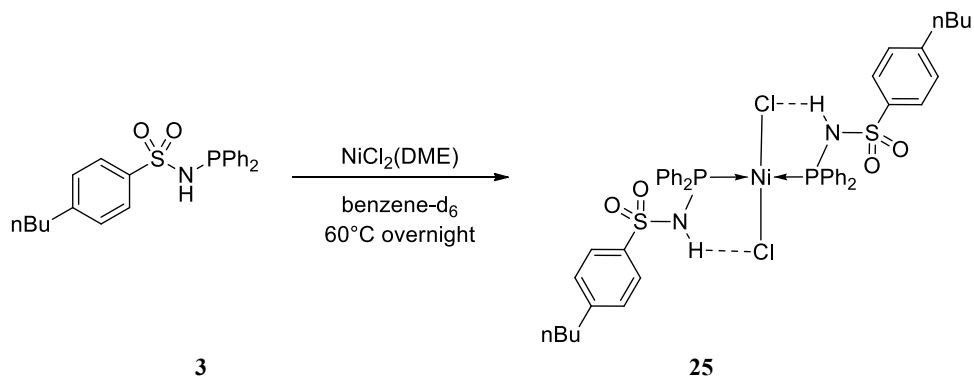
### 3 Coordination chemistry of sulphonamido-based phosphorus ligands with nickel precursors

The coordination chemistry of METAMORPhos ligands was first evaluated with nickel (II) precursors. The synthesis was performed in apolar and aprotic solvents to favour possible intermolecular hydrogen bonds between two ligands. We observed that the reaction of ligand **3** and  $\text{NiCl}_2(\text{DME})$  in a 2:1 ratio in benzene at  $60^\circ\text{C}$  was complete after 16 h leading to a red precipitate (Scheme 5). No more ligand was present in the benzene phase according to  $^{31}\text{P}$  NMR. To ensure full conversion of the precursor, we used a slight excess of ligands that was removed in the end of the reaction by filtration. The precipitate was only slightly soluble in dichloromethane and  $^{31}\text{P}$  NMR analysis of a saturated sample in  $\text{CD}_2\text{Cl}_2$  led to a broad signal at

$\delta(\text{CD}_2\text{Cl}_2)$ : 34.8 ppm that likely corresponds to the free ligand **3**; the complex might be paramagnetic and therefore not visible in  $^{31}\text{P}$  NMR.

Crystals of complex **25** were obtained from slow vapour diffusion of pentane in a dichloromethane solution of complex and the X-ray structure that was determined from diffraction experiments is presented in Figure 7. Both ligands in this complex are in the NH form and they coordinate *via* the phosphorus atom in *trans* with respect to each other. The arrangement around nickel is square planar (sum of angles =  $360^\circ$ ). The H-bond between the NH and the chloride that is coordinated to the nickel is very short (2.40(2) Å), constraining the two ligands in a square planar geometry. The geometry of ligand in the complex is very similar to that of the free METAMORPhos ligand with only a slightly shorter PN bond in the complex (ligand 1.720 Å, complex 1.696 Å) and slightly longer NS bond in the complex (ligand 1.624 Å, complex 1.642 Å). Complex **25** was evaluated for ethylene oligomerisation with MAO (300 eq.) as activator. The complex produced at  $45^\circ\text{C}$  and 35 bar, mainly butenes (92.5 % of oligomers) of which 88.1% accounted for 2-butene. Although the activity was very high at the start with a value of  $3.5 \cdot 10^6 \text{ g}_{\text{C}_2\text{H}_4} \cdot (\text{g}_{\text{Ni}} \cdot \text{h})^{-1}$ , the complex degraded to black material and turned inactive after 10 min.

Attempts to form coordination complex with ligand **11**, which exists exclusively as the PH tautomer, under similar conditions as described for ligand **25** with  $\text{NiCl}_2(\text{DME})$  did not lead to a clear transformation as no colour change was observed and analysis of the crude by  $^{31}\text{P}$  NMR showed only the starting material. Supposing that more electrophilic nickel would trigger the tautomer rearrangement with ligand **11** allowing a trivalent phosphorus coordination, we added  $\text{AgBF}_4$  in THF as abstracting halide agent. The reaction was also performed with nickel tetrafluoroborate as precursor but no reactivity was noticed.



**Scheme 5.** Synthesis of  $\text{Ni}(\text{METAMORPhos } \mathbf{3})_2\text{Cl}_2$  complex **25**.

Next we investigated if the presence of a base during the complexation would activate ligand **11** by inducing a shift in the tautomeric ratio. Complexation of ligand **11** (2 eq.) with  $\text{NiBr}_2(\text{DME})$  (1 eq.) in benzene and in the presence of triethylamine (4 eq.), immediately led to a brown solution with quick consumption of insoluble  $\text{NiBr}_2(\text{DME})$ . According to  $^{31}\text{P}$  NMR, a new nickel complex **26** formed, in which non-equivalent phosphines are coordinated to nickel as can be seen from two very broad signals shifted downfield (80-100 ppm region).

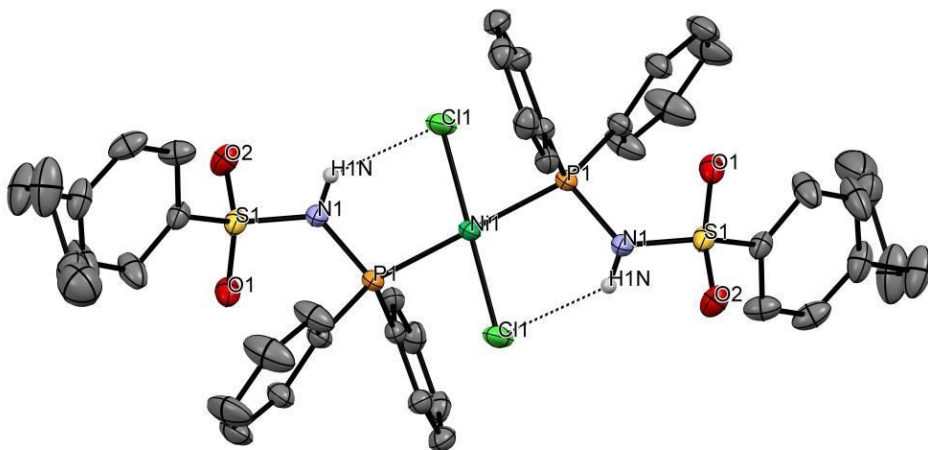
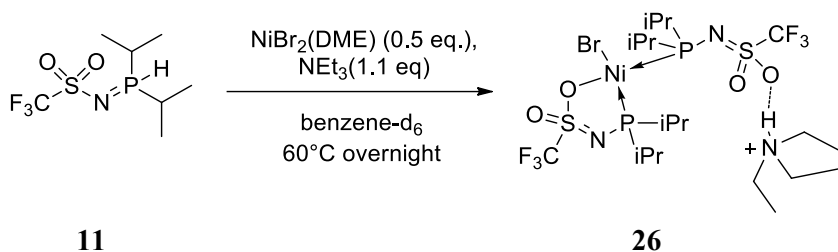


**Figure 7.** ORTEP plot (50% probability displacement ellipsoids) of complex **25**. Hydrogen atoms have been omitted for clarity (except for NH moiety). Selected bond lengths (Å) and angles (°): Ni1-Cl1 2.1610(5); Ni1-P1 2.2342(5); P1-N1 1.6964(15); N1-S1 1.6424(15); N1-H1N 0.80(3); S1-O1 1.4308(13); S1-O2 1.4333(16); Cl1-H1N 2.40(2); Cl1-Ni1-P1 86.43(2); Cl1-Ni-Cl1 180.00; P1-Ni1-P1 180.00.

A crystal of **26** was obtained from slow vapour diffusion of pentane into a dichloromethane crude solution of complex (see Figure 8). The X-ray structure shows some unusual features. The two ligands adopt a *cis* configuration in the solid state and coordinate in the anionic form. The primary ligand forms a PO chelate containing a double S-N bond, which is significantly shorter than the free ligand **11** (N1-S1 1.5232(15) Å vs. 1.5471(9) Å in the ligand) and two formal single bonds: P-N and S-O (P1-N1 1.6827(14) Å and S1-O1 1.4812(13) Å vs. N1-P1 1.6193(9) Å and S1-O1 1.4402(9) Å for ligand **11**). The second ligand is engaged in coordination to nickel but only through the phosphorus. The S-N bond length (N2-S2 1.5215(13) Å) is similar to the other S1-N1 double bond in the PO chelate and still very short compared to the free ligand, suggesting that this involves a double bond. Besides, the P-N and S-O bonds in the second ligand are of intermediate length between single and double, which suggests a delocalised structure on the PNSO moiety. This ligand is also obviously deprotonated by triethylamine as the proton is closer from the

triethylamine than for the original ligand ( $N_{\text{NEt}_3}\text{-H}$  0.83(2) Å and  $N_{\text{MET}}\text{-H}$  2.08(2) Å). It forms an ion pair that resides at the oxygen in the solid state meaning that once coordinated on nickel, METAMORPhos **11** may be deprotonated by triethylamine. These experiments show that sulphonamido-phosphorus based ligands coordinate in several modes to nickel.



**Scheme 6.** Synthesis of nickel complex **26** from METAMORPhos **11**,  $\text{NiBr}_2(\text{DME})$  and triethylamine.

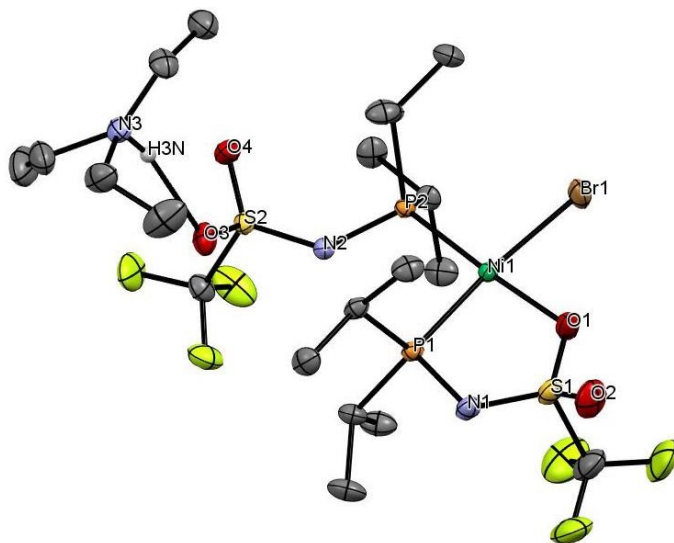
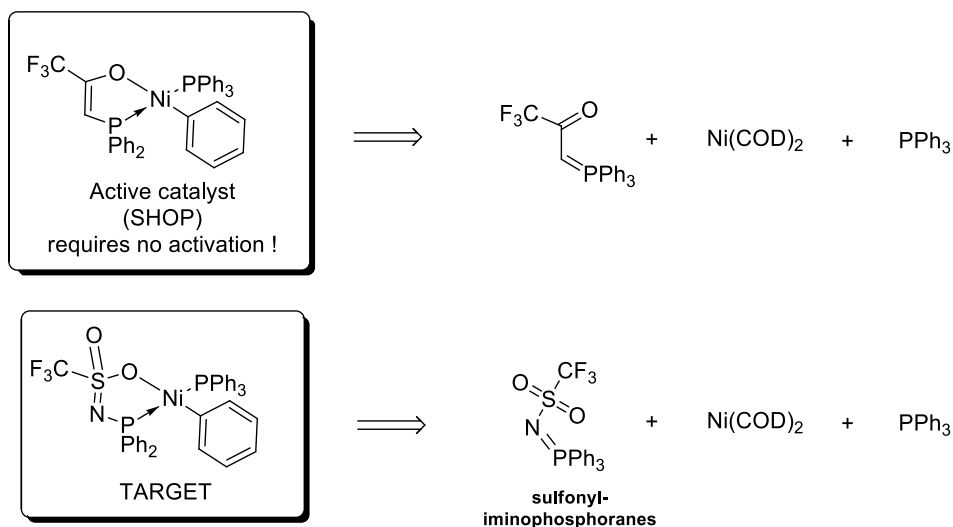


**Figure 8.** ORTEP plot (50% probability displacement ellipsoids) of complex **26**. Hydrogen atoms have been omitted for clarity (except for OH moiety). Selected bond lengths (Å) and angles (°): Ni1-P1 2.2099(4); P1-N1 1.6827(14); N1-S1 1.5232(15); S1-O1 1.4812(13); Ni1-Br1 2.3166(3); Ni1-O1 1.9771(13); Ni1-P2 2.1769(4); P2-N2 1.6579(14); N2-S2 1.5215(13); S2-O3 1.4511(13); S2-O4 1.4458(13); [H-bond: O3-N3 2.8881(19); O3-H3N 2.08(2); N3-H3N 0.83(2)].

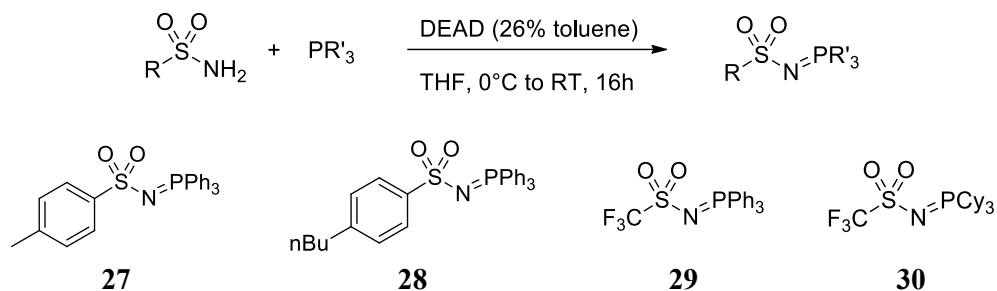
The use of single component catalysts in oligomerisation, such as nickel-aryl type complexes, offer active systems that do not need activation before the application in catalytic reaction. The direct preparation of Ni-H or Ni-R (R= aryl, alkyl) complexes based on these METAMORPhos ligands would be interesting as they can be directly used for ethylene oligomerisation catalysis. Indeed, the reaction of carboxymethylphosphanes ( $\text{R-CO-CH=PR}'_3$ ) or amidophosphanes ( $\text{R-CO-}$

$\text{N}=\text{PR}'_3$ ) with  $\text{Ni}(0)$  was successfully used to generate a plethora of  $\text{PCCO}^-$  (or  $\text{PCNO}^-$ ) chelated aryl nickel complexes that constitute the basis of SHOP catalyst.<sup>[18-22]</sup> These complexes were demonstrated to be active in ethylene oligomerisation producing linear alpha olefins with a large Schulz-Flory product distribution. By analogy, we thought that sulphonyl-iminophosphoranes of general formula  $\text{R-SO}_2\text{-N}=\text{P}(\text{R}')_3$  or METAMORPhos in the PH tautomeric form  $\text{R-SO}_2\text{-N}=\text{P}(\text{R}')_2\text{H}$  would be good candidates to form similar organometallic arrangements based on a  $\text{PNSO}^-$  chelate (Scheme 7).



**Scheme 7.** Structural analogy between sulphonyl-iminophosphoranes and carboxymethylphosphorane for the formation of single component Ni-Ar catalysts.

Sulphonyl iminophosphoranes were prepared by condensation of a sulphonamide and a tri-substituted phosphine in the presence of diethylazodicarboxylate (DEAD) in an overnight reaction at room temperature (Scheme 8).<sup>[23]</sup> This procedure is more suited than the reaction of sulphonyl azide on  $\text{PR}'_3$  or reaction of  $\text{N,N}'$ -dibrominated sulphonamides with  $\text{PR}'_3$ , which in both cases generated also a lot of phosphine oxide.<sup>[24-26]</sup> The approach with DEAD was smooth as the pure product precipitated from THF at the end of the reaction. This strategy afforded sulphonyl iminophosphoranes **27**, **28**, **29**, **30** in moderate yield (isolated up to 40 %) which were characterised by <sup>31</sup>P and <sup>1</sup>H NMR (Scheme 8).



**Scheme 8.** Sulphonyl iminophosphoranes synthesised by condensation of a sulphonamide and a phosphine in presence of DEAD.

The ability of this new class of sulphonyl-iminophosphoranes to form organometallic complexes was investigated with  $\text{Ni}(\text{COD})_2$  in presence of a phosphine ( $\text{PPh}_3$  or  $\text{PCy}_3$ ).<sup>[18,27,28]</sup> The presence of a coordinating phosphine is mandatory for the reaction to happen and probably relies on the intervention of  $\text{Ni}(\text{PR}_3)_n$  intermediates. In the presence of  $\text{PPh}_3$ , the solutions first turned red due to the initial coordination of  $\text{PPh}_3$  to  $\text{Ni}(0)$  but no further reactivity was observed with sulphonyl-iminophosphoranes at room temperature. We expected that the low solubility of the ligands would not be limiting, considering that carboxymethylphosphoranes or amidophosphoranes have similar low solubility but dissolve in the course of complex formation.<sup>[19]</sup> Increasing the reaction temperature to  $60^\circ\text{C}$  improved ligand dissolution but led also to complex decomposition, as indicated by the formation of a suspension of black insoluble material and loss of the red colour. In all experiments the sulphonyl-iminophosphoranes were very stable and did not react with the metal complex. Similar experiments performed in the presence of  $\text{PCy}_3$  led to the formation several compounds as indicated by  $^{31}\text{P}$  NMR that displayed several peaks whereas only a doublet was expected. We suggest that  $\text{PPh}_3$  is not strongly coordinating to nickel and therefore does not sufficiently stabilise the system.

## 4 Conclusion

In this Chapter we reported some synthetic aspects in the preparation of METAMORPhos ligands. We found that during the preparation of METAMORPhos, iminobisphosphines, the bis-addition product, form as by products under certain conditions. Iminobisphosphines and METAMORPhos are also in equilibrium *via* sort of disproportionation reaction, which is less dependent on the operating conditions. However, this equilibrium is suppressed by the use of bulky or alkyl substituents on the phosphorus. As a result, several METAMORPhos ligands could be isolated, depending on the properties of the starting materials. Similarly to amidophosphines and secondary phosphine oxides, METAMORPhos give rise to formation of several tautomers in solution with the PH ( $\text{P}^{\text{IV}}$ ) and the NH ( $\text{P}^{\text{III}}$ ) forms being the most



common. The domains of predominance of each tautomer (PH/NH) depend on the electronic properties of the ligand. Systems with electron donating groups on P and electron withdrawing groups at the S favour the PH form. Besides this electronic effect, the presence of a base (or hydrogen-bond acceptor moiety) may also induce a shift in the tautomer equilibrium. METAMORPhos ligands that are in tautomeric form with the trivalent phosphorus, coordinate to nickel(II) to form square planar bis-METAMORPhos complexes. In contrast, METAMORPhos ligands that are in the pentavalent state did not form coordination complexes when mixed with a nickel(II) precursor. However, the same reaction in the presence of triethylamine as a base, resulted in complex formation in which METAMORPhos acted as anionic PO<sup>-</sup> ligand. The X-ray structure of this complex confirmed that one such anionic ligand is chelated at the nickel complex, while a second ligand coordinated monotonically *via* the phosphorus. Importantly, a wide variety of METAMORPhos ligands can be prepared and they display interesting coordination behaviour to nickel.

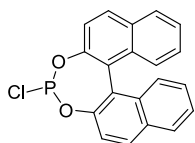
## 5 Experimental part

### 5.1 General

All reactions were carried out under an atmosphere of argon using standard Schlenk techniques. Sulphonamides, di(o-tolyl)chlorophosphine, di-tert-butylchlorophosphine, diethylchlorophosphine, dicyclohexylchlorophosphine were purchased from commercial suppliers and used without further purification. Diphenylchlorophosphine and diisopropylchlorophosphine were distilled trap to trap under reduced pressure. THF, pentane and Et<sub>2</sub>O were distilled from sodium benzophenone. CH<sub>2</sub>Cl<sub>2</sub> and triethylamine were distilled from CaH<sub>2</sub>, toluene from sodium, under nitrogen. Alternatively solvents from SPS (Solvent Purification System, MBraun) were used. NMR solvents were degassed by freeze-pump-thaw cycling under argon and stored over activated 3 Å molecular sieves. NMR spectra (<sup>1</sup>H, <sup>1</sup>H{<sup>31</sup>P}, <sup>31</sup>P, <sup>31</sup>P{<sup>1</sup>H} and <sup>13</sup>C{<sup>1</sup>H}) were measured on a BRUKER 300 MHz spectrometer at 25°C. Analysis of liquid phases was performed on a GC Agilent 6850 Series II equipped with a PONA column. The gas phase for ethylene oligomerisation were analysed by gas GC on HP 6890. Elemental analyses were performed by Stephen Boyer (London Metropolitan University). Values of pKa for sulphonamides and related compounds were gathered from Scifinder (06/2014) and correspond to the value of the first acidity at 25°C, calculated using ACD/Labs Software (© 1994-2014).

### 5.2 Synthesis of ligands METAMORPhos

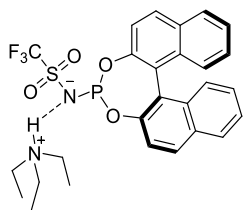
#### Synthesis of (R)-1,1'-Bi-2-naphthol-PCI (Binol PCI)



(R)-Binaphtol (11.05 g, 38.60 mmol, 1.00 eq.) was weighted in a 1000 mL round bottom flask and suspended in dry toluene (20 mL) stirred for 5 min at RT and then evaporated under vacuum. This operation was repeated twice. Then the solid was suspended in toluene (20 mL), phosphorus trichloride (50.00 mL, 78.70 g, 573 mmol, 14.80 eq.) and *N*-methylpyrrolidone (21 drops, acts as a catalyst). The mixture was heated at 60°C until complete dissolution of the (R)-binaphtol leading to a clear solution (15 min). Then toluene and phosphorus trichloride were evaporated. The resulting oil was co-

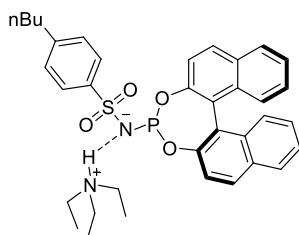
evaporated twice with toluene (2 x 50 mL) and triturated in pentane to give a powder (12.58 g, isolate yield: 93 %). The product was in accordance with the literature, contained no oxide and displayed a singlet in  $^{31}\text{P}$  NMR (121 MHz,  $\text{C}_6\text{D}_6$ , 300K):  $\delta(\text{ppm})$ : 177.

### Ligand 1



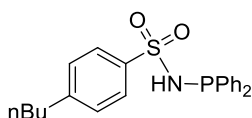
(R)-1,1'-Bi-2-naphthol-PCl (4.10 g, 11.70 mmol, 1.00 eq.) was dissolved in 20 mL of dry THF leading to an orange solution. In another Schlenk, commercially available 4-butylbenzene-1-sulphonamide (2.49 g, 11.70 mmol, 1.00 eq.) and triethylamine (9.80 mL, 70.20 mmol, 6.00 eq.) were dissolved in THF (30 mL). The phosphine was transferred to the sulphonamide solution by cannula under strong stirring leading to a white precipitate. The suspension was then filtered under argon atmosphere and the resulting clear solution was evaporated to sticky oil. The product was then washed with 30 mL of toluene/hexanes (1:2), and then with 30 mL  $\text{Et}_2\text{O}$ . The product was obtained as a white powder (2.21 g, isolated yield: 33 %). The NMR analysis of the product was in accordance with the literature.<sup>[6]</sup>  $^{31}\text{P}\{^1\text{H}\}$  NMR (121 MHz,  $\text{CD}_2\text{Cl}_2$ , 300 K):  $\delta$  (ppm): 165.22 (q,  $^4J_{\text{PF}} = 11.5$  Hz);  $^{31}\text{P}$  NMR (121 MHz,  $\text{CD}_2\text{Cl}_2$ , 300 K):  $\delta$  (ppm): 165.22 (q,  $^4J_{\text{PF}} = 11.5$  Hz);  $^1\text{H}$  NMR (300 MHz,  $\text{CD}_2\text{Cl}_2$ , 300K):  $\delta$  (ppm): 0.75 (t,  $^3J_{\text{HH}} = 7.3$  Hz,  $\text{CH}_2\text{H}_b\text{-CH}_3$ , 9H); 2.25 (br qd,  $-\text{CH}_2\text{H}_b\text{-CH}_3$ , 3H); 2.61 (br qd,  $-\text{CH}_2\text{H}_a\text{-CH}_3$ , 3H); 7.1-8.1 (aromatic region, 12  $\text{CH}_{\text{Ar}}$ ); 8.60 (br s, 1H, NH).

### Ligand 2



(R)-1,1'-Bi-2-naphthol-PCl (4.10 g, 11.70 mmol, 1.00 eq.) was dissolved in 20 mL of dry THF leading to an orange solution. In another Schlenk, commercially available 4-butylbenzene-1-sulphonamide (2.49 g, 11.70 mmol, 1.00 eq.) and triethylamine (9.80 mL, 70.20 mmol, 6.00 eq.) were dissolved in THF (30 mL). The phosphine was transferred to the sulphonamide solution by cannula under strong stirring leading to a white precipitate. The suspension was then filtered under argon atmosphere and the resulting clear solution was evaporated to sticky oil. The oil was dissolved in dichloromethane (15 mL) and evaporated, followed by a trituration in toluene (20 mL) leading to a solid. The solid was washed with toluene (2 x 20 mL) leading to a white solid. This solid was dried under vacuum to yield a powder (5.36 g, isolated yield: 73%). The NMR analysis of the product was in accordance with the literature.<sup>[6]</sup>  $^{31}\text{P}\{^1\text{H}\}$  NMR (121 MHz,  $\text{CD}_2\text{Cl}_2$ , 300 K):  $\delta$  (ppm): 171.07 (s);  $^{31}\text{P}$  NMR (121 MHz,  $\text{CD}_2\text{Cl}_2$ , 300 K):  $\delta$  (ppm): 171.07 (s);  $^1\text{H}$  NMR (300 MHz,  $\text{CD}_2\text{Cl}_2$ , 300K):  $\delta$  (ppm): 0.71 (t,  $^3J_{\text{HH}} = 7.2$  Hz,  $\text{CH}_3_{\text{NEt}_3}$ , 9H); 0.96 (t,  $^3J_{\text{HH}} = 7.3$  Hz,  $\text{CH}_3\text{-CH}_2\text{-CH}_2\text{-CH}_2\text{-Ar}$ , 3H); 1.40 (m,  $\text{CH}_3\text{-CH}_2\text{-CH}_2\text{-CH}_2\text{-Ar}$ , 2H); 2.21 (br dq,  $^3J_{\text{HH}} = 7$  Hz,  $^2J_{\text{HaHb}} = 13$  Hz,  $\text{N-CH}_2\text{H}_b\text{-CH}_3$ , 3H); 2.63 (br dq,  $^3J_{\text{HH}} = 7$  Hz,  $^2J_{\text{HaHb}} = 13$  Hz,  $\text{N-CH}_2\text{H}_a\text{-CH}_3$ , 3H); 2.71 (t,  $^3J_{\text{HH}} = 7.5$  Hz,  $\text{CH}_3\text{-CH}_2\text{-CH}_2\text{-CH}_2\text{-Ar}$ , 2H); 6.78-8.0 (aromatic region, 16H); 9.98 (br s, NH, 1H).

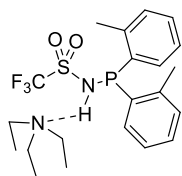
### Ligand 3



Commercially available 4-butylbenzene-1-sulphonamide (2.38 g, 11.14 mmol, 1.00 eq.) was placed in a Schlenk flask under argon. 3 mL of toluene was dropped on it leading to a blurred suspension which was stirred at room temperature for 5 minutes. The solvent was then evaporated. The process was repeated twice. The compound was then dissolved in THF (20 mL) and triethylamine (4.20 mL, 30.00 mmol, 2.70 eq.), leading to a clear colourless solution. Distilled chlorodiphenylphosphine (2 mL, 11.14

mmol, 1.0 eq.) was added dropwise under strong magnetic stirring at room temperature. The immediate formation of salt was observed as a white suspension. The suspension was left to stir overnight at room temperature. The suspension was then filtered under argon atmosphere and the resulting clear solution was evaporated to a white solid (87% of METAMORPhos and 13% iminobisphosphine). The solid was dissolved in 10 mL of THF and filtered over a short alumina gel column which was washed twice with 10 mL of THF. Evaporation of the solvent led to pure product in 53% yield. The NMR analysis of the product was in accordance with the literature.  $^{31}\text{P}\{^1\text{H}\}$  NMR (121 MHz,  $\text{C}_6\text{D}_6$ , 300K):  $\delta$  (ppm): 2.82 (s, PH); 32.75 (s, NH); ratio NH/PH= 18.9;  $^1\text{H}$  NMR (300 MHz,  $\text{C}_6\text{D}_6$ , 300K):  $\delta$  (ppm): 8.14 (d, 1H,  $^1J_{\text{H-P}} = 490$  Hz, tautomer PH), 8.10- 6.5 (aromatic region : tautomer NH and PH), 5.82 (d, 1H,  $^2J_{\text{H-P}} = 7$  Hz, NH tautomer NH), 2.34-2.14 (m,  $(\text{C}_3\text{H}_7)\text{-CH}_2\text{-Ar}$  : tautomer NH and PH), 1.27 (m., 2H,  $(\text{C}_2\text{H}_5)\text{-CH}_2\text{-CH}_2\text{-Ar}$  : tautomer NH), 1.26 (m., 2H,  $(\text{C}_2\text{H}_5)\text{-CH}_2\text{-CH}_2\text{-Ar}$  : tautomer PH), 1.16-1.02 (m.,  $\text{CH}_3\text{-CH}_2\text{-(C}_2\text{H}_4)\text{-Ar}$ , 2H tautomer NH and 2H tautomer PH), 0.84-0.77 (m.,  $\text{CH}_3\text{-(C}_3\text{H}_6)\text{-Ar}$ , 3H tautomer NH and 3H tautomer PH).

## Ligand 8



Trifluoromethanesulfonamide (1.2 g, 8.0 mmol, 1 eq.) was dried azeotropically three times by suspending the powder in toluene (3 mL), stirring for 5 min at RT and removing the solvent under vacuum. After that, the dry trifluoromethanesulfonamide was mixed with anhydrous triethylamine (2.1 g, 20 mmol, 2.6 eq., 3.0 mL) and dissolved in dry THF (20 mL). Di(o-tolyl)chlorophosphine was dissolved in another Schlenk with 10 mL of THF. The chlorophosphine solution (2.0 g, 8.0 mmol, 1.0 eq.) was added dropwise to the sulfonamide solution leading to a white thick precipitate. After 10 minutes, a  $^{31}\text{P}$  NMR indicated complete conversion of the chlorophosphine towards two tautomers at 15.77 ppm (NH— $\text{NEt}_3$ , 70%) and 22.6 ppm (PH,  $^1J_{\text{PH}} = 472.6$  Hz, 30%). The mixture was filtered by cannula to remove the triethylammonium salt and the filtrate was washed twice with THF (10 mL). The liquid phase was evaporated under reduced pressure to afford a colorless oil. The oil was heated to 50°C under vacuum to remove traces of volatile products and diethyl ether (20 mL) was finally added to the oil leading to a white powder upon trituration. This powder was washed with 3 x 5 mL of diethyl ether (solubilizing the PH tautomer only) and finally dried under vacuum to give the product under the NH— $\text{NEt}_3$  tautomer (isolated yield : 2.43 g, yield : 66%). Analyses were performed on the NH— $\text{NEt}_3$  tautomer.

$^{31}\text{P}\{^1\text{H}\}$  NMR (121 MHz,  $\text{CD}_2\text{Cl}_2$ ):  $\delta$ (ppm) = 26.4 (broad s);  $^{31}\text{P}$  NMR (121 MHz,  $\text{CD}_2\text{Cl}_2$ )  $\delta$ (ppm) = 26.5 (broad s);  $^{19}\text{F}$  NMR (282 MHz,  $\text{CD}_2\text{Cl}_2$ )  $\delta$ (ppm) = -78.2.  $^1\text{H}$  NMR (300 MHz,  $\text{CD}_2\text{Cl}_2$ ):  $\delta$ (ppm) = 1.08 (t,  $^3J_{\text{HH}} = 7.3$  Hz,  $\text{CH}_3\text{-CH}_2\text{-N}$ , 9H); 2.39 (br s,  $\text{-CH}_3$  tolyl, 6H); 2.69 (q,  $^3J_{\text{HH}} = 7.4$  Hz,  $\text{CH}_3\text{-CH}_2\text{-N}$ , 6H); 5.32 ( $\text{CDHCl}_2$  solvent signal); 6.8-7.9 (m,  $\text{H}_{\text{Ar}}$ , 8H); 8.83 (br s,  $\text{N-H}^+\text{N}$ , 1H).  $^{13}\text{C}$  NMR (75 MHz,  $\text{CD}_2\text{Cl}_2$ ):  $\delta$ (ppm) = 8.62 ( $\text{CH}_3$   $\text{NEt}_3$ ); 20.64 (d,  $^3J_{\text{CP}} = 19.5$  Hz,  $\text{CH}_3$  tolyl); 46.16 ( $\text{-CH}_2\text{-N}$ ); 121.86 (q,  $^1J_{\text{CF}} = 326$  Hz,  $\text{CF}_3$ ); 125.94 (d,  $J = 3.0$  Hz,  $\text{CH}_{\text{Ar}}$ ); 129.09 (br s,  $\text{CH}_{\text{Ar}}$ ); 130.41 (d,  $J_{\text{CP}} = 4.8$  Hz,  $\text{CH}_{\text{Ar}}$ ); 130.97 (br s,  $\text{CH}_{\text{Ar}}$ ); 141.50 (d,  $J = 2.5$  Hz and 24.3 Hz,  $\text{C}^{\text{IV}}$ ,  $\text{C}_{\text{Ar-CH}_3}$ , 2C), 140.5 (broad,  $\text{C}^{\text{IV}}_{\text{Ar-P}}$ , 2C). EA found (th): C: 54.38 (54.53), H: 6.64 (6.54), N: 5.85 (6.06). EA found (th): C: 54.38 (54.53); H: 6.64 (6.54); N: 5.85 (6.06).

### Crystal data

Chemical formula	$\text{C}_{15}\text{H}_{14}\text{F}_3\text{NO}_2\text{PS} \cdot \text{C}_6\text{H}_{16}\text{N}$
$M_r$	462.51
Crystal system, space group	Orthorhombic, $P2_12_12_1$
Temperature (K)	200
$a, b, c$ (Å)	8.854 (1), 14.840 (2), 18.005 (2)

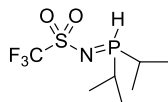
$V$ (Å <sup>3</sup> )	2365.7 (5)
$Z$	4
Radiation type	Mo $K\alpha$
$m$ (mm <sup>-1</sup> )	0.25
Crystal size (mm)	0.43 × 0.26 × 0.21

## Data collection

Diffractionmeter	Xcalibur, Atlas, Gemini ultra diffractometer
Absorption correction	Analytical <i>CrysAlis PRO</i> , Agilent Technologies, Version 1.171.37.33 (release 27-03-2014 CrysAlis171.NET) (compiled Mar 27 2014,17:12:48) Analytical numeric absorption correction using a multifaceted crystal model based on expressions derived by R.C. Clark & J.S. Reid. (Clark, R. C. & Reid, J. S. (1995). <i>Acta Cryst.</i> A51, 887-897) Empirical absorption correction using spherical harmonics, implemented in SCALE3 ABSPACK scaling algorithm.
$T_{\min}$ , $T_{\max}$	0.864, 0.924
No. of measured, independent and observed [ $I > 2.0\sigma(I)$ ] reflections	21076, 5703, 4673
$R_{\text{int}}$	0.047
$(\sin \theta/\lambda)_{\text{max}}$ (Å <sup>-1</sup> )	0.693

## Refinement

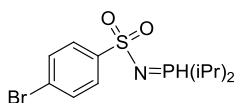
$R[F^2 > 2\sigma(F^2)]$ , $wR(F^2)$ , $S$	0.043, 0.080, 0.99
No. of reflections	5692
No. of parameters	273
H-atom treatment	H-atom parameters constrained
$\Delta_{\text{max}}$ , $\Delta_{\text{min}}$ (e Å <sup>-3</sup> )	0.44, -0.54
Absolute structure	Flack (1983), 3610 Friedel-pairs
Absolute structure parameter	0.05 (9)

**Ligand 11**


Commercially available trifluoromethyl sulphonamide (5.62 g, 37.70 mmol, 1.00 eq.) was placed in a 100 mL Schlenk. The powder was suspended in toluene (3 mL), stirred for 5 min and evaporated under vacuum. This operation was repeated twice (co-evaporation). Then, the sulphonamide was dissolved in dry THF (40 mL). Distilled chlorodiisopropylphosphine (6.00 mL, 37.70 mmol, 1.00 eq.) was added to the solution leading to a slightly blurred solution. To this solution was added dropwise triethylamine (13.10 mL, 98.30 mmol, 2.60 eq.) leading to a white precipitate. After stirring the suspension for 20 min at room temperature, unlocked <sup>31</sup>P NMR showed complete conversion of the chlorophosphine to a singlet at 40 ppm. The suspension was then filtered under argon atmosphere and the resulting clear solution was evaporated leading to a white powder (9.20 g, isolated yield: 92%). Crystals were grown from slow vapour diffusion of pentane in a toluene/

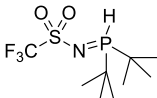
dichloromethane solution of the ligand. The NMR analysis of the product were in accordance with the literature.  $^{129}\text{I} \{^1\text{H}\}$  NMR (121 MHz,  $\text{CDCl}_3$ , 300 K):  $\delta$  (ppm): 42.32 (s);  $^{31}\text{P}$  NMR (121 MHz,  $\text{CDCl}_3$ , 300 K):  $\delta$  (ppm): 42.32 (d,  $^1J_{\text{PH}} = 451.7$  Hz);  $^1\text{H}$  NMR (300 MHz,  $\text{CDCl}_3$ , 300K):  $\delta$  (ppm): 1.30 (dd,  $^3J_{\text{HH}} = 7.06$  Hz &  $^3J_{\text{HP}} = 3.4$  Hz,  $\text{CH}_3_{\text{iPrA}}$ , 6H); 1.36 (dd,  $^3J_{\text{HH}} = 7.06$  Hz &  $^3J_{\text{HP}} = 1.0$  Hz,  $\text{CH}_3_{\text{iPrB}}$ , 6H); 2.31 (m, CH<sub>iPr</sub>, 2H); 6.37 (dt,  $^1J_{\text{HP}} = 450.2$  Hz & 3.7 Hz, PH, 1H).

### Ligand 12



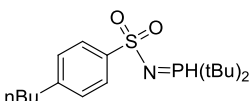
4-bromobenzene sulphonamide (2.00 g, 8.47 mmol, 1.00 eq.) was dissolved in dry THF (20 mL) and triethylamine (1.20 mL, 8.64 mmol, 1.02 eq.). Chlorodiisopropylphosphine (1.35 mL, 8.47 mmol, 1.00 eq.) was added dropwise under strong magnetic stirring at room temperature. The immediate formation of salt was observed as a white suspension. After stirring the solution at 10 min at RT, unlocked  $^{31}\text{P}$  NMR indicated the presence of the two tautomers (PH form at 35.8 ppm  $^1J_{\text{PH}} = 451.8$  Hz and NH form at 60.6 ppm: br signal with ratio NH/PH=0.19). The suspension was then filtered under argon atmosphere and the resulting clear solution was evaporated to a white solid. The solid was dissolved in 2 mL of dichloromethane and pentane (40 mL) was added slowly causing the product to crash out under in small crystallites. The pentane was then syringed out and the solid washed with pentane (2 x 10 mL) and dried under vacuum to yield a white powder (2.1g, isolated yield: 70%).  $^{31}\text{P}\{^1\text{H}\}$  NMR (121 MHz,  $\text{CD}_2\text{Cl}_2$ , 300 K):  $\delta$  (ppm): 36.5 (s);  $^{31}\text{P}$  NMR (121 MHz,  $\text{CD}_2\text{Cl}_2$ , 300 K):  $\delta$  (ppm): 36.5 (ddt,  $^1J_{\text{PH}} = 443.8$  Hz,  $^2J_{\text{PH}} = 28.9$  Hz,  $^2J_{\text{PH}} = 9.5$  Hz);  $^1\text{H}$  NMR (300 MHz,  $\text{CD}_2\text{Cl}_2$ , 300K):  $\delta$  (ppm): 1.12-1.30 (m,  $-\text{CH}_3$ , 12H); 2.24 (m,  $\text{CH}_{\text{iPr}}$ , 2H); 6.34 (dt,  $^1J_{\text{HP}} = 443.5$  Hz and  $^3J_{\text{HH}} = 3.7$  Hz, 1H, PH); 7.43-7.91 (m, aromatic region, 4H).

### Ligand 15



Commercially available trifluoromethyl sulphonamide (2.00 g, 13.40 mmol, 1.00 eq.) was placed in a 100 mL Schlenk and suspended in triethylamine (10.00 mL, 7.26 g, 71.77 mmol, 5.36 eq.) and THF (10 mL). Chlorodi(tertbutyl)phosphine (2.55 mL, 13.4 mmol, 1.00 eq.) was added to the sulphonamide and the mixture was heated at 60°C for 20 h to reach full conversion of the starting chlorophosphine. The solvents were evaporated to get rid of triethylamine and the solids resuspended in THF (20 mL). The suspension was then filtered under argon atmosphere and the resulting clear solution was evaporated leading to a white powder. The powder was dissolved in dichloromethane (5mL) and precipitated by slow addition of pentane (40 mL) to the solution. The solvents were syringed out and the solid was washed with pentane (2 x 10 mL) and dried to give a powder (2.44 g, isolated yield: 59 %). The NMR analysis of the product were in accordance with the literature.  $^{129}\text{I} \{^1\text{H}\}$  NMR (121 MHz,  $\text{CD}_2\text{Cl}_2$ , 300 K):  $\delta$  (ppm): 50.61(s);  $^{31}\text{P}$  NMR (121 MHz,  $\text{CD}_2\text{Cl}_2$ , 300 K):  $\delta$  (ppm): 50.61 (dm,  $^7J_{\text{PH}} = 441.3$  Hz,  $^3J_{\text{PH}} = 17.3$  Hz);  $^1\text{H}$  NMR (300 MHz,  $\text{CD}_2\text{Cl}_2$ , 300K):  $\delta$  (ppm): 1.36 (d,  $^3J_{\text{HP}} = 17.3$  Hz,  $\text{CH}_3_{\text{tBu}}$ , 18H); 6.13 (d,  $^1J_{\text{HP}} = 441$  Hz, PH, 1H).  $^{19}\text{F}$  NMR (282 MHz,  $\text{CD}_2\text{Cl}_2$ , 300K):  $\delta$  (ppm): 78.76 (s).

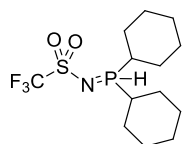
### Ligand 17



Commercially available 4-butylbenzene-1-sulphonamide (2.00 g, 9.37 mmol, 1.00 eq.) was dissolved in dry triethylamine (10 mL, 71.77 mmol, 7.70 eq.) and THF (2 mL). Distilled chloroditertbutylphosphine (1.78 mL, 9.37 mmol, 1.00 eq.) was added dropwise under strong magnetic stirring at room temperature. The mixture was then heated at 60°C for 3 days until the conversion reached a

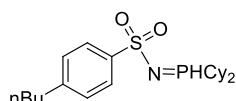
plateau at 84% according to NMR. The suspension was then filtered under argon atmosphere and the resulting clear solution was evaporated to a white solid. The solid was suspended in diethyl ether (10 mL) causing a solid to crash out. This solid was further washed with diethyl ether (4 x 20 mL) and dried under vacuum to yield a white powder (660 mg, isolated yield: 20%). The low yield may be explained by partial solubility of the product in diethyl ether. Using pentane instead of diethyl ether may increase yield.  $^{31}\text{P}\{^1\text{H}\}$  NMR (121 MHz, *tol-d*<sub>8</sub>, 300 K):  $\delta$  (ppm): 42.23 (s);  $^{31}\text{P}$  NMR (121 MHz, *tol-d*<sub>8</sub>, 300 K):  $\delta$  (ppm): 42.23 (dm,  $^1J_{\text{PH}} = 432.5$  Hz,  $^3J_{\text{PH}} = 16.4$  Hz);  $^1\text{H}$  NMR (300 MHz, *tol-d*<sub>8</sub>, 300K):  $\delta$  (ppm): 0.86 (t,  $^3J_{\text{HH}} = 7.3$  Hz,  $-\text{CH}_2-\text{CH}_3$ ); 0.97 (d,  $J = 16.3$  Hz,  $-\text{CH}_3$  *t*<sub>Bu</sub>, 18H); 1.21 (qd,  $^3J_{\text{HH}} = 7.8$  Hz,  $-\text{CH}_2-\text{CH}_3$ , 2H); 1.42 (m,  $-\text{CH}_2-\text{CH}_2-\text{CH}_3$ , 2H); 2.40 (t,  $^3J_{\text{HH}} = 7.8$  Hz,  $-\text{CH}_2-\text{Ar}$ , 2H); 6.09 (d,  $^1J_{\text{HP}} = 435.5$  Hz, PH, 1H); 6.99 (d,  $^3J_{\text{HH}} = 8.2$  Hz,  $\text{CH}_{\text{Ar}}$ , 2H); 8.08 (d,  $^3J_{\text{HH}} = 8.2$  Hz,  $\text{CH}_{\text{Ar}}$ , 2H);  $^{13}\text{C}$  NMR (75 MHz, *tol-d*<sub>8</sub>, 300K):  $\delta$  (ppm): 14.11 ( $-\text{CH}_2-\text{CH}_3$ ); 22.65 ( $-\text{CH}_2-\text{CH}_3$ ); 26.05 (d,  $^3J_{\text{CP}} = 1.6$  Hz,  $-\text{CH}_3$  *t*<sub>Bu</sub>); 33.39 ( $\text{C}^{\text{IV}}$  *t*<sub>Bu</sub>); 33.68 ( $-\text{CH}_2-\text{CH}_2-\text{CH}_3$ ); 34.18 ( $\text{C}^{\text{IV}}$  *t*<sub>Bu</sub>); 35.68 ( $-\text{CH}_2-\text{Ar}$ ); 126.49 ( $\text{CH}_{\text{Ar}}$ , 2C); 128.27 ( $\text{CH}_{\text{Ar}}$ , 2C); 144.97 ( $\text{C}^{\text{IV}}$  *c-n*<sub>Bu</sub>); 144.55 ( $\text{C}^{\text{IV}}$  *c-SO*<sub>2</sub>).

### Ligand 19



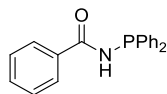
Commercially available trifluoromethyl sulphonamide (1.01 g, 6.79 mmol, 1.00 eq.) was placed in a 100 mL Schlenk and suspended THF (20 mL) and triethylamine (2.50 mL, 17.60 mmol, 2.60 eq.). Chlorodi(cyclohexyl)phosphine (1.5 mL, 6.79 mmol, 1 eq.) was added dropwise and under strong stirring to the sulphonamide at RT. After stirring the mixture for 10 min at RT, all the chlorophosphine had reacted to give the product along with 12% of iminobisphosphine. The suspension was then filtered under argon atmosphere and the resulting clear solution was evaporated leading to a white powder. The powder was washed with pentane (3 x 10 mL). Finally the product was dissolved in a minimum of dichloromethane and precipitated with pentane. The solid was dried under vacuum to give a white powder (1.3 g, isolated yield: 55 %).  $^{31}\text{P}\{^1\text{H}\}$  NMR (121 MHz,  $\text{CD}_2\text{Cl}_2$ , 300 K):  $\delta$  (ppm): 35.33 (s);  $^{31}\text{P}$  NMR (121 MHz,  $\text{CD}_2\text{Cl}_2$ , 300 K):  $\delta$  (ppm): 50.61 (d,  $^1J_{\text{PH}} = 450.9$  Hz);  $^1\text{H}$  NMR (300 MHz,  $\text{CD}_2\text{Cl}_2$ , 300K):  $\delta$  (ppm): 1.2-2.2 (m, Cy, 22H); 3.05 (dd,  $^2J_{\text{HP}} = 14.9$  Hz &  $^3J_{\text{HH}} = 7.4$  Hz, P-CH, 2H); 6.30 (dt,  $^1J_{\text{HP}} = 451.4$  Hz &  $^2J_{\text{HP}} = 3.9$  Hz, PH, 1H).  $^{19}\text{F}$  NMR (282 MHz,  $\text{CD}_2\text{Cl}_2$ , 300K):  $\delta$  (ppm): -79.22

### Ligand 20



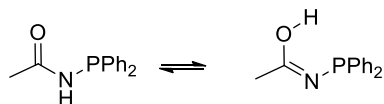
Commercially available 4-butylbenzene-1-sulphonamide (834 mg, 4.00 mmol, 1.00 eq.) and triethylamine (571  $\mu\text{L}$ , 4.10 mmol, 1.03 eq.) were dissolved in dry THF (20 mL) and commercial Chlorodicyclohexylphosphine (880  $\mu\text{L}$ , 4.00 mmol, 1.00 eq.) was added dropwise under strong magnetic stirring at room temperature leading to a white precipitate. The mixture was stirred until no more chlorophosphine was seen by  $^{31}\text{P}$  NMR (20 h). The suspension was then filtered under argon atmosphere and the resulting clear solution was evaporated to sticky oil. Diethyl ether was added to the oil (10 mL) and the mixture stirred for 5 min at RT after which the solvent was evaporated. This operation was repeated twice leading to a white solid. Diethyl ether (10 mL) and pentane (10 mL) were added to the powder and the solvents were syringed out. The solid was washed again with pentane (2 x 10 mL) and dried under vacuum to give a white powder (isolated yield: 980 mg, 60%).  $^{31}\text{P}\{^1\text{H}\}$  NMR (121 MHz,  $\text{CD}_2\text{Cl}_2$ , 300 K):  $\delta$  (ppm): 28.84 (s);  $^{31}\text{P}$  NMR (121 MHz,  $\text{CD}_2\text{Cl}_2$ , 300 K):  $\delta$  (ppm): 28.83 (d,  $^1J_{\text{PH}} = 443.0$  Hz);  $^1\text{H}$  NMR (300 MHz,  $\text{CD}_2\text{Cl}_2$ , 300K):  $\delta$  (ppm): 0.91 (t,  $^3J_{\text{HH}} = 7.4$  Hz,  $-\text{CH}_3$ , 3H); 1.1-2.1 (m, signals of the Cy and the  $-\text{CH}_2-\text{CH}_2-\text{CH}_3$ , 22H); 2.64 (t,  $^3J_{\text{HH}} = 7.5$  Hz,  $\text{Ar}-\text{CH}_2-$ , 2H); 6.28 (dt,  $^1J_{\text{HP}} = 441.4$  Hz,  $^2J_{\text{PH}} = 3.7$  Hz, PH, 1H); 7.23 (d,  $^3J_{\text{HH}} = 8$  Hz,  $\text{CH}_{\text{Ar}}$ , 2H); 7.72 (d,  $^3J_{\text{HH}} = 8.1$  Hz,  $\text{CH}_{\text{Ar}}$ , 2H).

**Ligand 21** (according to the procedure of Woolins et al.<sup>[30,31]</sup>)



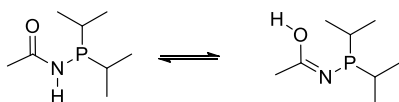
Benzamide (3.00 g, 24.76 mmol, 1.00 eq.) and 4-DMAP (187 mg, 1.55 mmol, 0.06 eq.) were placed in a Schlenk and degassed. To this Schlenk were added THF (90 mL) and triethylamine (6.80 mL, 49.20 mmol, 2.00 eq.). To this solution was added dropwise chlorodiphenylphosphine (4.44 mL, 24.76 mmol, 1 eq.) under strong magnetic stirring, causing a white solid to form. Immediately after addition, the crude product consisted only of iminobisphosphine at -16.3 (d,  $^1J_{PP} = 280$  Hz) and 23.8 (d,  $^1J_{PP} = 280$  Hz). The mixture was refluxed for 16 h which led to improved conversion to the monosubstituted product (85% of crude by  $^{31}\text{P}$  NMR). The mixture was filtered under inert argon atmosphere and the filtrate evaporated to a white viscous powder. The powder was washed with diethyl ether (2 x 40 mL) and dried under vacuum to give a white solid. The solid was crystallised from dichloromethane / diethyl ether to give white needles. (Isolate yield 2.48 g, 33 %).  $^{31}\text{P}\{^1\text{H}\}$  NMR (121 MHz,  $\text{CD}_2\text{Cl}_2$ , 300 K):  $\delta(\text{ppm})$ : 24.68 ppm (NH tautomer).  $^1\text{H}$  NMR ( $\text{CD}_2\text{Cl}_2$ , 300 MHz, 300K):  $\delta(\text{ppm})$ : 6.55 (br s, NH, 1H); 7.36-7.60 (m,  $\text{CH}_{\text{Ar}}$ , 13H); 7.79-7.85 (m,  $\text{CH}_{\text{Ar}}$ , 2H).

**Ligand 22** (According to the procedure of Braunstein and co-workers. <sup>[15,32]</sup>)



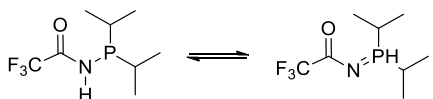
N(trimethylsilyl)-acetamide (1.46 g, 11.10 mmol, 1.00 eq.) was dissolved in toluene (20 mL). To this solution was added chlorodiphenylphosphine (1.00 mL, 6.28 mmol, 1.00 eq.). The mixture was then heated at 60°C for 1 h under dynamic bubbling of argon to remove  $\text{TMSCl}$  formed in the reaction mixture and an important precipitate formed. The solid that precipitated was filtered and washed with pentane (3 x 10 mL) and dried under vacuum. (Isolated yield: 2.2 g, 82 %).  $^{31}\text{P}\{^1\text{H}\}$  NMR (121 MHz,  $\text{CD}_2\text{Cl}_2$ , 300 K):  $\delta(\text{ppm})$ : 22.8 (s, NH form, 68 %); 30.3 (s, OH form, 32 %).  $^1\text{H}$  NMR (300 MHz,  $\text{C}_6\text{D}_6$ , 300K):  $\delta(\text{ppm})$ : 2.13 (s,  $-\text{CH}_3$ , 3H); 2.31 (s, 1H); 6.04 (br s, 1H); 7.43 (m,  $\text{CH}_{\text{Ar}}$ , 10H).

**Ligand 23** (According to the procedure of Braunstein and co-workers. <sup>[15,32]</sup>)



N(trimethylsilyl)-acetamide (824 mg, 6.28 mmol, 1.00 eq.) was dissolved in toluene (20 mL). To this solution was added chlorodiisopropylphosphine (1.00 mL, 6.28 mmol, 1.00 eq.) dropwise. The mixture was then heated at 70°C for 2 h under dynamic bubbling of argon to remove  $\text{TMSCl}$  formed in the reaction mixture. The solvent was removed to give a colourless solid in a quantitative yield.  $^{31}\text{P}\{^1\text{H}\}$  NMR (121 MHz,  $\text{C}_6\text{D}_6$ , 300 K):  $\delta(\text{ppm})$ : 49.7 (s, NH form, 14 %); 56.14 (s, OH form, 86 %). Only the signals of the major tautomer were reported.  $^1\text{H}$  NMR (300 MHz,  $\text{C}_6\text{D}_6$ , 300K):  $\delta(\text{ppm})$ : 0.85 (dd,  $^3J_{\text{HP}} = 16.2$  Hz,  $^3J_{\text{HH}} = 7.0$  Hz,  $-\text{CH}_3$   $_{i\text{Pr}}$ , 6H); 0.94 (dd,  $^3J_{\text{HP}} = 11.0$  Hz,  $^3J_{\text{HH}} = 6.9$  Hz,  $-\text{CH}_3$   $_{i\text{Pr}}$ , 6H); 1.58 (br s,  $-\text{CH}$   $_{i\text{Pr}}$ , 2H); 2.16 (d,  $^4J_{\text{HP}} = 2.4$  Hz,  $\text{H}_3\text{C}=\text{O}$ , 3H); 4.86 (weak signal tautomer OH, OH); 7.38 (br s, NH, 1H).

**Ligand 24** (adapted from Woolins et al. <sup>[30,31]</sup>)

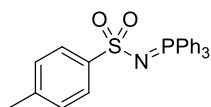


Trifluoroacetamide (2.80 g, 24.70 mmol, 1.00 eq.) and 4-(dimethylamino)pyridine (DMAP, 187 mg, 1.55 mmol, 0.006 eq.) were placed in a 100 mL Schlenk. The powders were co-evaporated twice with toluene to remove residual water (2 x 3 mL). The powders were then dissolved in THF (25 mL) and triethylamine, (3.78 mL, 27.20 mmol, 1.10 eq.) followed by the dropwise addition of diisopropylchlorophosphine (3.77 g, 3.93 mL, 24.70 mmol, 1.00 eq.) under strong magnetic stirring, leading to a white precipitate. Unlocked  $^{31}\text{P}$  NMR, measured immediately after addition showed the formation of 59% of

iminobisphosphine and 41 % of amidophosphine. The mixture was refluxed for 16h which led to 85 % of amidophosphine in the crude. The suspension was then filtered under argon atmosphere and the resulting clear solution was evaporated leading to an orange solid. The solid was dissolved in diethyl ether (20 mL) and precipitated with pentane (40 mL). The solvents were syringed out and the solid was washed with pentane (3 x 10 mL) and dried under vacuum to give a yellowish powder (1.5 g, isolated yield: 26%).  $^{31}\text{P}\{^1\text{H}\}$  NMR (121 MHz,  $\text{CD}_2\text{Cl}_2$ , 300 K):  $\delta$  (ppm): 40.1 (s, PH tautomer, 31%P); 56.9 (s, NH tautomer, 69%P);  $^{31}\text{P}$  NMR (121 MHz,  $\text{CD}_2\text{Cl}_2$ , 300 K):  $\delta$  (ppm): 40.1 (d, PH tautomer,  $^1J_{\text{PH}} = 447.2$  Hz); 56.9 (s, NH tautomer);  $^1\text{H}$  NMR (300 MHz,  $\text{CD}_2\text{Cl}_2$ , 300K):  $\delta$  (ppm): 1.0-1.2 (m,  $\text{CH}_3_{\text{IPr}}$ , NH tautomer, 12H); 1.22-1.44 (m,  $\text{CH}_3_{\text{IPr}}$ , PH tautomer, 12H); 1.96 (sept d,  $^3J_{\text{HH}} = 5.3$  Hz,  $^2J_{\text{HP}} = 1.7$  Hz,  $\text{CH}_{\text{IPr}}$ , NH tautomer, 2H); 2.40 (sept,  $^3J_{\text{HH}} = 3.2$  Hz,  $\text{CH}_{\text{IPr}}$ , PH tautomer, 2H); 6.05 (br s, NH, 1H); 6.46 (dt,  $^1J_{\text{HP}} = 440$  Hz,  $^3J_{\text{HH}} = 3.8$  Hz, PH, 1H). Signals of the residue from 4-DMAP at 3.2 ppm ( $-\text{CH}_3$ , 6H), 6.7 and 8.2 ppm.

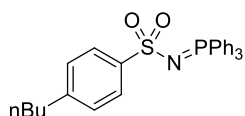
### 5.3 Synthesis of sulphonyl-iminophosphoranes

#### Sulphonyl iminophosphorane 27



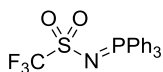
Tosylamide (856 mg, 5.00 mmol, 1.00 eq.) and triphenylphosphine (1.31 g, 5.00 mmol, 1.00 eq.) were placed in a 50 mL Schlenk with dry THF (10 mL). The solution was cooled to 0°C and diethylazodicarboxylate (solution at 45 mol% in toluene, 1.43 mL, 5.00 mmol, 1.00 eq.) was added dropwise to the solution. The orange DEAD solution immediately turned colourless in solution. After addition, the mixture was left to react at room temperature for 16h. A white precipitate formed which was filtered and washed with diethyl ether (2x 5 mL) and dried under vacuum. The product was conforming to the literature, isolated yield: 790 mg, 36%.  $^{31}\text{P}\{^1\text{H}\}$  NMR (121 MHz,  $\text{CDCl}_3$ , 300K):  $\delta$ (ppm): 14.40 (s);  $^{31}\text{P}$  NMR (121 MHz,  $\text{CDCl}_3$ , 300K):  $\delta$ (ppm): 14.40 (br s);  $^1\text{H}$  NMR (300 MHz,  $\text{CDCl}_3$ , 300K):  $\delta$ (ppm): 2.29 (s,  $-\text{CH}_3$ , 3H); 7.01 (d,  $^3J_{\text{HH}} = 8.6$  Hz,  $\text{H}_{\text{Ar}}$ , 2H), 7.38-7.52 (m,  $\text{H}_{\text{Ar}}$ , 8H) ; 7.52-7.62 (m,  $\text{H}_{\text{Ar}}$ , 3H) ; 7.67-7.82 (m,  $\text{H}_{\text{Ar}}$ , 6H).

#### Sulphonyl iminophosphorane 28



4-*n*-butyl phenyl sulphonamide (1.07 mg, 5.00 mmol, 1.00 eq.) and triphenylphosphine (1.31 g, 5.00 mmol, 1.00 eq.) were placed in a 50 mL Schlenk with dry THF (10 mL). The solution was cooled to 0°C and diethylazodicarboxylate (solution at 45 mol% in toluene, 1.43 mL, 5.00 mmol, 1.00 eq.) was added dropwise to the solution. The orange DEAD solution immediately turned colourless in solution. After addition, the mixture was left to react at room temperature for 16h. A white precipitate formed which was filtered and washed with diethyl ether (2 x 5 mL) and dried under vacuum. The product contained traces of carbamate from the DEAD. It was recrystallised from hot ethanol to give colourless crystals (isolated yield: 1.06 g, 45%).  $^{31}\text{P}\{^1\text{H}\}$  NMR (121 MHz,  $\text{CDCl}_3$ , 300K):  $\delta$ (ppm): 14.46 (s);  $^{31}\text{P}$  NMR (121 MHz,  $\text{CDCl}_3$ , 300K)  $\delta$ (ppm) = 14.46 (br s);  $^1\text{H}$  NMR (300 MHz,  $\text{CDCl}_3$ , 300K)  $\delta$ (ppm): 0.90 (t,  $^3J_{\text{HH}} = 7.3$  Hz,  $-\text{CH}_3$ ); 1.26 (m,  $-\text{CH}_2-\text{CH}_3$ , 2H); 1.52 (quad,  $^3J_{\text{HH}} = 7.4$  Hz,  $\text{CH}_3-\text{CH}_2-\text{CH}_2-\text{CH}_2-\text{Ar}$ , 2H); 4.19 (m,  $-\text{CH}_2-\text{Ar}$ , 2H); 7.00 (m,  $\text{CH}_{\text{Ar}}$ , 2H); 7.36-7.62 (m,  $\text{CH}_{\text{Ar}}$ , 11H); 7.68-7.86 (m,  $\text{CH}_{\text{Ar}}$ , 6H).

#### Sulphonyl iminophosphorane 29

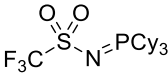


Trifluoromethane sulphonamide (746 mg, 5 mmol, 1 eq.) and triphenylphosphine (1.31 g, 5.00 mmol, 1.00 eq.) were placed in a 50 mL Schlenk with dry THF (10 mL). The solution was cooled to 0°C and diethylazodicarboxylate (solution at 45 mol% in toluene, 1.43 mL, 5 mmol,



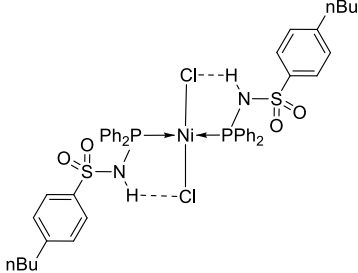
1 eq.) was added dropwise to the solution. The orange DEAD solution immediately turned colourless in solution. After addition, the mixture was left to react at room temperature for 16h. A white precipitate formed which was filtered and washed with diethyl ether (2 x 5 mL) and dried under vacuum. The product was recrystallised from ethanol / dichloromethane to give colourless crystals (isolated yield: 765 mg, 39%).  $^{31}\text{P}\{^1\text{H}\}$  NMR (121 MHz,  $\text{CDCl}_3$ )  $\delta(\text{ppm}) = 21.05$  (s);  $^{31}\text{P}$  NMR (121 MHz,  $\text{CDCl}_3$ , 300K):  $\delta(\text{ppm}) = 21.05$  (br s);  $^1\text{H}$  NMR (300 MHz,  $\text{CDCl}_3$ , 300K):  $\delta(\text{ppm}) = 7.38\text{--}7.52$  (m,  $\text{H}_{\text{Ar}}$ , 6H);  $7.52\text{--}7.62$  (m,  $\text{H}_{\text{Ar}}$ , 3H);  $7.67\text{--}7.82$  (m,  $\text{H}_{\text{Ar}}$ , 6H).

### Sulphonyl iminophosphorane 30

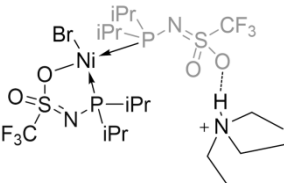

 Trifluoromethane sulphonamide (746 mg, 5.00 mmol, 1.00 eq.) and tricyclohexylphosphine (1.40 g, 5.00 mmol, 1.00 eq.) were placed in a 50 mL Schlenk with dry THF (10 mL). The solution was cooled to 0°C and diethylazodicarboxylate (solution at 45 mol% in toluene, 1.43 mL, 5.00 mmol, 1.00 eq.) was added dropwise to the solution. The orange DEAD solution immediately turned colourless in solution. After addition, the mixture was left to react at room temperature for 16h. A white precipitate formed which was filtered and washed with diethyl ether (2x 5 mL) and dried under vacuum. The product was recrystallised from ethanol / dichloromethane to give colourless crystals (isolated yield: 728 mg, 34%).  $^{31}\text{P}\{^1\text{H}\}$  NMR (121 MHz,  $\text{CDCl}_3$ , 300K):  $\delta(\text{ppm}) = 44.40$  (s);  $^{31}\text{P}$  NMR (121 MHz,  $\text{CDCl}_3$ , 300K):  $\delta = 44.39$  (br s);  $^1\text{H}$  NMR (300 MHz,  $\text{CDCl}_3$ , 300K):  $\delta(\text{ppm}) = 1.16\text{--}1.40$  (m, Cy, 9H);  $1.42\text{--}1.64$  (m, Cy, 6H);  $1.66\text{--}1.82$  (m, Cy, 3H);  $1.82\text{--}2.04$  (m, Cy, 12H);  $2.24$  (qt,  $^2J_{\text{HP}} = 12.2$  Hz and  $^3J_{\text{HH}} = 2.8$  Hz, Cy, 3H),  $^{19}\text{F}$  NMR (282 MHz,  $\text{CDCl}_3$ )  $\delta(\text{ppm}) = -79.05$ .

## 5.4 Synthesis of complexes

### Complex 25


 METAMORPhos ligand **3** (123 mg, 0.31 mmol, 2.20 eq.) and  $\text{NiCl}_2(\text{DME})$  (31 mg, 0.14 mmol, 1.00 eq.) were placed in a Schlenk with toluene (3 mL). The mixture was stirred for 16h at 60°C to give a dark red insoluble solid. The toluene was syringed out and the solid washed again with toluene to get rid of the ligand excess. The solid was dried under vacuum and dissolved in dichloromethane (10 mL). This solution was filtered through a syringe disc filter to remove traces of unreacted  $\text{NiCl}_2$  (pore diameter 0.15  $\mu\text{m}$ ) and the resulting liquid evaporated to give a red powder in almost quantitative yield. We were not able to analyse properly this complex by NMR, since only br signals attributed to the free ligand could be observed in  $^{31}\text{P}$  and  $^1\text{H}$  NMR.

### Complex 26


 METAMORPhos ligand **11** (82 mg, 0.31 mmol, 2.20 eq.) and triethylamine (100  $\mu\text{L}$ , 0.74 mmol, 5.30 eq.) were dissolved in a Schlenk with toluene (2 mL). In another Schlenk  $\text{NiBr}_2(\text{DME})$  (43 mg, 0.14 mmol, 1.00 eq.) was suspended in toluene (2 mL). The ligand mixture was added to the nickel suspension by cannula under strong stirring leading to an orange solution which progressively darkened to brown. The solution was heated at 60°C overnight and the solvents were evaporated to give a bright red powder. Crystals were obtained from slow vapour diffusion of

pentane in a toluene solution of the complex. NMR analyses were realised on the crude product with equimolar quantity of  $\text{NEt}_3\text{HBr}$ .  $^{31}\text{P}$  NMR (121 MHz,  $\text{CD}_2\text{Cl}_2$ , 300K):  $\delta$ (ppm): 88.9 (br s) and 106.57 (br d,  $^2J_{\text{PP}}$  ca. 75 Hz).

## 5.5 Procedure for unlocked NMR

As a general procedure, oven-dried NMR tubes were placed in a NMR tube holder connected to the Schlenk line, and purged. Then a portion of the reaction mixture was transferred under circulation of argon to the NMR tube *via* a cannula (or with a glass pipette); the tube was then sealed and analysed by NMR.

## 5.6 Procedure for ligand titration

The ligand was dissolved in  $\text{CDCl}_3$  (5 mL, 0.1 M) in a Schlenk. Triethylamine was added to this Schlenk by small portions (approx. 0.05 mmol). The mixture was shaken and a portion was transferred to a NMR tube under argon. Both  $^{31}\text{P}$  and  $^1\text{H}$  NMR were recorded and the content of the tube was replaced in the Schlenk. The operation was repeated several times with different concentrations of base. The exact molar ratio of base *vs.* ligand was determined from the relative integration of the  $\text{CH}_3$  signals of the triethylamine *vs.* the  $\text{CH}_3$  signals of the ligand.

## 5.7 Procedure for catalytic experiment

The reactor of 50 mL was dried under vacuum at  $100^\circ\text{C}$  for 2 hours and then filled at room temperature with ethylene at 1.4 bar. Catalyst solutions were injected through a septum (10  $\mu\text{mol}$  in 8mL of toluene) and methylaluminumoxane (2mL, 10% in toluene, 300 eq.) were injected. The temperature and pressure were set to  $45^\circ\text{C}$  and 35 bars. The reaction started with stirring and ethylene uptake and temperature were monitored. The reaction was stopped after 1 h. The reactor was cooled down to room temperature and the gas phase evacuated under stirring. The liquid was neutralised with aqueous  $\text{H}_2\text{SO}_4$  (20%) and the organic phase was analysed by GC.

# 6 References

- [1] F. W. Patureau, M. Kuil, A. J. Sandee, J. N. H. Reek, M. K. Frederic W. Patureau Albertus J. Sandee and Joost N.H. Reek, *Angew. Chem., Int. Ed.* **2008**, *47*, 3180–3183.
- [2] J. N. H. Reek, F. W. Patureau, M. Kuil, A. J. Sandee, J. Meeuwissen, *Coordination Complex System Comprising Tautomeric Ligands*, **2011**, U.S. Patent US 2011/0003959.
- [3] F. W. Patureau, M. a. Siegler, A. L. Spek, A. J. Sandee, S. Jugé, S. Aziz, A. Berkessel, J. N. H. Reek, *Eur. J. Inorg. Chem.* **2012**, *2012*, 496–503.
- [4] F. G. Terrade, M. Lutz, J. I. van der Vlugt, J. N. H. Reek, *Eur. J. Inorg. Chem.* **2014**, *2014*, 1826–1835.
- [5] T. León, M. Parera, A. Roglans, A. Riera, X. Verdaguer, *Angew. Chem., Int. Ed.* **2012**, *51*, 6951–6955.
- [6] F. W. Patureau, S. de Boer, M. Kuil, J. Meeuwissen, P.-A. R. Breuil, M. a. Siegler, A. L. Spek, A. J. Sandee, B. de Bruin, J. N. H. Reek, *J. Am. Chem. Soc.* **2009**, *131*, 6683–6685.
- [7] F. G. Terrade, M. Lutz, J. N. H. Reek, *Chem. Eur. J.* **2013**, *19*, 10458–10462.
- [8] T. Achard, L. Giordano, A. Tenaglia, Y. Gimbert, G. Buono, *Organometallics* **2010**, *29*, 3936–3950.
- [9] V. L. Foss, T. E. Chernykh, I. N. Staroverova, *J. Gen. Chem. USSR* **1983**, *10*, 1969–1976.

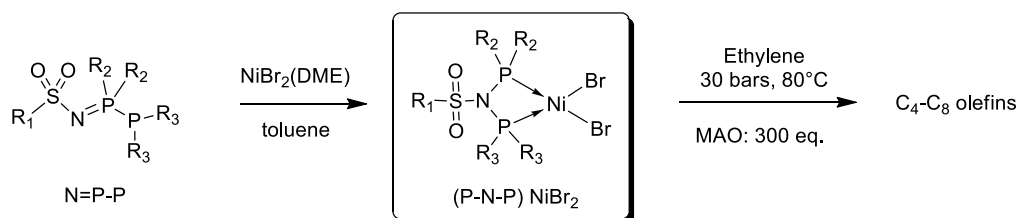
- [10] Z. Fei, R. Scopelliti, P. J. Dyson, *Dalt. Trans.* **2003**, 2772.
- [11] G. Ewart, D. S. Payne, A. L. Porte, A. P. Lane, *J. Chem. Soc.* **1962**, 3984–3990.
- [12] G. Ewart, A. P. Lane, J. Mckechnie, D. S. Payne, *J. Chem. Soc.* **1964**, 1543–1547.
- [13] D. S. Payne, D. A. Morton-Blake, A. P. Lane, *J. Chem. Soc.* **1967**, 1492–1498.
- [14] A. Schmidpeter, H. Rossknecht, *Angew. Chem., Int. Ed.* **1969**, 614–615.
- [15] M. Agostinho, V. Rosa, T. Avilés, R. Welter, P. Braunstein, *Dalton Trans.* **2009**, 814–822.
- [16] J. Gopalakrishnan, *Appl. Organomet. Chem.* **2009**, 23, 291–318.
- [17] D. Martin, D. Moraleda, T. Achard, L. Giordano, G. Buono, *Chem. Eur. J.* **2011**, 17, 12729–12740.
- [18] W. Keim, A. Behr, B. Gruber, B. Hoffmann, F. H. Kowaldt, U. Kürschner, B. Limbacher, F. P. Sístig, *Organometallics* **1986**, 5, 2356–2359.
- [19] W. Keim, F. H. Kowaldt, R. Goddard, C. Krüger, *Angew. Chem., Int. Ed.* **1978**, 17, 466–467.
- [20] A. Behr, W. Keim, G. Thelen, *J. Organomet. Chem.* **1983**, C38–C40.
- [21] P. Kuhn, D. Sémeril, D. Matt, M. J. Chetcuti, P. Lutz, *Dalt. Trans.* **2007**, 515–528.
- [22] P. Kuhn, D. Sémeril, C. Jeunesse, D. Matt, M. Neuburger, A. Mota, *Chem. Eur. J.* **2006**, 12, 5210–5219.
- [23] S. Bittner, Y. Assaf, P. Krief, I. M. Pomerantz, B. T. Ziemnicka, C. G. Smithld, *J. Org. Chem.* **1985**, 3, 1712–1718.
- [24] A. Khazaei, A. Rostami, Z. Tanbakouchian, Z. Zinati, *Catal. Commun.* **2006**, 7, 214–217.
- [25] I. Saikia, B. Kashyap, P. Phukan, *Chem. Commun.* **2011**, 47, 2967–2969.
- [26] L. Beaufort, L. Delaude, A. F. Noels, *Tetrahedron* **2007**, 63, 7003–7008.
- [27] P. Braunstein, Y. Chauvin, S. Mercier, L. Saussine, A. De Cian, J. Fischer, *Chem. Commun.* **1994**, 332, 2203.
- [28] P. Braunstein, Y. Chauvin, S. Mercier, L. Saussine, *C. R. Chim.* **2005**, 8, 31–38.
- [29] F. G. Terrade, Nature Inspired Catalytic Systems Using Sulfonamido-Phosphorus Based Complexes, University of Amsterdam, **2014**.
- [30] T. Q. Ly, A. M. Z. Slawin, J. D. Woollins, *Polyhedron* **1999**, 18, 1761–1766.
- [31] H. L. Milton, M. V. Wheatley, A. M. Z. Slawin, J. D. Woollins, *Polyhedron* **2004**, 23, 3211–3220.
- [32] P. Braunstein, C. Frison, X. Morise, R. D. Adams, *Dalt. Trans.* **2000**, 2205–2214.

# Chapter 3

---

## Iminobisphosphines to (non-) Symmetrical Di(phosphino)amine Ligands: Metal-Induced Synthesis of Diphosphorus Nickel and Chromium Complexes and Application in Olefin Oligomerisation Reactions

---



Part of this work has been published: P. Boulens, M. Lutz, E. Jeanneau, H. Olivier-Bourbigou, J. N. H. Reek, P. -A. R. Breuil *Eur. J. Inorg. Chem.* **2014**, 3754–3762

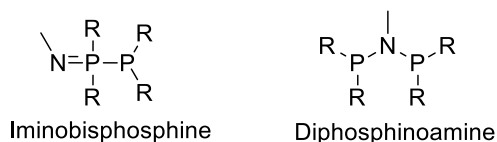
# 1 Introduction

The demand for short-chain olefins is still increasing and the need to develop robust and selective oligomerisation catalytic systems is of prime importance and pushed by the recent upswing in ethylene production. Over the past 60 years a great number of homogeneous nickel catalysts for olefin oligomerisation have been reported.<sup>[1-5]</sup> Among others, monophosphine ligands studied in the 1960s have shown to have significant positive effects on the selectivity in olefin oligomerisation, leading to industrial successes<sup>[6]</sup>. At that time, diphosphine ligands were scarce and the well-known 1,2-bis(diphenylphosphino)ethane (DPPE) led to nickel-based catalysts that display low activity in ethylene transformation<sup>[7,8]</sup>. A renewed interest in bidentate ligands, triggered by the advances in their synthesis, allowed the evaluation of symmetrical diphosphines with different bite angles and electronic properties. In the field of nickel-catalysed olefin oligomerisation, symmetrical carbon-bridged diphosphines ligands have shown activity leading to formation of oligomeric/polymeric products.<sup>[9-11]</sup> In addition, the groups of Le Floch<sup>[12]</sup> and Matt<sup>[13]</sup> respectively reported xanthene- and calixarene-based diphosphine nickel complexes associated to methylaluminumoxane (MAO) as active catalytic systems for ethylene dimerisation (butenes > 90%). Symmetrical di(phosphino)amine Ph<sub>2</sub>P-NR-PPh<sub>2</sub> nickel complexes (with R = Ph, CH<sub>2</sub>-C<sub>6</sub>H<sub>5</sub>, CH<sub>2</sub>-(C<sub>4</sub>H<sub>3</sub>O), CH<sub>2</sub>-(C<sub>4</sub>H<sub>3</sub>S), CH<sub>2</sub>-(C<sub>5</sub>H<sub>4</sub>N), CH<sub>2</sub>-CH<sub>2</sub>-(C<sub>4</sub>H<sub>3</sub>S)) were shown to oligomerise ethylene to light olefins with moderate activity when activated by MAO.<sup>[14,15]</sup> Introducing bulky groups (OMe, Me, Et, *i*Pr) on the *ortho* position of the arylphosphines switched the catalyst selectivity from oligomerisation to production of polyethylene.<sup>[16,17]</sup> So far the evaluation of ligands in this important reaction is limited to symmetrical bisphosphine ligated nickel complexes, mainly because of the lack of synthetic routes of non-symmetrical diphosphines. This has led us to develop, a synthetic route that allows the formation of nickel complexes based on non-symmetrical bidentate ligands. Herein, we report a metal-induced rearrangement strategy from iminobisphosphine ligands to symmetrical and non-symmetrical diphosphine nickel complexes. These nickel pre-catalysts can be activated using MAO, providing fast catalysts for ethylene and propylene oligomerisation reactions. Preliminary results are also reported, considering this rearrangement strategy for chromium in ethylene and propylene oligomerisation.

## 2 Results and Discussion

### 2.1 Synthesis of iminobisphosphines

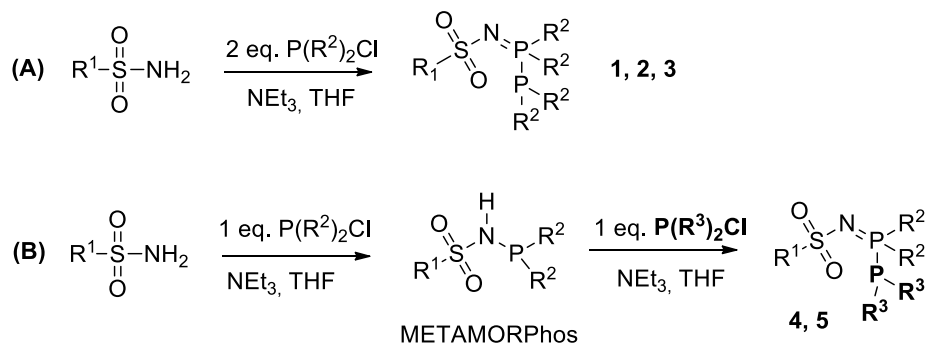
Iminobisphosphines (N=P-P) were described for the first time by Schmidpeter et al. in 1969.<sup>[18,19]</sup> However, their tendency to form oils (“schwer kristallisierbare Öle”) and to decompose were an obstacle to isolation and characterisation. Bulky and electron rich N-tosylamines have been described, leading to isolable iminobisphosphines TsN=PR<sub>2</sub>-PR<sub>2</sub> (with R = Et or *i*Pr).<sup>[20]</sup> More recently, Dyson et al. reported the preparation and isolation of stable aryl-substituted iminobisphosphines.<sup>[21]</sup> Generally these compounds are synthesised by reacting two equivalents of chlorophosphine with an amine. Iminobisphosphines may coexist with their di(phosphino)amine P-N-P isomer, in a ratio that depends on the nitrogen substitution (Scheme 1). Although homo-P substituted iminobisphosphines are now well described, the literature on hetero-P substituted iminobisphosphine ligands is scarce and limited to *in situ* NMR observations.<sup>[20]</sup> In the presence of Pt or Pd precursors, Dyson et al. showed that iminobisphosphines completely rearrange to the bidentate P-N-P system in which both phosphorus atoms are coordinated to the metal centre.<sup>[14,22,23]</sup> Recently, Shell also patented the synthesis of homo- and hetero-P substituted iminobisphosphine mixtures and their applications in chromium-catalysed ethylene oligomerisation.<sup>[24,25]</sup>



**Scheme 1.** Isomeric structures of iminobisphosphines (N=P-P) and di(phosphino)amines (P-N-P).

We recently introduced METAMORPhos as a new ligand scaffold that consists of a sulphonamide based phosphoramidite ligand.<sup>[26,27]</sup> The same sulphonamide building blocks were used in this work to prepare new iminobisphosphines, which were isolated as powders in moderate to good yields (up to 79%). The two different synthesis pathways explored: **(A)** or **(B)** are depicted in Scheme 2. Homo-P substituted iminobisphosphines were selectively obtained by reacting two equivalents of a chlorophosphine on a sulphonamide in presence of NEt<sub>3</sub> in THF **(A)**. On the other hand, hetero P-substituted iminobisphosphines were afforded *via* a two-step synthesis **(B)**. First, the sulphonamide reacted with a chlorophosphine to give an aminophosphine, which represents a typical METAMORPhos ligand. Then, in a

second step the aminophosphine reacted with a different chlorophosphine to yield the hetero-P substituted iminobisphosphine.



Ligand	R <sup>1</sup>	R <sup>2</sup>	R <sup>3</sup>	Isol. yield
<b>1</b>	(4-Br)C <sub>6</sub> H <sub>4</sub>	Ph	-	68 %
<b>2</b>	(4- <i>n</i> Bu)C <sub>6</sub> H <sub>4</sub>	Ph	-	79 %
<b>3</b>	(4-Br)C <sub>6</sub> H <sub>4</sub>	<i>i</i> Pr	-	58 %
<b>4</b>	(4- <i>n</i> Bu)C <sub>6</sub> H <sub>4</sub>	Ph	<i>i</i> Pr	34 %
<b>5</b>	(4- <i>n</i> Bu)C <sub>6</sub> H <sub>4</sub>	Ph	Cy	51 %

**Scheme 2.** Synthesis of homo- and hetero-P substituted iminobisphosphines.

## 2.2 Properties of iminobisphosphines

Single crystals were grown for homo- and hetero-P substituted ligands **2** and **4** by slow diffusion of pentane in a toluene solution of the ligand. The X-ray crystal structures confirmed the ligand structures. Importantly, the order of addition of chlorophosphines in the stepwise route during the synthesis is retained of the hetero-P substituted product, determines the final structure: i.e. the P(*i*Pr)<sub>2</sub> at the terminal P(III) position and PPh<sub>2</sub> at the central P(V) (Figure 1 and Figure 2). The formation of iminobisphosphines is probably due to a nucleophilic attack of the METAMORPhos phosphorus (route **B**) on the chlorophosphine, in agreement with the reaction-mechanism reported by Foss and co-workers.<sup>[28]</sup> P1-N1 and P1-P2 distances for both ligands in the solid state are close to that found in the literature.<sup>[21,23]</sup> The P(2)-P(1)-N(1) angle in ligand **2** is in the range of previously reported iminobisphosphines (115.00(5)°). However, for the hetero-P substituted ligand **4**, the P(2)-P(1)-N(1) angle is much shorter (99.5(1)°).

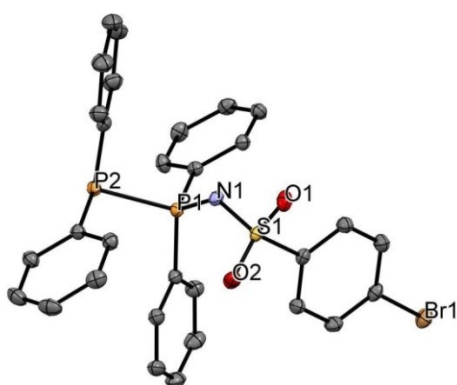


**Figure 1.** ORTEP plot (50% probability displacement ellipsoids) of ligand **1**. Hydrogen atoms have been omitted for clarity. Selected bond lengths (Å) and angles (°): S(1)-O(1) 1.4446(11); S(1)-O(2) 1.4448(11); S(1)-N(1) 1.5726(12); P(1)-P(2) 2.2221(5); P(1)-N(1) 1.6000(12); O(1)-S(1)-O(2) 116.50(7), O(1)-S(1)-N(1) 106.98(6); O(1)-S(1)-C(1) 105.97(7); O(2)-S(1)-N(1) 112.83(6); P(2)-P(1)-N(1) 115.00(5).

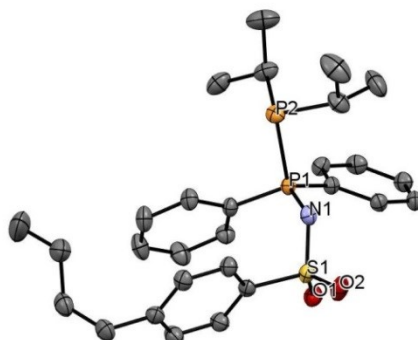


**Figure 2.** ORTEP plot (50% probability displacement ellipsoids) of ligand **4**. Hydrogen atoms have been omitted for clarity. Selected bond lengths (Å) and angles (°): S(1)-O(1) 1.441(3); S(1)-O(2) 1.446(3); S(1)-N(1) 1.591(2); P(1)-P(2) 2.200(1); P(1)-N(1) 1.615(2); O(1)-S(1)-O(2) 116.6(1), O(1)-S(1)-N(1) 107.5(1); O(1)-S(1)-C(25) 106.7(1); O(2)-S(1)-N(1) 113.0(1); P(2)-P(1)-N(1) 99.5(1).

The iminobisphosphines bear a central P(V) and a terminal P(III) atom, resulting in two characteristic doublets in the  $^{31}\text{P}$  NMR spectrum, with a  $^1J_{PP}$  coupling constants of ca. 300 Hz. From 2D  $^{31}\text{P}\{^1\text{H}\}$  experiment on the hetero-P substituted ligand **4**, we assigned the doublet upfield at  $\delta = 2.80$  ppm to terminal  $\text{P}(i\text{Pr})_2$  and the downfield chemical shift at  $\delta = 20.13$  ppm to central  $\text{PPh}_2$  leading to comprehensive  $^{31}\text{P}$  NMR characterisation of all ligands. The  $^{31}\text{P}\{^1\text{H}\}$  chemical shifts and the  $^1J_{PP}$  values for ligands **1-5** are reported in Table 1. Basic substituents on the phosphines induce a chemical shift displacement downfield. In addition,  $^1J_{PP}$  coupling constants increase with the phosphine basicity. Indeed, iminobisphosphines with basic substituents such as **3** ( $^1J_{PP} = 329$  Hz) have greater coupling constants compared to the aryl-substituted compounds ( $^1J_{PP} = 281$  Hz for **1**).

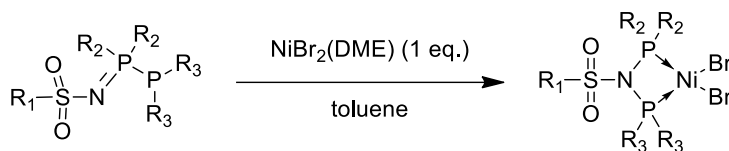
**Table 1.**  $^{31}\text{P}$  chemical shifts  $\delta$ (ppm) and coupling constants  $^1J_{PP}$ (Hz) of ligands **1-5** in  $\text{CD}_2\text{Cl}_2$ .

Ligand	P(V) - $\delta$	P(III) - $\delta$	$^1J_{PP}$ (Hz)
<b>1</b>	Ph: 19.72	Ph: -18.74	281
<b>2</b>	Ph: 19.47	Ph: -17.90	278
<b>3</b>	<i>i</i> Pr: 50.39	<i>i</i> Pr: -6.32	329
<b>4</b>	Ph: 20.13	<i>i</i> Pr: 2.80	312
<b>5</b>	Ph: 20.44	Cy: -4.98	315



### 2.3 Reaction of iminobisphosphines with nickel (II)

Upon reaction of ligands **1-5** with NiBr<sub>2</sub>(DME) (DME = dimethoxyethane) as the metal precursor, complete conversion into di(phosphino)amine-chelated nickel complexes **6-10**, respectively, was observed. Accordingly, the <sup>31</sup>P NMR spectra display a singlet for the symmetrical complexes **6-8** and two doublets with a small coupling constant (<sup>2</sup>J<sub>PP</sub> = 119.6 and 118.6 Hz for **9** and **10**, respectively), typical for *cis*-oriented ligands in nickel complexes. The red, diamagnetic complexes were obtained in moderate to good isolated yields (up to 80%, Scheme 3). This approach constitutes an elegant way to generate unprecedented symmetrical P-alkyl and non-symmetrical diphosphine nickel complexes. Crystals of complexes **6** (symmetrical), **9** and **10** (unsymmetrical) suitable for X-ray diffraction were grown from slow vapour diffusion of pentane into dichloromethane / toluene solutions. ORTEP diagrams are shown in Figure 3, Figure 4 and Figure 5 along with selected bond lengths and bond angles. All three nickel complexes adopt a square-planar geometry with a constrained *cis*-coordination of the ligand, similar to the published di(phosphino)amine nickel complexes. The bond lengths and angles of the various complexes in the solid state are very similar. The substitution only slightly affects the P-N bond length, which is longer for basic phosphines; in complex **9**, N-PPh<sub>2</sub>: 1.727(3) Å and N-P(*i*Pr)<sub>2</sub>: 1.752(3) Å and in complex **10**, N-PPh<sub>2</sub>: 1.7449(15) Å and N-PCy<sub>2</sub>: 1.7512(15) Å. The bite angles of all the complexes are in the same range (97.16(8) < P-N-P < 97.37(15) and 75.54(2) < P-Ni-P < 75.976(19)).



Complex	R <sub>1</sub>	R <sub>2</sub>	R <sub>3</sub>	Isol. yield %
<b>6</b>	4-BrPh	Ph	Ph	80
<b>7</b>	4- <i>n</i> BuPh	Ph	Ph	68
<b>8</b>	4-BrPh	<i>i</i> Pr	<i>i</i> Pr	57
<b>9</b>	4- <i>n</i> BuPh	Ph	<i>i</i> Pr	61
<b>10</b>	4- <i>n</i> BuPh	Ph	Cy	54

**Scheme 3.** Synthesis of di(phosphino)amine-NiBr<sub>2</sub> complexes.

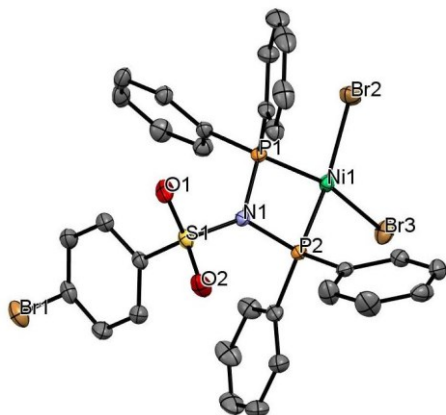


**Figure 3.** ORTEP plot (50% probability displacement ellipsoids) of complex **6**. Hydrogen atoms and  $\text{CH}_2\text{Cl}_2$  solvent molecules have been omitted for clarity. Selected bond lengths (Å) and angles (°): Br(2)-Ni(1) 2.3230(4); Br(3)-Ni(1) 2.3307(4); Ni(1)-P(1) 2.1277(6); Ni(1)-P(2) 2.1212(6); P(1)-N(1) 1.7316(18); P(2)-N(1) 1.7385(18); Br(2)-Ni(1)-Br(3) 99.703(13); Br(2)-Ni(1)-P(1) 91.250(19); Br(2)-Ni(1)-P(2) 163.48(2); Br(3)-Ni(1)-P(1) 164.82(2); Br(3)-Ni(1)-P(2) 95.203(19); P(1)-Ni(1)-P(2) 75.54(2); Ni(1)-P(1)-N(1) 93.33(6); Ni(1)-P(2)-N(1) 93.36(6); P(1)-N(1)-P(2) 97.17(9).

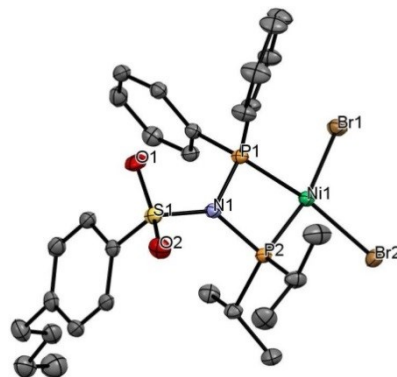


**Figure 4.** ORTEP plot (50% probability displacement ellipsoids) of complex **9**. Hydrogen atoms and  $\text{CH}_2\text{Cl}_2$  solvent molecules have been omitted for clarity. Selected bond lengths (Å) and angles (°): Br(1)-Ni(1) 2.3334(6); Br(2)-Ni(1) 2.3275(6); Ni(1)-P(1) 2.1189(10); Ni(1)-P(2) 2.1284(10); P(1)-N(1) 1.727(3); P(2)-N(1) 1.752(3); Br(1)-Ni(1)-Br(2) 98.87(2); Br(1)-Ni(1)-P(1) 92.91(3); Br(1)-Ni(1)-P(2) 168.24(3); Br(2)-Ni(1)-P(1) 168.00(3); Br(2)-Ni(1)-P(2) 92.44(3); P(1)-Ni(1)-P(2) 75.93(4); Ni(1)-P(1)-N(1) 93.85(10); Ni(1)-P(2)-N(1) 92.79(10); P(1)-N(1)-P(2) 97.37(15).

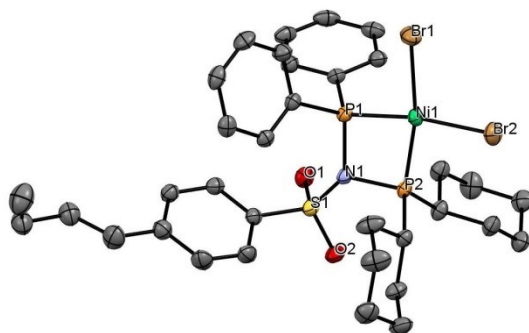
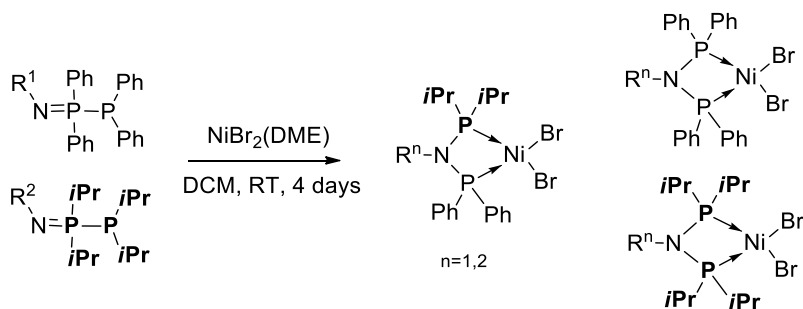


**Figure 5.** ORTEP plot (50% probability displacement ellipsoids) of complex **10**. Hydrogen atoms have been omitted for clarity. Selected bond lengths (Å) and angles (°): Br(1)-Ni(1) 2.3314(3); Br(2)-Ni(1) 2.3200(3); Ni(1)-P(1) 2.1194(5); Ni(1)-P(2) 2.1401(5); P(1)-N(1) 1.7449(15); P(2)-N(1) 1.7512(15); Br(1)-Ni(1)-Br(2) 97.109(12); Br(1)-Ni(1)-P(1) 92.018(16); Br(1)-Ni(1)-P(2) 167.949(18); Br(2)-Ni(1)-P(1) 170.843(18); Br(2)-Ni(1)-P(2) 94.884(16); P(1)-Ni(1)-P(2) 75.976(19); Ni(1)-P(1)-N(1) 93.78(5); Ni(1)-P(2)-N(1) 92.88(5); P(1)-N(1)-P(2) 97.16(8).

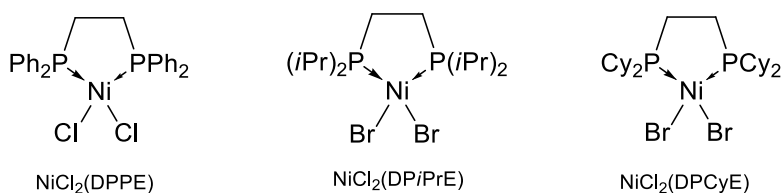
## 2.4 Nickel-induced rearrangement of iminobisphosphines

We were interested in the mechanism of the metal induced rearrangement of these ligands and therefore we performed some additional experiments. Upon mixing ligand **3** with NiBr<sub>2</sub>(DME), the signals of the free ligand disappeared and we observed two new resonances, at  $\delta(\text{CD}_2\text{Cl}_2)$ : 133.6 ppm and  $\delta(\text{CD}_2\text{Cl}_2)$ : 36.6 ppm. The resonance at 133.6 ppm is characteristic for di(isopropyl)phosphine bromide and is also observed when the synthesis is performed in halogen-free solvents such as toluene, showing that the halogen source is most likely the nickel precursor. The resonance at 36.6 ppm is in the range of the R-NH-PR<sub>2</sub> fragment. These observations are in line with the proposed metal-induced rearrangement reported by Dyson et al. for Pd and Pt.<sup>[15]</sup> In this mechanism the P-P bond of the iminobisphosphine is proposed to be homolitically cleaved, releasing a chlorophosphine and the remaining fragment. Additionally, we reasoned that this rearrangement may also involve intermolecular processes. Therefore we did an experiment in which we mixed the homo-P substituted iminobisphosphines **2** (Ph, Ph) and **3** (*i*Pr, *i*Pr) with 2 eq. of NiBr<sub>2</sub>(DME). After 5 min complete conversion of ligand **2** to the symmetrical complex **7** was observed in addition to free ligand **3**. After 4 days stirring, a mixture of homo- and hetero-substituted complexes was observed (Scheme 4). Surprisingly, the addition of one equivalent of ligand **3** (*i*Pr, *i*Pr) to a solution of isolated complex **7** (Ph, Ph), resulted in the formation of only one non-symmetrical complex (<sup>2</sup>J<sub>PP</sub> = 120 Hz) along with the starting materials, and the formation of homocomplex **8** was not observed. This demonstrates that the P-P bond is more likely to be cleaved in P-alkyl based systems and that the P-N bond as in the di(phosphino)amine complex **7** may also be broken. Importantly, mixing the two isolated complexes **7** (Ph, Ph) and **8** (*i*Pr, *i*Pr) did not lead to the formation of non-symmetrical complexes, indicating that the complexes themselves are sufficiently stable (in absence of triggers) for catalysis. Some decomposition products and paramagnetic compounds were, however, formed after 4 days.



**Scheme 4.** Scrambling experiment on complex formation: 2 symmetrical iminobisphosphines and NiBr<sub>2</sub>(DME) (2eq.) in DCM.

The symmetrical and non-symmetrical bidentate P-N-P nickel complexes **7-10** were evaluated in ethylene oligomerisation using methylaluminoxane (MAO, 10% wt. in toluene) as activator. Three diphosphine nickel complexes  $\text{NiCl}_2(\text{DPPE})$ ,  $\text{NiBr}_2(\text{DP}i\text{PrE})$  and  $\text{NiBr}_2(\text{DPCyE})$  were prepared to evaluate the electronic and chelating effects on the catalytic outcome (Scheme 5). Ethylene oligomerisation reactions were carried out under two different sets of conditions: 30 bar / 45°C and 5 bar / 30°C. All the reactions were duplicated and turned out to be reproducible (see Table 2 and Table 3).



**Scheme 5.** Reference diphosphine nickel complexes for ethylene oligomerisation:  $\text{NiCl}_2(\text{DPPE})$ ,  $\text{NiBr}_2(\text{DP}i\text{PrE})$  and  $\text{NiBr}_2(\text{DPCyE})$ .

## 2.5 Nickel complexes evaluation in ethylene oligomerisation

Upon activation with MAO at 30 bar and 45°C, complex **7** is moderately productive for short chain oligomers ( $14 \times 10^3 \text{ g}_{\text{oligomers}} \cdot (\text{g}_{\text{Ni}} \cdot \text{h})^{-1}$ , see Table 2). The deactivation, observed experimentally by a decrease in ethylene uptake in time, is attributed to an unstable active species as a black deposit was recovered at the end of the reaction. Interestingly, the novel alkyl-substituted (PNP') $\text{NiBr}_2$  complexes **8, 9, 10** were very active ( $70\text{-}81 \times 10^3 \text{ g}_{\text{oligomers}} \cdot (\text{g}_{\text{Ni}} \cdot \text{h})^{-1}$ ) and the exothermic reaction resulted in a temperature change (up to + 23°C). Compared to the aryl-disubstituted complex **7**, they were five times more active showing that basic phosphorus moieties are beneficial for the activity. In contrast, the ethylene-bridged diphosphine nickel complexes  $\text{NiCl}_2(\text{DPPE})$ ,  $\text{NiBr}_2(\text{DPCyE})$  and  $\text{NiBr}_2(\text{DP}i\text{PrE})$  gave oligomers with low activity and the reaction temperature could be controlled at 45-50°C during the reaction. The activity and selectivity displayed by  $\text{NiCl}_2(\text{DPPE})$  and  $\text{NiBr}_2(\text{DPCyE})$  is similar to the methylene-bridged diphosphine complexes reported by the group of Pringle and Wass.<sup>[4]</sup>

**Table 2.** Results of catalytic reactions of ethylene oligomerisation at 30 bar C<sub>2</sub>H<sub>4</sub>, 45°C for complexes **7-10** and references NiCl<sub>2</sub>(DPPE), NiBr<sub>2</sub>(DiPrPE) and NiBr<sub>2</sub>(DPCyE).

Complex	T <sub>max</sub> (°C)	Mass of products (g)	Prod. <sup>[a]</sup>	Product distribution <sup>[b]</sup>			1- C <sub>4</sub> <sup>[c]</sup>
				C <sub>4</sub>	C <sub>6</sub>	C <sub>8</sub> <sup>+</sup>	
<b>7</b>	52	8.4	14	92.4	6.6	1.0	57.7
<b>8</b> <sup>[d]</sup>	77	36.1	80	71.5	18.3	10.2	22.3
<b>9</b> <sup>[d]</sup>	65	36.2	81	71.7	17.9	10.4	20.9
<b>10</b> <sup>[d]</sup>	70	33.1	70	68.1	19.4	12.5	22.2
<b>NiCl<sub>2</sub>(DPPE)</b>	51	2.9	5	93.2	5.3	1.6	38.0
<b>NiBr<sub>2</sub>(DiPrPE)</b>	50	1.3	2	79.1	15.3	5.6	67.7

Reaction conditions: n<sub>Ni</sub> = 10 μmol, MAO (300 eq.), toluene (50 mL), 1h (unless stated otherwise).  
[a] Productivity x 10<sup>3</sup> g<sub>oligomers</sub>·(g<sub>Ni</sub>·h)<sup>-1</sup>; [b] Product analysis performed by GC (wt.%); [c] wt.% 1-C<sub>4</sub> in C<sub>4</sub> fraction; [d] stopped at 45 min.

Performing the catalytic experiments under milder conditions (5 bar and 30 °C) allowed full control of the reaction temperature. By applying these conditions it was possible to keep the ethylene uptake linear and catalysts were still active after 60 min. The symmetrical diphenyl-P substituted complex **7** was barely active at 5 bar and 30°C affording mainly dimers (Table 3) The nitrogen substitution of all the complexes, namely the -SO<sub>2</sub>- moiety did not have a crucial impact on the catalysis since N-alkyl substituted complexes of general formula R-CH<sub>2</sub>-N(PPh<sub>2</sub>)<sub>2</sub>, developed by the group of Wu<sup>[7]</sup> were equivalent in terms of activity to the symmetrical diphenyl-P substituted complex **7**. If not directly impacting catalysis, the sulphonyl group enhanced the stability of the synthetic intermediates and gave the possibility to reach a variety of homo- and hetero-substituted nickel complexes, especially some with basic phosphines. The corresponding isopropyl di-substituted analogue **8** showed high productivity and moderate selectivity for butenes (66.5 %) and low alpha selectivity (10.7 %). Selectivity in 1-C<sub>4</sub> is lower than that obtained in Table 2 demonstrating that isomerisation of 1-C<sub>4</sub> into 2-C<sub>4</sub> can be dependent on operating conditions. Lower ethylene concentration in the liquid phase induced by lower pressure at iso temperature favours this side reaction. The non-symmetric complexes **9** (Ph,*i*Pr) and **10** (Ph,Cy) activated by MAO were also very active and moderately selective to butenes formation (67.0 and 60.4 %, respectively).

**Table 3.** Results of catalytic reactions of ethylene oligomerisation at 5 bar C<sub>2</sub>H<sub>4</sub>, 30°C for complexes **7-10**.

Complex	Tmax (°C)	Mass of products (g)	Prod. <sup>[a]</sup>	Product distribution <sup>[b]</sup>			1-C <sub>4</sub> <sup>[c]</sup>
				C <sub>4</sub>	C <sub>6</sub>	C <sub>8</sub> <sup>+</sup>	
<b>7</b>	30	3.0	5	94.4	4.8	0.8	11.9
<b>8</b>	34	23.9	41	66.5	22.4	11.2	10.7
<b>9</b>	30	17.0	29	67.0	21.8	11.3	10.1
<b>10</b>	30	25.9	36	60.4	24.9	14.7	9.4

Reaction conditions : n<sub>Ni</sub> = 10 μmol , MAO (300 eq.), toluene (50 mL), 1h; <sup>[a]</sup> Productivity x 10<sup>3</sup> g<sub>oligomers</sub>·(g<sub>Ni</sub>·h)<sup>-1</sup>; <sup>[b]</sup> Product analysis performed by GC (wt.%); <sup>[c]</sup> wt.% 1-C<sub>4</sub> in C<sub>4</sub> fraction.

The moderate selectivity for the terminal linear olefins in the C<sub>4</sub> and C<sub>6</sub> fractions obtained when complexes **7-10** were used as catalysts (see Table 3) is likely to result from two different processes, *i.e.* isomerisation that converts for instance 1-C<sub>4</sub> into 2-C<sub>4</sub> and/or co-dimerisation of butenes and ethylene to branched hexenes. We therefore looked in detail at the C<sub>6</sub> products to attempt to understand the mechanistic pathways. The identification of all the C<sub>6</sub> isomers (1-hexene, 2-hexene (*cis* + *trans*), 3-hexene (*cis* + *trans*), ethyl-2-butene-1, methyl-3-pentene-1, methyl-3-pentene-2 (*cis* + *trans*)) was possible by coupling GC and GC-MS analyses and is presented for systems **7-10** in Table 4.

**Table 4.** Isomer distribution in the C<sub>6</sub> cut for complexes **7-10** determined by GC.

% of C <sub>6</sub>	HEX1	HEX2	HEX3	M3P1	M3P2	E2B1
<b>7</b>	4,4	24,5	9,3	12,0	35,6	14,2
<b>8</b>	0,7	6,2	1,6	12,2	59,6	19,7
<b>9</b>	0,7	7,2	1,6	12,1	61,6	17,3
<b>10</b>	0,5	5,4	1,3	10,9	63,5	18,4

Reaction conditions: see Table 3. HEX1: 1-hexene; HEX2: 2-hexenes (*cis* and *trans*); HEX3: 3-hexenes (*cis* and *trans*); M3P1: methyl-3-pentene-1; M3P2: methyl-3-pentenes-2 (*cis* and *trans*); E2B1: ethyl-2-butene-1.

Analysis of the C<sub>6</sub> products formed from the experiment in which precatalyst **7** was used, revealed the presence of up to 38.2 % of linear C<sub>6</sub> olefins compared to 9.6 % maximum for precatalysts **8-10** containing P-alkyl moieties. Remarkably, the symmetrical and non-symmetrical precatalysts **8-10** present the same product distribution pattern in C<sub>6</sub> oligomers, methylpentenes being the predominant isomers with up to 74.4 wt.% in the C<sub>6</sub> fraction. While linear isomers are expected to be formed from parallel ethylene reactions, branched products are likely formed from consecutive co-dimerisation reactions of ethylene and butenes and not by parallel polyaddition of ethylene. To gain understanding on co-dimerisation, we monitored

the product formation in the liquid phase using **8** as the precatalyst. Samples of the reaction mixture taken after 12 min showed that the linear C<sub>6</sub> / branched C<sub>6</sub> ratio was identical to the one quantified after 1h reaction time. This demonstrates that co-dimerisation is not only observed when butenes are accumulated in the medium but also at the start of the reaction. Considering the very high content of branched isomers at different reaction times, we conclude that for our alkyl-based di(phosphino)amine nickel catalysts the co-dimerisation reactions are competitive with ethylene oligomerisation.

## 2.6 Nickel catalyst evaluation in propylene oligomerisation

The dimerisation of propylene with a nickel(II) catalyst precursors that does not contain any phosphine ligand and activated with EADC (ethylchloroaluminium) usually gives oligomers with uncontrolled regioselectivity, typically a mixture of dimethylbutenes (4%), methylpentenes (87%) and n-hexenes (9%).<sup>[29]</sup> It is well-known that the use of bulky and basic phosphine ligands, such as triisopropylphosphine or tricyclohexylphosphine (PCy<sub>3</sub>), can drive the reaction to high selectivity in 2,3-dimethylbutenes (2,3-DMB-1 and 2,3-DMB-2). 2,3-Dimethylbutenes are especially important since they can be used as key starting olefins for fine chemical intermediates. 2,3-DMB-2 is used for the synthesis of Danitol<sup>TM</sup>, which is a high performance pyrethroid insecticide invented by Sumitomo in 1976, and to produce other intermediates (Pinacolone). 2,3-DMB-1 is a key intermediate for the production of musk fragrances (Tonalid<sup>TM</sup>).<sup>[30-32]</sup> A lot of studies have been made on the Ni-phosphine catalytic systems in order to improve the activity and the selectivity,<sup>[33,34]</sup> but the use of diphosphine ligands associated with MAO as activator of nickel precursors has not been reported so far.

The reference complex NiCl<sub>2</sub>(PCy<sub>3</sub>)<sub>2</sub> and the precatalysts **7-10** were evaluated upon MAO activation in chlorobenzene for propylene oligomerisation (Table 8). The experimental conditions had to be adapted to the manipulation and reactivity of liquid propylene and are the following. The solvent was first introduced with *n*-heptane as internal standard in the reactor. Propylene (4 g) was then introduced and the reactor was cooled to 10°C. Then the nickel complex solution was introduced, followed by the MAO cocatalyst. The mass of propylene introduced was then increased to 20 g and the reaction was performed in closed batch. Starting the reaction at low temperature (10°C) allowed controlling the initial reaction exotherm due to the high concentration of propylene in the liquid phase. After 10 minutes, the reactor was heated and maintained at 45°C. The reaction progress could be followed by the decrease of pressure in the reactor and by analysis of aliquot of liquid products formed.

For  $\text{NiCl}_2(\text{PCy}_3)_2$ , low propylene conversion (9 wt.%) was observed after 10 minutes at  $10^\circ\text{C}$ , while a rapid increase in product formation was measured at  $45^\circ\text{C}$  (73 % after 20 additional minutes and up to 85% after 110 minutes, Table 5, Entries 1-3). The product analysis showed a change in selectivity depending on propylene conversion. Indeed, a shift towards heavier products ( $\text{C}_9$ ,  $\text{C}_{12}$ ) was observed at higher conversions. This is explained by an increase of hexenes concentration relative to propylene concentration in time, favouring the co-dimerisation reactions ( $\text{C}_3+\text{C}_6$  or  $\text{C}_6+\text{C}_6$ ).

The complexes **7-10** were then evaluated under identical conditions ( $T = 45^\circ\text{C}$ ) and product selectivity was compared at similar ( $> 65$  wt.%) propylene conversions (Table 5, Entries 4-7). After 110 minutes, up to 81% conversion was obtained with excellent selectivity of 95.8 % in hexenes when complex **7** bearing a symmetrical aromatic diphosphinoamine ligand was applied. This result is surprising since the same catalyst is almost inactive for ethylene oligomerisation (see Table 3). However, monitoring the pressure decrease in the reactor for catalytic reactions with complexes **7-10** shows that complex **7** is more active at low temperature ( $10^\circ\text{C}$  for the first 10 min) than at higher temperature ( $45^\circ\text{C}$ ). This suggests catalyst decomposition of phenyl substituted phosphines at higher temperature, a phenomenon already observed by the group of Wu.<sup>[14]</sup> Complex **7** afforded a poor selectivity of 19.1 % in DMBs (Table 6, Entry 4) under these conditions. Complex **8**, based on a symmetrical alkyl di(phosphino)amine ligand, gave much more formation of heavier products  $\text{C}_9$  to  $\text{C}_{15}^+$  (59.8 % dimers relative to all products) compared to complex **7**, despite a lower propylene conversion.

An enhanced selectivity in DMBs in the  $\text{C}_6$  fraction was obtained for complex **8** (52.4 %) (Table 6, Entry 5) compared to complex **7**. This result shows that the effect of alkyl-based phosphine ligands is maintained in the case of bidentate symmetrical alkyl diphosphine ligand.

The use of dissymmetrical complexes **9** and **10** lead to the formation of mainly dimers (80%) even at high propylene conversions (64 and 75 wt.%, respectively, Table 5, entries 6-7). In addition, the selectivity in DMB in the  $\text{C}_6$  fraction is  $> 40\%$  (Table 6, entries 5-7). This demonstrates that the introduction of only one alkyl-based phosphino group already affects the catalytic properties of the nickel complex.

As a conclusion, the nature of the di(phosphino)amine ligands has a great impact on the nickel catalysed propylene dimerisation. Symmetrical aromatic di(phosphino)amine ligands gave rise to the formation of dimers with uncontrolled



regioselectivity (methylpentenes are the main dimers). The introduction of at least one alkyl-phosphino group on the chelating bidentate ligand leads to a more controlled reaction resulting in the formation of 2,3-DMB-1 as the main dimer.

**Table 5.** Oligomerisation of propylene: product distribution.

Entry	Complex	Conversion <sup>[d]</sup> (wt.%)	Oligomer distribution (wt.%) <sup>[a]</sup>			
			C <sub>6</sub>	C <sub>9</sub>	C <sub>12</sub>	C <sub>15</sub> <sup>+</sup>
1	<b>NiCl<sub>2</sub>(PCy<sub>3</sub>)<sub>2</sub></b> <sup>[b]</sup>	9	70.2	15.5	5.3	9.0
2	<b>NiCl<sub>2</sub>(PCy<sub>3</sub>)<sub>2</sub></b> <sup>[c]</sup>	73	62.7	19.4	8.0	9.9
3	<b>NiCl<sub>2</sub>(PCy<sub>3</sub>)<sub>2</sub></b>	85	56.5	23.3	10.8	9.4
4	<b>7</b>	35-40	95.8	3.3	0.7	0.2
5	<b>8</b>	75-80	59.8	23.0	9.0	8.2
6	<b>9</b>	60-65	81.3	12.3	3.9	2.5
7	<b>10</b>	50-53	80.1	14.0	4.3	1.6

Reaction conditions: 20 g C<sub>3</sub>H<sub>6</sub>, 45°C unless stated, co-catalyst: MAO (300 eq.) n<sub>Ni</sub> = 10 μmol, solvent: chlorobenzene, reaction volume: 50 mL, reaction time: 110 min unless stated, <sup>[a]</sup> Determined by GC based on analysis of an aliquot of the liquid phase and in reference to n-heptane. 1-3 <sup>[b]</sup> Reaction time: 10mn, T= 10°C. <sup>[c]</sup> Reaction time: 30mn T=10-45°C. <sup>[d]</sup> Conversion determined by GC for entries 1-3, and by pressure monitoring at 85 min for entries 4-7 (estimation).

**Table 6.** Oligomerisation of propylene: dimer selectivity<sup>[a]</sup>

Entry	Complex	4M1P	1-DMB	4M2P	2M1P	2M2P	Hex	2-DMB
3	<b>NiCl<sub>2</sub>(PCy<sub>3</sub>)<sub>2</sub></b>	0.6	72.8	6.3	12.9	4.1	2.4	0.9
4	<b>7</b>	1.3	17.8	9.6	29.2	29.7	11.1	1.3
5	<b>8</b>	3.9	47.0	5.8	25.8	9.1	3.0	5.4
6	<b>9</b>	1.9	37.9	11.8	25.3	13.9	6.4	2.8
7	<b>10</b>	1.8	44.7	7.8	25.5	12.3	4.8	3.1

<sup>[a]</sup> For reaction conditions, see Table 8. Dimer selectivity (wt.%) determined by GC/MS. **4M1P**: 4-methyl-1-pentene; **1-DMB**: 2,3-dimethylbut-1-ene; **4M2P**: 4-methyl-2-pentene; **2M1P**: 2-methyl-1-pentene; **2M2P**: 2-methyl-2-pentene; **Hex**: hexenes; **2-DMB**: 2,3-dimethylbut-2-ene. <sup>[b]</sup> 10 min. <sup>[c]</sup> 30 min.

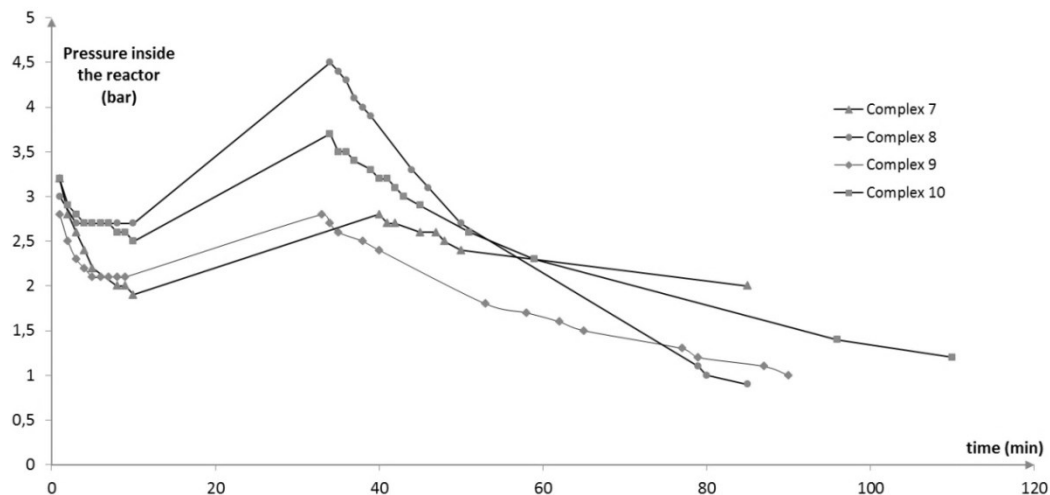


**Figure 6.** Pressure monitoring for the catalytic oligomerisation reactions of propylene with catalysts 7-10 in batch reactor; From 0-10 min:  $T=10^{\circ}\text{C}$ , from 10 to (35-40) min temperature increase to  $45^{\circ}\text{C}$ , from (35-40) min to 90 min:  $T=45^{\circ}\text{C}$ .

## 2.7 Ligand evaluation in chromium-catalysed ethylene oligomerisation

Di(phosphino)amine ligands  $\text{R}_2\text{PN}(\text{R})\text{PR}_2$  (Figure 7) associated with chromium have been reported by BP<sup>[35,36]</sup> and Sasol<sup>[37-43]</sup> as efficient catalysts upon MAO activation for selective ethylene trimerisation or tetramerisation to 1-hexene or 1-octene, respectively. Up to now, the iminobisphosphine rearrangement to di(phosphino)amine known for late transition metals as palladium, platinum or nickel has not been explicitly described with early transition metals. Shell, however, claimed in a patent that mixtures of iminobisphosphines (Figure 7), a chromium precursor and MAO led to the formation of selective catalysts for 1-octene production.<sup>[24,25,44]</sup> These results suggested the chromium mediated rearrangement of iminobisphosphines to di(phosphino)amine. We therefore sought to determine how the introduction of electron withdrawing sulphonyl fragment on the nitrogen atom could impact the ligand rearrangement in presence of chromium and the selectivity of these associations with MAO in ethylene oligomerisation.



injected in the different reactors as a suspension while limpid solutions were obtained from mixing the different ligands with  $\text{CrCl}_3(\text{THF})_3$ . For comparison, we also evaluated the di(phosphino)amines reported by Sasol (Figure 7) with  $\text{Cr}(\text{acac})_3$  in similar reaction conditions. High activity and selectivity were obtained for the reference catalyst, with up to  $130 \times 10^3 \text{ g}_{\text{oligomers}} \cdot (\text{g}_{\text{Cr}} \cdot \text{h})^{-1}$  and 70% of octenes relative to all other products with 98.8% of 1-octene in this  $\text{C}_8$  fraction. The other products formed were hexenes (16%), a distribution of heavier products (13%) and polyethylene (< 1%). The systems formed by the different ligands **1-3** and chromium precursors displayed very low reactivity within one hour reaction time and ethylene uptake did not exceeded 2 g. Such low ethylene consumption did not allow calculating representative activities. GC analysis of the different liquid phases showed wide oligomer distributions with similar Schulz-Flory constant ( $K_{\text{SF}} = 0.57 - 0.68$ ) showing no specific ligand effect on the catalytic outcome. These preliminary tests suggested that either the complex formation with the different ligands was not effective or that these ligands have a detrimental effect on chromium-catalysed ethylene oligomerisation.

### 3 Conclusion

Starting from sulphonamide moieties, we prepared several stable iminobisphosphines bearing P-aryl, P-alkyl or mixture of both groups. We showed that the metal-induced rearrangement to di(phosphino)amine complexes is likely initiated by P-P bond cleavage and that the ligand redistribution can involve an intermolecular process. This path allows easy generation of new alkylphosphine substituted complexes  $(\text{PNP})\text{NiBr}_2$  and non-symmetrical complexes  $(\text{PNP}')\text{NiBr}_2$ . Activated by MAO, the alkyl-P containing catalysts are efficient for ethylene oligomerisation. Besides displaying a high productivity, these systems display an unusual product distribution of butenes along with oligomers ( $\text{C}_6$  and  $\text{C}_8^+$ ) that are mainly composed of branched olefins that are favoured by co-dimerisation processes. In propylene oligomerisation, we observed a clear influence of the di(phosphino)amine moiety on the product distribution, the dimers being favoured over the heavier products ( $\text{C}_9^+$ ) with aromatic phosphino groups while alkyl moieties enhanced the dimethylbutene formation within the  $\text{C}_6$  fraction. Using dissymmetrical disphosphinoamine complexes allows combining both effects leading to an overall yield of 29% in DMBs for complex **10** bearing a diphenylphosphino and a dicyclohexylphosphino group. Different iminobisphosphines were evaluated for *in situ* chromium-catalysed ethylene oligomerisation revealing low activity and no particular selectivity for the different combinations.

## 4 Experimental Section

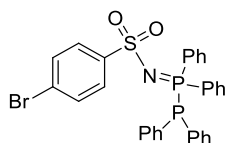
### 4.1 General

All reactions were carried out under an atmosphere of nitrogen using standard Schlenk techniques. Sulphonamides and reference ligands were purchased from commercial suppliers and used without further purification. Chlorophosphines were distilled trap to trap under reduced pressure. MAO (10% in toluene) was purchased from Chemtura and stored cold. THF, pentane and Et<sub>2</sub>O were distilled from sodium and benzophenone. CH<sub>2</sub>Cl<sub>2</sub>, chlorobenzene and triethylamine were distilled from CaH<sub>2</sub>, toluene from sodium, under nitrogen. NMR spectra (<sup>1</sup>H, <sup>1</sup>H{<sup>31</sup>P}, <sup>31</sup>P, <sup>31</sup>P{<sup>1</sup>H} and <sup>13</sup>C{<sup>1</sup>H}) were measured on a Varian MERCURY 300 MHz, or a BRUKER 300 MHz spectrometer at 300K. High resolution FAB (Fast Atom Bombardment) mass spectra were recorded on a JEOL JMS SX/SX102A four sector mass spectrometer. Calculated spectra were obtained with JEOL Isotopic Simulator (version 1.3.0.0). Analyses of liquid phases were performed on a GC Agilent 6850 Series II equipped with a PONA column. The gas phases for ethylene oligomerisation were analysed by gas GC on HP 6890.

### 4.2 Ligand synthesis

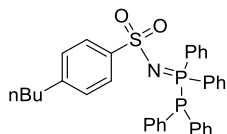
The syntheses of metamorphos ligands were described in Chapter 2 and run accordingly<sup>[23,45]</sup>

#### Synthesis of 4-bromo-N-(1,1,2,2-tetraphenyldiphosphanylidene) benzenesulphonamide 1:



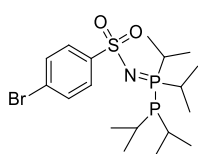
4-bromobenzene-1-sulphonamide (500 mg, 2.12 mmol, 1.0 eq.) was dissolved in tetrahydrofuran (10 mL) and triethylamine (1.6 mL, 11.2 mmol, 5.3 eq.) leading to a clear colourless solution. Distilled diphenylchlorophosphine (0.760 mL, 4.24 mmol, 2.0 eq.) was added dropwise under strong magnetic stirring at room temperature. The suspension was left to stir 5 min at room temperature. The suspension was then filtered under nitrogen atmosphere and the resulting clear solution was evaporated to a white solid. The solid was dissolved in a minimum of dichloromethane and pentane (20 mL) was added. Upon evaporation under reduced pressure, a precipitate formed. The liquid was syringed out and the powder was washed twice with pentane (10 mL). Finally the product was dried under reduced pressure affording a white powder (isolate yield: 870 mg, 68%). Crystals suitable for XR diffraction were obtained by slow diffusion of pentane in a saturated dichloromethane solution of the product. <sup>1</sup>H NMR (300 MHz, CD<sub>2</sub>Cl<sub>2</sub>, 300K) δ(ppm) 7.82 – 6.89 (m, 24H). <sup>31</sup>P NMR (121 MHz, CD<sub>2</sub>Cl<sub>2</sub>, 300K) 19.72 (d, <sup>1</sup>J<sub>PP</sub> = 281.1 Hz), -18.74 (d, <sup>1</sup>J<sub>PP</sub> = 281.1 Hz). <sup>31</sup>P{<sup>1</sup>H} NMR (121 MHz, CD<sub>2</sub>Cl<sub>2</sub>, 300K) δ(ppm) 19.72 (d, <sup>1</sup>J<sub>PP</sub> = 279.9 Hz), -18.74 (d, <sup>1</sup>J<sub>PP</sub> = 281.2 Hz). <sup>13</sup>C NMR (75 MHz, CD<sub>2</sub>Cl<sub>2</sub>, 300K) δ(ppm) 124.96 (s, C<sup>IV</sup>, C-Br); 127.42 (dd, <sup>2</sup>J<sub>CP</sub> = 81.8 Hz, <sup>3</sup>J<sub>CP</sub> = 10.2 Hz, C<sup>IV</sup><sub>Ph2 ipso</sub>, 4C); 127.81 (s, CH<sub>ArSO2</sub>, 2C); 129.00 (d, <sup>3</sup>J<sub>CP</sub> = 12.3 Hz, CH<sub>Ar meta</sub>, 4C); 129.17 (dd, <sup>3</sup>J<sub>CP</sub> = 7.9, <sup>4</sup>J<sub>CP</sub> = 1.1 Hz, CH<sub>Ar meta</sub>, 4C); 130.95 (d, <sup>4</sup>J<sub>CP</sub> = 2.4 Hz, CH<sub>Ar para</sub>, 2C); 131.56 (s, CH<sub>ArSO2</sub>, 2C); 133.22 (d, <sup>4</sup>J<sub>CP</sub> = 3.1 Hz, CH<sub>Ar para</sub>, 2C); 133.47 (dd, <sup>2</sup>J<sub>CP</sub> = 9.71 Hz, <sup>3</sup>J<sub>CP</sub> = 4.54 Hz, CH<sub>Ar ortho</sub>, 4C); 135.75 (dd, <sup>2</sup>J<sub>CP</sub> = 21.1 Hz, <sup>3</sup>J<sub>CP</sub> = 7.2 Hz, CH<sub>Ar ortho</sub>, 4C); 145.90 (d, <sup>3</sup>J<sub>CP</sub> = 3.2 Hz, C<sup>IV</sup>, C-SO<sub>2</sub>). MS(FAB<sup>+</sup>): m/z calcd. for C<sub>30</sub>H<sub>25</sub>NO<sub>2</sub>P<sub>2</sub>BrS ([MH]<sup>+</sup>): 606,0248; obsd.: 606,0255. Anal. found (calcd.) for C<sub>30</sub>H<sub>25</sub>NO<sub>2</sub>P<sub>2</sub>BrS: C, 59.53 (59.61); H, 3.85 (4.00); N, 2.26 (2.32).

### Synthesis of 4-butyl-N-(1,1,2,2-tetraphenyldiphosphanylidene)benzenesulphonamide 2:



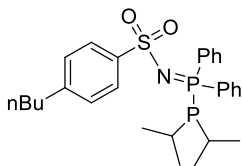
4-butylbenzene-1-sulphonamide (500 mg, 2.34 mmol, 1 eq.) was dissolved in tetrahydrofuran (20 mL) and triethylamine (1 mL, 7.17 mmol, 3 eq.) leading to a clear colourless solution. Distilled diphenylchlorophosphine (0.945 mL, 4.98 mmol, 2.1 eq.) was added dropwise under strong magnetic stirring at room temperature. The suspension was left to stir 5 min at room temperature. The suspension was then filtered under nitrogen atmosphere and the resulting clear solution was evaporated to an oil. The oil was dissolved in Et<sub>2</sub>O (10 mL) and evaporated without heating means. This step was repeated 4 times until the combined increase in concentration and loss in temperature caused the product to precipitate. The solid was vacuum dried to obtain a white powder (isolate yield: 1.07 g, 79%). <sup>1</sup>H NMR (300 MHz, CD<sub>2</sub>Cl<sub>2</sub>, 300K): δ(ppm)= 7.91 – 6.33 (m, -CH<sub>Ar</sub>, 24H), 2.59 (t, <sup>3</sup>J<sub>HH</sub> = 7.7 Hz, CH<sub>3</sub>-CH<sub>2</sub>-CH<sub>2</sub>-CH<sub>2</sub>-CAr, 2H), 1.57 (m, CH<sub>3</sub>-CH<sub>2</sub>-CH<sub>2</sub>-CH<sub>2</sub>-CAr, 2H), 1.33 (m, CH<sub>3</sub>-CH<sub>2</sub>-CH<sub>2</sub>-CH<sub>2</sub>-CAr, 2H), 0.93 (t, <sup>3</sup>J<sub>HH</sub> = 7.3 Hz CH<sub>3</sub>-CH<sub>2</sub>-CH<sub>2</sub>-CH<sub>2</sub>-Ar, 3H). <sup>13</sup>C NMR (75 MHz, CD<sub>2</sub>Cl<sub>2</sub>, 300K): δ(ppm)= 14.09 (CH<sub>3</sub>); 22.63 (CH<sub>2</sub>-CH<sub>3</sub>); 33.87 (CH<sub>2</sub>-CH<sub>2</sub>-CH<sub>3</sub>); 35.72 (Ar-CH<sub>2</sub>); 125.98 (C<sub>Ar-SO<sub>2</sub></sub>, 2C); 127.89 (dd, <sup>1</sup>J<sub>PC</sub> = 81.5 Hz, <sup>2</sup>J<sub>CP</sub> = 10.2 Hz, C<sup>IV</sup><sub>PPh2 ipso</sub>, 4C); 128.80 (C<sub>Ar-SO<sub>2</sub></sub>, 2C); 128.88 (d, <sup>3</sup>J<sub>CP</sub> = 12.3 Hz, CH<sub>PPh2 meta</sub>, 4C); 129.08 (dd, <sup>3</sup>J<sub>CP</sub> = 7.8 Hz, <sup>4</sup>J<sub>CP</sub> = 0.9 Hz, CH<sub>PPh2 meta</sub>, 4C); 130.81 (d, <sup>4</sup>J<sub>CP</sub> = 2.3 Hz, CH<sub>PPh2 para</sub>, 2C); 133.03 (d, <sup>4</sup>J<sub>CP</sub> = 3.0 Hz, CH<sub>PPh2 para</sub>, 2C); 133.46 (dd, <sup>2</sup>J<sub>CP</sub> = 9.6 Hz, <sup>3</sup>J<sub>CP</sub> = 4.4 Hz, CH<sub>PPh2 ortho</sub>, 2C); 135.76 (dd, <sup>2</sup>J<sub>CP</sub> = 21.05 Hz, <sup>3</sup>J<sub>CP</sub> = 7.3 Hz, CH<sub>PPh2 ortho</sub>, 2C); 144.20 (d, <sup>3</sup>J<sub>CP</sub> = 3.3 Hz, C<sup>IV</sup><sub>C-SO<sub>2</sub></sub>); 145.99 (C<sup>IV</sup><sub>C-nBu</sub>). <sup>31</sup>P{<sup>1</sup>H} NMR (121 MHz, CD<sub>2</sub>Cl<sub>2</sub>, 300K): δ(ppm)= 19.47 (d, <sup>1</sup>J<sub>PP</sub> = 277.9 Hz), -17.90 (d, <sup>1</sup>J<sub>PP</sub> = 278.0 Hz). MS (FAB+): m/z calcd. For C<sub>34</sub>H<sub>34</sub>O<sub>2</sub>NP<sub>2</sub>S ([M+H]<sup>+</sup>): 582.1786; obsd.: 582.1790; Anal. found (calcd.) for C<sub>34</sub>H<sub>34</sub>O<sub>2</sub>NP<sub>2</sub>S: C, 70.11 (70.21); H, 5.93 (5.72); N, 2.50 (2.41).

### Synthesis of 4-bromo-N-(1,1,2,2-tetraisopropyldiphosphanylidene)benzenesulphonamide 3:



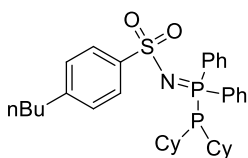
4-bromobenzene-1-sulphonamide (2 g, 8.47 mmol, 1 eq.) was dissolved in tetrahydrofuran (20 mL) and triethylamine (3.6 mL, 25.4 mmol, 3 eq.) leading to a clear colourless solution. Commercial diisopropylchlorophosphine (2.95 mL, 18.5 mmol, 2.2 eq.) was added dropwise under strong magnetic stirring at room temperature. The suspension was left to stir for 2 days at room temperature. The suspension was then filtered under nitrogen atmosphere and the resulting clear solution was evaporated to a white solid. The solid was suspended in pentane (10 mL) and evaporated without heating means. This step was repeated once. The solid was dissolved in a minimum of dichloromethane (4 mL) and pentane (60 mL) was added causing a solid to form. The liquid was syringed out and the powder was washed twice with pentane (10 mL). Finally the product was dried under reduced pressure affording a white powder (isolate yield: 2.3 g, 58%). <sup>1</sup>H NMR (300 MHz, CD<sub>2</sub>Cl<sub>2</sub>, 300K): δ(ppm)= 7.87 – 7.30 (m, CH<sub>Ar</sub> 4H), 2.72 (m, CH<sub>iPr</sub>, 2H), 2.49 (m, CH<sub>iPr</sub>, 2H), 1.63 – 0.97 (m, CH<sub>3</sub>, 24H). <sup>31</sup>P{<sup>1</sup>H} NMR (121 MHz, CD<sub>2</sub>Cl<sub>2</sub>, 300K): δ(ppm)= 50.39 (d, <sup>1</sup>J<sub>PP</sub> = 329.5 Hz), -6.30 (d, <sup>1</sup>J<sub>PP</sub> = 329.8 Hz). <sup>13</sup>C NMR (75 MHz, CD<sub>2</sub>Cl<sub>2</sub>, 300K) δ(ppm) 17.50 (m, CH<sub>3 iPr</sub>, 4C); 21.09 (dd, <sup>2</sup>J<sub>CP</sub> = 9.6 Hz, <sup>3</sup>J<sub>CP</sub> = 7.9 Hz, CH<sub>3 iPr</sub>, 2C); 22.33 (dd, <sup>1</sup>J<sub>CP</sub> = 21.8 & <sup>2</sup>J<sub>CP</sub> = 4.15 Hz, CH<sub>iPr</sub>, 2C); 23.15 (dd, <sup>2</sup>J<sub>CP</sub> = 20.9 Hz, <sup>3</sup>J<sub>CP</sub> = 6.9 Hz, CH<sub>3 iPr</sub>, 2C); 28.86 (dd, <sup>1</sup>J<sub>CP</sub> = 42.14 Hz, <sup>2</sup>J<sub>CP</sub> = 6.9 Hz, CH<sub>iPr</sub>, 2C); 124.73 (C<sup>IV</sup><sub>C-Br</sub>); 127.65 (CH<sub>Ar-SO<sub>2</sub></sub>, 2C); 131.69 (CH<sub>Ar-SO<sub>2</sub></sub>, 2C); 146.69 (C<sup>IV</sup><sub>C-SO<sub>2</sub></sub>). Anal. found (calcd.) for C<sub>18</sub>H<sub>32</sub>BrNO<sub>2</sub>P<sub>2</sub>S: C, 46.11 (46.16); H, 6.98 (6.89); N, 3.01 (2.99).

### Synthesis of 4-butyl-N-(1,1-diisopropyl-2,2-diphenyldiphosphanilydene)benzenesulphonamide 4:



4-butylbenzene-1-sulphonamide-bisphenyl-phosphine (1g, 4.68 mmol, 1 eq.) was dissolved in tetrahydrofuran (20 mL) and triethylamine (1.3 mL, 9.36 mmol, 2 eq.) leading to a clear colourless solution. Commercial diisopropylchlorophosphine (0.746 mL, 4.68 mmol, 1 eq.) was added dropwise under strong magnetic stirring at room temperature. The suspension was left to stir 10 min at room temperature. The suspension was then filtered under nitrogen atmosphere and the resulting clear solution was evaporated to an oil. Pentane (20 mL) was added to the oil under strong stirring then after decantation, the upper layer was syringed out. The oil was suspended in pentane (10 mL) and evaporated without heating means. This step was repeated once with pentane (10 mL) and twice with Et<sub>2</sub>O (10 mL). The combined increase in concentration and loss in temperature caused the product to precipitate. Pentane (20 mL) was added to wash the powder and was syringed out and the solvent vacuum dried affording a white solid (isolate yield: 808 mg, 34%). <sup>1</sup>H NMR (300 MHz, CD<sub>2</sub>Cl<sub>2</sub>, 300K): δ(ppm)= 7.98 – 7.83 (m, 4H, -PPh<sub>2</sub>), 7.76 – 7.64 (m, -CH<sub>2</sub>-Ar-SO<sub>2</sub>, 2H), 7.60 – 7.35 (m, -PPh<sub>2</sub>, 6H), 7.23 – 7.12 (m, -CH<sub>2</sub>-Ar-SO<sub>2</sub>, 2H), 2.69 – 2.57 (t, <sup>2</sup>J<sub>HH</sub> = 7.4 Hz, CH<sub>3</sub>-CH<sub>2</sub>-CH<sub>2</sub>-CH<sub>2</sub>-Ar, 2H), 2.44 (m, 2H, CH<sub>2</sub>-Ar), 1.69 – 1.48 (m, CH<sub>3</sub>-CH<sub>2</sub>-CH<sub>2</sub>-CH<sub>2</sub>-Ar, 2H), 1.35 (m, CH<sub>3</sub>-CH<sub>2</sub>-CH<sub>2</sub>-CH<sub>2</sub>-Ar, 2H), 1.18 – 0.99 (m, CH<sub>3</sub>-CH<sub>2</sub>-CH<sub>2</sub>-CH<sub>2</sub>-Ar, 2H), 0.93 (t, <sup>3</sup>J<sub>HH</sub> = 7.3 Hz, CH<sub>3</sub>-CH<sub>2</sub>-CH<sub>2</sub>-CH<sub>2</sub>-Ar, 3H). <sup>31</sup>P{<sup>1</sup>H} NMR (121 MHz, CD<sub>2</sub>Cl<sub>2</sub>, 300K): δ(ppm)= 20.13 (d, <sup>1</sup>J<sub>PP</sub> = 311.6 Hz); 2.80 (d, <sup>1</sup>J<sub>PP</sub> = 311.6 Hz). <sup>13</sup>C NMR (75 MHz, CD<sub>2</sub>Cl<sub>2</sub>, 300K): δ(ppm)= 14.10 (CH<sub>3</sub>); 20.70 (dd, J<sub>CP</sub> = 10.6 & 9.2 Hz, CH<sub>3</sub>-CH<sub>2</sub>-CH<sub>2</sub>-CH<sub>2</sub>-Ar, 2H); 22.67 (CH<sub>2</sub>-CH<sub>2</sub>-CH<sub>2</sub>-CH<sub>2</sub>-Ar, 2H); 22.75 (d, J<sub>CP</sub> = 3.0 Hz, CH<sub>2</sub>-CH<sub>2</sub>-CH<sub>2</sub>-CH<sub>2</sub>-Ar, 2H); 23.01 (CH<sub>2</sub>-CH<sub>2</sub>-CH<sub>2</sub>-CH<sub>2</sub>-Ar, 2H); 23.18 (dd, <sup>2</sup>J<sub>CP</sub> = 18.1 Hz, <sup>3</sup>J<sub>CP</sub> = 7.6 Hz, CH<sub>3</sub>-CH<sub>2</sub>-CH<sub>2</sub>-CH<sub>2</sub>-Ar, 2H); 35.77 (Ar-CH<sub>2</sub>-CH<sub>2</sub>-Ar, 2H); 126.02 (C<sub>Ar-SO<sub>2</sub></sub>, 2C); 128.63 (C<sub>Ar-SO<sub>2</sub></sub>, 2C); 129.11 (d, <sup>3</sup>J<sub>CP</sub> = 12.4 Hz, CH<sub>2</sub>-CH<sub>2</sub>-CH<sub>2</sub>-CH<sub>2</sub>-Ar, 2H); 130.78 (dd, <sup>1</sup>J<sub>CP</sub> = 83.6, <sup>2</sup>J<sub>CP</sub> = 9.7 Hz, C<sup>IV</sup><sub>PPH<sub>2</sub></sub> ipso, 4C); 132.61 (dd, J<sub>CP</sub> = 9.4 & 6.0 Hz, CH<sub>2</sub>-CH<sub>2</sub>-CH<sub>2</sub>-CH<sub>2</sub>-Ar, 6C); 144.60 (d, <sup>3</sup>J<sub>CP</sub> = 4.9 Hz, C<sup>IV</sup><sub>CSO<sub>2</sub></sub>, 2C); 146.15 (C<sup>IV</sup><sub>CSO<sub>2</sub></sub>, 2C); 146.15 (C<sup>IV</sup><sub>C-nBu</sub>). Anal. found (calcd.) for C<sub>28</sub>H<sub>37</sub>N<sub>2</sub>O<sub>2</sub>P<sub>2</sub>S: C, 65.53 (65.48); H, 7.34 (7.16); N, 2.60 (2.73).

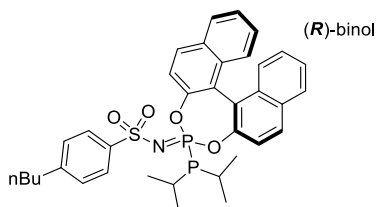
### Synthesis of 4-butyl-N-(1,1-dicyclohexyl-2,2-diphenyldiphosphanilydene)benzenesulphonamide 5:



4-butylbenzene-1-sulphonamide-bisphenyl-phosphine (360 mg, 0.91 mmol, 1 eq.) was dissolved in tetrahydrofuran (10 mL) and triethylamine (0.126 mL, 1.82 mmol, 2 eq.) leading to a clear colourless solution. Commercial dicyclohexylchlorophosphine (0.200 mL, 0.91 mmol, 1 eq.) was added dropwise under strong magnetic stirring at room temperature. The suspension was left to stir 5 min at room temperature. The suspension was then filtered under nitrogen atmosphere and the resulting clear solution was evaporated to an oil. The oil was suspended in pentane (10 mL) and evaporated without heating means. This step was repeated once with pentane (10 mL) and twice with Et<sub>2</sub>O (10 mL). The combined increase in concentration and loss in temperature caused the product to precipitate. Pentane (20 mL) was added to wash the powder and the powder was vacuum dried affording a white solid (isolate yield: 273 mg, 51%). <sup>1</sup>H NMR (300 MHz, CD<sub>2</sub>Cl<sub>2</sub>, 300K): δ(ppm)= 7.90 (dd, J = 12.5 and 7.6 Hz, PPh<sub>2</sub>, 4H), 7.78 – 7.67 (dd, J = 8.4, 2.0 Hz, Ar-SO<sub>2</sub>, 2H), 7.61 – 7.40 (m, PPh<sub>2</sub>, 6H), 7.18 (dd, J = 8.4 Hz and 2.0 Hz, Ar-SO<sub>2</sub>, 2H), 2.63 (t, <sup>2</sup>J<sub>HH</sub> = 7.6 Hz, -CH<sub>2</sub>-Ar, 2H), 2.30 – 2.01 (m, Cy, 2H), 1.81 (m, Cy, 2H), 1.73 – 1.49 (m, Cy, 8H), 1.73 – 1.49 (m, -CH<sub>2</sub>-CH<sub>2</sub>-Ar, 2H) 1.33 (dt, <sup>2</sup>J<sub>HH</sub> = 16.3, 7.3 Hz, -CH<sub>2</sub>-CH<sub>2</sub>-CH<sub>2</sub>-Ar, 2H), 1.17 (m, Cy, 10H), 0.93 (t, <sup>3</sup>J<sub>HH</sub> = 7.3 Hz, H<sub>3</sub>C-CH<sub>2</sub>-CH<sub>2</sub>-CH<sub>2</sub>-Ar, 3H). <sup>31</sup>P{<sup>1</sup>H} NMR (121 MHz, CD<sub>2</sub>Cl<sub>2</sub>, 300K): δ(ppm)= 20.44 (d, <sup>1</sup>J<sub>PP</sub> = 314.9 Hz), -4.98 (d, <sup>1</sup>J<sub>PP</sub> = 314.4 Hz). <sup>13</sup>C NMR (75 MHz, CD<sub>2</sub>Cl<sub>2</sub>, 300K): δ(ppm)= 4.08 (CH<sub>3</sub>); 22.65 (CH<sub>2</sub>-CH<sub>2</sub>-CH<sub>2</sub>-CH<sub>2</sub>-Ar, 2H); 26.31 (d, J<sub>CP</sub> = 0.8 Hz, CH<sub>2</sub>-CH<sub>2</sub>-CH<sub>2</sub>-CH<sub>2</sub>-Ar, 2H); 27.47 (d, J<sub>CP</sub> = 8.9 Hz, CH<sub>2</sub>-CH<sub>2</sub>-CH<sub>2</sub>-CH<sub>2</sub>-Ar, 2H);

27.74 (d,  $J_{CP} = 12.4$  Hz,  $\text{CH}_2$  Cy, 2C); 30.88 (m,  $J_{CP} = 8.9$  Hz,  $\text{CH}_2$  Cy, 2C); 32.81 (dd,  $^1J_{CP} = 20.54$  Hz,  $^2J_{CP} = 2.91$  Hz,  $\text{CH-P}$  Cy, 2C); 33.30 (dd,  $J_{CP} = 15.8$ ,  $J = 7.4$  Hz,  $\text{CH}_2$  Cy, 2C); 33.88 ( $-\text{CH}_2-\text{CH}_2-\text{CH}_3$ ); 35.71 (Ar- $\text{CH}_2-\text{CH}_2$ ); 126.02 ( $\text{CH}_{\text{Ar-SO}_2}$ , 2C); 128.59 ( $\text{CH}_{\text{Ar-SO}_2}$ , 2C); 129.03 (d,  $^3J_{CP} = 12.2$  Hz,  $\text{CH}_{\text{PPh}_2 \text{ meta}}$ , 4C); 131.30 (dd,  $^1J_{CP} = 84.0$  Hz,  $^2J_{CP} = 9.2$  Hz,  $\text{C}_{\text{PPh}_2 \text{ ispo}}$ , 2C); 132.51 (d,  $^4J_{CP} = 3.1$  Hz,  $\text{CH}_{\text{PPh}_2 \text{ para}}$ , 2C); 132.55 (dd,  $^2J_{CP} = 9.8$  &  $^3J_{CP} = 6.0$  Hz,  $\text{CH}_{\text{PPh}_2 \text{ ortho}}$ , 4C); 144.76 (d,  $^3J_{CP} = 5.0$  Hz,  $\text{C}_{\text{IV}}$ , C-SO<sub>2</sub>); 146.06 (s,  $\text{C}_{\text{IV}}$ , C-nBu). MS (FAB<sup>+</sup>): m/z calcd. For  $\text{C}_{34}\text{H}_{34}\text{O}_2\text{NP}_2\text{S}$  ([M+H]<sup>+</sup>): 594.2725; obsd.: 594.2732. Anal. found (calcd.) for  $\text{C}_{34}\text{H}_{34}\text{O}_2\text{NP}_2\text{S}$ : C, 68.76 (68.78); H, 7.73 (7.64); N, 2.38 (2.36).

### Synthesis of ligand iminophosphite-phosphine:

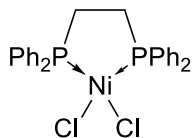


Chiral metamorphos (ligand **2** of Chapter 2, 1.0 g, 1.6 mmol, 1.0 eq.) was suspended in dry THF (20 mL). To this solution chlorodiisopropylphosphine (253  $\mu\text{L}$ , 1.6 mmol, 1.0 eq.) was added dropwise leading to a white precipitate and the suspension was stirred for 16 h at RT. The suspension was then filtered under argon atmosphere and the resulting clear solution was evaporated to white foam. The foam was submitted twice to co-evaporation with diethyl ether (2 x 5 mL)

followed by twice with pentane (2 x 5 mL) to give a sticky solid. The solid was re-suspended in pentane (5 mL) and left in an ultrasonic bath for 10 min at RT and the solvent was co-evaporated. The previous operation was repeated twice to give a solid which was washed with pentane (3 x 20 mL) and dried under vacuum to a white powder (isolated: 828 mg, 81 % yield).  $^{31}\text{P}\{^1\text{H}\}$  NMR (121 MHz,  $\text{CD}_2\text{Cl}_2$ , 300K):  $\delta$  (ppm): -2.77 (d,  $^1J_{PP} = 350.1$  Hz); 49.89 (d,  $^1J_{PP} = 350.2$  Hz);  $^{31}\text{P}$  NMR (121 MHz,  $\text{CD}_2\text{Cl}_2$ , 300 K):  $\delta$  (ppm): -2.78 (br d,  $^1J_{PP} = 350.1$  Hz); 49.88 (ddd,  $^1J_{PP} = 350.1$  Hz,  $^xJ_{PH} = 21.2$  Hz,  $^yJ_{PH} = 16.3$  Hz).  $^1\text{H}$  NMR (300 MHz,  $\text{CD}_2\text{Cl}_2$ , 300K):  $\delta$  (ppm): 0.86 (t,  $^3J_{HH} = 7.2$  Hz,  $-\text{CH}_3$ , 3H); 1.05-1.50 (m,  $\text{CH}_3-\text{CH}_2-\text{CH}_2-\text{CH}_2-\text{Ar}$  and  $\text{CH}_3$   $_{\text{iPr}}$ , 16H); 2.30-2.53 (m, Ar- $\text{CH}_2-$  and  $\text{CH}_{\text{iPr}}$ , 3H); 2.74 (m,  $\text{CH}_{\text{iPr}}$ , 1H); 6.76 (d,  $^3J_{HH} = 8.3$  Hz,  $\text{CH}_{\text{Ar}}$ , 2H); 7.20-7.41 (m,  $\text{CH}_{\text{binol}}$ , 4H); 7.37 (d,  $^3J_{HH} = 8.4$  Hz,  $\text{CH}_{\text{Ar}}$ , 2H); 7.43-7.60 (m,  $\text{CH}_{\text{binol}}$ , 4H); 7.84-8.10 (m,  $\text{CH}_{\text{binol}}$ , 4H). MS(FAB<sup>+</sup>): m/z calcd. for  $\text{C}_{36}\text{H}_{39}\text{NO}_4\text{P}_2\text{S}$  ([MH]<sup>+</sup>): 644.2153; obsd. 644.2156.

### 4.3 Complex synthesis

#### Synthesis of nickel (II) dichloride (1,2-bis(diphenylphosphino)ethane): $\text{NiCl}_2(\text{DPPE})$ :

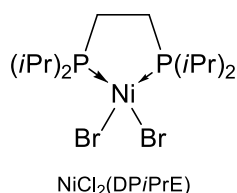


$\text{NiCl}_2(\text{DPPE})$

To a suspension of nickel (II) chloride dimethoxyethane adduct (325 mg, 1.48 mmol, 1 eq.) in dichloromethane (50 mL) was added a solution of 1,2-bis(diphenylphosphino)ethane (653 mg, 1.64 mmol, 1.1 eq.) dissolved in dichloromethane (20 mL). The mixture was stirred overnight at RT to give a red precipitate. The solvents are evaporated under reduced pressure and the powder was washed with pentane (3x 20 mL) and dried under vacuum to give a dark red solid (isolate yield: 444 mg, 54%).  $^1\text{H}$  NMR (300 MHz,  $\text{CD}_2\text{Cl}_2$ , 300K):  $\delta$ (ppm)= 2.15 (t,  $^3J_{PP} = 18$  Hz,  $-\text{CH}_2-$ , 4H); 7.50-7.63 (m, 12  $\text{H}_{\text{Ar}}$ ); 7.90-8.02 (m,  $\text{CH}_{\text{PPh}_2}$  8H).  $^{31}\text{P}\{^1\text{H}\}$  NMR (121 MHz,  $\text{CD}_2\text{Cl}_2$ , 300K)  $\delta$ (ppm) 57.55 (s).  $^{13}\text{C}$  NMR (75 MHz,  $\text{CD}_2\text{Cl}_2$ , 300K)  $\delta$ (ppm) 28.17 (t,  $^1J_{CP} = 25$  Hz,  $\text{CH}_2$ , 2C); 128.90 (t,  $^1J_{CP} = 25$  Hz,  $\text{C}_{\text{IV}}^{\text{PPh}_2}$ , 4C); 129.37 (t,  $^3J_{CP} = 5.4$  Hz,  $\text{CH}_{\text{PPh}_2 \text{ meta}}$ , 8C); 132.25 (s,  $\text{CH}_{\text{PPh}_2 \text{ para}}$ , 4C); 134.05 (t,  $^2J_{CP} = 4.7$  Hz,  $\text{CH}_{\text{PPh}_2 \text{ ortho}}$ , 8C).



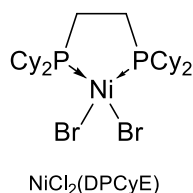
### Synthesis of nickel (II) dibromide (1,2-bis(diisopropylphosphino)ethane): NiCl<sub>2</sub>(DPiPrE):



To a suspension of nickel (II) bromide dimethoxyethane adduct (324 mg, 1.05 mmol, 1 eq.) in dichloromethane (20 mL) was added commercial 1,2-bis(diisopropylphosphino)ethane (300 mg, 1 mmol, 1.1 eq.). The insoluble mixture was stirred for 16 h after which the solvent was evaporated under vacuum. The resulting powder was washed with pentane (4 x 10 mL) to get rid of the excess ligand and the DME. The resulting powder was dried under vacuum. Isolate yield: 360 mg, 75%. The product was conform to the literature.<sup>[46]</sup>

<sup>1</sup>H NMR (300 MHz, CD<sub>2</sub>Cl<sub>2</sub>, 300K) overlapping signals of CH<sub>2</sub> and *i*Pr; <sup>31</sup>P{<sup>1</sup>H} NMR (121 MHz, CD<sub>2</sub>Cl<sub>2</sub>, 300K) δ(ppm) 95.37 (s). <sup>13</sup>C NMR (75 MHz, CD<sub>2</sub>Cl<sub>2</sub>, 300K) δ(ppm) 18.89 (s, -CH<sub>3</sub>); 20.90 (s, -CH<sub>3</sub>); 21.68 (t, <sup>1</sup>J<sub>CP</sub> = 19.3 Hz, -CH<sub>2</sub>); 28.08 (t, <sup>1</sup>J<sub>CP</sub> = 13.4 Hz, CH *i*Pr). Anal. found (calcd.) for C<sub>14</sub>H<sub>32</sub>Br<sub>2</sub>NiP<sub>2</sub>: C, 34.87 (34.97); H, 6.78 (6.71).

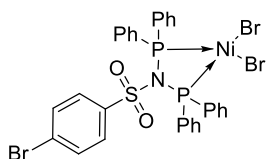
### Synthesis of nickel (II) dibromide (1,2-bis(dicyclohexylphosphino)ethane): NiCl<sub>2</sub>(DPCyE):



To a suspension of nickel (II) bromide dimethoxyethane adduct (322 mg, 1.04 mmol, 1.1 eq.) in dichloromethane (20 mL) was added commercial 1,2-bis(dicyclohexylphosphino)ethane (400 mg, 0.946 mmol 1 eq.). The mixture turned brown red after a few seconds and the solid was consumed. After 10 min, the mixture was passed through a syringe filter and the red solution evaporated under reduced pressure. The orange solid formed was washed with 3 x 10 mL of pentane. The solid was then dried under vacuum to yield 440 mg of an orange powder

(isolate yield: 73%). <sup>1</sup>H NMR (300 MHz, CD<sub>2</sub>Cl<sub>2</sub>, 300K) overlapping signals of CH<sub>2</sub> and Cy. <sup>31</sup>P{<sup>1</sup>H} NMR (121 MHz, CD<sub>2</sub>Cl<sub>2</sub>, 300K) δ(ppm) 88.84 (s). <sup>13</sup>C NMR (75 MHz, CD<sub>2</sub>Cl<sub>2</sub>, 300K) δ(ppm) 22.68 (t, <sup>1</sup>J<sub>CP</sub> = 19.3 Hz, CH<sub>2</sub>). 26.29 (s, Cy); 27.24 (t, <sup>1</sup>J<sub>CP</sub> = 4.8 Hz, Cy); 27.58 (t, <sup>1</sup>J<sub>CP</sub> = 6.57 Hz, Cy); 29.59 (t, <sup>1</sup>J<sub>CP</sub> = 1.88 Hz, Cy); 30.75 (s, Cy); 37.69 (t, <sup>1</sup>J<sub>CP</sub> = 12.78 Hz, Cy).

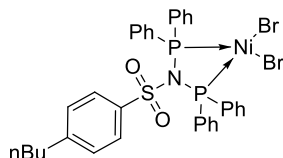
### Synthesis of complex 6:



4-bromo-N-(1,1,2,2-tetraphenyldiphosphanylidene)benzene sulphona-mide (ligand 1, 200 mg, 0.331 mmol, 1.01 eq.) and nickel (II) bromide dimethoxyethane adduct (101 mg, 0.327 mmol, 1 eq.) were suspended in toluene (3 mL). The mixture was stirred at 60°C until complete consumption of nickel (II) bromide dimethoxyethane adduct. A solid formed and the liquid was syringed out. The precipitate was washed 3 times with pentane (5

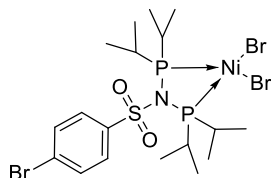
mL) and dried under reduced pressure to yield a reddish brown solid (isolate yield: 215 mg, 80%). Crystals suitable from diffraction were obtained by slow diffusion of pentane in a dichloromethane/toluene solution of the product <sup>1</sup>H NMR (300 MHz, CD<sub>2</sub>Cl<sub>2</sub>, 300K): δ(ppm)= 8.16 (m, PPh<sub>2</sub>, 8H), 7.76 (t, *J* = 7.3 Hz, CH <sub>PPh<sub>2</sub> para</sub>, 4H), 7.59 (m, PPh<sub>2</sub>, 8H), 7.06 (d, <sup>3</sup>*J*<sub>HH</sub> = 8.2 Hz, -Ar-SO<sub>2</sub>, 2H), 6.18 (d, <sup>3</sup>*J*<sub>HH</sub> = 8.5 Hz, -Ar-SO<sub>2</sub>, 2H). <sup>31</sup>P{<sup>1</sup>H} NMR (121 MHz, CD<sub>2</sub>Cl<sub>2</sub>, 300K): δ(ppm)= 65.52. <sup>13</sup>C NMR (75 MHz, CD<sub>2</sub>Cl<sub>2</sub>, 300K): δ(ppm)= 125.46 (t, <sup>1</sup>*J*<sub>CP</sub> = 26.5 Hz, C<sup>IV</sup>, C<sub>PPh<sub>2</sub> ipso</sub>, 4C); 125.63 (C<sup>IV</sup>, C-Br); 128.81 (CH<sub>ArSO<sub>2</sub></sub>, 2C); 129.50 (CH<sub>Ar meta</sub>, 8C); 132.50 (CH<sub>ArSO<sub>2</sub></sub>, 2C); 134.20 (CH<sub>Ar para</sub>, 4C); 135.11 (CH<sub>Ar ortho</sub>, 8C); 137.8 (C<sup>IV</sup>, C-SO<sub>2</sub>). MS(FAB<sup>+</sup>): *m/z* calcd. for C<sub>30</sub>H<sub>24</sub>NO<sub>2</sub>P<sub>2</sub>Br<sub>2</sub>SNi ([M- HBr]<sup>+</sup>): 741.8701; obsd.: 741.8702.

### Synthesis of complex 7:



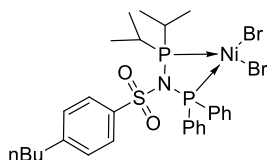
4-butyl-N-(1,1,2,2-tetraphenyldiphosphan-1-ylidene)benzenesulphona-mide (ligand **2**, 200 mg, 0.344 mmol, 1 eq.) and nickel (II) bromide dimethoxyethane adduct (106 mg, 0.344 mmol, 1 eq.) were suspended in benzene (2 mL). The mixture was stirred at 65°C until complete consumption of nickel (II) bromide dimethoxyethane adduct (**1h**). A solid formed and the liquid was syringed out. The precipitate was washed 3 times with pentane (3 x 5 mL) and dried under reduced pressure to yield a brown solid (isolate yield: 188 mg, 68%). <sup>1</sup>H NMR (300 MHz, CD<sub>2</sub>Cl<sub>2</sub>, 300K): δ(ppm)= 8.91 – 5.91 (m, H<sub>Ar</sub>, 24H), 2.72 – 2.24 (m, CH<sub>3</sub>-CH<sub>2</sub>-CH<sub>2</sub>-CH<sub>2</sub>-CAr, 2H), 1.51 (m, CH<sub>3</sub>-CH<sub>2</sub>-CH<sub>2</sub>-CH<sub>2</sub>-CAr, 2H), 1.31 (m, CH<sub>3</sub>-CH<sub>2</sub>-CH<sub>2</sub>-CH<sub>2</sub>-CAr, 2H), 0.95 (m, CH<sub>3</sub>-CH<sub>2</sub>-CH<sub>2</sub>-CH<sub>2</sub>-CAr 3H). <sup>31</sup>P{<sup>1</sup>H} NMR (121 MHz, CD<sub>2</sub>Cl<sub>2</sub>, 300K): δ(ppm)= 64.07. <sup>13</sup>C NMR (75 MHz, CD<sub>2</sub>Cl<sub>2</sub>, 300K): δ(ppm)= 13.94 (-CH<sub>3</sub>); 22.59 (-CH<sub>2</sub>-CH<sub>3</sub>); 33.38 (-CH<sub>2</sub>-CH<sub>2</sub>-CH<sub>3</sub>); 35.69 (Ar-CH<sub>2</sub>-); 125.58 (t, <sup>1</sup>J<sub>CP</sub> = 26.7 Hz, C<sup>IV</sup>, C<sub>PPh2 ipso</sub>); 127.44 (CH<sub>Ar-SO<sub>2</sub></sub>, 2C); 129.24 (CH<sub>Ar-SO<sub>2</sub></sub>, 2C); 129.31 (t, <sup>3</sup>J<sub>CP</sub> = 6.1 Hz, CH<sub>PPh2 meta</sub>, 8C); 133.98 (br. s., CH<sub>para</sub>, 4C); 135.05 (t, <sup>2</sup>J<sub>CP</sub> = 6.0 Hz, CH<sub>PPh2 ortho</sub>); 135.94 (C<sup>IV</sup>, C-*n*Bu); 150.76 (C<sup>IV</sup>, C-SO<sub>2</sub>). Anal. found (calcd.) for C<sub>34</sub>H<sub>33</sub>Br<sub>2</sub>NNiO<sub>2</sub>P<sub>2</sub>S: C, 51.22 (51.04); H 4.23 (4.16); N 1.69 (1.75).

### Synthesis of complex 8:



4-bromo-N-(1,1,2,2-tetraisopropyldiphosphan-1-ylidene)benzenesulpho-namide (ligand **3**, 200 mg, 0.427 mmol, 1.01 eq.) and nickel (II) bromide dimethoxyethane adduct (130 mg, 0.422 mmol, 1 eq.) were suspended in toluene (3 mL). The mixture was stirred at 60°C until complete consumption of nickel (II) bromide dimethoxyethane adduct. A solid formed and the liquid was syringed out. The precipitate was washed 3 times with pentane (3 x 5 mL) and dried under reduced pressure to yield a reddish solid (isolate yield: 174 mg, 57%). <sup>1</sup>H NMR (300 MHz, CD<sub>2</sub>Cl<sub>2</sub>, 300K): δ(ppm)= 7.97 – 7.57 (m, 4H, Ar-SO<sub>2</sub>), 2.82 (sept, CH<sub>iPr</sub>, <sup>3</sup>J<sub>HH</sub> = 7.0 Hz, 4H), 1.97 – 1.02 (m, CH<sub>3 iPr</sub>, 24H). <sup>31</sup>P{<sup>1</sup>H} NMR (121 MHz, CD<sub>2</sub>Cl<sub>2</sub>, 300K): δ(ppm)= 111.26. <sup>13</sup>C NMR (75 MHz, CD<sub>2</sub>Cl<sub>2</sub>, 300K): δ(ppm)= 19.82 (d, <sup>2</sup>J<sub>CP</sub> = 84.82 Hz, CH<sub>3 iPr</sub>, 8C); 31.29 (m, CH<sub>iPr</sub>, 4C); 125.27 (C<sup>IV</sup>, C-Br); 129.73 (CH<sub>Ar-SO<sub>2</sub></sub>, 2C); 133.84 (CH<sub>Ar-SO<sub>2</sub></sub>, 2C); 138.41 (C<sup>IV</sup>, C-SO<sub>2</sub>). Anal. found (calcd.) for C<sub>18</sub>H<sub>32</sub>Br<sub>3</sub>NNiO<sub>2</sub>P<sub>2</sub>S: C, 31.46 (31.48); H, 4.87 (4.70); N 1.91 (2.04).

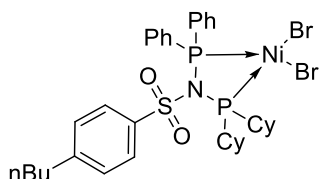
### Synthesis of complex 9:



4-butyl-N-(1,1-diisopropyl-2,2-diphenyldiphosphan-1-ylidene)benzenesulphona-mide (ligand **4**, 400 mg, 0.786 mmol, 1 eq.) and nickel (II) bromide dimethoxyethane adduct (266 mg, 0.864 mmol, 1.1 eq.) were dissolved in dichloromethane (20 mL) and stirred for 5 min at RT. The red solution was passed through a glass filter and the filtrate evaporated to dryness. The solid was washed 3 times with pentane (10 mL) and dried under reduced pressure to afford a red powder (isolate yield: 350 mg, 61%). Crystals suitable from diffraction were obtained by slow diffusion of pentane in a dichloromethane/toluene solution of the product. <sup>1</sup>H NMR (300 MHz, CD<sub>2</sub>Cl<sub>2</sub>, 300K): δ(ppm)= 8.77 – 6.21 (m, CH<sub>Ar</sub>, 14H), 3.29 (m, 4H, CH<sub>3</sub>-CH-CH<sub>3</sub> and -CH<sub>2</sub>-Ar), 2.43 (m, CH<sub>2</sub>-CH<sub>2</sub>-Ar, 2H), 1.66 – 1.00 (m, CH<sub>3</sub>-CH-CH<sub>3</sub> and CH<sub>3</sub>-CH<sub>2</sub>-CH<sub>2</sub>-CH<sub>2</sub>-Ar, 14H), 0.78 (t,

$^3J_{HH} = 7.8$  Hz,  $\text{CH}_3\text{-CH}_2\text{-CH}_2\text{-CH}_2\text{-Ar}$ , 3H).  $^{31}\text{P}\{^1\text{H}\}$  NMR (121 MHz,  $\text{CD}_2\text{Cl}_2$ , 300K):  $\delta(\text{ppm}) = 117.10$  (d,  $^2J_{PP} = 119.6$  Hz), 61.16 (d,  $^2J_{PP} = 121.4$  Hz).  $^{13}\text{C}$  NMR (75 MHz,  $\text{CD}_2\text{Cl}_2$ , 300K):  $\delta(\text{ppm}) = 13.78$  ( $-\text{CH}_3$ ,  $n\text{Bu}$ ); 18.15 (d,  $^2J_{CP} = 3.0$  Hz,  $\text{CH}_3$ ,  $i\text{Pr}$ , 2C); 18.46 (d,  $^2J_{CP} = 2.0$  Hz,  $\text{CH}_3$ ,  $i\text{Pr}$ , 2C); 22.33 ( $-\text{CH}_2\text{-CH}_3$ ); 29.62 (d,  $^1J_{CP} = 16.8$  Hz,  $\text{CH}$ ,  $i\text{Pr}$ , 2C); 33.23 ( $-\text{CH}_2\text{-CH}_2\text{-CH}_3$ ); 35.66 (Ar- $\text{CH}_2$ ); 126.57 (d,  $^1J_{CP} = 53.2$  Hz,  $\text{C}^{\text{IV}}_{\text{PPh}_2 \text{ ipso}}$ , 2C); 127.93 ( $\text{CH}_{\text{Ar-SO}_2}$ , 2C); 133.68 (d,  $^4J_{CP} = 3.0$  Hz,  $\text{CH}_{\text{PPh}_2 \text{ para}}$ , 2C); 135.46 (d,  $^2J_{CP} = 12.6$  Hz,  $\text{CH}_{\text{PPh}_2 \text{ ortho}}$ , 4C); 136.05 ( $\text{C}^{\text{IV}}$ , C- $n\text{Bu}$ ); 151.64 ( $\text{C}^{\text{IV}}$ , C- $\text{SO}_2$ ). Anal. found (calcd.) for  $\text{C}_{28}\text{H}_{37}\text{Br}_2\text{NNiO}_2\text{P}_2\text{S}$ : C, 45.89 (45.94); H, 4.96 (5.09); N, 1.86 (1.91).

## Synthesis of complex 10:



4-butyl-N-(1,1-dicyclohexyl-2,2-diphenyldiphosphanylidene) benzenesulphonamide (ligand **5**, 98 mg, 0.165 mmol, 1.02 eq.) and nickel (II) bromide dimethoxyethane adduct (50 mg, 0.162 mmol, 1 eq.) were dissolved in dichloromethane and stirred for 2 h at RT. The red solution was passed through a glass filter and the filtrate evaporated to dryness. The solid was washed 3 times with pentane (5 mL) and dried under reduced pressure to afford a red powder (isolate yield: 73 mg, 54%). Crystals suitable for diffraction were obtained by slow diffusion of pentane in a dichloromethane/toluene solution of the product.  $^{31}\text{P}\{^1\text{H}\}$  NMR (121 MHz,  $\text{CD}_2\text{Cl}_2$ , 300K):  $\delta(\text{ppm}) = 108.15$  (d,  $^2J_{PP} = 118.6$  Hz), 60.28 (d,  $^2J_{PP} = 119.2$  Hz).  $^{13}\text{C}$  NMR (75 MHz,  $\text{CD}_2\text{Cl}_2$ , 300K):  $\delta(\text{ppm}) = 13.93$  ( $-\text{CH}_3$ ); 22.64 ( $-\text{CH}_2\text{-CH}_3$ ); 25.94 ( $\text{CH}_2$ ,  $\text{Cy}$ , 2C); 26.87 (d,  $J_{CP} = 12.5$  Hz,  $\text{CH}_2$ ,  $\text{Cy}$ , 2C); 27.22 (d,  $J_{CP} = 13.4$  Hz,  $\text{CH}_2$ ,  $\text{Cy}$ , 2C); 28.57 ( $\text{CH}_2$ ,  $\text{Cy}$ , 2C); 28.88 (d,  $J_{CP} = 4.0$  Hz,  $\text{CH}_2$ ,  $\text{Cy}$ , 2C); 33.43 ( $-\text{CH}_2\text{-CH}_2\text{-CH}_3$ ); 35.87 (Ar- $\text{CH}_2$ -); 38.77 (d,  $J_{CP} = 15.2$  Hz,  $\text{CH}$ ,  $\text{Cy}$ , 2C); 126.96 (d,  $^1J_{CP} = 53.9$  Hz,  $\text{C}^{\text{IV}}_{\text{PPh}_2 \text{ ipso}}$ , 2C); 128.15 ( $\text{CH}_{\text{Ar-SO}_2}$ , 2C); 128.92 (d,  $^3J_{CP} = 12.5$  Hz,  $\text{CH}_{\text{PPh}_2 \text{ meta}}$ , 4C); 129.94 ( $\text{CH}_{\text{Ar-SO}_2}$ , 2C); 133.78 (d,  $^4J_{CP} = 2.9$  Hz,  $\text{CH}_{\text{para}}$ , 2C); 135.68 (d,  $^2J_{CP} = 12.5$  Hz,  $\text{CH}_{\text{ortho}}$ , 4C); 136.61 ( $\text{C}^{\text{IV}}$ , C- $n\text{Bu}$ ); 151.74 ( $\text{C}^{\text{IV}}$ , C- $\text{SO}_2$ ). MS(FAB<sup>+</sup>):  $m/z$  calcd. for  $\text{C}_{34}\text{H}_{45}\text{Br}_2\text{NO}_2\text{P}_2\text{SNi}$  ( $[\text{M}]^+$ ): 811.0354; obsd.: 811.0337. Anal.: found (calcd.) for  $\text{C}_{34}\text{H}_{45}\text{Br}_2\text{NO}_2\text{P}_2\text{SNi}$ : C, 47.23 (50.28); H, 5.90 (5.58); N, 1.64 (1.72) probably traces of solvent.

## Crystal structures

CCDC 980069 (compound **1**), 980681 (**4**), 980070 (**6**), 980071 (**9**), and 980072 (**10**) contain the supplementary crystallographic data.

## 4.4 Catalytic reactions procedures

### 1.1.1. Procedure for the nickel-catalysed oligomerisation of ethylene / MAO

The reactor of 250 mL was dried under vacuum at 100°C for 2 hours and then pressurised at 5 bar with ethylene. The reactor was cooled down at room temperature and the ethylene was evacuated, leaving a slight over pressure inside the reactor. Toluene (43 mL) was injected to the reactor and either heated to 45°C or cooled to 10 °C (for tests at 30°C) under stirring. When the temperature inside the reactor was stabilised, stirring was stopped, the toluene solution of catalyst (10  $\mu\text{mol}$ , 5 mL) was injected, followed by MAO (10% in toluene, 2 mL, 300 eq). Then the reactor was filled with 30 bar of ethylene pressure (ca. 8.3 g) and magnetic stirring was started ( $t=0$ ). The reaction ran for 1h or shorter for very active systems at the desired temperature. The pressure was kept by connecting the reactor to an ethylene ballast by using a manometer (grove) and the ethylene uptake was monitored by mass difference of the ballast on a balance. The reaction was stopped by closing the ethylene supply and cooling the reactor to 25°C with moderate stirring. The gas phase was evacuated, quantified (flow meter)

and collected in 30L plastic drum by water displacement (stirring the liquid phase was necessary). The drum was shaken with residual water to homogenise the gas phase and it was injected in GC. The reactor was opened, the liquid phase transferred by pipette to a glass bottle and neutralised with 20% aqueous H<sub>2</sub>SO<sub>4</sub>. The toluene phase was weighted and injected in GC.

### 1.1.2. Procedure for the nickel-catalysed oligomerisation of propylene / MAO

The reactor of 250 mL was dried under vacuum at 100°C for 2 hours, cooled at 10°C then filled with propylene slightly over atmospheric pressure (1.4 bar). Chlorobenzene (33.0 mL) and *n*-heptane (10.0 mL, internal standard accurately weighed) were introduced, followed by propylene (4.0 g). The MAO (1.5 M in toluene, 300 eq., 2.0 mL) was then injected followed by the precatalyst (0.10 mmol in 5.0 mL chlorobenzene). After that, propylene (16.0 g) was introduced, the uptake closed and stirring is started (t=0 min). The temperature was maintained at 10°C for 10 min and then was gradually brought to 45°C. Consumption of the propylene was followed by the reduction of the pressure inside the reactor. Sampling was performed for the reference complex NiCl<sub>2</sub>(PCy<sub>3</sub>)<sub>2</sub> after 10 and 30 minutes. After 110 min, the reaction was stopped, the reactor cooled to 25°C under moderate stirring, residual pressure was evacuated and the reactor was opened. The liquid phase was then drawn off and neutralised with 20% aqueous H<sub>2</sub>SO<sub>4</sub>. The resulting organic phase was weighted and analysed by GC apparatus equipped with a cryostat. The conversion was measured as the ratio of the mass of products formed (based on the internal standard) on the mass of propylene introduced.

### 1.1.3. Procedure for the oligomerisation of ethylene with chromium / MAO

The reactor of 250 mL was dried under vacuum at 100°C for 2 hours and then filled at room temperature with ethylene at atmospheric pressure (1.4 bar). A mixture of Cr(acac)<sub>3</sub> (19.2 mg, 55 μmol, 1 eq.) or CrCl<sub>3</sub>(THF)<sub>3</sub> (20.6 mg, 55 μmol, 1 eq.) and ligand (110 μmol, 2.0 eq.) were suspended in toluene (50 mL) and stirred for 10 min at RT. A part of this solution was injected in the reactor (3 mL, 3.3 μmol Cr, 6.6 μmol ligand) followed by introduction of methylaluminoxane (MAO, 0.7 mL, 10% in toluene, 300 eq.). The temperature and pressure were set to 45°C and 35 bars. The reaction was started by stirring and was stopped after 60 min. The reactors were cooled down to room temperature and the gas phase evacuated under stirring. The liquid was neutralised with 20 % aqueous H<sub>2</sub>SO<sub>4</sub> and the organic phase analysed by GC.

Approach of supposed chromium complexes synthesis: CrCl<sub>3</sub>(THF)<sub>3</sub> (10 μmol, 1 eq.) and the iminobisphosphine (10 μmol, 1 eq.) were dissolved in 5 mL of THF. The mixture was stirred for 10 min at room temperature, and then the mixture was heated to 60°C leading to a blue silvery solid that crashed out. No further details could be recovered from the complexes due to the low solubility and paramagnetic nature of these complexes.

## 5 References

- [1] S. D. Ittel, L. K. Johnson, M. Brookhart, *Chem. Rev.* **2000**, *100*, 1169–204.
- [2] F. Speiser, P. Braunstein, L. Saussine, *Acc. Chem. Res.* **2005**, *38*, 784–793.
- [3] P. Kuhn, D. Sémeril, D. Matt, M. J. Chetcuti, P. Lutz, *Dalt. Trans.* **2007**, 515–528.

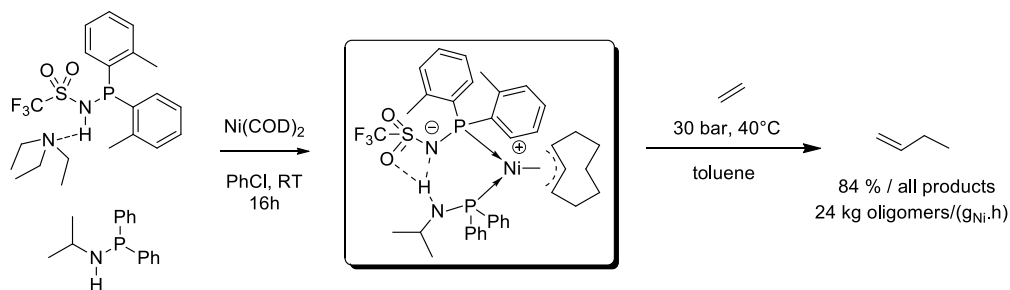
- [4] C. Bianchini, G. Giambastiani, I. G. Rios, G. Mantovani, A. Meli, A. M. Segarra, *Coord. Chem. Rev.* **2006**, *250*, 1391–1418.
- [5] S. Wang, W.-H. Sun, C. Redshaw, *J. Organomet. Chem.* **2014**, *751*, 717–741.
- [6] B. Cornils, W. A. Herrmann, in *Appl. Homog. Catal. with Organomet. Compd. A Compr. Handb. Three Vol.*, **2002**.
- [7] G. Wilke, B. Bogdanovic, *Angew. Chem., Int. Ed.* **1966**, *5*, 151–266.
- [8] B. Bogdanovic, B. Henc, H. Karmann, *Ind. Eng. Chem. Res.* **1963**, *62*, 34–44.
- [9] J. N. L. Dennett, A. L. Gillon, K. Heslop, D. J. Hyett, J. S. Fleming, C. E. Lloyd-Jones, A. G. Orpen, P. G. Pringle, D. F. Wass, J. N. Scutt, et al., *Organometallics* **2004**, *23*, 6077–6079.
- [10] I. Albers, E. Álvarez, J. Cámpora, C. M. Maya, P. Palma, L. J. Sánchez, E. Passaglia, *J. Organomet. Chem.* **2004**, *689*, 833–839.
- [11] C. Bianchini, L. Gonsalvi, W. Oberhauser, D. Sémeril, R. Gutmann, *Dalt. Trans.* **2003**, 3869–3875.
- [12] G. Mora, S. van Zutphen, C. Klempe, L. Ricard, Y. Jean, P. Le Floch, *Inorg. Chem.* **2007**, *46*, 10365–71.
- [13] M. Lejeune, D. Sémeril, C. Jeunesse, D. Matt, F. Peruch, P. J. Lutz, L. Ricard, *Chem. Eur. J.* **2004**, *10*, 5354–60.
- [14] K. Song, H. Gao, F. Liu, J. Pan, L. Guo, S. Zai, Q. Wu, *Eur. J. Inorg. Chem.* **2009**, *2009*, 3016–3024.
- [15] Z. Sun, F. Zhu, Q. Wu, S. Lin, *Appl. Organomet. Chem.* **2006**, *20*, 175–180.
- [16] L. Lavanant, A.-S. Rodrigues, E. Kirillov, J.-F. Carpentier, R. F. Jordan, *Organometallics* **2008**, *27*, 2107–2117.
- [17] N. a. Cooley, S. M. Green, D. F. Wass, K. Heslop, a. G. Orpen, P. G. Pringle, *Organometallics* **2001**, *20*, 4769–4771.
- [18] A. Schmidpeter, H. Rossknecht, *Angew. Chem., Int. Ed.* **1969**, 614–615.
- [19] A. Schmidpeter, H. Rossknecht, *Zeitschrift fuer Naturforsch. /B* **1971**, *54*, 81–82.
- [20] V. L. Foss, Y. A. Veits, I. F. Lutsenko, *Zhurnal Obs. khimii* **1984**, *54*, 2670–2684.
- [21] Z. Fei, R. Scopelliti, P. J. Dyson, *Dalt. Trans.* **2003**, 2772.
- [22] Z. Fei, W. H. Ang, D. Zhao, R. Scopelliti, P. J. Dyson, *Inorganica Chim. Acta* **2006**, *359*, 2635–2643.
- [23] Z. Fei, N. Biricik, D. Zhao, R. Scopelliti, P. J. Dyson, *Inorg. Chem.* **2004**, *43*, 2228–30.
- [24] E. De Boer, H. Van Der Heijden, Q. A. On, J. P. Smit, A. Van Zon, *Ligands and Catalyst Systems Thereof for the Catalytic Oligomerization of Olefinic Monomers*, **2009**, U.S. Patent US 2009/0062493 A1.
- [25] E. De Boer, H. Van Der Heijden, Q. A. On, J. P. Smit, A. Van Zon, *Ligands and Catalyst Systems for the Oligomerization of Olefinic Monomers*, **2009**, U.S. Patent US 2009/0069517 A1.
- [26] F. W. Patureau, M. Kuil, A. J. Sandee, J. N. H. Reek, M. K. Frederic W. Patureau Albertus J. Sandee and Joost N.H. Reek, *Angew. Chem., Int. Ed.* **2008**, *47*, 3180–3183.
- [27] F. G. Terrade, M. Lutz, J. I. van der Vlugt, J. N. H. Reek, *Eur. J. Inorg. Chem.* **2014**, *2014*, 1826–1835.
- [28] V. L. Foss, T. E. Chernykh, I. N. Staroverova, *J. Gen. Chem. USSR* **1983**, *10*, 1969–1976.
- [29] M. Uchino, Y. Chauvin, G. Lefebvre, *C. R. Acad. Sc. Paris* **1967**, *265/2*, 103–106.
- [30] H. Sato, H. Tojima, K. Ikimi, *J. Mol. Catal. A* **1999**, *144*, 285–293.

- [31] H. Sato, H. Tojima, *Bull. Chem. Soc. Jpn.* **1993**, *66*, 3079–3084.
- [32] M. Itagaki, G. Suzukalo, K. Nomura, *Bull. Chem. Soc. Jpn.* **1998**, *71*, 79–82.
- [33] C. Carlini, M. Marchionna, R. Patrini, A. Maria, R. Galletti, G. Sbrana, *Appl. Catal. A Gen.* **2001**, *207*, 387–395.
- [34] F. Benvenuto, C. Carlini, M. Marchionna, A. M. R. Galletti, G. Sbrana, *J. Mol. Catal. A Chem.* **2002**, *178*, 9–20.
- [35] A. Carter, S. a Cohen, N. a Cooley, A. Murphy, J. Scutt, D. F. Wass, *Chem. Commun. (Camb)*. **2002**, *3*, 858–9.
- [36] J. T. Dixon, M. J. Green, F. M. Hess, D. H. Morgan, *J. Organomet. Chem.* **2004**, *689*, 3641–3668.
- [37] M. J. Overett, K. Blann, A. Bollmann, J. T. Dixon, F. Hess, E. Killian, H. Maumela, D. H. Morgan, A. Neveling, S. Otto, *Chem. Commun. (Camb)*. **2005**, 622–4.
- [38] A. Bollmann, K. Blann, J. T. Dixon, F. M. Hess, E. Killian, H. Maumela, D. S. McGuinness, D. H. Morgan, A. Neveling, S. Otto, et al., *J. Am. Chem. Soc.* **2004**, *126*, 14712–14713.
- [39] K. Blann, A. Bollmann, J. T. Dixon, F. M. Hess, E. Killian, H. Maumela, D. H. Morgan, A. Neveling, S. Otto, M. J. Overett, *Chem. Commun. (Camb)*. **2005**, 620–1.
- [40] M. J. Overett, K. Blann, A. Bollmann, J. T. Dixon, D. Haasbroek, E. Killian, H. Maumela, D. S. McGuinness, D. H. Morgan, *J. Am. Chem. Soc.* **2005**, *127*, 10723–10730.
- [41] K. Blann, A. Bollmann, J. T. Dixon, A. Neveling, D. H. Morgan, H. Maumela, E. Killian, F. M. Hess, S. Otto, L. Pepler, et al., *Trimerization of Olefins*, **2004**, U.S. Patent WO 2004/056479 A1.
- [42] J. T. Dixon, P. Wasserscheid, D. S. McGuinness, F. M. Hess, H. Maumela, D. H. Morgan, *Trimerisation and Oligomerisation of Olefins Using a Chromium Based Catalyst*, **2003**, U.S. Patent WO 03053891.
- [43] J. T. Dixon, D. H. Morgan, H. Maumela, P. Nongodlwana, J. A. Willemse, *Two Stage Activation of Oligomerisation Catalyst and Oligomerization of Olefinic Compounds in the Presence of an Oligomerisation Catalyst so Activated*, **2008**, U.S. Patent WO2008/146215 A1.
- [44] E. De Boer, H. Van Der Heijden, Q. A. On, J. P. Smit, A. Van Zon, *Ligands and catalytic systems thereof for the catalytic oligomerization of olefinic monomers*, **2008**, U.S. Patent WO2008/077908.
- [45] F. W. Patureau, S. de Boer, M. Kuil, J. Meeuwissen, P.-A. R. Breuil, M. a Siegler, A. L. Spek, A. J. Sandee, B. de Bruin, J. N. H. Reek, *J. Am. Chem. Soc.* **2009**, *131*, 6683–6685.
- [46] M. Tenorio, M. Puerta, P. Valerga, *J. Chem. Soc., Dalt. Trans.* **1996**, 1305–1308.



# Chapter 4

## Self-Assembled Organometallic Nickel Complexes as Catalysts for Selective Oligomerisation of Ethylene





# 1 Introduction

Since the discovery by Keim and co-workers that nickel complexes can be highly active catalysts for the oligomerisation of ethylene (Figure 1),<sup>[1,2]</sup> this reaction has been one of the showcase examples of homogeneous catalysis as it led to one of the key industrial processes, Shell Higher Olefin Process (SHOP).<sup>[3,4]</sup> Due to the commercial success, the nickel-catalysed ethylene oligomerisation reaction was studied in detail at the fundamental level.<sup>[5-10]</sup> The market for olefins has slowly changed and there is a growing commercial interest in obtaining selectively shorter linear alpha olefins such as 1-butene, which is only a minor product when the traditional nickel catalysts giving a broad Schulz-Flory product distribution are employed. As such, re-exploring nickel-based catalysts with a different approach could be scientifically and commercially rewarding.

Sulphonamido-phosphorus ligands (METAMORPhos) were recently introduced as a family of highly versatile building blocks for late transition metal complexes (Figure 1).<sup>[11-16]</sup> They display interesting adaptive coordination behaviour as they coordinate in P and P,O chelating form and in both neutral and anionic states of the ligand. Tuning of the substituents on the sulphonamide allows for the optimisation of specific catalytic properties, e.g. a more acidic character of the  $R^1SO_2-NH-R^2$  is anticipated to disfavour the reductive elimination reaction leading to the neutral ligand and inactive Ni(0), resulting in an improved catalyst life time. Moreover, these ligands proved to be particularly suited to construct supramolecular bidentate or tridentate complexes through hydrogen bonding. As it is known that the additional  $PPh_3$  ligand coordinated to the SHOP catalyst displayed in Figure 1 has a great influence on catalyst stability and product distribution,<sup>[5-7]</sup> we anticipated that nickel complexes based on METAMORPhos and aminophosphine ligands would form supramolecular pincer ligands that due to the dynamic nature of the supramolecular complexes would favour the catalyst stability, but at the same time retain the vacant site required for adequate catalytic activity. While self-assembled ligands by hydrogen bonding, metal-ligand, ionic, and stacking interactions have successfully been developed for noble transition metals such as rhodium, palladium and platinum, and have been applied in various catalytic transformations,<sup>[17-31]</sup> this approach has hardly been applied for first-row transition metals. To the best of our knowledge, the *in situ* generated Ni(0) complex that was used as catalyst in the hydrocyanation reaction is the only example, reported by Breit *et al.*<sup>[32]</sup> Considering the frequent use of nickel for industrial catalytic transformations there is, however, still a lot of potential for the use of self-assembled ligands. We report here such a supramolecular ligand approach for the formation of stable nickel complexes based on hydrogen bonds, by self-assembly of a METAMORPhos and an aminophosphine ligand. The

organometallic nickel complexes are remarkably stable and at the same time form very active and selective dimerisation catalysts for ethylene to form 1-butene as the main product.

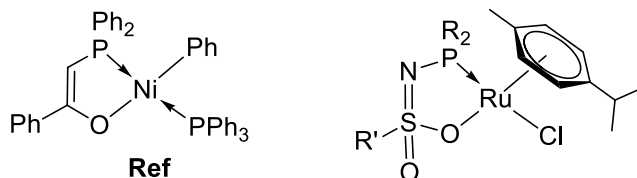


**Figure 1.** Representative anionic P,O ligand that forms the active nickel based SHOP catalyst (left) and a typical coordination mode of METAMORPhos, an adaptive sulphonamido-phosphorus ligand (right).

## 2 Discussion

Mixing equimolar amounts of nickel(0) bis(1,5-cyclooctadiene) ( $\text{Ni}(\text{COD})_2$ ), *i*Pr - NH- PPh<sub>2</sub> and 1.NE<sub>3</sub> (or 2) in a chlorobenzene solution led to the selective formation of nickel(II) complex 3 (or 4) in which METAMORPhos coordinates as an anionic ligand. During the formation of the complex the COD ligand was converted to the  $\pi$ -allyl (Figure 2). Such complexes can be formed after oxidative addition of the acidic sulphonamide ligand, and subsequent insertion of the hydride in the double bond of the COD fragment. The supramolecular nickel complexes were isolated as yellow powders (yields up to 57 %) and characterised by <sup>1</sup>H, <sup>13</sup>C and <sup>31</sup>P NMR and the molecular structure was confirmed by X-ray analysis (see experimental part).

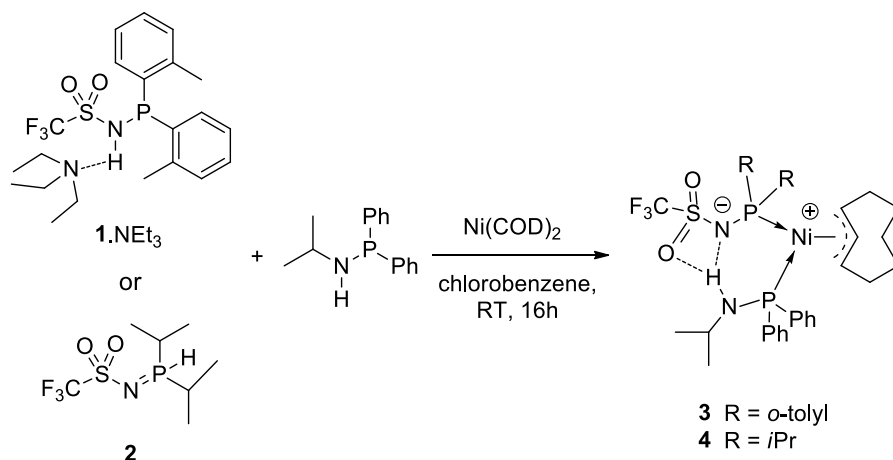


**Figure 2.** Synthesis of supramolecular nickel complexes 3 and 4.

Crystals of complexes **3** and **4** suitable for X-ray analysis were obtained by slow diffusion of pentane in a toluene solution of the complex. The complexes **3** and **4**, displayed in Figures 3 and 4, adopt a square planar coordination geometry, with the phosphorus ligands in *cis*-position with respect to one another. The nickel atom is formally cationic, whereas the negative charge is delocalised on the NSO fragment of the METAMORPhos ligand, as is also clear from the P-N and N-S bond lengths (intermediate between single and double bond) and the S-N-P angles (typically between  $sp^2$  or  $sp^1$  hybridised nitrogen,  $131.0^\circ$  for **3** and  $134.17^\circ$  for **4**). The anionic NSO site forms a good hydrogen bond acceptor, and indeed there is a hydrogen bond formed with the NHP of the adjacent ligand. Interestingly, for complex **3** the hydrogen bond distance is significantly longer ( $2.994 \text{ \AA}$ ) compared to that found in complex **4** (N2-H $\cdots$ N1 bond of  $2.190 \text{ \AA}$ , consistent with literature),<sup>[14]</sup> suggesting that there is a weaker interaction between the ligands in complex **3**. The difference in steric bulk between the two METAMORPhos ligands likely accounts for this. Inspection of the solid state structures reveals that in complex **4** the two isopropyl substituents are transversal to the coordination plane, whereas in complex **3** the *o*-tolyl substituents are opposite to the allyl moiety. The latter geometry results in a rotation of the sulphonamido fragment, increasing the distance to the hydrogen bond donor. This geometry difference in the two complexes is further supported by the switch of the dihedral angle P-Ni-P-N<sub>METAMORPhos</sub> from  $28.5^\circ$  for **4** to  $79.3^\circ$  for **3**.

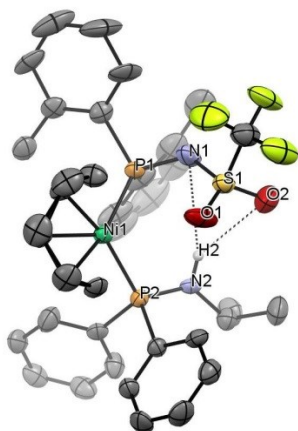


**Figure 3.** ORTEP plot (50% probability displacement ellipsoids) of complex **3**. Hydrogen atoms have been omitted for clarity (except for NH moiety). Selected bond lengths ( $\text{\AA}$ ) and angles ( $^\circ$ ): Ni1-P1 2.222(2); Ni1-P2 2.206(2); N2-H2 0.859; N1--H2 2.994; O1--H2 2.844; P2-Ni1-P1 104.55(9).

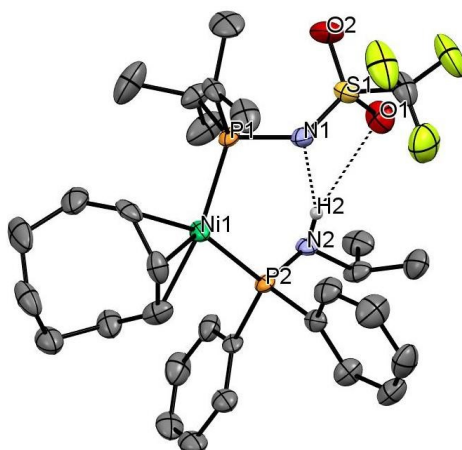


**Figure 4.** ORTEP plot (50% probability displacement ellipsoids) of complex **4**. Hydrogen atoms have been omitted for clarity (except for NH moiety). Selected bond lengths ( $\text{\AA}$ ) and angles ( $^\circ$ ): Ni1-P1 2.2165(17); Ni1-P2 2.2007(13); N2-H2 0.852; N1--H2 2.190; O1--H2 2.588; P2-Ni1-P1 103.96(6).

These diamagnetic complexes also form in solution as is clear from the  $^{31}\text{P}$  NMR and  $^1\text{H}$  NMR spectra. The two doublets observed in  $^{31}\text{P}$  NMR are shifted downfield with respect to the corresponding ligands and the small coupling constant is in agreement with *cis*-geometries ( $^2J_{PP} = 30$  Hz) as seen in Figure 5. In the  $^1\text{H}$  NMR spectra the signals for the  $\pi$ -allyl fragment are clearly observed at  $\delta(\text{ppm}, \text{C}_6\text{D}_6)$ : 3.71 (2H) and 5.09 (1H) for complex **3** and 3.36 (1H), 4.19 (1H) and 4.48 (1H) for complex **4** (Figure 6 and Figure 7, respectively). Moreover the NH proton of the co-ligand *i*Pr - NH- PPh<sub>2</sub>, initially appearing at 1.56 ppm (in C<sub>6</sub>D<sub>6</sub>) was shifted to 2.85 ppm for complex **3** and to 5.85 ppm for complex **4** in agreement with a H-bonding interaction between the two ligands.

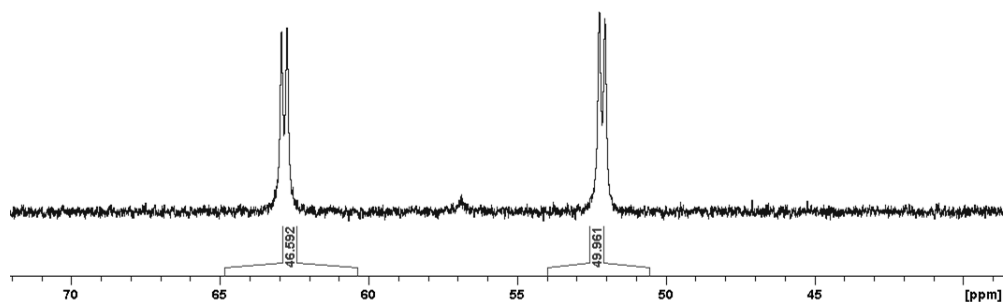


**Figure 5.**  $^{31}\text{P}$  NMR (121 MHz, C<sub>6</sub>D<sub>6</sub>) spectrum of complex **3** showing two doublets with small coupling constants ( $^2J_{PP} = 23$  Hz) attributed to a *cis* arrangement of phosphines around nickel.

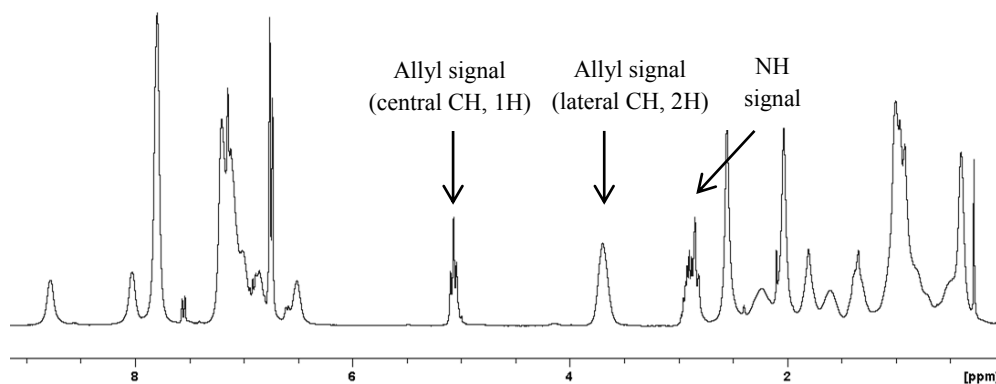


**Figure 6.**  $^1\text{H}$  NMR (300 MHz, C<sub>6</sub>D<sub>6</sub>) of complex **3** showing two signals of the allyl moiety (the 2 lateral allylic protons are overlapping).

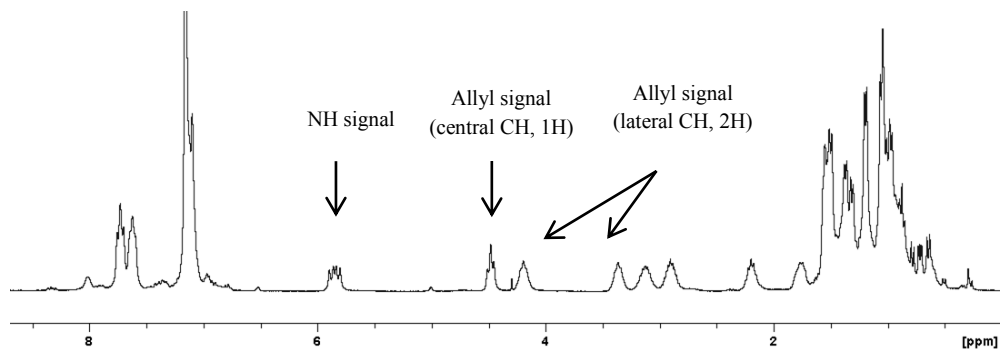


**Figure 7.**  $^1\text{H}$  NMR (300 MHz,  $\text{C}_6\text{D}_6$ ) of complex **4** with the three signals of the allyl moiety and the signal of the NH proton engaged in a hydrogen bonding.

These complexes were evaluated as catalysts in the ethylene oligomerisation at  $40^\circ\text{C}$  under an ethylene atmosphere with a pressure of 30 bar in the absence of any additional activator. High selectivity for the formation 1-butene (up to 84 % / all products) and good productivity ( $24 \text{ kg}_{\text{oligo}}/(\text{g}_{\text{Ni}}\cdot\text{h})$ ) were obtained with steady ethylene uptake over a period of 90 minutes for complex **3** (Table 1 and Figure 8). Based on these results, we formed a new class of nickel complexes which are, to our knowledge, the most robust and efficient organometallic nickel catalyst for 1-butene formation.<sup>[5–7,33–40]</sup> The high selectivity for short terminal olefins ( $1\text{-C}_4 > 99.0\%$ ), *i.e.* little isomerisation, was also observed when complex **4** was applied as the catalyst. A lower productivity and a clear shift in selectivity to a larger alpha-olefin distribution (Schulz-Flory with  $K_{\text{SF}} = 0.45$ ) were, however, observed. In comparison, the representative industrial benchmark complex (**Ref**, Figure 1), at higher concentration, required a slightly higher temperature for activation ( $50^\circ\text{C}$ ) and led to a very large Schulz-Flory distribution with a low productivity under equal reaction conditions ( $K_{\text{SF}} > 0.90$ ).

**Table 1.** Catalytic evaluation of **3**, **4** and benchmark complex **Ref**.

Complex	$n_{\text{Ni}}$ ( $\mu\text{mol}$ )	T( $^\circ\text{C}$ )	Prod. <sup>[a]</sup>	Product distribution <sup>[b]</sup>			
				$\text{C}_4$	$\text{C}_6$	$\text{C}_8^+$	$1\text{-C}_4$ <sup>[c]</sup>
<b>3</b>	10	40	24	85	13	2	99.0
<b>4</b>	10	40	12	35	28	37	99.7
<b>Ref</b>	50	50	5	1	2	97	76.7

Test conditions : 30 bar  $\text{C}_2\text{H}_4$ , solvent : toluene (55 mL), 90 min, [a] productivity in  $\text{kg}_{\text{oligo}}/(\text{g}_{\text{Ni}}\cdot\text{h})$ , [b] in wt. %, determined by GC, [c]  $1\text{-C}_4$  wt. % in  $\text{C}_4$  fraction, determined by GC.

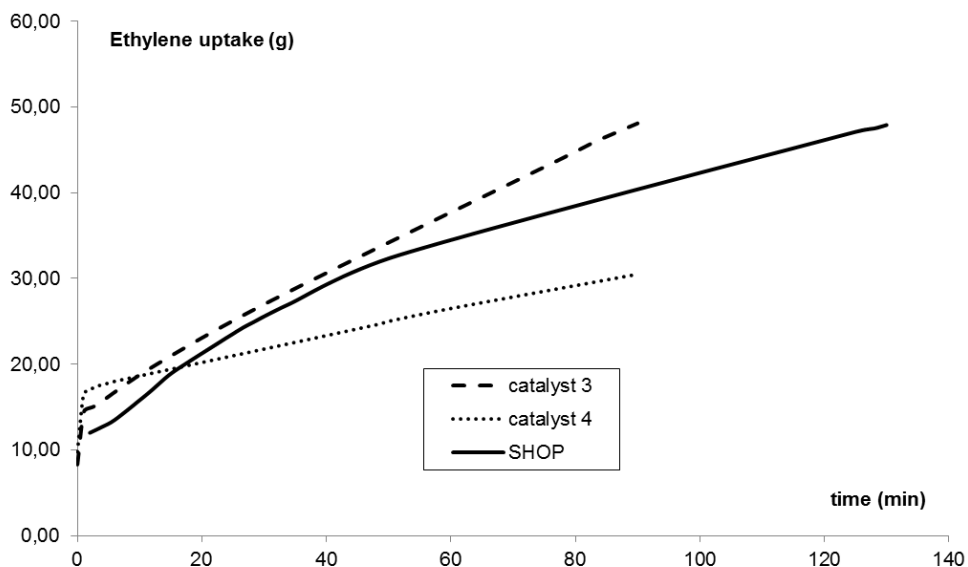


**Figure 8.** Ethylene uptake for catalysts **3**, **4** and **Ref** during the oligomerisation reaction. Initial uptake corresponds to the dissolution of ethylene into the solvent (ca. 13 g of ethylene).

More information on the active species was obtained from *in situ* NMR, revealing the rearrangement of both complexes under ethylene pressure. Indeed, at room temperature and under 5 bar of ethylene, the original complex **3** solution turned from orange to green and a new complex formed with two phosphines in *trans* position as evidenced by the large coupling observed in  $^{31}\text{P}$  NMR (55.5 ppm (d,  $J = 271$  Hz); 69.2 ppm (d,  $J = 271$  Hz)) illustrated in Figure 9. In the  $^1\text{H}$  NMR no hydride was observed. Similar reactivity was observed with complex **4** leading to a new species (53.5 ppm (d,  $J = 275$  Hz); 89.8 ppm (d,  $J = 275$  Hz)) illustrated in Figure 10. GC and GC/MS analyses of the NMR solution revealed the presence of short chain olefins (butenes and hexenes) and vinylcyclooctene. These experiments suggest ethylene insertion in catalyst precursor **3** (and **4**) with subsequent beta-H elimination or beta-H transfer with ethylene leading to vinylcyclooctene and the nickel-ethyl complex as the resting state (see Figure 11). Concomitantly, the rearrangement of the METAMORPhos ligand under the monoanionic P,O chelating ligand is proposed.

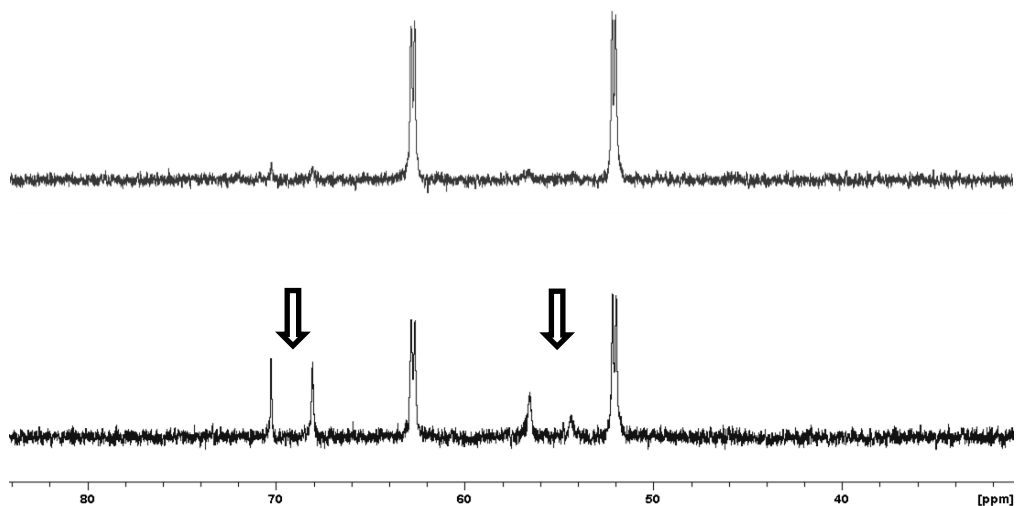


**Figure 9.** High pressure  $^{31}\text{P}$  NMR (131 MHz,  $\text{C}_6\text{D}_6$ , 300 K) NMR experiment on complex **3** under 5 bar of ethylene. Above: complex **3** with ethylene (5 bar) immediately after introduction, below complex **3** with ethylene (5 bar) after 45 min.

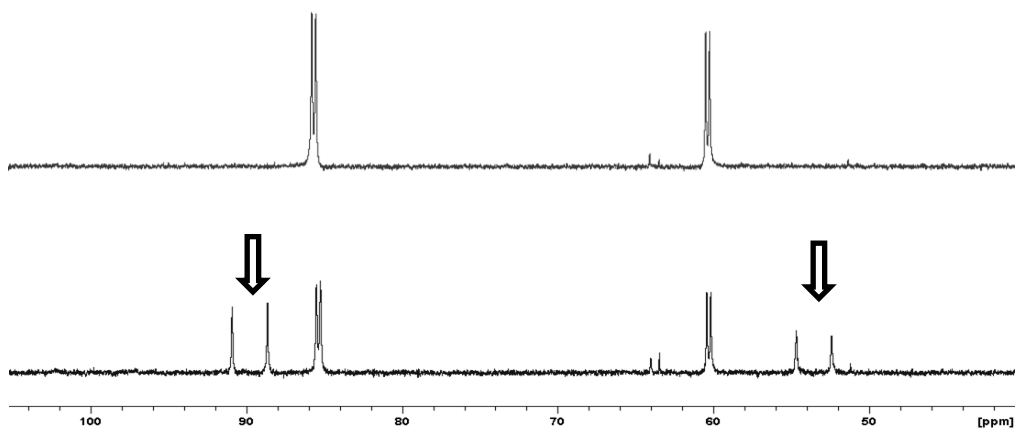


**Figure 10.** High pressure  $^{31}\text{P}$  NMR (131 MHz,  $\text{C}_6\text{D}_6$ , 300 K) NMR experiment on complex **4** under 5 bar of ethylene: complex **4** without ethylene, below complex **4** with ethylene (5 bar) after 45 min.

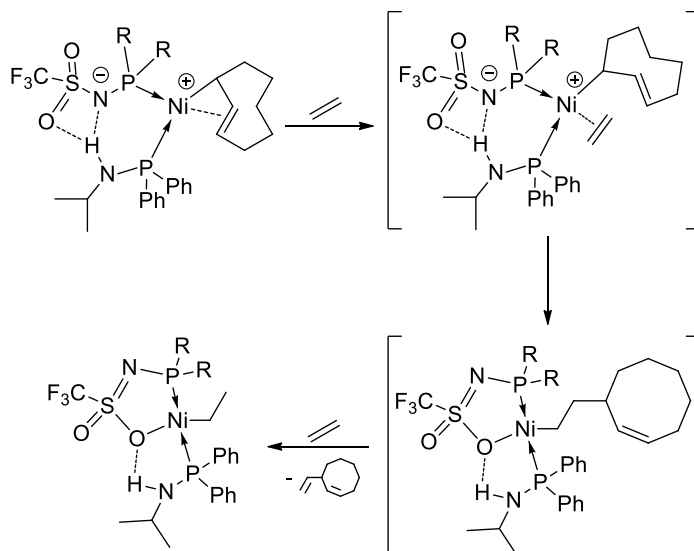


**Figure 11.** Suggested mechanism for catalyst rearrangement under ethylene.

### 3 Conclusion

In conclusion, we report the synthesis and detailed characterisation of stable nickel complexes supported by supramolecular bidendate ligands based on sulphonamido-phosphorus and aminophosphine ligands. The hydrogen-bond between the ligands in the zwitterionic nickel complexes was unambiguously proven in two X-ray structures. Importantly, this novel class of complexes reveals highly active and selective catalyst for ethylene oligomerisation with up to 84 wt. % of 1-butene compared to all products formed. This high selectivity for short linear alpha olefins is interesting considering the change in the market towards such products, and as such these results may renew the interest in the development of a new generation of nickel catalysts. *In situ* NMR experiments under ethylene pressure show the rearrangement of these structures to the proposed monoanionic P,O-P nickel complex as the resting state, that may explain the specific properties displayed by the catalyst. This provides a good starting point for further development and detailed understanding of this new class of nickel catalysts.

## 4 Experimental part

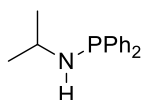
### 4.1 General

All reactions were carried out under an atmosphere of argon using standard Schlenk techniques. The trifluoromethanesulphonamide, 1,5-cyclooctadiene, di(*o*-



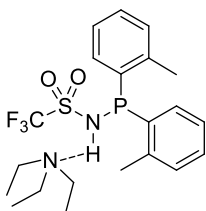
tolyl)chlorophosphine and diisopropylchlorophosphine were purchased from commercial suppliers and used without further purification. The ligand **2** and benchmark complex **Ref** were prepared according to known literature procedure.<sup>[1,16]</sup> THF, pentane and Et<sub>2</sub>O were distilled from sodium / benzophenone. CH<sub>2</sub>Cl<sub>2</sub>, chlorobenzene and triethylamine were pre-dried and distilled with CaH<sub>2</sub>, toluene from sodium, under nitrogen. Alternatively solvents from Solvent Purification System (M-Braun SPS 800) were used. NMR solvents were degassed by freeze-pump-thaw cycling under argon and stored over activated 3 Å molecular sieves. NMR spectra (<sup>1</sup>H, <sup>1</sup>H{<sup>31</sup>P}, <sup>31</sup>P, <sup>31</sup>P{<sup>1</sup>H} and <sup>13</sup>C{<sup>1</sup>H}) were measured on a BRUKER 300 MHz spectrometer at 25°C with C<sub>6</sub>D<sub>6</sub> as solvent. The calibration of the spectrum was performed on NMR solvent signal (C<sub>6</sub>D<sub>5</sub>H for proton at δ = 7.16 ppm and C<sub>6</sub>D<sub>6</sub> carbon at δ = 128.06 ppm). Analysis of liquid phase was performed on a GC Agilent 6850 Series II equipped with a PONA column. The gas phase for ethylene oligomerisation was analysed by GC on a HP 6890.

## 4.2 Synthesis of N-isopropyl-1,1-diphenylphosphinamine



Isopropylamine (1.8 mL, 22.3 mmol, 2.0 eq.) and triethylamine (4.7 mL, 33.4 mmol, 3.0 eq.) were placed in a Schlenk with 10 mL of dry THF. To this mixture was added chlorodiphenylphosphine dropwise (2.0 mL, 11.1 mmol, 1.0 eq.). The mixture was stirred for 10 min at room temperature and the precipitate which formed was filtered off. The filtrate was submitted to vacuum to give a colourless oily liquid. Trituration of the oil in pentane led to a white powder which was washed with pentane (2 x 10 mL). A pure compound was obtained by distillation of the solid under reduced pressure with an isolated yield of 2.1 g (77%). The product was stored at -18°C. <sup>31</sup>P{<sup>1</sup>H} NMR (121 MHz, C<sub>6</sub>D<sub>6</sub>): δ(ppm) = 34.94; <sup>1</sup>H NMR (300 MHz, C<sub>6</sub>D<sub>6</sub>): δ(ppm) = 0.95 (s, -CH<sub>3</sub>, 3H); 0.97 (s, -CH<sub>3</sub>, 3H); 1.56 (m, NH, 1H); 3.22 (m, CH, 1H); 7.0-7.22 (m, CH<sub>Ar</sub>, 6H); 7.4-7.6 (m, CH<sub>Ar</sub>, 4H). <sup>13</sup>C (C<sub>6</sub>D<sub>6</sub>): δ(ppm) = 26.17 (d, <sup>3</sup>J<sub>CP</sub> = 6.7 Hz, CH<sub>3</sub>, 2C); 48.72 (d, <sup>2</sup>J<sub>CP</sub> = 23.1 Hz, CH, 1C); 128.4 (m, CH<sub>Ar</sub>, 6C); 131.53 (d, J<sub>CP</sub> = 20 Hz, CH<sub>Ar</sub>, 4C), C<sup>IV</sup> not observed.

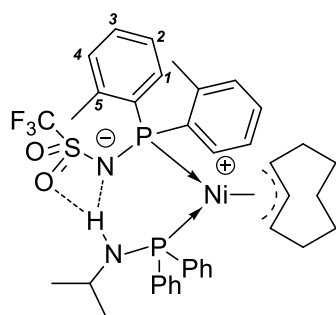
## 4.3 Synthesis of ligand 1



Trifluoromethanesulphonamide (2.4 g, 16.1 mmol, 1 eq.) and triethylamine (5.8 g, 41.8 mmol, 6.0 mL 2.6 eq.) were dissolved in dry THF (30 mL). Di(o-tolyl)chlorophosphine was dissolved in another Schlenk in 10 mL of THF. The chlorophosphine solution (4.0 g, 16.1 mmol, 1.0 eq.) was added dropwise to the sulphonamide solution leading to a white precipitate. After 20 minutes, the mixture was filtered to remove the salt and the filtrate was rinsed twice with 10 mL of THF. The liquid phase was evaporated under reduced pressure to give a colorless oil. A white powder was obtained by addition of diethyl ether (20 mL) to the oil. This powder was washed with diethyl ether (3 x 5 mL) and finally dried under vacuum to give the product (isolate yield : 2.5 g, yield : 34%). <sup>31</sup>P{<sup>1</sup>H} NMR (121 MHz, C<sub>6</sub>D<sub>6</sub>): δ(ppm) = 15.77 (s, PH form 12%); 22.62 (broad s, NH-NEt<sub>3</sub> form, 88%); <sup>31</sup>P NMR (121 MHz, C<sub>6</sub>D<sub>6</sub>) δ(ppm) = 15.77 (d,

PH form,  $^1J_{PH} = 472.6$  Hz); 22.62 (broad s);  $^{19}\text{F}$  NMR (282 MHz,  $\text{C}_6\text{D}_6$ )  $\delta(\text{ppm}) = -77.57$ .  $^1\text{H}$  NMR (300 MHz,  $\text{C}_6\text{D}_6$ ):  $\delta(\text{ppm}) =$  only the signals of the NH-NEt<sub>3</sub> form are reported  $\delta(\text{ppm}) = 0.66$  (m,  $\underline{\text{CH}_3\text{-CH}_2\text{-N}}$ , 9H); 2.14 (q,  $^3J_{HH} = 7.4$  Hz,  $\text{CH}_3\text{-CH}_2\text{-N}$ , 6H); 2.36 (br s,  $-\text{CH}_3$  tolyl, 6H); 6.7-7.1 (m,  $\text{H}_{\text{Ar}}$ , 6H); 7.5-8.0 (m,  $\text{H}_{\text{Ar}}$ , 2H); 8.94 (br s,  $\text{N-H}^+\cdots\text{N}$ , 1H).  $^{13}\text{C}$  NMR (75 MHz,  $\text{C}_6\text{D}_6$ ): only the signals of the NH-NEt<sub>3</sub> form are reported:  $\delta(\text{ppm}) = 8.51$  ( $\text{CH}_3$  NEt<sub>3</sub>); 20.75 (d,  $^3J_{CP} = 19.5$  Hz,  $\text{CH}_3$  tolyl); 45.83 ( $-\text{CH}_2\text{-N}$ ); 122.40 (q,  $^1J_{CF} = 326$  Hz,  $\text{CF}_3$ ); 126.03 (d,  $J = 3.0$  Hz,  $\text{CH}_{\text{Ar}}$ ); 129.54 (br s,  $\text{CH}_{\text{Ar}}$ ); 130.57 (d,  $J_{CP} = 4.8$  Hz,  $\text{CH}_{\text{Ar}}$ ); 131.65 (br s,  $\text{CH}_{\text{Ar}}$ ); 141.45 (d,  $J = 2.5$  Hz and 24.3 Hz,  $\text{C}^{\text{IV}}$ ,  $\underline{\text{C}}_{\text{Ar-CH}_3}$ , 2C),  $\text{C}^{\text{IV}}_{\text{Ar-P}}$  not observed.

#### 4.4 Synthesis and characterisation of complex 3



A solid mixture of ligand **1** (463 mg, 1.0 mmol, 1.0 eq.), N-isopropyl-1,1-diphenylphosphinamine (244 mg, 1.0 mmol, 1.0 eq.) and Ni(COD)<sub>2</sub> (275 mg, 1.0 mmol, 1.0 eq.) was dissolved in chlorobenzene (20 mL) at 0°C. This mixture was left to stir for 16 h at room temperature, leading to a dark solution. Then the solvents were removed under reduced pressure leading to a dark oil. This oil was triturated in diethylether (10 mL) and the solvent evaporated under vacuum. This operation was repeated twice until a solid formed. The solid was washed with

diethyl ether (2 x 10 mL) until the solution became clear. The solid was finally dried under reduced pressure to give the product (isolated yield 190 mg, 25%). A second fraction might be recovered from the ether filtrate. Crystals suitable for X-Ray diffraction analysis were obtained by slow evaporation of a concentrated benzene solution containing complex **3**.  $^{31}\text{P}\{^1\text{H}\}$  NMR (121 MHz,  $\text{C}_6\text{D}_6$ ):  $\delta(\text{ppm}) = 52.13$  (d,  $^2J_{PP} = 23.1$  Hz); 62.82 (d,  $^2J_{PP} = 23.3$  Hz);  $^{19}\text{F}$  NMR (282 MHz,  $\text{C}_6\text{D}_6$ ):  $\delta(\text{ppm}) = -77.70$  ppm;  $^1\text{H}$  NMR (300 MHz,  $\text{C}_6\text{D}_6$ ):  $\delta(\text{ppm}) = 0.41$  (m,  $\text{CH}_3$  *iPr*, 3H); 0.52 (m,  $\text{CH}_2$  COD, 1H); 0.93 (m,  $\text{CH}_2$  COD, 5H); 1.01 (m,  $-\text{CH}_3$  *iPr*, 3H); 1.36 (m,  $\text{CH}_2$  COD, 1H); 1.61 (m,  $\text{CH}_2$  COD, 1H); 1.81 (m,  $\text{CH}_2$  COD, 1H); 2.05 (s,  $\text{CH}_3$  tolyl, 3H); 2.23 (m,  $\text{CH}_2$  COD, 1H); 2.57 (s,  $\text{CH}_3$  tolyl, 3H); 2.85 (t,  $^2J_{HP} = 10.1$  Hz, NH, 1H); 2.92 (m,  $\text{CH}$  *iPr*, 1H); 3.71 (m,  $\text{CH}_{\text{allyl COD}\beta}$ , 2H); 5.09 (t,  $^3J_{HH} = 8.4$  Hz,  $\text{CH}_{\text{allyl COD}\alpha}$ , 1H); 6.53 (m,  $\text{H}_{\text{tolyl } 2b}$ , 1H); 6.75 (d,  $^4J_{HP} = 3.9$  Hz,  $\text{H}_{\text{tolyl } 4b}$ , 1H); 6.77 (d,  $^4J_{HP} = 4.0$  Hz,  $\text{H}_{\text{tolyl } 4a}$ , 1H); 6.87 (m,  $\text{H}_{\text{tolyl } 3b}$ , 1H); 7.02 (m,  $\text{H}_{\text{tolyl } 3a}$ , 1H); 7.17 (m,  $\text{H}_{\text{PPh}_2}$ , 6H); 7.20 (m,  $\text{H}_{\text{tolyl } 2a}$ , 1H); 7.81 (m,  $\text{H}_{\text{PPh}_2}$ , 4H); 8.04 (m,  $\text{H}_{\text{tolyl } 1b}$ , 1H); 8.78 (m,  $\text{H}_{\text{tolyl } 1a}$ , 1H).  $^{13}\text{C}$  NMR (75 MHz,  $\text{C}_6\text{D}_6$ ):  $\delta(\text{ppm}) = 21.7$  ( $\text{CH}_3$  tolyl); 22.1 ( $\text{CH}_3$  tolyl); 22.9 ( $\text{CH}_2$  COD); 24.9 ( $\text{CH}_3$  *iPr*); 25.5 ( $\text{CH}_3$  *iPr*); 26.5 (2  $\text{CH}_2$  COD); 29.2 (2  $\text{CH}_2$  COD); 46.9 (d,  $^2J_{CP} = 12.2$  Hz,  $\text{CH}_{\text{iPr}}$ ); 79.3 (d,  $^2J_{CP} = 18.6$  Hz,  $\text{CH}_{\text{allyl COD}\beta}$ ); 86.4 (d,  $^2J_{CP} = 20.6$  Hz,  $\text{CH}_{\text{allyl COD}\beta}$ ); 110.9 ( $\text{CH}_{\text{allyl COD}\alpha}$ ); 122.0 (qd,  $^1J_{CF} = 322.0$  Hz &  $^3J_{CP} = 6.0$  Hz,  $\text{CF}_3$ ); 123.68 (d,  $^3J_{CP} = 11.9$  Hz,  $\text{CH}_{\text{tolyl } 2b}$ ); 125.69 (m,  $\text{CH}_{\text{tolyl } 2a}$ ); 128.31 (m, 3C,  $\text{CH}_{\text{PPh}_2}$ ); 129.9 (d,  $^4J_{CP} = 22$  Hz,  $\text{CH}_{\text{tolyl } 3a}$ ); 130.2 (d,  $^4J_{CP} = 22$  Hz,  $\text{CH}_{\text{tolyl } 3b}$ ); 131.1 (m,  $\text{CH}_{\text{tolyl } 4a}$ ); 131.6 (m,  $\text{CH}_{\text{tolyl } 1a}$ ); 132.2 (m,  $\text{CH}_{\text{tolyl } 4a}$ ); 134.2 (m,  $\text{CH}_{\text{PPh}_2}$ , 4C); 135.0 (m or d,  $\text{C}^{\text{IV}}_{\text{tolyl ipso}}$ ); 136.9 (d,  $^1J_{CP} = 48.1$  Hz,  $\text{C}^{\text{IV}}_{\text{PPh}_2 \text{ ipso}}$ , 2C); 138.3 (m,  $\text{C}^{\text{IV}}_{\text{tolyl C-Me}}$ ); 139.6 (d,  $^1J_{CP} = 48.6$  Hz;  $\text{C}^{\text{IV}}_{\text{tolyl ipso}}$ ); 143.6 (m,  $\text{C}^{\text{IV}}_{\text{tolyl C-Me}}$ ).

X-Ray structure of complex **3** (see text for picture)

$C_{38}H_{45}F_3N_2NiO_2P_2S$	$F(000) = 1616$
$M_r = 771.50$	$D_x = 1.369 \text{ Mg m}^{-3}$
Monoclinic, $P2_1/n$	Cu $K\alpha$ radiation, $\lambda = 1.5418 \text{ \AA}$
Hall symbol: -P 2yn	Cell parameters from 3983 reflections
$a = 10.811 (2) \text{ \AA}$	$\theta = 4.5\text{--}67.1^\circ$
$b = 18.315 (2) \text{ \AA}$	$\mu = 2.50 \text{ mm}^{-1}$
$c = 18.962 (3) \text{ \AA}$	$T = 150 \text{ K}$
$\beta = 94.70 (1)^\circ$	Needle, light yellow
$V = 3741.9 (10) \text{ \AA}^3$	$0.11 \times 0.04 \times 0.03 \text{ mm}$
$Z = 4$	

**Data collection**

Xcalibur, Atlas, Gemini ultra diffractometer	6515 independent reflections
Radiation source: Enhance Ultra (Cu) X-ray Source	4438 reflections with $I > 2.0\sigma(I)$
mirror	$R_{\text{int}} = 0.130$
Detector resolution: $10.4685 \text{ pixels mm}^{-1}$	$\theta_{\text{max}} = 90.0^\circ$ , $\theta_{\text{min}} = 3.4^\circ$
$\omega$ scans	$h = -12 \rightarrow 12$
Absorption correction: analytical <i>CrysAlis PRO</i> , Agilent Technologies, Version 1.171.36.28 (release 01-02-2013 CrysAlis171.NET) (compiled Feb 1 2013, 16:14:44) Analytical numeric absorption correction using a multifaceted crystal model based on expressions derived by R.C. Clark & J.S. Reid. (Clark, R. C. & Reid, J. S. (1995). <i>Acta Cryst.</i> A51, 887-897)	$k = 0 \rightarrow 21$
$T_{\text{min}} = 0.608$ , $T_{\text{max}} = 0.844$	$l = 0 \rightarrow 22$
11721 measured reflections	

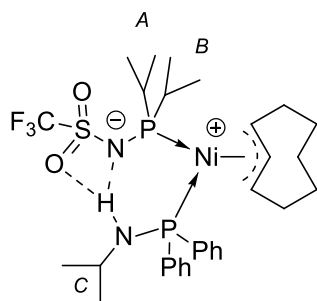
**Refinement**

Refinement on $F^2$	Primary atom site location: structure-invariant direct methods
Least-squares matrix: full	Hydrogen site location: difference Fourier map
$R[F^2 > 2\sigma(F^2)] = 0.096$	H-atom parameters constrained
$wR(F^2) = 0.210$	Method, part 1, Chebychev polynomial, (Watkin, 1994, Prince, 1982) [weight] = $1.0/[A_0 * T_0(x) + A_1 * T_1(x) + \dots + A_{n-1} * T_{n-1}(x)]$ where $A_i$ are the Chebychev coefficients listed below and $x = F / F_{\text{max}}$ Method = Robust Weighting (Prince, 1982) $W = [\text{weight}] * [1 - (\Delta F / 6 * \sigma F)^2]^2$ $A_i$ are: 269. 327. 156. 18.8
$S = 1.03$	$(\Delta/\lambda)_{\text{max}} = 0.0001$
6794 reflections	$\Delta >_{\text{max}} = 1.59 \text{ e \AA}^{-3}$
442 parameters	$\Delta >_{\text{min}} = -1.44 \text{ e \AA}^{-3}$
36 restraints	

**Hydrogen-bond geometry ( $\text{\AA}$ ,  $^\circ$ )**

$D\text{---}H\cdots A$	$D\text{---}H$	$H\cdots A$	$D\cdots A$	$D\text{---}H\cdots A$
N2—H2 $\cdots$ N1	0.859	2.995	3.775	148.53
N2—H2 $\cdots$ O2	0.859	2.844	3.481	132.27

#### 4.5 Synthesis and characterisation of complex 4



Ligand **2** (395 mg, 1.5 mmol, 1.0 eq.), N-(diphenylphosphino)isopropylamine (365 mg, 1.5 mmol, 1.0 eq.) and Ni(COD)<sub>2</sub> (415 mg, 1.5 mmol, 1.0 eq) were placed in a Schlenk with toluene (30 mL) and 4 drops of 1,5-cyclooctadiene. Upon dissolution, the mixture turned red. To reach completion, the solution was heated to 50°C for 20 minutes. The solvents were then evaporated to give a sticky solid. This oily solid was co-evaporated twice with 10 mL of pentane to give a solid which was washed with pentane (3 x

10 mL). The powder was re-dissolved in toluene and this solution was filtered to remove solid residue. The filtrate was evaporated and the solid residue submitted to co-evaporation with pentane (2 x 10 mL) followed with washing with pentane (2 x 10 mL). The solid was finally dried under reduced pressure to give a yellow powder (isolated: 574 mg, yield: 57%). Crystals suitable for X-ray diffraction were obtained from slow vapour diffusion of pentane in a toluene solution of **4**. <sup>31</sup>P {<sup>1</sup>H} NMR (300 MHz, C<sub>6</sub>D<sub>6</sub>): δ(ppm) = 85.76 (d, *J*<sub>PP</sub> = 30.9 Hz); 60.22 (d, *J*<sub>PP</sub> = 31.3 Hz); <sup>19</sup>F NMR (282 MHz, C<sub>6</sub>D<sub>6</sub>): δ(ppm) = -78.04 (s) <sup>1</sup>H NMR (300 MHz, C<sub>6</sub>D<sub>6</sub>): δ(ppm) = 0.8-1.9 (region of -CH<sub>2</sub> COD, 10H); 0.99 (dd, *J* = 5.9 & 14.4 Hz, -CH<sub>3</sub><sub>iPrA</sub>, 3H); 1.05 (d, *J* = 5.9 Hz, CH<sub>3</sub><sub>iPrC</sub>, 3H); 1.19 (d, *J* = 6.1 Hz, -CH<sub>3</sub><sub>iPrC</sub>, 3H); 1.34 (dd, *J* = 16.6 & 6.6 Hz, -CH<sub>3</sub><sub>iPrA</sub>, 3H); 1.52 (m, -CH<sub>3</sub><sub>iPrB</sub>, 6H); 2.19 (sept; *J* = 6.7 Hz, -CH<sub>iPrB</sub>, 1H); 2.90 (m, -CH<sub>iPrC</sub>, 1H); 3.36 (m, CH<sub>allyl</sub> COD β, 1H); 4.19 (m, CH<sub>allyl</sub> COD β, 1H); 4.48 (t, <sup>3</sup>*J*<sub>HH</sub> = 7.9 Hz, CH<sub>allyl</sub> COD α, 1H); 5.85 (dd, *J* = 10.5 & 18.2 Hz, NH, 1H); 7.09 (m, CH<sub>Ar-m-p</sub>, 6H); 7.62 (m, CH<sub>Ar-o</sub>, 2H); 7.72 (m, CH<sub>Ar-o</sub>, 2H). <sup>13</sup>C NMR (75 MHz, C<sub>6</sub>D<sub>6</sub>): δ(ppm) = 18.35 (CH<sub>3</sub><sub>B</sub>); 18.50 (CH<sub>3</sub><sub>A</sub>); 19.43 (CH<sub>3</sub><sub>A</sub>); 19.99 (CH<sub>3</sub><sub>B</sub>); 22.64 (CH<sub>2</sub> COD); 24.75 (CH<sub>3</sub><sub>C</sub>); 25.25 (CH<sub>3</sub><sub>C</sub>); 26.92 (CH<sub>2</sub> COD); 27.71 (CH<sub>2</sub> COD); 29.92 (CH<sub>2</sub> COD); 30.72 (d, <sup>1</sup>*J*<sub>CP</sub> = 19.2 Hz, CH<sub>iPrA</sub>); 31.37 (CH<sub>2</sub> COD); 32.74 (d, <sup>1</sup>*J*<sub>CP</sub> = 19.1 Hz, CH<sub>iPrB</sub>); 46.78 (d, <sup>1</sup>*J*<sub>CP</sub> = 12.4 Hz, CH<sub>iPrC</sub>); 72.86 (d, *J* = 15.7 Hz, CH<sub>allylβ</sub>); 81.42 (d, *J* = 18.2 Hz, CH<sub>allylβ</sub>); 110.50 (CH<sub>allylα</sub>); 121.9 (q, *J* = 323.32 Hz, CF<sub>3</sub>); 127.58 (CH<sub>Ar-m</sub>); 128.52 (CH<sub>Ar-m</sub>); 130.44 (d, *J* = 26.0 Hz, CH<sub>Ar-p</sub>); 132.90 (d, *J* = 12.05 Hz, C<sub>Ar-o</sub>); 136.08 (dd, *J* = 32.3 & 43.0 Hz, C<sub>Ar-ippo</sub>).

X-Ray structure determination of complex **4** (see text for picture)

C <sub>30</sub> H <sub>45</sub> F <sub>3</sub> N <sub>2</sub> NiO <sub>2</sub> P <sub>2</sub> S	<i>F</i> (000) = 712
<i>M</i> <sub>r</sub> = 675.42	<i>D</i> <sub>x</sub> = 1.358 Mg m <sup>-3</sup>
Monoclinic, <i>P</i> 2 <sub>1</sub>	Mo <i>K</i> α radiation, λ = 0.7107 Å
Hall symbol: <i>P</i> 2 <sub>1</sub> yb	Cell parameters from 5639 reflections
<i>a</i> = 10.1525 (5) Å	θ = 3.6–28.7°
<i>b</i> = 15.9444 (7) Å	μ = 0.79 mm <sup>-1</sup>
<i>c</i> = 10.9061 (5) Å	<i>T</i> = 150 K
β = 110.670 (5)°	Block, yellow
<i>V</i> = 1651.79 (14) Å <sup>3</sup>	0.35 × 0.26 × 0.17 mm
<i>Z</i> = 2	

#### Data collection

Xcalibur, Eos, Nova diffractometer	7365 independent reflections
Radiation source: Mova (Mo) X-ray Source	5943 reflections with $I > 2.0\sigma(I)$
mirror	$R_{\text{int}} = 0.080$
Detector resolution: 15.9897 pixels $\text{mm}^{-1}$	$\theta_{\text{max}} = 29.8^\circ$ , $\theta_{\text{min}} = 3.2^\circ$
$\omega$ scans	$h = -13 \rightarrow 13$
Absorption correction: analytical <i>CrysAlis PRO</i> , Agilent Technologies, Version 1.171.36.28 (release 01-02-2013 CrysAlis171 .NET) (compiled Feb 1 2013,16:14:44) Analytical numeric absorption correction using a multifaceted crystal model based on expressions derived by R.C. Clark & J.S. Reid. (Clark, R. C. & Reid, J. S. (1995). Acta Cryst. A51, 887-897)	$k = -21 \rightarrow 20$
$T_{\text{min}} = 0.846$ , $T_{\text{max}} = 0.910$	$l = -13 \rightarrow 14$
16282 measured reflections	

### Refinement

Refinement on $F^2$	Hydrogen site location: difference Fourier map
Least-squares matrix: full	H-atom parameters constrained
$R[F^2 > 2\sigma(F^2)] = 0.070$	Method, part 1, Chebyshev polynomial, (Watkin, 1994, Prince, 1982) [weight] = $1.0/[A_0 * T_0(x) + A_1 * T_1(x) + \dots + A_{n-1} * T_{n-1}(x)]$ where $A_i$ are the Chebyshev coefficients listed below and $x = F / F_{\text{max}}$ Method = Robust Weighting (Prince, 1982) $W = [\text{weight}] * [1 - (\Delta F / 6 * \sigma F)^2]$ $A_i$ are: 227. 285. 102.
$wR(F^2) = 0.116$	$(\Delta/\sigma)_{\text{max}} = 0.0001$
$S = 0.99$	$\Delta_{\text{max}} = 2.41 \text{ e } \text{\AA}^{-3}$
7365 reflections	$\Delta_{\text{min}} = -1.81 \text{ e } \text{\AA}^{-3}$
371 parameters	Absolute structure: Flack (1983), 3201 Friedel-pairs
1 restraint	Flack parameter: 0.03 (2)
Primary atom site location: structure-invariant direct methods	

### Hydrogen-bond geometry ( $\text{\AA}$ , $^\circ$ )

$D-H \cdots A$	$D-H$	$H \cdots A$	$D \cdots A$	$D-H \cdots A$
$\text{N2}-\text{H2} \cdots \text{N1}$	0.85	2.19	2.977 (11)	153 (1)
$\text{N2}-\text{H2} \cdots \text{O1}$	0.85	2.59	3.323 (11)	145

Symmetry code: (i)  $-x, y+1/2, -z$ .

## 4.6 High pressure ethylene NMR experiments

For NMR experiments, ca. 20 mg of complex were charged in a high pressure NMR tube in the glove box under argon and dissolved in 0.6 mL of dry, degassed  $\text{C}_6\text{D}_6$ . The tube was closed and connected outside of the glove box to ethylene supply by the screw cap. The line was purged 5 times (vacuum / ethylene) to get rid of residual oxygen. The ethylene pressure was set at 5 bars and then the screw cap was gently opened to pressurise the tube which was then closed, disconnected and vigorously shaken. All these operations were repeated twice to ensure saturation of ethylene inside the solution contained in the NMR tube.

#### 4.7 Procedure for the oligomerisation of ethylene (semi-batch)

The reactor of 250 mL was dried under vacuum at 100°C for 2 hours and then pressurised to 5 bar of ethylene. The ethylene supply was closed and the reactor was cooled down at room temperature. Ethylene inside the reactor was evacuated, maintaining however a slight over pressure inside the reactor (1.4 bar). The solvent used for catalysis (toluene, 50 mL) was injected and then heated to 40°C (or 50°C) under magnetic stirring (1000 rpm). When the temperature inside the reactor was stabilised, stirring was stopped and the catalyst solution (10 or 50  $\mu\text{mol}$  in toluene: 5 mL) was injected. Then the reactor was pressurised to 30 bar of ethylene and the pressure maintained by connection to an ethylene supply cylinder (80 bar) positioned on a balance (semi-batch). The reaction started ( $t=0$ ) with magnetic stirring (1000 rpm) and the test ran for 90 min with a regular monitoring the ethylene uptake by the mass reduction of the ethylene supply cylinder. The reaction was stopped by closing the ethylene supply and cooling the reactor to 25°C (250 rpm). The gas phase was evacuated, quantified through a flowmeter and collected in a 30L plastic drum by water displacement (stirring the liquid phase to 1000 rpm was necessary to degas completely the liquid phase). The plastic drum containing the gas phase was shaken with residual water to homogenise the gas and a portion of this gas phase was collected in a glass ampulla and injected in GC. After all the gas fraction had been evacuated, stirring was stopped and the reactor was carefully opened. The liquid phase was transferred with a plastic pipette to a glass bottle cooled to 0°C (to minimise butene losses). The liquid phase was quantified by mass and a cold sample injected directly in GC.

Catalytic reactions were carried out to have significant ethylene uptake, therefore complexes **3** and **4** were run at 10  $\mu\text{mol}$  of nickel while the less active benchmark complex **Ref** was evaluated at 50  $\mu\text{mol}$  of nickel. Moreover catalytic reaction for **Ref** requested to be run at 50°C to trigger catalyst activation, as seen by ethylene consumption. Ethylene uptake was monitored as function of time during the catalytic reaction. Dissolution occurs at the start (0-5 min), followed by a linear uptake. In the test conditions (30 bar and 40°C, 50 mL toluene) complex **3** led to an uptake of 48.6 g of ethylene, which corresponds to 21.0 g of oligomers formed, the mass difference being unreacted ethylene. Complex **4**, in the same conditions led to an uptake of 30.5 g of ethylene which correspond to 10.2 g of oligomers, the rest consisting of unreacted ethylene. The benchmark complex (**Ref**) at 30 bar and 50°C, and  $n_{\text{Ni}} = 50 \mu\text{mol}$  (five times more concentrated than **3** and **4**) led to an uptake of 47.9 g of ethylene which corresponds to 32 g of oligomers and waxes and unreacted ethylene. The Schulz-Flory constant ( $K_{\text{SF}}$ ) was established based on the mass percentage of  $\text{C}_8\text{-C}_{18}$  cuts.

## 5 References

- [1] W. Keim, F. H. Kowaldt, R. Goddard, C. Krüger, *Angew. Chem., Int. Ed.* **1978**, *17*, 466–467.
- [2] W. Keim, *Angew. Chem., Int. Ed.* **2013**, *52*, 12492–12496.
- [3] B. Cornils, W. A. Herrmann, in *Appl. Homog. Catal. with Organomet. Compd.*, Wiley-VCH Verlag GmbH, **2008**, pp. 213–385.
- [4] A. Forestière, H. Olivier-Bourbigou, L. Saussine, *Oil Gas Sci. Technol.* **2009**, *64*, 649–667.
- [5] P. Kuhn, D. Sémeril, C. Jeunesse, D. Matt, M. Neuburger, A. Mota, *Chem. Eur. J.* **2006**, *12*, 5210–5219.
- [6] P. Kuhn, D. Sémeril, D. Matt, M. J. Chetcuti, P. Lutz, *Dalt. Trans.* **2007**, 515–528.
- [7] A. Kermagoret, P. Braunstein, *Dalton Trans.* **2008**, *33*, 822–831.
- [8] S. Mecking, *Coord. Chem. Rev.* **2000**, *203*, 325–351.
- [9] F. Speiser, P. Braunstein, L. Saussine, *Acc. Chem. Res.* **2005**, *38*, 784–793.
- [10] S. Wang, W.-H. Sun, C. Redshaw, *J. Organomet. Chem.* **2014**, *751*, 717–741.
- [11] F. W. Patureau, M. Kuil, A. J. Sandee, J. N. H. Reek, M. K. Frederic W. Patureau Albertus J. Sandee and Joost N.H. Reek, *Angew. Chem., Int. Ed.* **2008**, *47*, 3180–3183.
- [12] F. W. Patureau, S. de Boer, M. Kuil, J. Meeuwissen, P.-A. R. Breuil, M. a Siegler, A. L. Spek, A. J. Sandee, B. de Bruin, J. N. H. Reek, *J. Am. Chem. Soc.* **2009**, *131*, 6683–6685.
- [13] T. León, M. Parera, A. Roglans, A. Riera, X. Verdager, *Angew. Chem., Int. Ed.* **2012**, *51*, 6951–6955.
- [14] F. W. Patureau, M. a Siegler, A. L. Spek, A. J. Sandee, S. Jugé, S. Aziz, A. Berkessel, J. N. H. Reek, *Eur. J. Inorg. Chem.* **2012**, *2012*, 496–503.
- [15] F. G. Terrade, M. Lutz, J. N. H. Reek, *Chem. Eur. J.* **2013**, *19*, 10458–10462.
- [16] F. G. Terrade, M. Lutz, J. I. van der Vlugt, J. N. H. Reek, *Eur. J. Inorg. Chem.* **2014**, *2014*, 1826–1835.
- [17] M. J. W. Joost N. H. Reek Piet W. N. M. van Leeuwen, *Org. Biomol. Chem.* **2005**, *3*, 2371–2383.
- [18] J. Meeuwissen, J. N. H. Reek, *Nat. Chem.* **2010**, *2*, 615–621.
- [19] M. Raynal, P. Ballester, A. Vidal-Ferran, P. W. N. M. van Leeuwen, *Chem. Soc. Rev.* **2014**, *43*, 1660–1733.
- [20] M. Raynal, P. Ballester, A. Vidal-Ferran, P. W. N. M. van Leeuwen, *Chem. Soc. Rev.* **2014**, *43*, 1734–1787.
- [21] N. V Dubrovina, A. Börner, *Angew. Chem. Int. Ed. Engl.* **2004**, *43*, 5883–5886.
- [22] B. Breit, *Angew. Chem. Int. Ed. Engl.* **2005**, *44*, 6816–6825.
- [23] C. Machut, J. Patriceon, S. Tilloy, H. Bricout, F. Hapiot, E. Monflier, *Angew. Chem., Int. Ed.* **2007**, *46*, 3040–3042.
- [24] S. B. Owens, G. M. Gray, *Organometallics* **2008**, *27*, 4282–4287.
- [25] S. a Moteki, J. M. Takacs, *Angew. Chem., Int. Ed.* **2008**, *47*, 894–897.
- [26] P.-A. R. Breuil, F. W. Patureau, J. N. H. Reek, *Angew. Chem., Int. Ed.* **2009**, *48*, 2162–2165.
- [27] Y. Hasegawa, I. D. Gridnev, T. Ikariya, *Angew. Chem. Int. Ed. Engl.* **2010**, *49*, 8157–8160.
- [28] A. Christiansen, D. Selent, A. Spannenberg, M. Köckerling, H. Reinke, W. Baumann, H. Jiao, R. Franke, A. Börner, *Chem. Eur. J.* **2011**, *17*, 2120–2129.

- [29] L. Pignataro, M. Boghi, M. Civera, S. Carboni, U. Piarulli, C. Gennari, *Chemistry* **2012**, *18*, 1383–1400.
- [30] S. a Moteki, K. Toyama, Z. Liu, J. Ma, A. E. Holmes, J. M. Takacs, *Chem. Commun.* **2012**, *48*, 263–265.
- [31] U. Gellrich, W. Seiche, M. Keller, B. Breit, *Angew. Chem. Int. Ed. Engl.* **2012**, *51*, 11033–11038.
- [32] M. de Greef, B. Breit, B. B. Michiel de Greef, *Angew. Chem., Int. Ed.* **2009**, *48*, 551–554.
- [33] J. Malinoski, M. Brookhart, *Organometallics* **2003**, *22*, 5324–5335.
- [34] R. Ceder, G. Muller, J. Sales, J. Vidal, D. Neibecker, I. Tkatchenko, *J. Mol. Catal.* **1991**, *68*, 23–31.
- [35] B. Boardman, G. C. Bazan, *Acc. Chem. Res.* **2009**, *42*, 1597–1606.
- [36] I. Albers, E. Alvarez, J. Campora, C. M. Maya, P. Palma, L. J. Sanchez, E. Passaglia, *J. Organomet. Chem.* **2004**, *689*, 833–839.
- [37] T. R. Younkin, *Science (80-. )*. **2000**, *287*, 460–462.
- [38] D. V. Gutsulyak, A. L. Gott, W. E. Piers, M. Parvez, *Organometallics* **2013**, *32*, 3363–3370.
- [39] H.-F. Klein, M. He, O. Hetche, A. Rau, D. Walther, T. Wieczorek, G. Luft, *Inorganica Chim. Acta* **2005**, *358*, 4394–4402.
- [40] D. Chandran, C. Bae, I. Ahn, C.-S. Ha, I. Kim, *J. Organomet. Chem.* **2009**, *694*, 1254–1258.



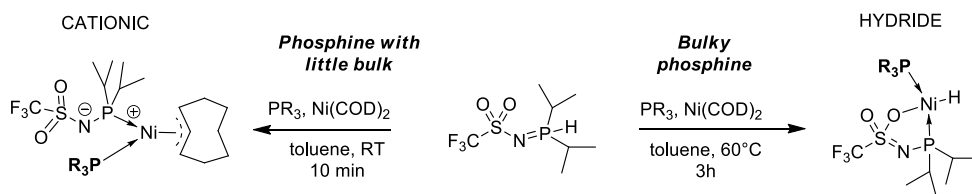


# Chapter 5

---

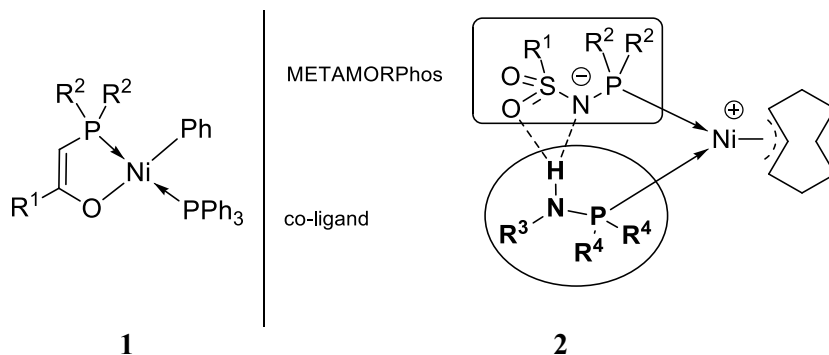
## Zwitterionic and Nickel Hydride Complexes based on METAMORPhos Ligand: a Parameter Study on their Formation

---



# 1 Introduction

Single component and well-defined nickel catalysts are of particular interest for olefins oligomerisation as they do not require an additional activator. These systems greatly simplify the operability of the catalytic reactions. Besides they allow identifying the reaction intermediates (active species). One of the prominent examples is the neutral (PO)-coordinated nickel aryl phosphine complex **1** that affords linear alpha olefins (LAO) and allowed for the development of the SHOP process in the late 70s.<sup>[1-5]</sup> This single system was extensively reviewed and key structural factors such as phosphorus substituents, ligands and chelate backbone have been identified and linked to performances in oligomerisation reaction.<sup>[6-8]</sup> In Chapter 4, we disclosed a new class of single component nickel catalysts based on structure **2**. These complexes, stabilised by hydrogen bonding, readily oligomerise ethylene with high activity ( $24 \text{ kg}_{\text{oligo}}/(\text{g}_{\text{Ni}}\cdot\text{h})$ ) but most importantly possess unprecedented selectivity features. A simple change in phosphorus substituents allows a shift between a broad LAO distribution, (comparable to SHOP) to a more interesting selective 1-butene formation.



We sought to understand the structural parameters allowing the formation of such architectures through self-assembly. We studied the combination of METAMORPhos ligands (Figure 1) with aminophosphines as well as non-functionalised phosphines on the complex formation and stability. We observed the formation of supramolecular assemblies, zwitterionic and hydride complexes. The influence of steric and electronic parameters of both ligands applied on the complex formation is described and a mechanism that accounts for their formation is suggested.

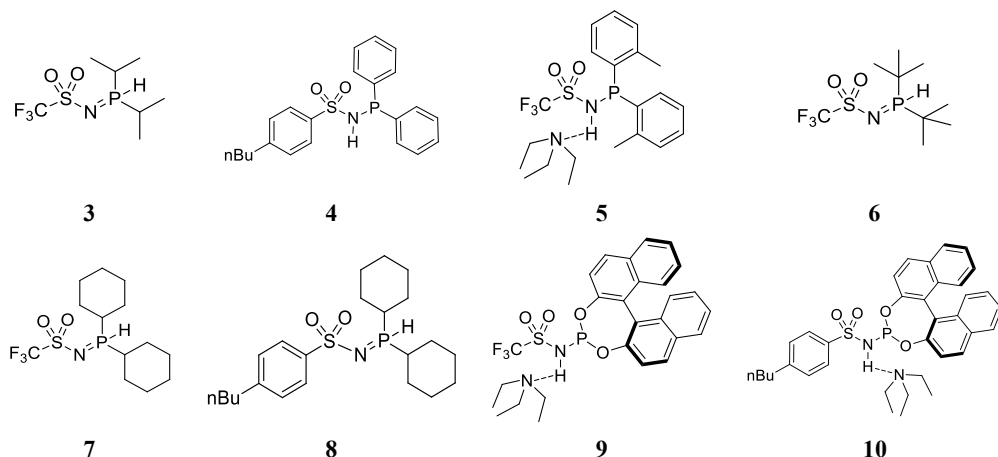


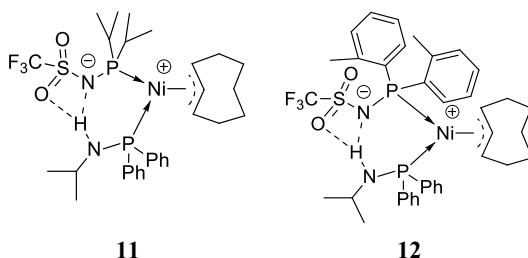
**Figure 1.** METAMORPhos ligands used in this study, exist in different tautomeric forms and can be associated to a triethylamine adduct. For more information see Chapter 2.

## 2 Synthesis of the complexes

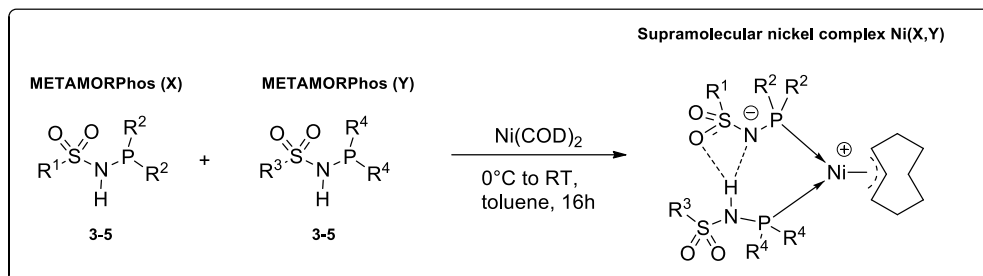
### 2.1 Reactivity of the system METAMORPhos / aminophosphine with Ni(COD)<sub>2</sub>

#### 2.1.1 Access to zwitterionic bis(METAMORPhos) nickel complexes

In the previous Chapter we reported that METAMORPhos ligand **3** or **5** reacted with Ni(COD)<sub>2</sub> and the aminophosphine (*i*Pr-NH-PPh<sub>2</sub>) leading to the corresponding supramolecular complexes **11** and **12**. The selective formation of the heterocomplex was interesting, and proposed to be (partly) driven by hydrogen bond formation. Complex formation from two monodentate ligands and a metal, leads (in principle) to the statistical combinations of 2 homocomplexes and the heterocomplex in a 2/3 and 1/3 ratio respectively.



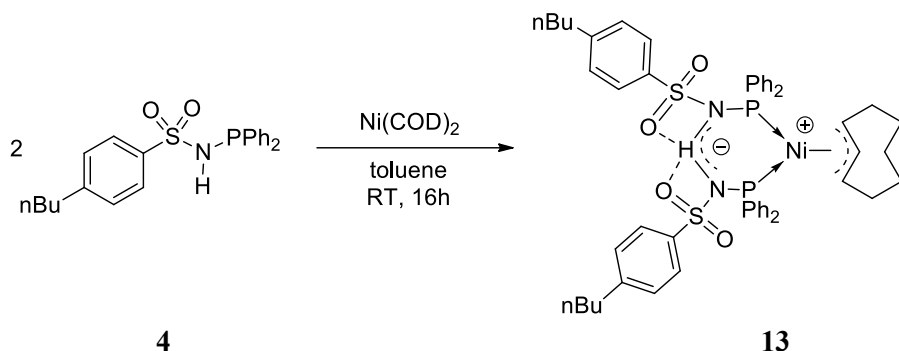
To understand the formation of these complexes and potentially broaden the scope of available single component nickel complexes, we investigated the synthesis of METAMORPhos-based homocomplexes by reacting METAMORPhos ligand (2 eq.) with Ni(COD)<sub>2</sub> (1 eq.) according to Scheme 1.



**Scheme 1.** Reaction of two METAMORPhos ligands with  $\text{Ni}(\text{COD})_2$  aiming to form bis(METAMORPhos) nickel zwitterionic cationic supramolecular complexes

When two equivalents of METAMORPhos **3** (PH tautomer) were added to a solution of  $\text{Ni}(\text{COD})_2$  no reaction was observed and therefore the synthesis of the corresponding homocomplex was not possible. In contrast, a quick colour change from yellow to dark greenish was observed when two equivalents of ligand **4** were added to a solution of  $\text{Ni}(\text{COD})_2$ . The complex **13** that formed had a broad peak appearing in the  $^{31}\text{P}$  NMR spectrum at  $\delta$ : 55 ppm.<sup>1</sup> We suggest that the peak broadness is the result of signal overlap and fast intermolecular proton exchange at room temperature, leading to equivalent ligands at the NMR timescale. Decreasing the temperature should limit the rate of exchange of the proton between the two moieties and therefore should lead to splitting of this broad signal. Indeed, a slow decrease in the temperature (to  $-80^\circ\text{C}$ ) led to disappearance of the original broad signal in  $^{31}\text{P}$  NMR and the appearance of new broad signals at  $\delta(\text{CD}_2\text{Cl}_2)$ : 57 and 30 ppm. These chemical shift values are close to those of a phosphine coordinated to nickel and of free ligand **4** respectively (see experimental part). Typical proton signals attributed to the allyl fragment were also observed for **13** and the ligand **4** NH signal at 5.81 ppm ( $\text{C}_6\text{D}_6$ ) was shifted to 9.64 ppm ( $\text{C}_6\text{D}_6$ ) in the complex, suggesting that a hydrogen-bond is present between the two ligand moieties. As a consequence complex **13** is likely to adopt a *cis* arrangement, as proposed in the structure of Scheme 2.

<sup>1</sup> The crude reaction mixture consisted of the product **13** at 55 ppm (80%) and the other product was a doublet system at  $\delta(\text{ppm})$ : 12 (d,  $^2J_{\text{PP}} = 17.0$  Hz) and 53 (d,  $^2J_{\text{PP}} = 17.0$  Hz) for 20% corresponding to the thermal degradation product (see experimental part for further details).



**Scheme 2.** Synthesis of bis METAMORPhos zwitterionic nickel complex **13** from METAMORPhos ligand **4** and  $\text{Ni(COD)}_2$ .

METAMORPhos **5** was not very reactive with  $\text{Ni(COD)}_2$  but a broad signal observed in  $^{31}\text{P}$  NMR at 62 ppm suggests that the homocomplex had formed similarly to what observed for ligand **4**. The peak broadness also suggests quick proton exchange at RT. Other products observed in  $^{31}\text{P}$  NMR probably correspond to the decomposition products of the homocomplex (37 and 61 ppm). Unfortunately the homocomplex could not be isolated.

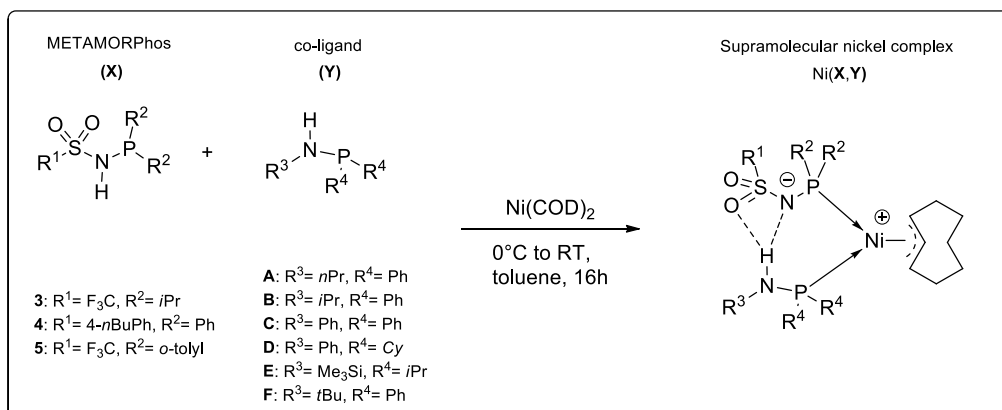
Synthetic access to the heterocomplex (**3,4**) was also investigated with ligands **3** and **4**. NMR analysis of the crude reaction mixture shows that it consists of a mixture of the heterocomplex (**3,4**), ligand **3** and the homocomplex (**4,4**) as concluding from broad signals around 90 ppm and 54 ppm. No product could however be isolated.

In summary, the reactivity of METAMORPhos +  $\text{Ni(COD)}_2$  to form the homocomplexes depends on the tautomeric form of the ligand. METAMORPhos ligands under the  $\text{P}^{\text{III}}$  coordinating NH tautomer led to homocomplexes (**4,4**) and (**5,5**) while ligands under the PH tautomer are not reactive with  $\text{Ni(COD)}_2$ , whereas when combined with a proper co-ligand, they do form complexes. Therefore, the choice of METAMORPhos in the PH tautomer is a way to suppress the formation of the homocomplexes and favour clean hetero-combinations. However a co-ligand (aminophosphine) is required to achieve complex formation. The choice of this co-ligand is crucial as clean formation of the heterocomplex (**3,4**), using **4** (NH tautomer) as co-ligand, was hampered by competitive side reactions leading to homocomplexes.

### 2.1.2 Diversification of the aminophosphines of the zwitterionic nickel complexes

The synthesis of homocomplexes, based on METAMORPhos ligands presented above, stresses the importance of the co-ligand properties to prevent the formation of homocomplexes. In order to have a clearer idea of the parameters that rule this selectivity, we studied the influence of several aminophosphine co-ligands (**A-F** presented in Figure 2) on the synthesis of supramolecular nickel complexes. For this study, METAMORPhos ligands **3**, **4**, **5** with different electronic contributions have been selected and the experimental conditions followed are presented in Scheme 3

*Nickel complexes will be abbreviated by Ni(X,Y) where X refers to the METAMORPhos under the anionic form and Y corresponds to the neutral co-ligand. In addition to this abbreviation, isolated complexes will be indexed with a number.*



**Scheme 3.** General synthetic approach used for the preparation of zwitterionic complexes from METAMORPhos, aminophosphine and Ni(COD)<sub>2</sub>.

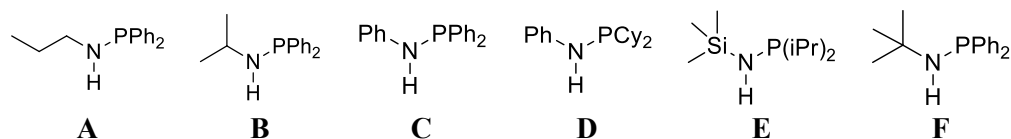


**Figure 2.** Aminophosphine co-ligands A-F used in this study of general formula R<sup>1</sup>-NH-P(R<sup>2</sup>)<sub>2</sub>; they are potentially H-donor moieties

Using a similar procedure to the one affording Ni(**3,B**):**11** and Ni(**5,B**):**12**, the heterocomplexes containing the co-ligand **A** Ni(**3,A**):**14** and Ni(**5,A**):**15** were formed quantitatively and isolated. The NMR spectra are very similar to those of complexes **11** and **12**. Crystal structures were determined for **14** and **15** (see Figure 3 and Figure 4 respectively). The resemblance of both crystal structures with those of **11** and **12**,

suggests that an increase of steric bulk on the nitrogen from (*n*-Pr to *i*Pr) had little influence on the geometry of the complex. The use of the very bulky aminophosphine **F** (*t*Bu-NH-PPh<sub>2</sub>) for the synthesis of Ni(**3,F**) led to a slow reaction and we could not observe clear complex formation by NMR. This suggests that a threshold exists above which too much steric hindrance at the R<sup>3</sup> prevents the formation of supramolecular zwitterionic nickel complexes. Similarly, a decrease of the steric bulk on METAMORPhos phosphine (P(*o*-tolyl)<sub>2</sub> to PPh<sub>2</sub>) led to the formation of complex Ni(**4,B**) in good yields (> 95%). This complex was sensitive to heat and could not be isolated in pure form. This suggests that bulky substituents on METAMORPhos phosphorus increase the stability of the heterocomplexes with respect to the homocomplex.

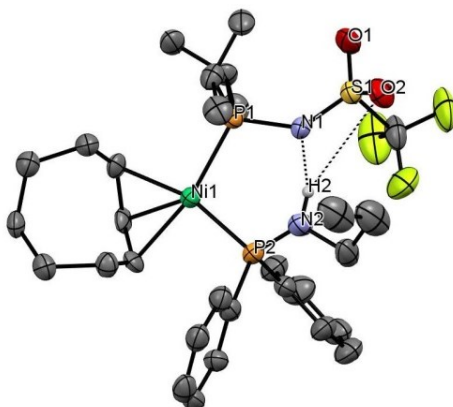
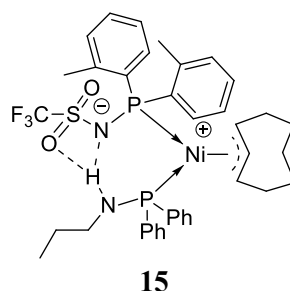
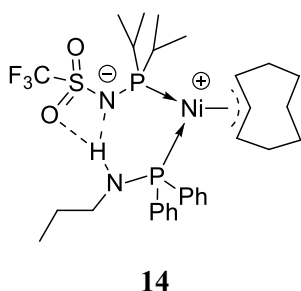


**Figure 3.** ORTEP plot (50% probability displacement ellipsoids) of complex **14**. Hydrogen atoms have been omitted for clarity (except for NH moiety). Selected bond lengths (Å) and angles (°): Ni1-P1 2.221(2); Ni1-P2 2.197(2); N2-H2 0.869; N1-H2 2.074; O2-H2 3.033; P1-Ni1-P2 102.44(7).

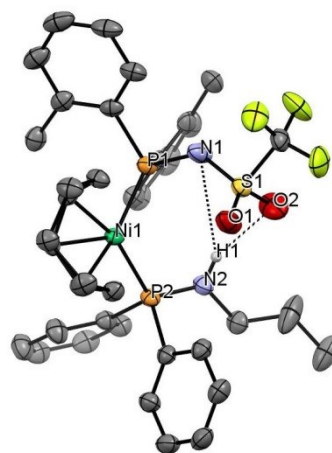


**Figure 4.** ORTEP plot (50% probability displacement ellipsoids) of complex **15**. Hydrogen atoms have been omitted for clarity (except for NH moiety). Selected bond lengths (Å) and angles (°): Ni1-P1 2.2173(9); Ni1-P2 2.2024(9); N2-H1 0.851; N1-H1 3.304; O--H1 2.373; P1-Ni1-P2 106.56(3).



Next, the use of aminophosphine **C** (Ph-NH-PPh<sub>2</sub>) was explored. The phenyl group attached to the nitrogen reduces the electronic density of this aminophosphine at the nitrogen. Moreover, as **C** is unable to form a zwitterionic homocomplex with Ni(COD)<sub>2</sub> it should favour the formation of heterocomplexes to the same extent as co-ligand **A** and **B** with METAMORPhos **3** and **5**. The synthesis of Ni(**3,C**), Ni(**4,C**), Ni(**5,C**) led indeed to the respective heterocomplexes in solution, however with limited conversion (up to 66% according to <sup>31</sup>P NMR of the crude mixture). A competitive ligand coordination was observed for complex Ni(**4,C**), (similarly to complex Ni(**4,3**)) leading to the formation of the homocomplex Ni(**4,4**). This shows the importance of strong electron donating groups on the nitrogen of the aminophosphine co-ligands (such as **A** or **B**) to favour the selective formation of heterocomplexes.

Co-ligands **A**, **B**, **C**, **F** and **4** used so far, all have in common the -NH-PPh<sub>2</sub> group. Although very similar, a clear difference is noted in their reactivity. This suggests that the substitution at the nitrogen atom affects the H-bonding and probably also the electronic properties at the phosphorus atom. We sought to determine if increasing the electron density on the phosphorus by using directly attached substituents would also lead to the corresponding zwitterionic complexes as shown in Scheme 3. For this, we introduced P-alkyl substituted aminophosphine ligand **D** and **E**. The heterocomplex Ni(**3,D**) was observed (<sup>31</sup>P and <sup>1</sup>H NMR) in solution but the presence of several other products in the crude mixture prevented its isolation. Attempts to form Ni(**4,D**) led to numerous products. Similarly the heterocomplex Ni(**5,E**) was observed in solution at very low conversion but could not be isolated. Increasing the electron density on the phosphorus by using directly attached substituents also led to the formation of the heterocomplexes but also by-products were observed in reaction mixtures that probably correspond to degradation products of the cationic complex. In comparison, co-ligands with a diphenyl substituted phosphorus (e.g. **A** and **B**) led to more stable nickel heterocomplexes.

In summary, the access to supramolecular zwitterionic heterocomplexes in the reaction of METAMORPhos + aminophosphine + Ni(COD)<sub>2</sub> depends on several parameters. The phosphorus atom at the co-ligand needs to be sufficiently electron-rich for stable coordination to the nickel atom to occur. This was realised by employing phenyl P-substituted aminophosphines having donating groups on the nitrogen. Moreover, hetero-complexes formed selectively when by themselves both ligand and co-ligand did not perform oxidative addition on Ni(COD)<sub>2</sub> and only a mixture of the two formed the desired complex. This was particularly the case for METAMORPhos in the PH tautomer and electron rich aminophosphines (see **11-15**). In the case of reactive METAMORPhos (NH), it was important that the co-ligand

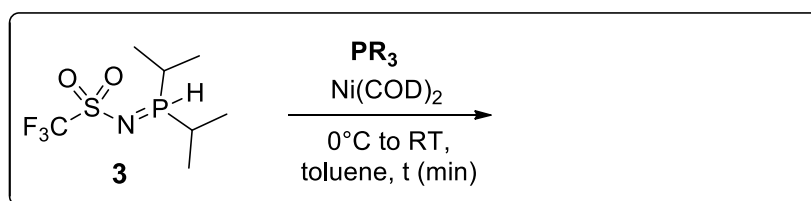
was more electron-donating than METAMORPhos itself to favour pure hetero-combinations. By following this strategy 4 heterocomplexes and 1 homocomplex were synthesised in pure form. This class of complexes was not particularly stable because degradation in solution occurred already at 60°C. The overall stability depends mainly on the nature of the co-ligand. Co-ligands with bulky phosphine substituents such as *t*Bu led to slow complex formation. An increase in the basicity of the phosphorus atom by using directly attached substituents led to complicated mixtures.

## 2.2 Reactivity of the system METAMORPhos / phosphine (or phosphite) with Ni(COD)<sub>2</sub>

Aminophosphines and in particular diphenyl P-substituted analogues have been successfully used to selectively form stable zwitterionic heterocomplexes **11**, **12**, **14**, **15**. We wondered if other electron-rich ligands would function similarly. Non-functionalised phosphines (and phosphites) were introduced as co-ligands instead of aminophosphines with the aim to further diversify the properties of the complexes. METAMORPhos ligand **3** was selected for this study since it does not form the homocomplex Ni(**3**,**3**) by itself in the presence of Ni(COD)<sub>2</sub>.

### 2.2.1 Trimethylphosphine (PMe<sub>3</sub>) as co-ligand

Trimethylphosphine, a strongly electron donating phosphine with limited bulk, was first evaluated as co-ligand in the reaction of ligand **3** with Ni(COD)<sub>2</sub> at room temperature according to Scheme 4.

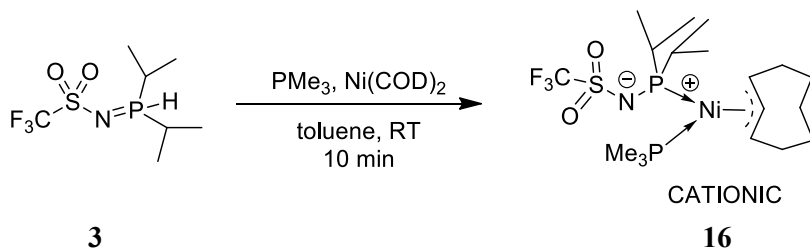


**Scheme 4.** General procedure used for the preparation of complexes based on different phosphines **PR**<sub>3</sub> and ligand **3**.

Upon addition of trimethylphosphine to a mixture of ligand **3** and Ni(COD)<sub>2</sub> a clear brown colour developed and the solution slowly darkened upon stirring. When monitoring the reaction by unlocked <sup>31</sup>P NMR, first the formation of a peak at -23 ppm was observed, which corresponds to Ni(PMe<sub>3</sub>)<sub>4</sub> according to literature.<sup>[9]</sup> This signal, together with the one of METAMORPhos ligand **3**, decreased upon time with the formation of two doublets at 87 ppm and -11 ppm, both having a coupling

constant of 31 Hz. The reaction was complete and neat already after 10 min as evidenced by  $^{31}\text{P}$  NMR.

The isolated product had typical features of previously reported zwitterionic supramolecular complexes: two phosphorus atoms with small  $^2J_{PP}$  *cis* coupling and the allylic protons between 3.5 and 4.4 ppm in the  $^1\text{H}$  NMR spectrum (see Scheme 5 and Figure 5). Further NMR characterisation and proper elemental analysis confirmed the formation of complex **16**. The absence of a proton donor moiety in the co-ligand ( $\text{PMe}_3$ ) proved that hydrogen bonding was not a crucial element for the formation of the hetero ligated complex.



**Scheme 5.** Synthesis of zwitterionic cationic complex **16** from METAMORPhos ligand **3**,  $\text{PMe}_3$  and  $\text{Ni}(\text{COD})_2$

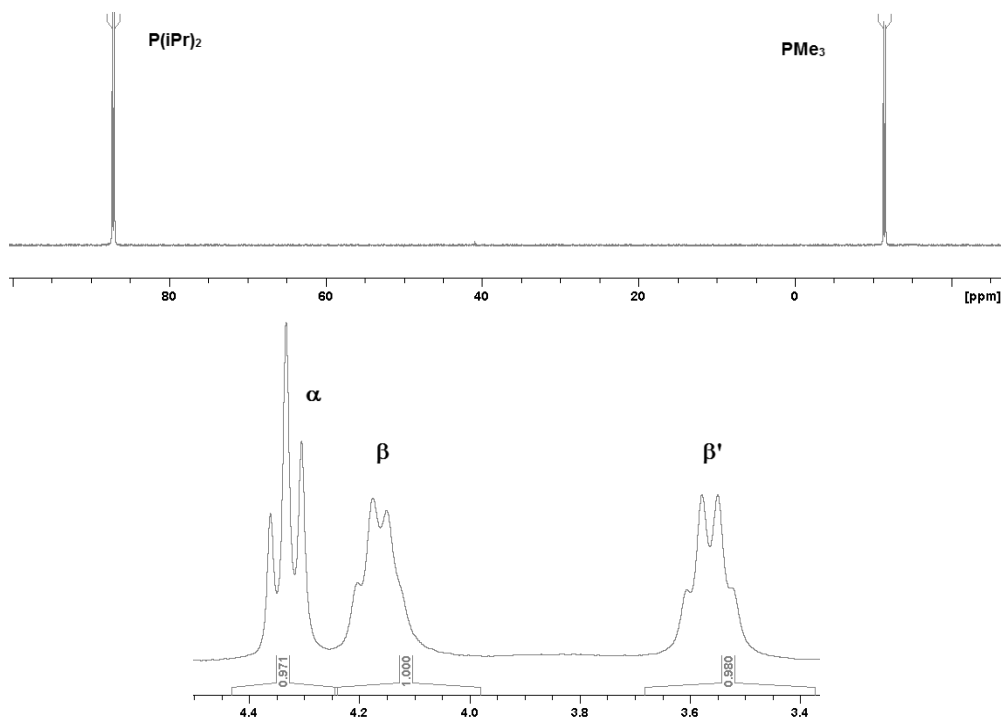


**Figure 5.**  $^{31}\text{P}$  NMR (121 MHz,  $\text{C}_6\text{D}_6$ , 300K) spectrum (above) and  $^1\text{H}$  NMR (300 MHz,  $\text{C}_6\text{D}_6$ , 300K) spectrum (allyl region, below) for complex **16** ( $\alpha$ : central allylic proton,  $\beta$  and  $\beta'$ : side allylic protons).

Crystals of complex **16** suitable for X ray diffraction were grown by slow diffusion of pentane in a toluene solution of the complex. The corresponding ORTEP plot is presented in Figure 6. Zwitterionic complex **16** adopts a square planar environment around the metal (sum of angles =  $360.7^\circ$ ), which was in line with the diamagnetic nature of this complex and its observation by NMR. Moreover, the solid-state arrangement for zwitterionic complex **16** was very similar to the supramolecular complexes **11-15** (similar angles and bond lengths). This means that replacing aminophosphines by phosphines also has limited effect on the complex geometry.

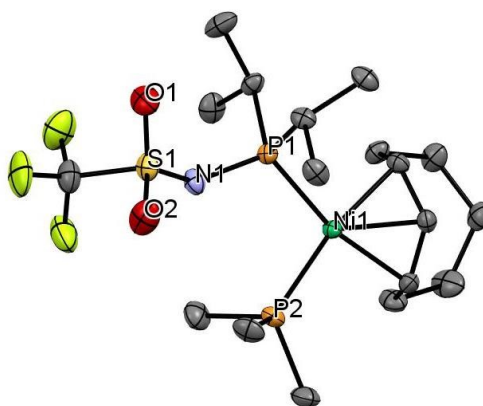


**Figure 6.** ORTEP plot (50% probability displacement ellipsoids) of complex **16**. Hydrogen atoms have been omitted for clarity. Selected bond lengths (Å) and angles ( $^\circ$ ): Ni1-P2 2.1889 (5); Ni1-P1 2.2127 (5); Ni1-C21 2.0825 (18); Ni1-C22 1.9744 (18); Ni1-C23 2.0864 (17); P1-N1 1.6592 (16); N1-S1 1.5313 (16); S1-O1 1.4482 (17); S1-O2 1.4492 (17); P2-Ni1-P1 100.34 (2); P1-N1-S1 133.88 (11)

By a similar approach we synthesised  $\text{PMe}_3$ -based zwitterionic complexes **16**, **17**, **18**, **19**, **20**, **21**, **22** based on METAMORPhos ligands **3**, **4**, **5**, **7**, **8**, **9**, **10**. Their structures are presented in Figure 7. Complexes **16**, **17** and **18** were synthesised on a larger scale and isolated for further analysis and catalytic experiments (see Chapter 6). The clean formation of hetero ligated complex was ensured thanks to the strong basicity and certainly the small size of  $\text{PMe}_3$ , which for instance prevented the formation of the homocombination **13** ( $\text{Ni}(\mathbf{4},\mathbf{4})$ ), observed in absence of  $\text{PMe}_3$  with ligand **4** and  $\text{Ni}(\text{COD})_2$ .

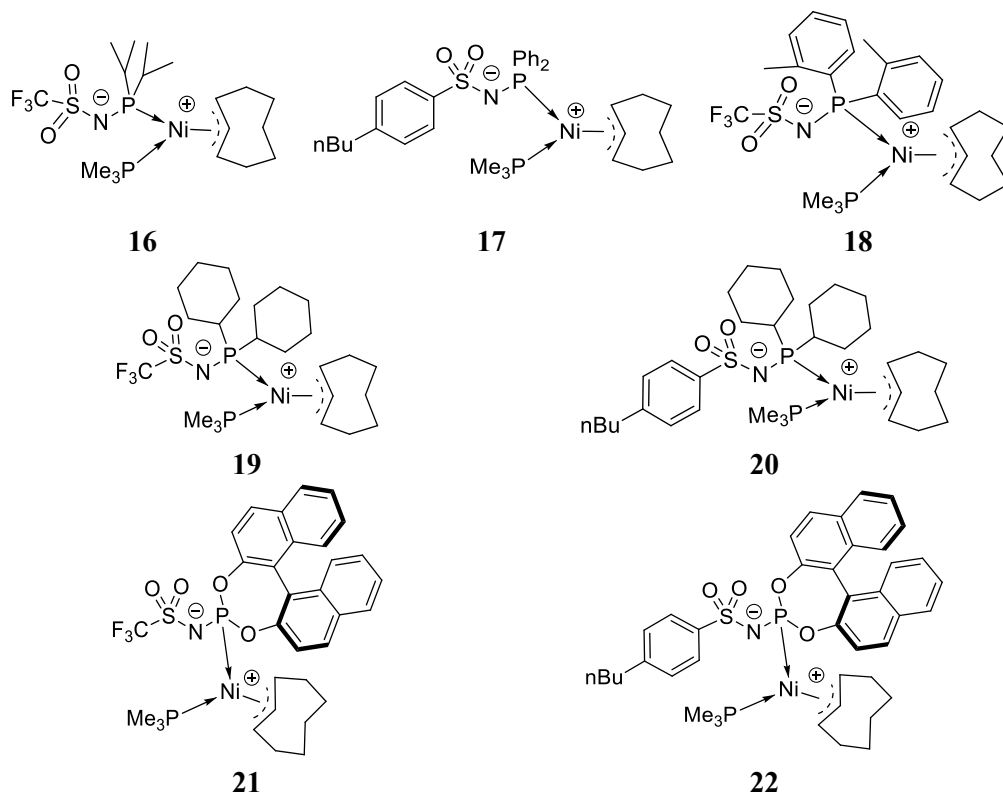


**Figure 7.** Zwitterionic complexes based on  $\text{PMe}_3$  isolated (**16**, **17**, **18**) or observed from the crude reaction mixture (**19**, **20**, **21**, **22**) based on  $^{31}\text{P}$  NMR chemical shifts. Conditions:  $[\text{METAMORPhos}] = [\text{PMe}_3] = [\text{Ni}(\text{COD})_2] = 50 \text{ mM}$  in toluene, stirring 10 min at RT, almost quantitative reactions.

Crystals of complex **17** were grown by slow vapour diffusion of pentane in a toluene solution of the complex. The corresponding ORTEP plot is presented in Figure 8. According to the crystal structures, both zwitterionic complexes **16** (Figure 6) and **17** adopt a square planar environment around the metal (sum of angles =  $360.67^\circ$  for **16** and  $360.03^\circ$  for **17**). Both are diamagnetic with similar characteristics. The  $\text{P}_{\text{METAMORPhos}}\text{-Ni}$  bond (P1-Ni1) bond was longer for complex **16** with  $\text{P}(\text{iPr})_2$  (Ni1-P1 2.2127 (5) Å) than that of complex **17** with  $\text{PPh}_2$  (Ni1-P29 2.1929 (10) Å). The bite angle (P1-Ni-P2) for complex **16** was  $100.34(2)^\circ$  while the one for **17** is  $102.15(4)^\circ$ , which is close to that of the supramolecular complex **11** with a value of  $103.96(6)^\circ$ .

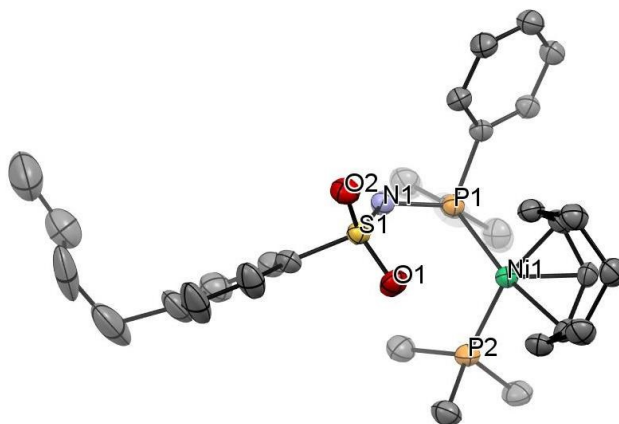


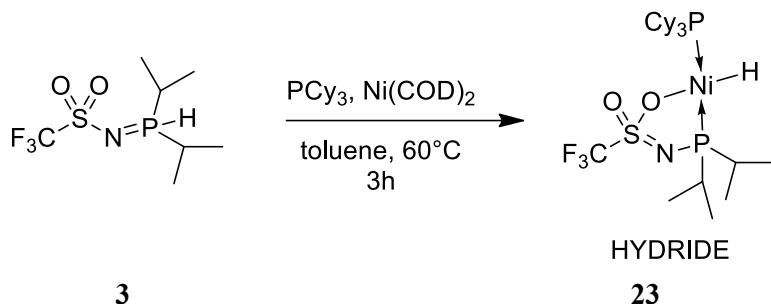
**Figure 8.** ORTEP plot (50% probability displacement ellipsoids) of complex **17**. Hydrogen atoms and a pentane molecule have been omitted for clarity. Selected bond lengths (Å) and angles (°): Ni1-P1 2.1929 (10); Ni1-P2 2.1828 (11); Ni1-C33 2.093 (4); Ni1-C34 1.970 (4); Ni1-C35 2.058 (4); P1-N1 1.660 (3); N1-S1 1.558 (3); S1-O1 1.455 (3); S1-O2 1.445 (3); P1-Ni1-P2 102.15 (4); P1-N1-S1 123.0 (2).

The stability of these  $\text{PMe}_3$ -based complexes is excellent compared to the aminophosphine-based complexes described before as they did not show degradation at room temperature. Heating the complexes was necessary to observe degradation. Indeed, irreversible degradation of **17** started around  $80^\circ\text{C}$  in 1-octene (used to mimic ethylene) leading to a new species (quantitatively) as observed by  $^{31}\text{P}$  NMR at  $\delta(\text{tol-}d_8)$ :  $-40.67$  (dd,  $J = 7.8$  and  $18.3$  Hz),  $73.95$  (dd,  $J = 7.8$  and  $18.4$  Hz) in which both phosphines are still coordinated to nickel. The very small coupling constant was similar to the degradation product of supramolecular complex **13** and probably indicates that the decomposition of the complex occurs by loss of the COD moiety.

### 2.2.1 Tricyclohexylphosphine ( $\text{PCy}_3$ ) as co-ligand

Having studied the behaviour of **3** with  $\text{PMe}_3$ , we wondered if a diversification of the co-ligand was possible by using other phosphines. In order to have an overview at both sides of the steric range, we evaluated the very bulky  $\text{PCy}_3$  (with similar electron donating properties) for this reaction to prepare an analogue of **16**. Under similar conditions, the reaction mixture showed almost no conversion after 10 min at RT and only the signals of  $\text{PCy}_3$  and ligand **3** were observed by  $^{31}\text{P}$  NMR at 10 ppm and 40 ppm respectively ( $\text{Ni}(\text{PCy}_3)_n$  was not observed). After leaving this mixture to stir for 16 h, the colour had changed to brown and unlocked  $^{31}\text{P}$  (and  $^{31}\text{P}\{^1\text{H}\}$ ) NMR indicated a new set of signals at 37 and 103 ppm with a multiplicity different from zwitterionic complexes (Figure 9). Each signal was a doublet of doublet with a large coupling of 236 Hz, consistent with two phosphorus atoms in a *trans* position with respect to each other. Next to this, two smaller couplings of 64 Hz and 77 Hz were

observed for the peaks at 37 and 103 ppm, respectively, which would correspond to a *cis* coupling. Heating the mixture at 60°C for two more hours led to full conversion towards complex **23**. The reaction was faster by heating the mixture at 60°C for 3 h as depicted in Scheme 6.



**Scheme 6.** Synthesis of hydride complex **23** from METAMORPhos ligand **3**, PCy<sub>3</sub> and Ni(COD)<sub>2</sub>.

Further characterisation by <sup>1</sup>H NMR showed that the product contained a hydride, observed at δ(C<sub>6</sub>D<sub>6</sub>): -26.8 ppm (dd, <sup>2</sup>J<sub>PH</sub> = 64 Hz, <sup>2</sup>J<sub>PH</sub> = 78 Hz) (see Figure 10). The similar coupling constant observed for this hydride and the phosphorus signals indicate that this constant corresponds to <sup>2</sup>J<sub>PH</sub> coupling between the hydride and phosphines in *cis* position to nickel.<sup>2</sup> Also the chemical shift for the P(*i*Pr)<sub>2</sub> signal was significantly different in both complexes: while the phosphorus signal of P(*i*Pr)<sub>2</sub> for zwitterionic complex **16** appears at 87.3 ppm, it is observed at 103.4 ppm for the hydride PO-chelated nickel complex **23**. This shows that the change between a zwitterionic diphosphine complex and a PO chelated nickel hydride complex has a direct influence on the chemical shift of the phosphorus.

<sup>2</sup> The observation of the *J*<sub>PH</sub> coupling in the <sup>31</sup>P{<sup>1</sup>H} NMR spectrum is explained by a limited range of proton decoupling set in routine experiments, which did not include the hydride signal in <sup>1</sup>H NMR at δ = -26.9 ppm. To decouple efficiently hydrides from <sup>31</sup>P {<sup>1</sup>H} experiments, the O2P frequency and the decoupling range should be modified accordingly.

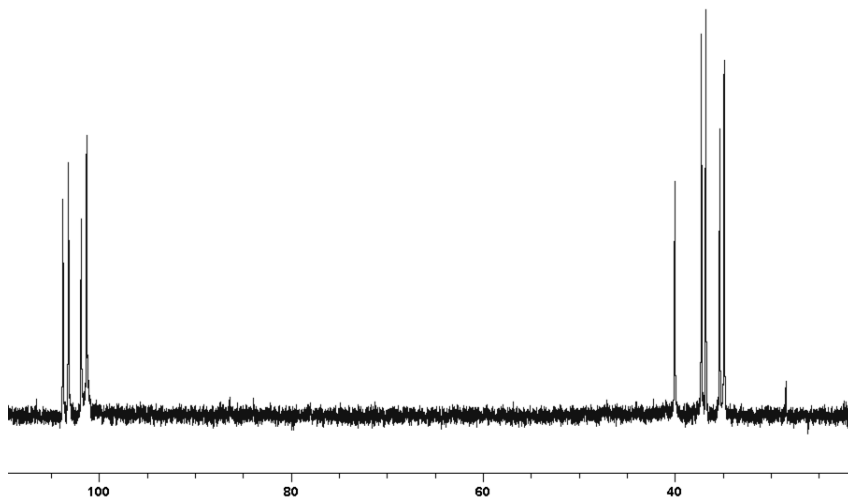


**Figure 9.**  $^{31}\text{P}$  NMR (121 MHz,  $\text{C}_6\text{D}_6$ , 300K) spectrum for complex **23** (the signal at 40 ppm in  $^{31}\text{P}$  NMR corresponds to impurity of ligand **3**)

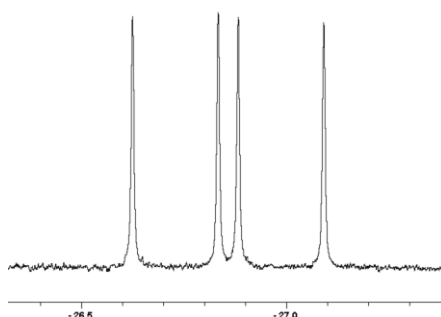


**Figure 10.**  $^1\text{H}$  NMR (300 MHz,  $\text{C}_6\text{D}_6$ , 300K) spectrum (hydride region) for complex **23** evidencing the coupling of the hydride with two different phosphorus atoms in *cis* position.

Crystals suitable for diffraction were grown by slow diffusion of pentane in a toluene solution of complex **23** and the ORTEP plot of the solid state structure is presented in Figure 11. This complex confirms the presence of two phosphines in *trans* position with respect to one another as well as an hydride being in *cis* with respect to the phosphines.

The complex has a square planar geometry, as is evident from the sum of angles around nickel ( $360.0^\circ$ ). A major difference with zwitterionic complex **16** is the formation of a PO anionic chelate, resulting in a neutral complex. This also results in a clear N=S bond (S(1)-N(1) 1.5276(17) Å) and the two single bonds at N-P and S-O (2.2092(6) Å and 1.4867(14) Å respectively).



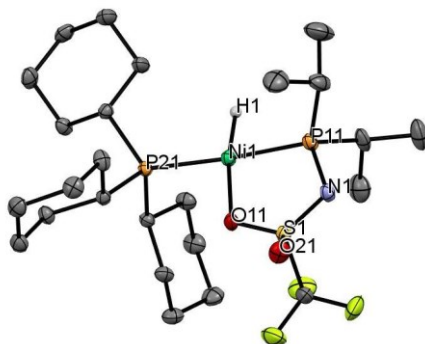


**Figure 11.** ORTEP plot (50% probability displacement ellipsoids) of complex **23**. Hydrogen atoms (excepted for the Ni-H) have been omitted for clarity. Selected bond lengths (Å) and angles (°): Ni(1)-P(11) 2.1496(6); Ni(1)-P(21) 2.2092(6); Ni(1)-O(11) 1.9953(13); S(1)-O(11) 1.4867(14); S(1)-O(21) 1.4333(15); S(1)-N(1) 1.5276(17); P(11)-N(1) 1.6918(17); Ni(1)-H(1) 1.42(2); P(11)-Ni(1)-P(21) 174.04(2); P(11)-Ni(1)-O(11) 87.76(4); P(21)-Ni(1)-O(11) 98.06(4); S(1)-N(1)-P(11) 115.49(10).

On the basis of chelated hydride **23**, we investigated whether other hydride complexes could be synthesised. METAMORPhos ligands **3**, **5**, **6** and **7** were used in combination with PCy<sub>3</sub> and Ni(COD)<sub>2</sub>; these combinations all led to the formation of hydride complexes (**23**, **24**, **25** and **26** respectively). These hydrides were remarkably stable as no decomposition occurred in solution below a temperature of 60°C. METAMORPhos ligand **4** (NH tautomer), however, did not lead to the selective formation of the nickel hydride complex when reacted with a mixture of Ni(COD)<sub>2</sub> and PCy<sub>3</sub>. The major product consisted of the homocomplex Ni(**4,4**) suggesting a competition between the formation of the homo and the heterocomplex. The nickel hydride complexes **23-26** were all diamagnetic and their chemdraw structures are displayed in Figure 12. Complexes **23** and **26** were isolated, whereas **24** and **25** were observed in solution (at high conversion).<sup>3</sup> This extension shows again the potential of METAMORPhos ligands to generate stable hydrides, which are not common in the literature.<sup>[10–23]</sup>

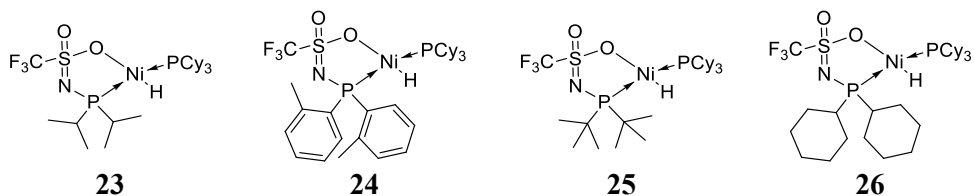
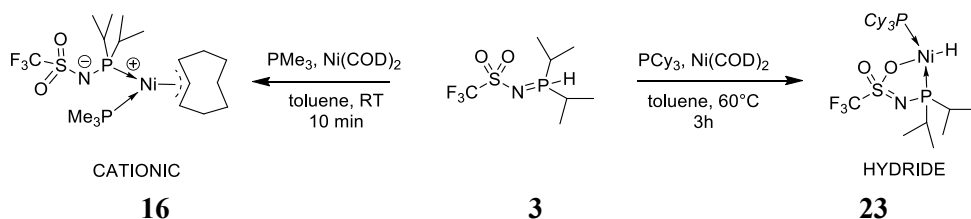


**Figure 12.** Nickel hydride complexes generated from the combination of METAMORPhos, Ni(COD)<sub>2</sub> and PCy<sub>3</sub>.

<sup>3</sup> see experimental part for more details

## 2.2.2 Extension to other phosphines and phosphites

The structural change at the metal complex caused by a simple change between  $\text{PMe}_3$  and  $\text{PCy}_3$  (summarised in Scheme 7), led us to investigate the factors that ruled the complex formation. As the co-ligand was obviously the pivotal element, other types of phosphines or phosphites were selected and assessed as co-ligands for this transformation.



**Scheme 7.** Reactivity of METAMORPhos ligand **3** with the system  $\text{Ni}(\text{COD})_2 + \text{PR}_3$  ( $\text{R} = \text{Me}, \text{Cy}$ ): Either zwitterionic nickel complex **16** or a neutral nickel hydride complex **23** is formed depending on the phosphine co-ligand used.

The geometry of complexes in solution was determined by recording a  $^{31}\text{P}$  NMR spectrum of the crude reaction mixture (see Table 1). The results of these experiments (reactivity and chemical shifts from the crude) are summarised in Table 2.

**Table 1.** Determination grid to distinguish hydride from zwitterionic nickel complexes by  $^{31}\text{P}$  and  $^1\text{H}$  NMR spectroscopy.

	Zwitterionic complex	Hydride complex
$^{31}\text{P}$ NMR (unlocked)	Two signals at x ppm and y ppm x and y are doublets with a coupling constant $J \approx 30$ Hz	Two signals at x ppm and y ppm x and y are doublets of doublets with a great coupling constant ( $J \approx 230$ Hz) and two smaller ( $J \approx 50-70$ Hz)
$^1\text{H}$ NMR	2 or 3 signals of the allyl in the 4-5 ppm region (no signal < 0 ppm)	One signal (dd) in the hydride region around -36 ppm

**Table 2.** Study of the reactivity of the system [ligand **3** + Ni(COD)<sub>2</sub> + Phosphine (or phosphite)].

	P(OMe) <sub>3</sub>	P(OPh) <sub>3</sub>	PMe <sub>3</sub>	P( <i>n</i> Bu) <sub>3</sub>	PPh <sub>2</sub> Me	PCy <sub>2</sub> H	PPh <sub>3</sub>
	no reactivity	no reactivity	zwitterionic	zwitterionic	zwitterionic (broad)	zwitterionic	broad signals
$\delta_1, \delta_2$ (ppm) $^2J_{PP}$ (Hz)	/	/	86.8 11.4 $J=31$ Hz	86.2 11.9 $J=28$ Hz	43.4 11.1 $J=nd$	86.9 26.5 $J=29$ Hz	nd. decomp.
Tolman's cone angle $\Theta$ (°)	107°	128°	118°	132°	136°	142°	145°
Electronic parameter $\nu_{CO}$ (cm <sup>-1</sup> )	2079.5	2085.3	2064.1	2060.3	2067.0	2065.3	2068.9

( <i>i</i> Pr)NHPPh <sub>2</sub> *	( <i>i</i> Pr) <sub>2</sub> NPPh <sub>2</sub> *	P( <i>i</i> Pr) <sub>3</sub>	PBz <sub>3</sub>	PCy <sub>3</sub>	P( <i>t</i> Bu) <sub>3</sub>	P( <i>o</i> tolyl) <sub>3</sub>	P(Mes) <sub>3</sub>
zwitterionic	reactivity decomp.	Ni-H	broad signals	Ni-H	Ni-H	no reactivity decomp.	no reactivity decomp.
85.8 60.2 $J=31$ Hz	/	103.7 48.6 $J=234$ Hz	/	103.4 36.1 $J=233$ Hz	102.2 77.5 $J=224$ Hz	/	/
149°	149°	160°	165°	170°	182°	194°	212°
2067.3	2067.3	2059.2	2066.4	2056.4	2056.1	2066.6	2064.4

Conditions: Ni(COD)<sub>2</sub> (0.1 mmol, 1 eq.), METAMORPhos (0.1 mmol, 1 eq.) and phosphine (0.1 mmol, 1 eq.) are dissolved in toluene (2 mL) under stirring at RT. If no reaction, the mixture was heated at 60°C for at least 10 min. The chemical shifts are indicative and based on unlocked <sup>31</sup>P NMR experiments.\* *i*PrNHPPh<sub>2</sub> and (*i*Pr)<sub>2</sub>NPPh<sub>2</sub> approximated from the calculated values of Me<sub>2</sub>NPPh<sub>2</sub> that appear in the table. nd.: not determined, decomp.: decomposition to black nickel.

Similar to PMe<sub>3</sub> and PCy<sub>3</sub>, the other phosphines (with different steric and electronic properties) reacted in solution with ligand **3** and Ni(COD)<sub>2</sub> to generate either the hydride or the zwitterionic nickel complex in solution. The electron-poor P(OPh)<sub>3</sub> in combination with ligand **3** and Ni(COD)<sub>2</sub> led to two new signals at 131 ppm and 142 ppm, which according to the literature, correspond to Ni(P(OPh)<sub>3</sub>)<sub>4</sub> and most certainly to Ni(P(OPh)<sub>3</sub>)<sub>4</sub>(COD).<sup>[9]</sup> Ligand **3** did not react, even after 16 h at RT (signal at 40 ppm). Similarly, stirring a solution of P(OMe)<sub>3</sub>, **3** and Ni(COD)<sub>2</sub> only led to the formation of Ni(P(OMe)<sub>3</sub>)<sub>4</sub> as indicated by the presence of a peak at 164 ppm in the <sup>31</sup>P NMR spectrum. Employing the electron rich ligand P(*n*Bu)<sub>3</sub> led to a clear brown solution and after 10 min the <sup>31</sup>P NMR signal consisted quantitatively of two doublets at 86.2 and 11.4 ppm with a small coupling ( $^2J_{PP} = 28$  Hz) in line with a zwitterionic complex. Using the PCy<sub>2</sub>H as co-ligand led also to a brown solution with two broad signals at 26.5 and 86.9 ppm, displaying a small coupling ( $^2J_{PP} = 29$  Hz).

Changing from alkyl to arylphosphines led to two very broad signals, especially for PPh<sub>2</sub>Me which formed a zwitterionic species on the basis of the signal integration

and chemical shifts but for which the coupling constant could not be measured. Triphenylphosphine led to low-intensity broad and undefined signals, which indicates either complex decomposition or the formation of paramagnetic species.

In comparison,  $P(iPr)_3$ , an alkyl phosphine with higher steric bulk, led to a clear orange solution and after 1 h no  $P(iPr)_3$  nickel-based chelates were observed (only the signals of free  $P(iPr)_3$  at 19.9 ppm and free METAMORPhos at 40 ppm were observed). After stirring for a longer period of time (16 h at RT) a typical pattern consisting of two doublets of doublets was observed by  $^{31}P$  NMR, which is characteristic of the hydride complex formation. In a similar way, the use of  $P(tBu)_3$  led to a characteristic hydride pattern at 63 and 104 ppm, but heating ( $60^\circ C$ ) was required to improve the conversion as the reaction was very slow at RT. Neither the very bulky  $P(o\text{-tolyl})_3$  nor  $P(Mes)_3$  reacted with **3**. Indeed, the peaks of both free phosphines were monitored at -30 ppm and -36 ppm, respectively, without any signals of phosphine-nickel chelates. Instead, after a few minutes the reaction mixtures formed black particles, which indicates decomposition of  $Ni(COD)_2$ . In contrast, the bulky tribenzylphosphine was reactive. However the presence of multiple broad peaks that showed up in the  $^{31}P$  NMR after a reaction at  $60^\circ C$  revealed that several species had formed.

The Tolman's cone angle  $\Theta$  and Tolman electronic parameter  $\nu_{CO}$  ( $cm^{-1}$ ), relative to the phosphine co-ligand, were found to be suitable reactivity descriptors for this study.<sup>[24]</sup> Regardless of zwitterionic or hydride complexes, the reactivity of the systems was in line with the phosphine basicity represented by the Tolman electronic parameter  $\nu_{CO}$ . Within the range covered by this study ( $2056.1\text{ cm}^{-1}$ :  $P(tBu)_3$  to  $2085.3\text{ cm}^{-1}$ :  $P(OMe)_3$ ), only phosphines with  $\nu_{CO}$  between  $2056.1$  and  $2068.9\text{ cm}^{-1}$  reacted as shown on the Tolman plot, Figure 13. Less basic phosphites such as  $P(OMe)_3$  or  $P(OPh)_3$  coordinated to nickel without reactivity. Moderately basic phosphines such as  $PPh_3$  reacted but led to complicated mixture and broad signals in  $^{31}P$  NMR and  $^1H$  NMR hinting at a paramagnetic nature of the formed complexes. Finally very basic and electron rich phosphines reacted quickly and led selectively to the isolation of nickel complexes (zwitterionic or hydride).

Among the reactive systems, steric bulk, as represented by Tolman's cone angle  $\Theta$ , was in line with the type of complex formed (zwitterionic or hydride). Phosphines with low steric bulk ( $118^\circ < \Theta < 143^\circ$ ), such as  $PMe_3$ ,  $P(nBu)_3$ ,  $PMePh_2$  and  $PCy_2H$  led selectively to zwitterionic nickel complexes. Phosphines of intermediate size ( $136^\circ < \Theta < 160^\circ$ ) such as  $PPh_2Me$ ,  $PCy_2H$ ,  $PPh_3$  and  $iPr_2NPPH_2$  did not lead to selective complex formation (some paramagnetic species were probably formed during the reaction). Finally, bulky phosphines ( $160^\circ < \Theta < 182^\circ$ ) generated

selectively nickel hydride complexes. There was no observable reaction with the most bulky phosphines  $P(o\text{-tolyl})_3$  and  $P(\text{Mes})_3$  with  $\Theta > 182$ .

The aminophosphine co-ligands that led to supramolecular complexes **11-15** can also be ranked within the series of classical phosphines in terms of electronic and steric contribution. Indeed, aminophosphine  $i\text{Pr-NH-PPh}_2$  would be comparable to  $\text{PPh}_3$  or to  $(i\text{Pr})_2\text{-N-PPh}_2$ , which are the two closest intermediates for which the Tolman parameters can be calculated (see experimental part for the calculation).

Whereas aminophosphines ( $i\text{Pr-NH-PPh}_2$ ,  $n\text{Pr-NH-PPh}_2$  and  $4\text{-}n\text{BuPh-SO}_2\text{-NH-PPh}_2$ ) led to the supramolecular H-bonded complexes **11-15**, their electronic and steric equivalents,  $\text{PPh}_3$  and  $\text{Ph}_2\text{P-N}(i\text{Pr})_2$ , did not lead to isolable complexes. This difference at *iso* electronic and *iso* steric suggests an important role for the supramolecular hydrogen bonding in complex stability for arylphosphine-containing co-ligands. This interaction could stabilise the *cis* configuration leading to zwitterionic complexes.

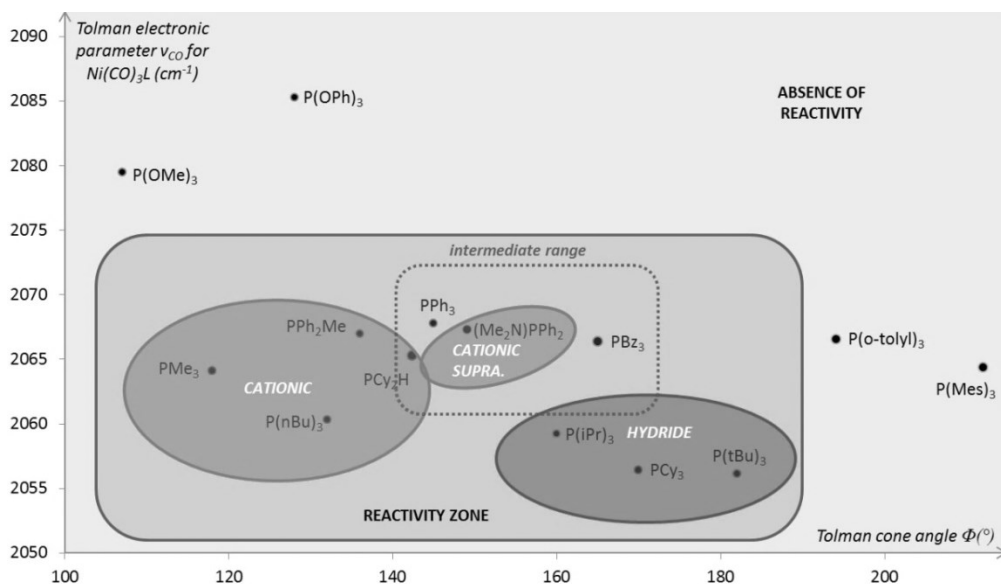


**Figure 13.** Tolman plot of phosphines used in this study and their reactivity towards nickel complex formation with METAMORPhos **3**.

The formation of complexes with an allyl nickel moiety on a cyclooctadiene ring has been reported.<sup>[9,25,26]</sup> Indeed, this moiety was described to exist in two isomers that are in equilibrium: a  $\eta^3$ -allylic form and a 4-enyl form (paramagnetic). Even though the 4-enyl isomer was not detected in the METAMORPhos-based zwitterionic complexes, it could exist as a new type of complex next to zwitterionic and hydride complexes. This hypothesis would fit well with the change in the geometry of the

complex when increasing the Tolman angle. Also it would clarify the situation for the “intermediate” range ( $136^\circ < \Theta < 160^\circ$ ) for which no clear formation of hydride or cationic was established due to undefined and broad signals. Therefore, this new species could well exist for co-ligands with a Tolman cone angle:  $136^\circ < \Theta < 160^\circ$  according to Figure 14.

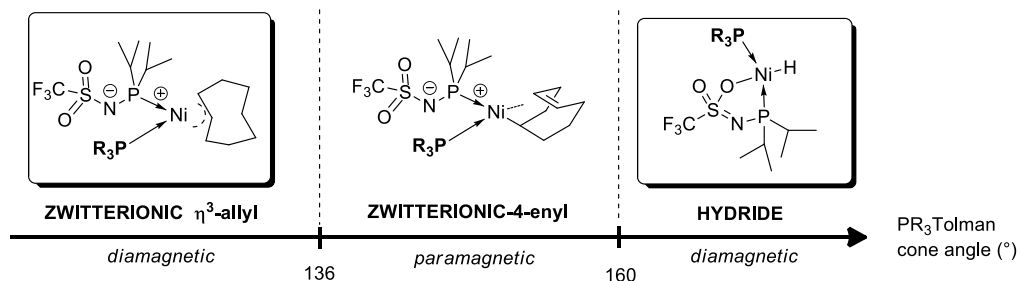


**Figure 14.** Influence of the Tolman cone angle for  $\text{PR}_3$  on the complex geometry based on METAMORPhos 3.

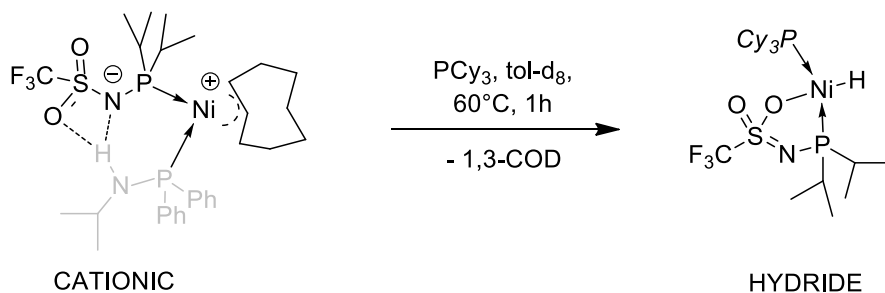
In summary, aiming to create a small library of catalysts derived from complexes **11** and **12** and understanding the effect of the co-ligand on complex stability, we found that aminophosphines could be replaced by more classical phosphine ligands. The formation of zwitterionic complexes with phosphines, free of hydrogen-donors, showed that hydrogen-bonding is not the crucial factor for complex formation. However hydrogen bonding between a H-donor co-ligand and METAMORPhos (with H-acceptor properties) stabilises the complexes and allows their isolation as co-ligands having no H-donor properties lead to complex decomposition. Phosphines used as co-ligand must be sufficiently basic (electron-rich) for the formation of stable complexes to occur. Increasing the steric bulk of the phosphine at iso-basicity resulted in a severe geometry change from a zwitterionic diphosphine complex to a PO-chelated nickel hydride complex. This new class of hydride complexes based on METAMORPhos, is promising as it is a clear extension of the showcase SHOP-type complexes.

### 3 Mechanism of complex formation

#### 3.1 Are zwitterionic and nickel hydride complexes interconvertible?

Through ligand variation of the phosphine in the METAMORPhos /  $\text{Ni}(\text{COD})_2$  system (METAMORPhos, co-ligand, nickel = 1:1:1), two classes of complexes with different geometries were obtained *via* identical synthetic procedure: those with a zwitterionic structure and those containing a metal hydride. We set out to investigate if these two complexes were interconvertible.

Attempts to convert zwitterionic complexes by thermal cleavage of the COD, did not lead to formation of the metal hydride species but led instead to several decomposition products. However, the addition of a five-fold excess of PCy<sub>3</sub> to the supramolecular zwitterionic nickel complex **11** (1 eq.) at 60°C in toluene-*d*<sub>8</sub> led to the emergence of two doublets of doublets in the <sup>31</sup>P NMR spectrum at δ(tol-*d*<sub>8</sub>, ppm): 36.6 (dd, <sup>2</sup>J<sub>PP</sub> = 235 Hz, <sup>2</sup>J<sub>PH</sub> = 64 Hz) and 103.0 (dd, <sup>2</sup>J<sub>PP</sub> = 230 Hz, <sup>2</sup>J<sub>PH</sub> = 74 Hz). Furthermore, in the <sup>1</sup>H NMR spectrum, a hydride signal was clearly observable at δ(tol-*d*<sub>8</sub>): -26.8 ppm alongside with the characteristic signals of unbound 1,3-COD (already reported in Figure 20). All these signals corresponded to those measured for hydride **23** and proved that zwitterionic complex **11** in presence of PCy<sub>3</sub> rearranges to the hydride complex **23** by loss of 1,3-COD according to Scheme 8. This experiment proved that the zwitterionic and hydride complexes are two closely-related structures and that the steric bulk of the phosphine co-ligand determines which of the two classes of compounds is formed.



**Scheme 8.** Conversion of zwitterionic cationic complex **11** to hydride **23** mediated by PCy<sub>3</sub>

We suggest that the formation of **23**, starting from **11** involves first the competitive coordination of tricyclohexylphosphine and aminophosphine to the metal centre (by displacement of the aminophosphine). This first step is likely to be directed towards the coordination of the more electron rich PCy<sub>3</sub> despite its steric bulk. Once the bulky phosphine is coordinated to nickel, it is likely that it destabilises the allyl moiety to form the enyl (mentioned in Figure 14). In a second step 1,3-COD is released by β-H elimination to form the hydride. We believe that steric bulk is the main driver of this reaction provided that the phosphine basicity is sufficient (Figure 13). To discriminate the implication of steric bulk from electronics in the complex rearrangement, additional experiments should involve changing PCy<sub>3</sub> in Scheme 8 by PMe<sub>3</sub> (same basicity, different steric bulk) or P(*o*-tolyl)<sub>3</sub> (same steric bulk, different basicity) and see if the corresponding hydride would form (which we do not expect).

To prove completely that zwitterionic and hydride species are interconvertible, we should also prove that the reverse pathway is possible (hydride to zwitterionic). The

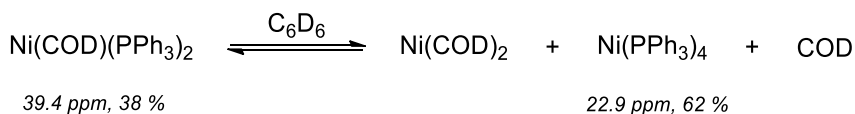
insertion of a hydride into a diene is known, however, this was not investigated for the current system.<sup>[9,25,26]</sup>

### 3.2 Role of the co-ligand in the mechanism

Developing an overall mechanism to account for the formation of both zwitterionic and hydride complexes formation is challenging. Indeed, it requires identifying which intermediate between the allyl and the hydride would form initially. The transformation of a zwitterionic complex to a non-charged complex appears more facile and is shown experimentally (with PCy<sub>3</sub> in Scheme 8). We propose a pathway in which the zwitterionic species forms first and then evolves to a hydride depending on the steric bulk of the co-ligand.

We have already reported in this Chapter that the phosphine (co-ligand) was compulsory for hetero-complexes formation (hydride or zwitterionic). Also, at the start of complex formation, we detected by NMR spectroscopy a peak corresponding to Ni(co-ligand)<sub>4</sub>, of which the intensity was decreasing in time while complex formation was observed (this was especially clear for the co-ligand PMe<sub>3</sub>). This is a strong indication that the co-ligand is important for the first step in the mechanism as it coordinates to the nickel centre.

To understand the different interactions between phosphine co-ligand, nickel and 1,5-COD, we synthesised the bright yellow model complex Ni(COD)(PPh<sub>3</sub>)<sub>2</sub> according to the procedure of Maciejewski *et al.*<sup>[27]</sup> Dissolved in C<sub>6</sub>D<sub>6</sub>, the complex shows in the <sup>31</sup>P NMR spectrum two peaks at δ(C<sub>6</sub>D<sub>6</sub>): 22.9 ppm (62 %) and 39.4 ppm (38 %) that we assigned to Ni(PPh<sub>3</sub>)<sub>4</sub> and Ni(COD)(PPh<sub>3</sub>)<sub>2</sub>, respectively, according to literature.<sup>[27–29]</sup> This equilibrium confirmed the occurrence of ligand fast exchange in solution (see Scheme 9).



**Scheme 9.** Ligand exchange in a system Ni(COD)<sub>2</sub>, PPh<sub>3</sub>: equilibrium between Ni(COD)(PPh<sub>3</sub>)<sub>2</sub> and Ni(PPh<sub>3</sub>)<sub>4</sub> in C<sub>6</sub>D<sub>6</sub>.

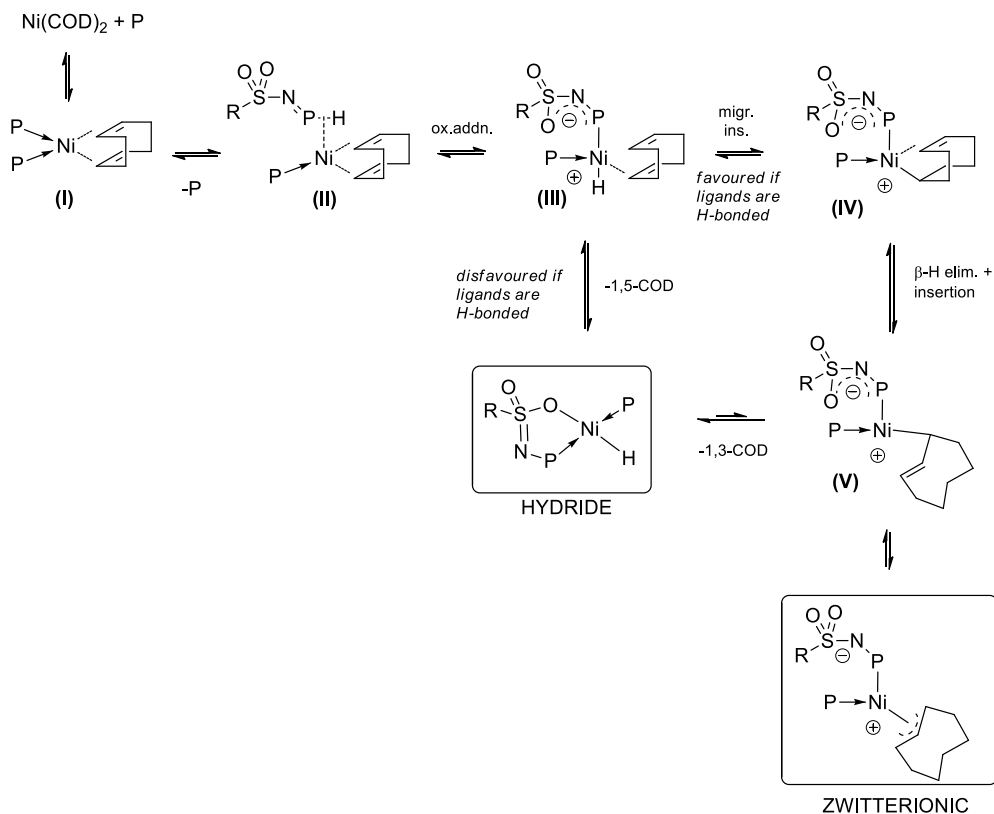
Furthermore, upon addition of co-ligand **B** (*i*Pr-NH-PPh<sub>2</sub>) (2 eq.) to Ni(COD)<sub>2</sub> in *d*<sub>8</sub>-toluene at RT, two signals appeared in the <sup>31</sup>P NMR spectrum at 63 ppm and 79 ppm in a ratio of 1 : 0.3. The same procedure in 1,5-COD led to a ratio of 1 : 2.2, suggesting that the signal at 79 ppm corresponds to a complex containing COD. Also, the difference in chemical shift between the two signals of 16 ppm fits with the hypothesis that both Ni(COD)(**B**)<sub>2</sub> (79 ppm) and Ni(**B**)<sub>4</sub> (63 ppm) are formed when **B**



is added to a solution containing  $\text{Ni}(\text{COD})_2$ . Based on the above, we propose a pathway (Scheme 10) that summarises the different pathways that lead to the formation of either zwitterionic or nickel hydride complexes.

Depending on the relative basicity of METAMORPhos and  $\text{PR}_3$ , there is a competitive coordination between phosphorus ligands to nickel. A complex of type  $\text{Ni}(\text{COD})(\text{METAMORPhos})_2$  could form initially in the absence of  $\text{PR}_3$  (see  $\text{Ni}(\mathbf{4,4})$  or  $\text{Ni}(\mathbf{5,5})$ ) or if the METAMORPhos ligand is more electron rich than  $\text{PR}_3$  (see the synthesis of  $\text{Ni}(\mathbf{4,C})$  leading to complex formation  $\text{Ni}(\mathbf{4,4})$ ). This competition could happen at the start but also probably at the end of the reaction.

Starting from  $\text{NiP}_2(\text{COD})$  (**I**), METAMORPhos can coordinate by exchange with a co-ligand to form (**II**). Then, by intramolecular oxidative addition of METAMORPhos, a zwitterionic nickel (II) hydride complex (**III**), with a negatively charged METAMORPhos fragment can form. This intermediate could lead to the hydride complex by loss of 1,5-COD and coordination of a bulky co-ligand ( $\text{PCy}_3$  for example). Alternatively, the migratory insertion of the hydride in the coordinated 1,5-COD double bond could generate (**IV**). The 1,4-enyl form, which upon isomerisation will lead to the zwitterionic complex. Two different pathways can explain the experiment displayed in Scheme 8 (zwitterionic to hydride): a)  $\text{ZW} - (\mathbf{V}) - \text{HY}$  or b)  $\text{ZW} - (\mathbf{V}) - (\mathbf{IV}) - (\mathbf{III}) - \text{HY}$ . In pathway a) the system would release 1,3-COD by  $\beta$ -H elimination while pathway b) it would release 1,5-COD. Given the observation of 1,3-COD by  $^1\text{H}$  NMR at the end of the reaction, pathway a) is most likely. However, given that nickel hydrides are also considered as isomerisation catalysts, it is possible that the free 1,3-COD observed by NMR come from the isomerisation of free 1,5-COD to the conjugated diene.



**Scheme 10.** Proposed mechanism leading to zwitterionic or nickel hydride complexes by oxidative addition of METAMORPhos ligand on zerovalent nickel phosphine COD complex. P: co-ligand and  $\text{RSO}_2\text{N}=\text{PH}$ : METAMORPhos ligand.

## 4 Conclusion

By the evaluation of different combinations of aminophosphines, we have identified that the formation of zwitterionic and cationic supramolecular nickel complexes is favoured when METAMORPhos ligands and bulky phosphines are involved. Also basic aminophosphines of type alkyl-NH-PPh<sub>2</sub> leads to such complexes. The high selectivity of the reaction towards the heterocomplex was ensured by a difference in basicity between the two ligands. Homocomplexes form when METAMORPhos ligand is present in the NH or the NH—NEt<sub>3</sub> tautomer. More conventional and unsubstituted phosphines were introduced and in combination with METAMORPhos and Ni(COD)<sub>2</sub> they also lead to the formation of zwitterionic heterocomplexes. By modulating the electronic and steric properties of the co-ligand, we found that this phosphine was crucial for the formation of the complex. We established that the basicity of the phosphine, described by the Tolman Electronic Parameter ( $\nu_{\text{CO}}$ ) has to be above a certain threshold for the complex formation to take place ( $\nu_{\text{CO}} < 2068.9$

$\text{cm}^{-1}$ ). Also, the steric bulk of the phosphine (described by the Tolman cone angle  $\theta$ ) has an influence on the geometry of the complex. Electron rich phosphines with limited steric bulk lead to zwitterionic nickel complexes, whereas more bulky phosphines lead to the formation of *trans*-(PO,P) chelated nickel hydride complexes. These two types of complexes are interrelated as a zwitterionic complex may be converted to a hydride complex. A mechanism leading to either a zwitterionic complex or a hydride complex was proposed. It most certainly involves the oxidative addition of a METAMORPhos ligand to a  $\text{Ni}(\text{COD})(\text{ligand})_2$  intermediate, which is only realised when the co-ligand brings sufficient electron density to the metal. The discrimination between zwitterionic and hydride complex certainly happens in a second step and is directed by the steric bulk of the co-ligand.

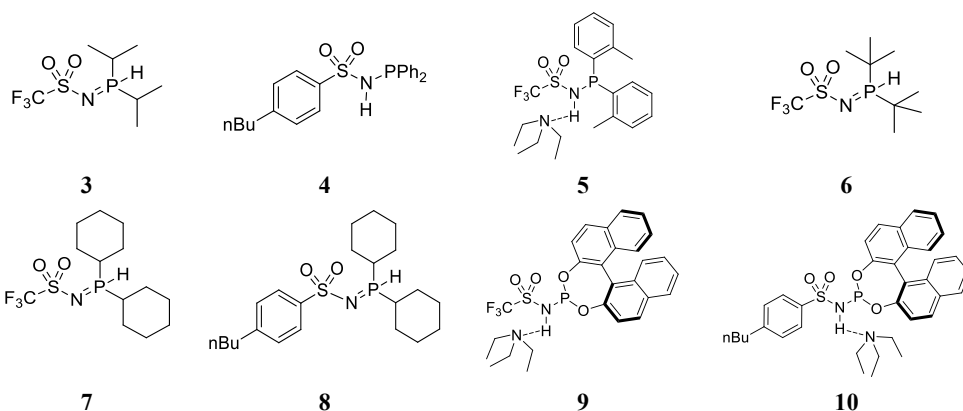
## 5 Experimental part

### 5.1 General

All reactions were carried out under an atmosphere of argon using standard Schlenk techniques. Phosphines, sulphonamides, 1,5-cyclooctadiene, di(*o*-tolyl)chlorophosphine were purchased from commercial suppliers and used without further purification. The benchmark complex **Ref** was prepared according to known literature procedure and NMR analysis was conform.<sup>[5]</sup> Chlorophosphines were distilled trap to trap under reduced pressure. THF, pentane and  $\text{Et}_2\text{O}$  were distilled from sodium benzophenone.  $\text{CH}_2\text{Cl}_2$  and chlorobenzene were distilled from  $\text{CaH}_2$ , toluene from sodium, under nitrogen. Alternatively solvents from SPS (Solvent Purification System MBraun) were used. NMR solvents were degassed by freeze-pump-thaw cycling under argon and stored over activated 3 Å molecular sieves. NMR spectra ( $^1\text{H}$ ,  $^1\text{H}\{^31\text{P}\}$ ,  $^{31}\text{P}$ ,  $^{31}\text{P}\{^1\text{H}\}$  and  $^{13}\text{C}\{^1\text{H}\}$ ) were measured on a BRUKER 300 MHz spectrometer. Elemental analyses were performed by Stephen Boyer (London Metropolitan University).

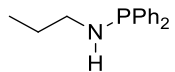
### 5.2 Ligand synthesis

METAMORPhos ligands **3-10** were synthesised according to literature procedure described in chapter 2.



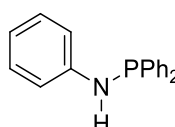
The ligand *N*-isopropyl-1,1-diphenylphosphinamine **31** (*i*Pr-NH-PPh<sub>2</sub>) was synthesised in Chapter 5. The synthesis of ligands amidophosphines **27**, **28**, **29**, **30** were reported in Chapter 2.

### Ligand A (*N*-propyl-1,1-diphenylphosphinamine)

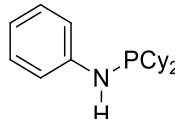
 *n*-propylamine (3.00 mL, 36.70 mmol, 3.00 eq.) was placed in a Schlenk in THF (10 mL). Chlorodiphenylphosphine was then added dropwise (2.00 mL, 11.14 mmol, 1.00 eq.) to this mixture. The mixture was then stirred for 10 min at room temperature and the precipitate formed was filtered off. The filtrate was submitted to vacuum to give a colourless oil. Isolated yield 2.3 g (85%). <sup>31</sup>P{<sup>1</sup>H} NMR (121 MHz, CDCl<sub>3</sub>, 300K): δ(ppm): 41.05 (s); <sup>1</sup>H NMR (300 MHz, CDCl<sub>3</sub>, 300K): δ(ppm): 0.91 (t, <sup>3</sup>J<sub>HH</sub> = 7.5 Hz, CH<sub>3</sub>, 3H); 1.51 (sext, <sup>3</sup>J<sub>HH</sub> = 7.2 Hz, CH<sub>2</sub>-CH<sub>3</sub>, 2H); 1.95 (d, <sup>2</sup>J<sub>HP</sub> = 5.0 Hz, NH, 1H); 2.93 (quint., <sup>3</sup>J<sub>HH</sub> = 7.6 Hz, CH<sub>2</sub>-N, 2H); 7.0-7.8 (m, H<sub>Ar</sub>, 10H). <sup>13</sup>C NMR (75 MHz, CDCl<sub>3</sub>, 300K): δ(ppm): 11.5 (s, CH<sub>3</sub>); 26.22 (d, <sup>3</sup>J<sub>CP</sub> = 6.1 Hz, CH<sub>2</sub>-CH<sub>3</sub>); 48.3 (d, <sup>2</sup>J<sub>CP</sub> = 14.0 Hz, CH<sub>2</sub>-N); 128.3 (d, J<sub>CP</sub> = 6.3 Hz, C<sub>Ar</sub>); 128.46 (s, C<sub>Ar</sub>); 131.4 (d, J<sub>CP</sub> = 19.5 Hz); 141.9 (d, J<sub>CP</sub> = 12.6 Hz, C<sub>Ar</sub>).

**Ligand B** (prepared in Chapter 4)

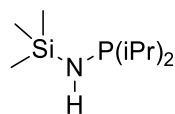
### Ligand C (*N*,1,1-triphenylphosphinamine)

 Dry aniline (6.00 mL, 5.22 g, 66.0 mmol, 3.0 eq.) was dissolved in a first Schlenk in THF (30 mL). In another Schlenk chlorodiphenylphosphine (4 mL, 4.92 g, 22 mmol, 1.0 eq.) was dissolved in THF (10 mL). Then the solution of chlorophosphine was added dropwise under strong stirring to the aniline solution leading to the formation of a white solid. After stirring the mixture for 10 min, unlocked <sup>31</sup>P NMR indicated that the reaction was complete. The precipitate that formed was filtered off and the filtrate evaporated under vacuum to an oil. This oil was submitted to vacuum and heated to 50°C to remove the excess of aniline leading to a white solid. The powder was then dissolved in a minimum amount of dichloromethane and *n*-pentane was added dropwise leading to a white precipitate. The solvent was then syringed out and the solid washed with *n*-pentane (3 x 20 mL) and finally dried under vacuum to give a white powder (isolated yield: 2.0 g, 33%). <sup>31</sup>P{<sup>1</sup>H} NMR (121 MHz, CD<sub>2</sub>Cl<sub>2</sub>, 300K): δ(ppm): 27.45 (s); <sup>1</sup>H NMR (300 MHz, CD<sub>2</sub>Cl<sub>2</sub>, 300K): δ(ppm): 4.53 (d, <sup>2</sup>J<sub>HP</sub> = 7.5 Hz, NH, 1H); 6.81 (t, <sup>3</sup>J<sub>HH</sub> = 7.7 Hz, CH<sub>Ar</sub>, 1H); 6.95-7.10 (m, CH<sub>Ar</sub>, 2H); 7.13-7.27 (m, CH<sub>Ar</sub>, 2H); 7.33-7.62 (m, CH<sub>Ar</sub>, 9H).

### Ligand D (1,1-dicyclohexyl-*N*-phenylphosphinamine)

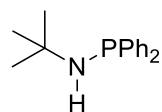
 Dry aniline (1.00 mL, 1.04 g, 11.3 mmol, 2.5 eq.) was dissolved in THF (10 mL). To this solution was added chlorodicyclohexylphosphine (1 mL, 1.05 g, 4.5 mmol, 1 eq.) dropwise under strong stirring leading to a thick precipitate. The mixture was stirred at RT for 10 min and <sup>31</sup>P unlocked NMR indicated full conversion to the product. The precipitate that formed was filtered off and the filtrate evaporated under vacuum to form a white powder (isolated yield 1.24 g, 96%). <sup>31</sup>P{<sup>1</sup>H} NMR (121 MHz, CD<sub>2</sub>Cl<sub>2</sub>, 300K): δ(ppm): 41.01 (s); <sup>1</sup>H NMR (300 MHz, CD<sub>2</sub>Cl<sub>2</sub>, 300K): δ(ppm): 0.52-1.97 (m, CH<sub>Cy</sub>, 22H); 3.34 (d, <sup>2</sup>J<sub>PH</sub> = 10.5 Hz, NH, 1H); 6.61-6.83 (m, CH<sub>Ar</sub>, 1H); 6.93-7.05 (m, CH<sub>Ar</sub>, 2H); 7.08-7.18 (m, CH<sub>Ar</sub>, 2H).

### Ligand E (1,1-diisopropyl-N-(trimethylsilyl)phosphinamine)



Chlorodiisopropylphosphine (4.00 mL, 3.84 g, 25.1 mmol, 1 eq.) was added dropwise to a HMDS (Hexamethyldisilazane) solution in toluene (5.25 mL, 4.06 g, 25.1 mmol, 1 eq. in 20 mL of toluene). The mixture was left to stir for 3 days at RT. Unlocked NMR of the crude mixture indicated complete conversion of the chlorophosphine but that two peaks formed at 47.3 ppm (monoaddition product 54%) and 66.4 ppm (bis addition product, 46%). The solvent and TMSCl were then removed under static vacuum leading to an oily residue. This residue was distilled under reduced pressure to give an oil (yield 45%).  $^{31}\text{P}\{^1\text{H}\}$  NMR (121 MHz,  $\text{C}_6\text{D}_6$ , 300K):  $\delta(\text{ppm})$ : 48.4 (s);  $^1\text{H}$  NMR (300 MHz,  $\text{C}_6\text{D}_6$ , 300K):  $\delta(\text{ppm})$ : 0.16 (s,  $(\text{CH}_3)_3\text{-Si}$ , 9H); 0.92 (dd,  $^3J_{\text{HH}} = 6.9$  Hz and  $^3J_{\text{HP}} = 10.1$  Hz,  $\text{CH}_3$  *iPr*, 6H); 0.98 (dd,  $^3J_{\text{HH}} = 7.0$  Hz and  $^3J_{\text{HP}} = 15.3$  Hz,  $\text{CH}_3$  *iPr*, 6H); 1.35 (tdd,  $^3J_{\text{HH}} = ^3J_{\text{HH}}' = 7.0$  Hz and  $^2J_{\text{HP}} = 1.4$  Hz; CH *iPr*, 2H), NH not observed.

### Ligand F (N-tert-butyl-1,1-diphenylphosphinamine)



Dry tert-butyl amine (1.76 mL, 1.22 g, 16.7 mmol, 3 eq.) was dissolved in THF (10 mL). To this solution was added chlorodiphenylphosphine dropwise (1 mL, 1.23 g, 5.57 mmol, 1 eq.) leading to a white precipitate. The mixture was left to stir for 16 h at room temperature. The precipitate that formed was filtered off and the filtrate evaporated under vacuum to form a white solid soluble in pentane (isolated yield: 2.45 g, 85 %).  $^{31}\text{P}\{^1\text{H}\}$  NMR (121 MHz,  $\text{C}_6\text{D}_6$ , 300K):  $\delta(\text{ppm})$ : 22.5 (s);  $^1\text{H}$  NMR (300 MHz,  $\text{C}_6\text{D}_6$ , 300K):  $\delta(\text{ppm})$ : 1.13 (s,  $\text{CH}_3$  *tBu*, 9H); 1.82 (d,  $^2J_{\text{PH}} = 11.5$  Hz, NH, 1H); 6.69-7.17 (m,  $\text{CH}_{\text{Ar}}$ , 3H); 7.43 (ddd,  $J = 8.1$  Hz, 3.2 Hz and 1.5 Hz,  $\text{CH}_{\text{Ar}}$ , 2H).

## 5.3 In situ approach for complex synthesis

*In situ* approaches described in the first part of this Chapter were first assessed by means of unlocked NMR to evaluate several combinations quickly. We focussed mainly on doublets systems with couplings around 30 Hz or greater to distinguish cationic complexes from hydride complexes. The values of the chemical shifts obtained without field locking were generally good with a reproducibility of  $\pm 2$  ppm, sufficient for a first screening of ligands combinations (with  $\text{Ni}(\text{COD})_2$ ). The results of the screening are summarised in Table 3. Grey entries correspond to isolated compounds.

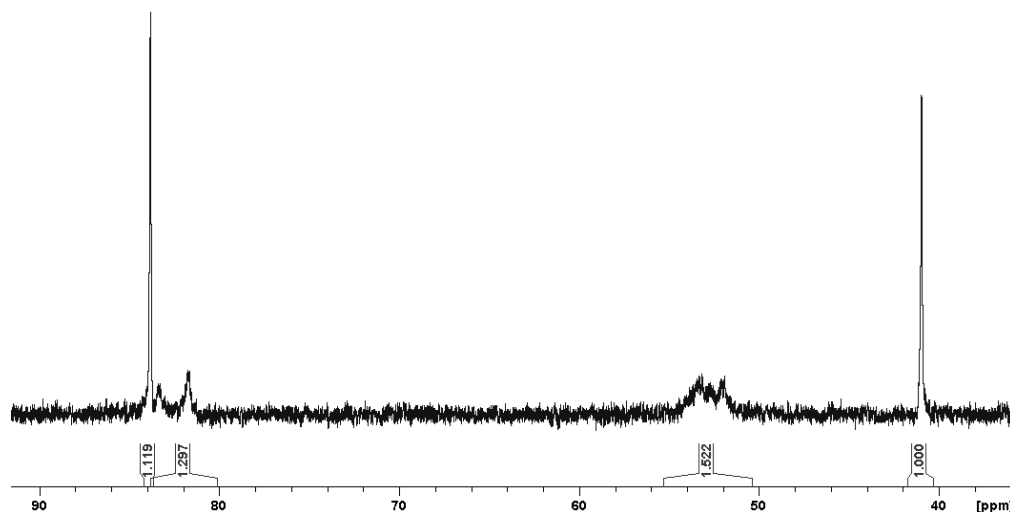
**Table 3.** Chemical shifts of the supramolecular complexes resulting from the coupling of two aminophosphines with  $\text{Ni}(\text{COD})_2$  on the basis of unlocked  $^{31}\text{P}$  NMR

	3	4	5	A	B	C	D	E	F
3	no reac.	54 (br) 82 (br)	nd	<u>Ni(3,A)</u> 65 (32) 92 (32)	<u>Ni(3,B)</u> 60 (31) 86 (31)	56 (28) 82 (30)	84 (br) 101 (br)	nd	slow dec.
4	-	<u>Ni(4,4)</u> 54 (br)	nd	nd	60 (27) 44 (27)	43 (28) 55 (28)	nd	nd	nd
5	-	-	62 (br)	<u>Ni(5,A)</u> 52 (25) 65 (25)	<u>Ni(5,B)</u> 52 (23) 63 (23)	53 (23) 59 (24)	nd	53 (23) 75 (23)	nd

*Chemical shifts of the observed complexes on the basis of unlocked  $^{31}\text{P}$  NMR. The values correspond to the chemical shift and the numbers between parentheses are the coupling constant. Grey entries correspond to isolated and characterised complexes (see expt. part). nd: not determined, no reac.: no reactivity, br: broad signals, slow dec. slow synthesis leading to decomposition products.*

Ni(3,4):

Formation of several combinations Ni(4,4), Ni(3,3) and Ni(3,4).

Ni(3,C), Ni(4,C), Ni(5,C)

Unlike co-ligands **A** and **B**, aminophosphine **C** reacted promptly with Ni(COD)<sub>2</sub> in toluene forming a yellow insoluble compound that likely consisted of neutral chelates of proposed formula Ni(C)<sub>4</sub> or [Ni(C)<sub>2</sub>]<sub>2</sub>.<sup>4</sup> To counteract the formation of these complexes, the solvent was then replaced by a mixture of chlorobenzene / 1,5-COD (10:1) favouring precursor solubility and dissociation.

The synthesis of Ni(3,C) was very slow compared to Ni(3,B). For any significant complexation to occur, the temperature of the reactant solution had to be increased to 60°C. The zwitterionic complex was observed by NMR at δ(ppm): 56 (d,  $J_{PP} = 28$  Hz); 82 (d,  $J_{PP} = 29$  Hz). However, the integration of the complex signals constituted only in 47 %P of the crude and the presence of black particles suggested that the complex decomposed in solution.

The synthesis of Ni(4,C) led to the expected product, found in <sup>31</sup>P NMR at δ(ppm): 43 (d,  $^2J_{PP} = 28$  Hz); 55 (d,  $^2J_{PP} = 28$  Hz) for 66 %P. Surprisingly, the other products consisted of the homocomplex Ni(4,4) at 53 ppm (br s) and its decomposition product at δ(ppm): 14 (d,  $^2J_{PP} = 17$  Hz); 42 (d,  $^2J_{PP} = 17$  Hz) see Figure 15. The presence of the homocomplex and its degradation product substantiated a competitive coordination behaviour of co-ligands **4** and **C**, as already observed in the synthesis of Ni(4,3). It also underlined that **4** and **C** had resembling basicity at the phosphorus and therefore a comparable ability to bind to nickel. In contrast, the co-ligand **B** with an electron donating group at R<sup>3</sup> had a stronger binding ability, as supported by the selective formation of Ni(4,B).

<sup>4</sup> bright yellow solid; <sup>31</sup>P NMR at δ(CD<sub>2</sub>Cl<sub>2</sub>): 52.4 ppm (sharp s), DEPT135 aromatic signals at 120-140 ppm, no allyl and no CH<sub>2</sub> (expected in the 20-35 ppm): absence of COD in the structure. Postulated: Ni(C)<sub>4</sub> or a dimer [Ni(C)<sub>2</sub>]<sub>2</sub> yet a clear resolution of this structure was not investigated.

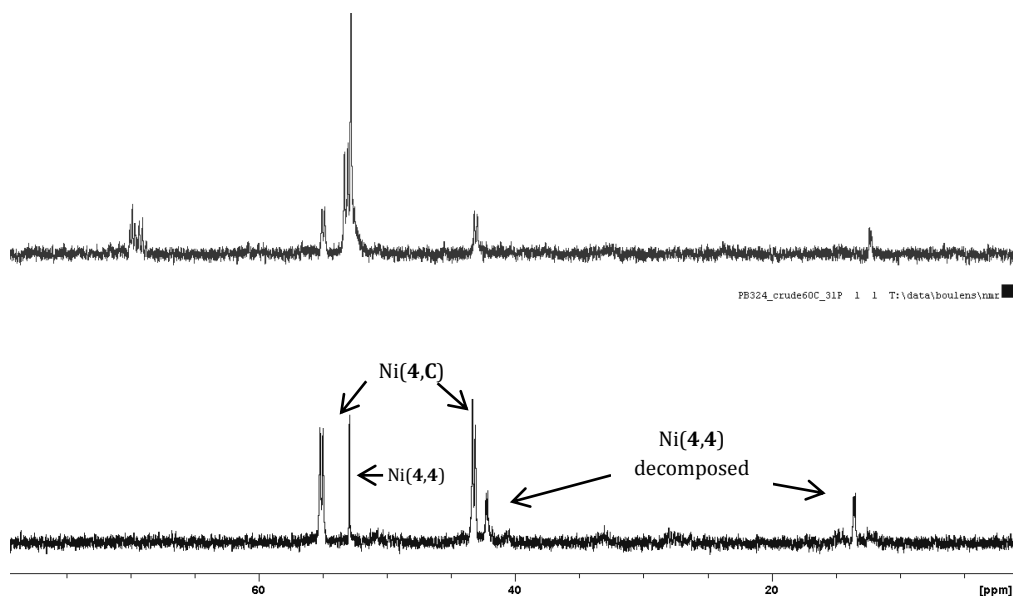


**Figure 15.** Crude  $^{31}\text{P}$  NMR recorded after reacting an equimolar mixture of  $\text{Ni}(\text{COD})_2$ , METAMORPhos **4** and co-ligand **C** (0.1 mmol) in toluene. Above after 1 h at RT, below 1h at RT followed by 1h at  $60^\circ\text{C}$ .

The synthesis of  $\text{Ni}(\mathbf{5},\mathbf{C})$  led after 16 h to the expected product as shown by  $^{31}\text{P}$  NMR ( $\text{CD}_2\text{Cl}_2$ ) at  $\delta(\text{ppm})$  52.64 (d,  $^2J_{\text{PP}} = 23.4$  Hz); 58.58 (d,  $^2J_{\text{PP}} = 23.7$  Hz). Also in this case, many black particles were formed. The product was isolated as a yellow powder which was poorly soluble in toluene; however, this complex was not pure enough to be used in catalysis.

### Ni(3,D)

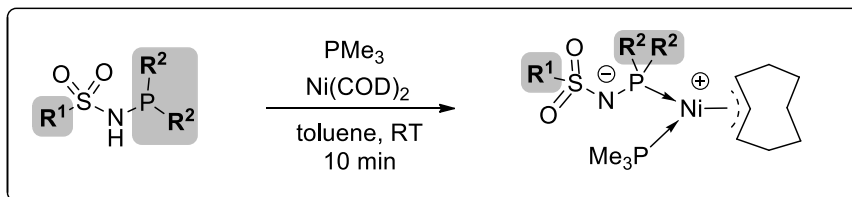
When **3** and **D** were added to a solution of  $\text{Ni}(\text{COD})_2$  at room temperature, no complexation was observed. The formation of  $\text{Ni}(\mathbf{3},\mathbf{D})$  was apparent when the same mixture was heated to  $60^\circ\text{C}$ ; this led to two broad signals in the NMR spectrum at  $\delta(\text{C}_6\text{D}_6)$ : 84.2 ppm and 101.7 ppm but also a characteristic signal for the allyl was observed by  $^1\text{H}$  NMR at  $\delta(\text{C}_6\text{D}_6)$ : 4.71 ppm (t,  $^3J_{\text{HH}} = 8.2$  Hz) in the range of reported signals. These data are in good agreement with the generation of a zwitterionic complex. Further isolation, however, was not attempted due to the formation of many other complexes in the crude reaction mixture.

### Ni(5,E)

Ligand **E** also generated a lot of products when reacted with  $\text{Ni}(\text{COD})_2$  and **5** according to NMR in which a doublet system was observed at 53 ppm (d,  $J_{\text{PP}} = 26$  Hz) and 75 ppm (d,  $J_{\text{PP}} = 23$  Hz), suggesting zwitterionic complex formation. However no selective complex formation was evidenced.

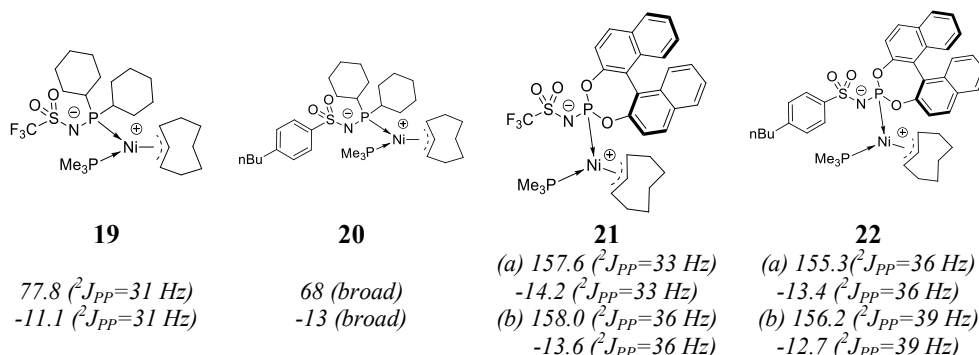
### PMe<sub>3</sub>-based METAMORPhos zwitterionic complexes

Since  $\text{PMe}_3$  showed very quick and quantitative conversion for the synthesis of zwitterionic complex **16**, the METAMORPhos ligands were tested according to the procedure depicted in Scheme 11.

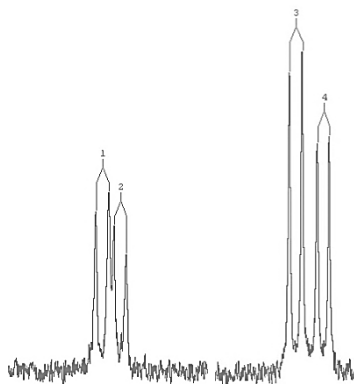


**Scheme 11.** General procedure adopted to evaluate the influence of different METAMORPhos on the synthesis on the zwitterionic and cationic  $\text{PMe}_3$ -based nickel complexes.

Chemical shifts (ppm) and coupling constant (Hz) for  $\text{PMe}_3$ -based complexes **19-22** (the other  $\text{PMe}_3$ -based complexes were isolated, see following section for experimental details)



The reaction of METAMORPhos ligands **9** and **10**, having a chiral centre with  $\text{Ni}(\text{COD})_2$  and  $\text{PMe}_3$  led to the formation of the corresponding zwitterionic complexes with however a “splitting” of each signal in the NMR spectrum in a 1:1 ratio as shown in Figure 16.



( $a_{2,4}$ ):  $157.6$  &  $-14.2$  ( $^2J_{PP}=33$  Hz)  
 ( $b_{1,3}$ )  $158.0$  &  $-13.6$  ( $^2J_{PP}=36$  Hz).

**Figure 16.** Phosphorus NMR spectrum of complex **21** (*in situ*) and respective chemical shifts for both diastereoisomers (a) and (b).

This splitting of signals, observed upon the insertion of a chiral element in the complex structure, suggested that two diastereoisomers had formed and consequently that the



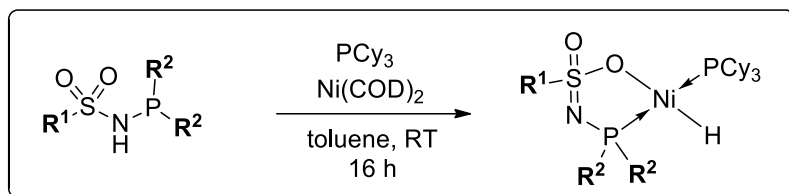
zwitterionic complex itself had its own source of chirality expressed in a 1:1 ratio. The origin of this chirality probably resulted in the position of the COD. Indeed on the basis of the crystal structures that were presented in Chapter 4, we observed that the 5 methylene groups of the COD could point either above or below the coordination plane compared with the two phosphines as shown in Figure 17.



**Figure 17.** Position of the COD in the complexes that can be located above or below the  $P_1, Ni, P_2$  coordination plane according to the solid state crystal structures of zwitterionic cationic nickel complexes.

### PCy<sub>3</sub>-based METAMORPhos zwitterionic complexes

The reaction conditions presented in Scheme 12 were adopted as a general procedure for the screening of the synthesis of PCy<sub>3</sub>-based METAMORPhos zwitterionic complexes.



**Scheme 12.** General procedure adopted for screening of different METAMORPhos ligands with PCy<sub>3</sub> and Ni(COD)<sub>2</sub>

METAMORPhos **4** (NH tautomer with  $R^1 = 4\text{-}n\text{Bu-Ph}$  and  $R_2 = \text{Ph}$ ) was very reactive with Ni(COD)<sub>2</sub> and PCy<sub>3</sub> producing several decomposition products, suggesting complex instability. A small peak in <sup>1</sup>H NMR spectrum of the mixture could be observed at – 26 ppm, which signals that a hydride had formed. However this product only accounted for a small fraction of the total yield of products and Ni(**4,4**) was also observed. The presence of Ni(**4,4**) suggested that there was a competitive reaction between hydride or zwitterionic complex formation. This competition was mainly directed towards Ni(**4,4**) which can be explained by the easier formation of the less bulky Ni(**4,4**) complex compared with the PCy<sub>3</sub>-based hydride.

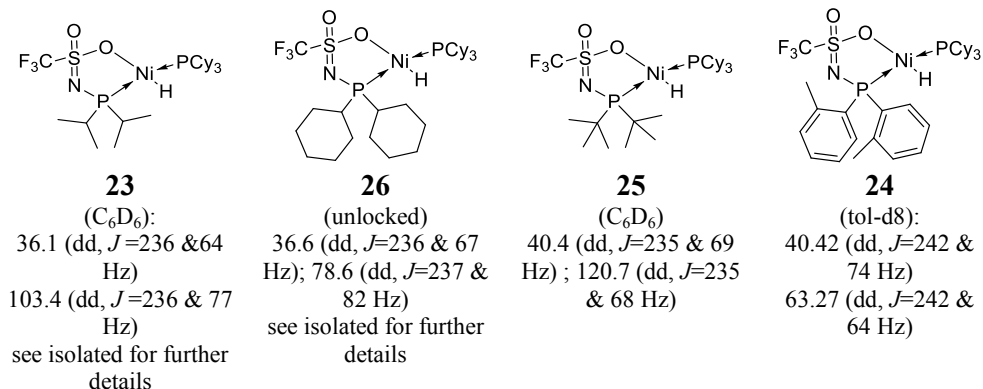
METAMORPhos ligands **5** and **6** (PH tautomer) bearing bulky phosphines PCy<sub>2</sub> and P(*t*-Bu)<sub>2</sub> reacted very slowly with Ni(COD)<sub>2</sub> and PCy<sub>3</sub> to form hydride complexes **26** and **25**, respectively. Full conversion of ligand **5** to hydride **26** was possible by heating the reaction mixture to 60°C for 16 h. The resulting complex was stable and soluble in toluene but precipitated in pentane. Analysis of the isolated product by NMR and elemental analysis also confirmed that complex **26** formed. Unfortunately no crystals could be obtained from these complexes.

Increasing again the steric bulk on the P atom ( $R^1 = \text{CF}_3$ ,  $R^2 = t\text{Bu}$ ), going through the tert-butyl substituted METAMORPhos ligand **6** decreased again system reactivity since the

system had to be heated up to 90°C for one hour; this led to the formation of a typical hydride pattern in the  $^{31}\text{P}$  NMR spectrum (doublets of doublets) with good conversion (85 %).

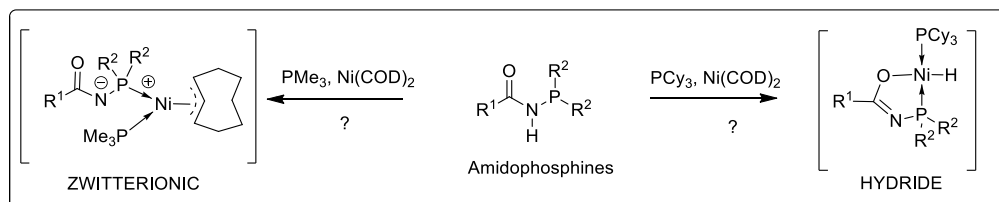
We investigated the reactivity of the analogue METAMORPhos **7** ( $\text{R}^1 = \text{CF}_3$ ,  $\text{R}^2 = \text{Cy}$ ) with the bulky cyclohexyl group on P. In the conditions of Scheme 12, already after 1 h ligand **7** had converted for 73 % to doublets of doublets in the  $^{31}\text{P}$  NMR spectrum. Surprisingly leaving this mixture in toluene for one week led to an orange precipitate which was insoluble in toluene or benzene and that we could not identify because of its low solubility. The higher reactivity of **7** (reaction at RT) compared with **3**, **5** and **6** suggests that less electron withdrawing groups on the METAMORPhos led to easier complex formation.

Chemical shifts observed for the hydride species:

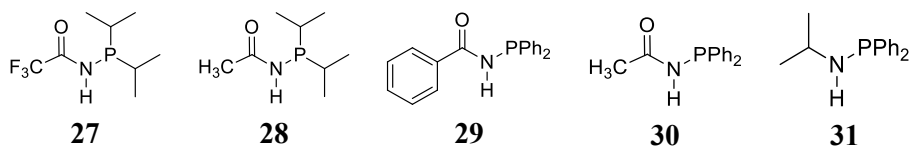


Extension to amidophosphines + ( $\text{PMe}_3/\text{Ni}(\text{COD})_2$ ) or + ( $\text{PCy}_3/\text{Ni}(\text{COD})_2$ ).

Because different METAMORPhos ligands allowed for the facile formation of either hydride or zwitterionic complexes as seen in Figure 7 and Figure 12, we wondered if changing METAMORPhos ligands for the more common amidophosphines would display equivalent reactivity under similar conditions. Zwitterionic or hydride complexes based on these ligands have not been reported to date with nickel. However, nickellacycles with P-N-C-O atoms have been described by Keim for Ni-aryl complexes suggesting the apparent stability of this arrangement.<sup>[30]</sup> This motivated our investigations into the synthesis of amidophosphine based zwitterionic or hydride complexes according to Scheme 13.<sup>5</sup>



<sup>5</sup> Amidophosphine ligands **27-31** were described and synthesised in Chapter 2 and they are represented under the NH tautomer for simplicity.

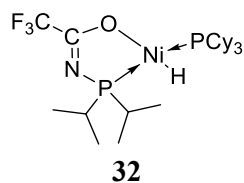


**Scheme 13.** General procedure for screening amidophosphine ligands with  $\text{PMe}_3/\text{Ni}(\text{COD})_2$  or  $\text{PCy}_3/\text{Ni}(\text{COD})_2$ .

The reaction of amidophosphine **27** (the direct carbonyl analogue of METAMORPhos ligand **3**) with  $\text{PMe}_3$  and  $\text{Ni}(\text{COD})_2$  led to a clear brown solution. The  $\text{PMe}_3$  signal observed initially at  $-62$  ppm in the  $^{31}\text{P}$  NMR spectrum had disappeared completely and several multiplet structures were observed at  $\delta(\text{ppm})$ :  $-21$  (s);  $-26.3$  (d,  $J_{\text{PP}} = 28.9$  Hz);  $110$  (br s);  $115.5$  (d,  $J_{\text{PP}} = 30.3$  Hz);  $116.4$  (br s). The two small doublets at  $-26.3$  ppm and  $115.5$  ppm corresponded to the resonances of two phosphorus atoms in *cis* position to a nickel centre (small value of  $J$ ). Heating this mixture to  $60^\circ\text{C}$  did not lead to any appreciable change in the product ratio, suggesting that a ligand equilibrium established between  $\text{Ni}(0)$ ,  $\text{PMe}_3$  and **27** without formation of the zwitterionic complex.

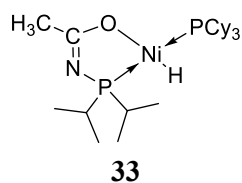
Through the same general procedure, the compounds **28-31** led to simple metal coordination without oxidative addition. This coordination was particularly visible for ligands **29** and **30** which generated in the  $^{31}\text{P}$  NMR spectrum in the  $-20$  ;  $-30$  ppm region simultaneously, a singlet, a doublet, a triplet and a quadruplet  $\delta(\text{ppm})$ :  $-21.6$  (s,  $\text{Ni}(\text{PMe}_3)_4$ );  $-22.8$  (d,  $J_{\text{PP}} = 33$  Hz,  $\text{Ni}(\text{29})(\text{PMe}_3)_3$ );  $-24.9$  (dd,  $J_{\text{PP}} = 35$  Hz  $\text{Ni}(\text{29})_2(\text{PMe}_3)_2$ );  $-28.0$  (dd,  $J_{\text{PP}} = 40$  Hz  $\text{Ni}(\text{29})_3(\text{PMe}_3)$ ). A similar pattern was also observed downfield (around  $65$  ppm). These signals accounted for all the possible chelates combinations containing  $\text{PMe}_3$  and **29**, according to Wilke for  $\text{Ni}(\text{PMe})_n(\text{PPh}_3)_{4-n}$ .<sup>[9]</sup>

Subsequently, we explored the second reaction, that is, the reactivity of several amidophosphines with  $\text{Ni}(\text{COD})_2$  and  $\text{PCy}_3$ . Ligands **27** and **28** with a basic diisopropylphosphine, converted quickly at RT to hydrides **32** and **33**, respectively, as confirmed by NMR. These amidophosphine-based hydrides were not isolated but their chemical shifts and coupling constants very close to those of METAMORPhos-based complexes **32** and **23** suggested that they had identical structure structures based on a PO chelate and two phosphines in *trans* position. Amido(aryl)phosphines **29** and **30** showed formation of the expected complexes when subjected to the general reaction conditions but also a number of by-products were formed according to  $^{31}\text{P}$  NMR, suggesting fast degradation. The aminophosphine **31** did not form hydrides even upon prolonged heating.



$^{31}\text{P}$  ( $\delta$  ppm):

$37$  (dd,  $^2J_{\text{PP}}=243$  Hz,  $^2J_{\text{PH}}=55$  Hz)  
 $118$  (dd,  $^2J_{\text{PP}}=240$  Hz,  $^2J_{\text{PH}}=66$  Hz).  
 $^1\text{H}$ : hydride at  $\delta$ :  $-24.4$  ppm (dd)



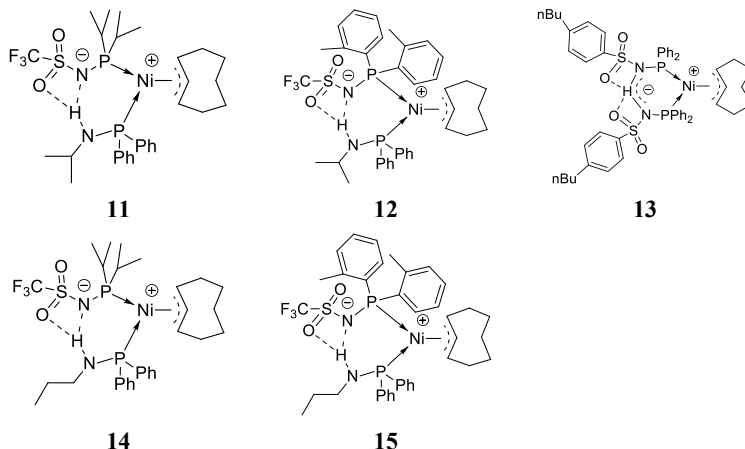
$^{31}\text{P}$  ( $\delta$  ppm):

$36.5$  ppm (dd,  $^2J_{\text{PP}}=240$  Hz,  $^2J_{\text{PH}}=53$  Hz)  
 $115$  ppm (dd,  $^2J_{\text{PP}}=240$  Hz,  $^2J_{\text{PH}}=63$  Hz);  
 $^1\text{H}$  hydride at  $\delta$ :  $-23.7$  ppm (dd)

Amidophosphines did not lead to zwitterionic complexes with  $\text{PMe}_3$  while in the presence of  $\text{PCy}_3$ , bulky ligands led to hydride complex formation. This suggested that the sulphonyl group in METAMORPhos offered a better stabilisation of zwitterionic complexes on the delocalised PNSO backbone, compared with the PNCO system. Moreover we anticipated that

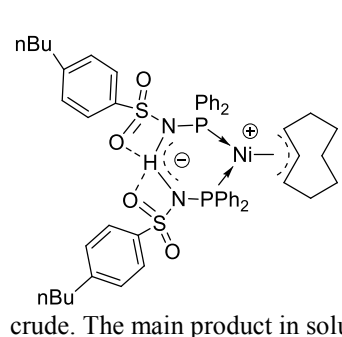
other ligands such as P-NH-P=O<sup>[31]</sup> could function similarly to sulphonamides based analogues and would produce zwitterionic or nickel hydride complexes.

## 5.4 Synthesis and characterisation of supramolecular complexes 11-15



Complexes **11** and **12** have been described previously (chapter 4)

### Complex 13



The synthesis of this complex was first performed in toluene and at RT. The reaction mixture quickly turned from yellow to dark greenish. The corresponding <sup>31</sup>P NMR of the crude mixture stirred overnight consisted in majority of a broad peak (complex **13**) at  $\delta$ : 55 ppm (80%) and in minority (20%) of a double doublet system at  $\delta$ (ppm): 12 (d, <sup>2</sup>J<sub>PP</sub> = 17.0 Hz) and 53 (d, <sup>2</sup>J<sub>PP</sub> = 17.0 Hz) attributed to the thermal degradation product of complex **13**: see Figure 18. The minor product was removed quantitatively by selective precipitation of a green solid from the crude mixture, by careful addition of pentane to a toluene solution of the crude. The main product in solution was obtained by evaporation of the solution.

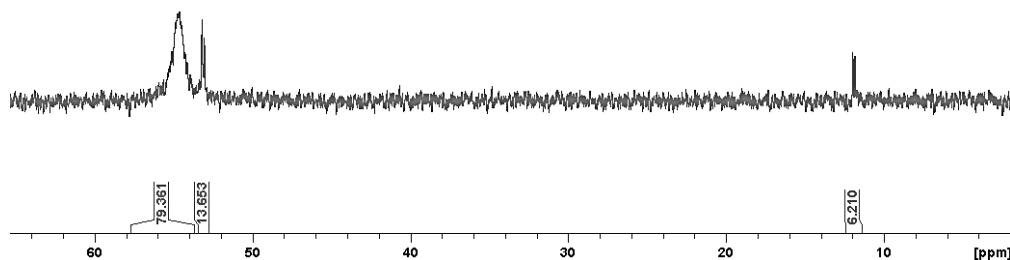


**Figure 18.** Unlocked <sup>31</sup>P NMR spectrum of the crude mixture during the synthesis of **13** with broad signals of the complex and the decomposition product at 12 and 53 ppm (values slightly differ in C<sub>6</sub>D<sub>6</sub>:  $\delta$  (C<sub>6</sub>D<sub>6</sub>): 54.0 ppm for the main product, by-product at  $\delta$ (C<sub>6</sub>D<sub>6</sub>): 12.6 ppm (d, <sup>2</sup>J<sub>PP</sub>=17.0 Hz) and 52.6 ppm (d, <sup>2</sup>J<sub>PP</sub>=17.0 Hz)

Changing toluene for chlorobenzene as the solvent for the synthesis did not change the product ratio. Surprisingly when 1,5-bis(cyclooctadiene) (1,5-COD) was used as reaction solvent, only the signal at 54 ppm was observed by  $^{31}\text{P}$  NMR. *Via* this optimised procedure, described below the pure product **13** was isolated with no decomposition product.

METAMORPhos ligand **4**, 4-*n*BuPh-SO<sub>2</sub>-NH-PPh<sub>2</sub> (397 mg, 1.00 mmol, 2.00 eq.) and Ni(COD)<sub>2</sub> (138 mg, 0.50 mmol, 1.00 eq.) were dissolved in dry 1,5-cyclooctadiene (10 mL) and stirred overnight. The solvent was evaporated under reduced pressure to yield a greenish oil. The resulting oil was co-evaporated several times with pentane to get rid of the traces of cyclooctadiene. The oil was extracted several times with heptane/ toluene mixtures (4:1) and the liquid fractions collected and evaporated to dryness to give an orange powder. The powder was dried and washed twice with 10 mL of pentane. to give an orange powder (131 mg). Isolate yield 27%.  $^{31}\text{P}\{^1\text{H}\}$  NMR (121 MHz, C<sub>6</sub>D<sub>6</sub>, 300K):  $\delta$ (ppm): 54.06;  $^1\text{H}$  NMR (300 MHz, C<sub>6</sub>D<sub>6</sub>, 300K):  $\delta$ (ppm): 0.82 (t,  $^3J = 7.2$  Hz, CH<sub>3</sub>, 6H); 1.15 (sex,  $^3J = 7.5$  Hz, CH<sub>2</sub>-CH<sub>3</sub>, 4H), 1.34 (q,  $^3J = 7.7$  Hz, CH<sub>2</sub>-CH<sub>2</sub>-CH<sub>3</sub>, 4H); 2.30 (t,  $^3J = 7.8$  Hz, CH<sub>2</sub>-Ar, 4H); 1.04 (m, CH<sub>2</sub> COD, 4H); 1.45 (m, CH<sub>2</sub> COD, 4H); 1.94 (m, CH<sub>2</sub> COD, 2H); 3.95 (dd,  $J = 17.2$  & 8.6 Hz, CH COD allyl  $\beta$ , 2H); 4.85 (t,  $^3J = 8.6$  Hz, CH COD allyl  $\alpha$ , 1H); 6.85 (d,  $^2J_{ortho} = 8.1$  Hz, CH<sub>Ar-SO<sub>2</sub></sub>, 4H); 7.01 (broad s, CH PPh<sub>2</sub>, 12H); 7.96 (broad s, CH PPh<sub>2</sub>, 8H); 8.04 (d,  $^3J_{HH} = 7.99$  Hz, CH<sub>Ar-SO<sub>2</sub></sub>, 4H); 9.64 (br s, NH, 1H);  $^{13}\text{C}$  NMR (75 MHz, C<sub>6</sub>D<sub>6</sub>, 300K):  $\delta$ (ppm): 14.07 (CH<sub>3</sub>, 2C); 22.54 (CH<sub>2</sub>-CH<sub>3</sub>, 2C); 23.09 (CH<sub>2</sub> COD, 1C); 27.05 (CH<sub>2</sub> COD, 2C); 29.95 (CH<sub>2</sub> COD, 2C); 33.54 (CH<sub>2</sub>-CH<sub>2</sub>-CH<sub>3</sub>, 2C); 35.65 (Ar-CH<sub>2</sub>, 2C); 82.12 (CH COD allyl  $\beta$ , 2C); 110.08 (CH COD allyl  $\alpha$ ); 127.34 (CH<sub>Ar-SO<sub>2</sub></sub>, 4C); 128.2 (m, CH PPh<sub>2</sub> meta, 8C); 128.46 (CH<sub>Ar-SO<sub>2</sub></sub>, 4C); 129.75 (CH PPh<sub>2</sub> para, 4C); 132.26 (m, CH PPh<sub>2</sub> ortho, 8C); 136.58 (m, C<sup>IV</sup> PPh<sub>2</sub> ipso, 4C); 143.14 (C<sup>IV</sup> C-*n*Bu, 2C); 146.06 (C<sup>IV</sup> C-SO<sub>2</sub>, 2C). EA (th): C: 64.17 (64.94); H: 6.64 (6.29); N: 3.15 (2.91).

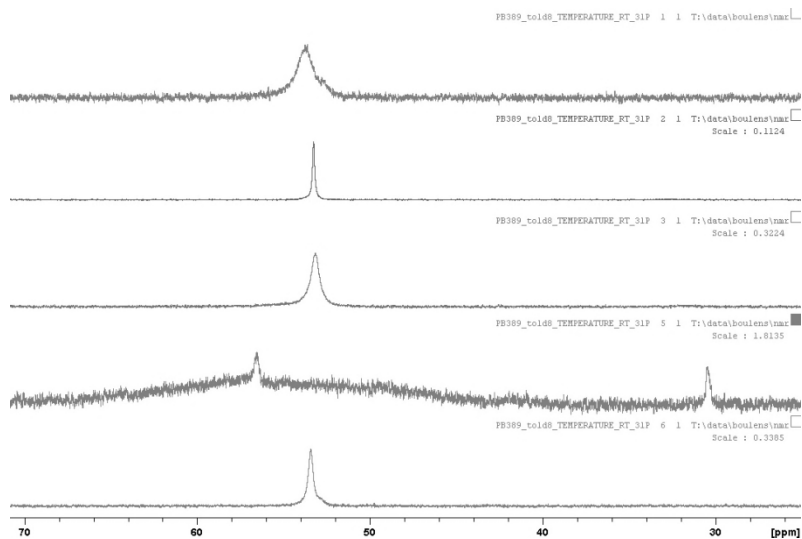
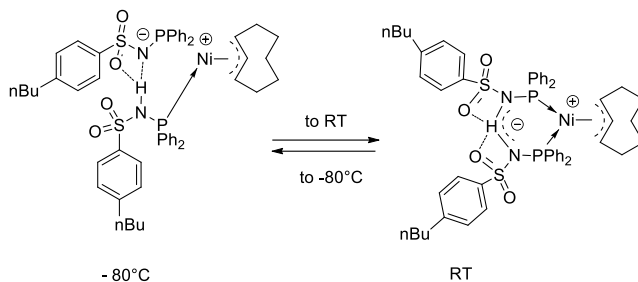


**Figure 19.** Low temperature  $^{31}\text{P}$  NMR (121 MHz, tol-*d*<sub>8</sub>) experiment on complex **13** in tol-*d*<sub>8</sub>. From top to bottom: 30°C, -10°C, -40°C, -80°C and back to 30°C.



**Scheme 14.** Complex **13** H-bond dynamics at  $-80^{\circ}\text{C}$  and room temperature.

### Thermal stability of complex **13**

Given the stability improvement induced by 1,5-COD in the course of the synthesis of **13**, we suspected that one possible degradation pathway for these complexes could be the loss of COD of the allyl moiety by beta-H elimination.<sup>6</sup> To check this hypothesis, we tested the effect of a reaction temperature increase on the structure of complex **13**. Already at  $60^{\circ}\text{C}$ , a solution of complex **13** in toluene went from yellow to green and we observed by  $^{31}\text{P}$  NMR a decrease of the signals of **13** with an increase of signals of the by-product at 12.6 ppm and 52.6 ppm. Simultaneously the signals of the allyl fragment disappeared from  $^1\text{H}$  NMR and new signals appeared at 5.6-6.2 ppm (see Figure 20), corresponding to free 1,3-COD according to the simulated  $^1\text{H}$  NMR pattern. However, we could not formally determine this degradation product structure and did not observe any hydride formation.

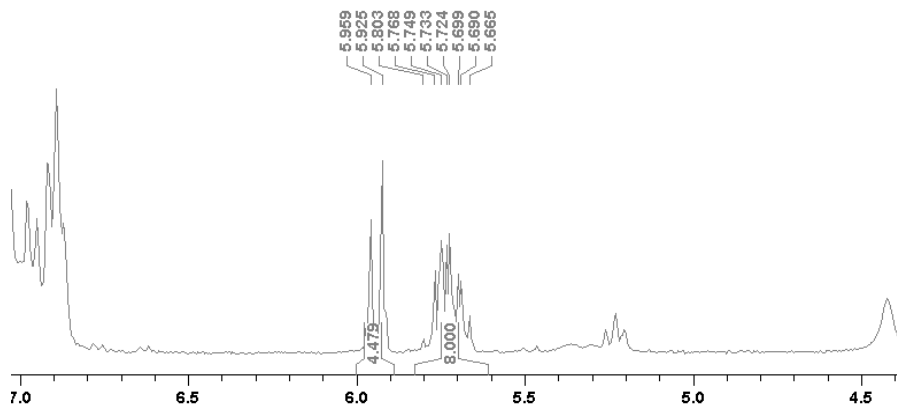
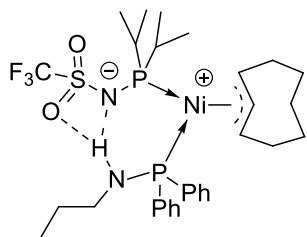


**Figure 20.**  $^1\text{H}$  NMR (300MHz,  $\text{C}_6\text{D}_5\text{Cl}$ ) spectrum of complex **13** at  $80^{\circ}\text{C}$ , detail of the characteristic 1,3-COD signals between 5.5 and 6.1 ppm corresponding to one of the thermal degradation product of the complex.

<sup>6</sup> In the absence of COD in the reaction mixture (replacing  $\text{Ni}(\text{COD})_2$  by  $\text{Ni}(\text{PPh}_3)_4$ ) there was no signal at 54 ppm and only the two doublet system at 12.6 and 52.6 ppm and corresponding to the side-product were formed.

## Complex 14



METAMORPhos ligand **3**,  $F_3C-SO_2-N=P(iPr)_2$  (265 mg, 1.00 mmol, 1.00 eq.) was placed in a Schlenk and dissolved in toluene (5 mL). In another Schlenk,  $Ni(COD)_2$  (275 mg, 1.00 mmol, 1.00 eq.), and propyl-1,1-diphenylphosphinamine (244 mg, 1.00 mmol, 1.00 eq.) and some 1,5-cyclooctadiene (0.5 mL for complex stabilisation) were dissolved in toluene (10 mL) in an ice bath. Both solutions were cooled to 0°C and the solution of METAMORPhos ligand **3** was added dropwise to the other Schlenk. The mixture was left to stir for 5h30 at room temperature leading to a brown solution. The solvents

were evaporated under vacuum to give a dark yellow solid. This solid was washed and triturated (ultrasound bath) with pentane (2 x 10 mL) to give a yellow powder. It was finally washed with cold diethyl ether (2 x 10 mL) to give a bright yellow solid. The solid was dried under vacuum. To get rid of  $Et_2O$  traces, the solid was suspended in toluene (5 mL) and the solvent evaporated under vacuum (co-evaporation). This operation was repeated once to give a yellow powder. The solid was then dissolved in dichloromethane (5 mL) to give an orange solution. This solution was passed through a syringe filter to eliminate residual solids or black nickel. The resulting solution was finally evaporated to an oil which is submitted to co-evaporation with toluene (2 x 5 mL). A yellow solid was obtained (isolate yield: 325 mg, 47 %). Due to a very low solubility in aromatic hydrocarbons the NMR was recorded in  $CD_2Cl_2$ .  $^{31}P\{^1H\}$  NMR (121 MHz,  $CD_2Cl_2$ , 300K):  $\delta$ (ppm): 64.55 (d,  $^2J_{PP} = 31.5$  Hz); 92.16 (d,  $^2J_{PP} = 31.6$  Hz);  $^1H$  NMR (300 MHz,  $CD_2Cl_2$ , 300K):  $\delta$ (ppm): 0.45-2.30 (COD signals of  $CH_2$ , 10H); 0.86 (t,  $^3J_{HH} = 7.4$  Hz,  $\underline{CH_3-CH_2}$ , 3H); 1.10-1.30 (m,  $CH_3$   $iPr$  a, 6H); 1.38 (dd,  $^3J_{HH} = 6.7$  Hz,  $^3J_{HP} = 13.4$  Hz, 3H,  $CH_3$   $iPr$  b, 6H); 1.44-1.63 (m,  $CH_3$   $iPr$  b and  $\underline{CH_2-CH_3}$ , 5H); 2.20 (m, CH  $iPr$  b, 1H); 2.53 (m,  $CH_2-N$ , 2H); 3.07 (m, CH  $iPr$  a, 1H); 3.90 (quint,  $^3J_{HH} = 8.5$  Hz, CH  $COD$  allyl  $\beta$ , 1H); 4.76 (quint.,  $^3J_{HH} = 7.4$  Hz, CH  $COD$  allyl  $\beta$ , 1H); 5.05 (t,  $^3J_{HH} = 8.5$  Hz, CH  $COD$  allyl  $\alpha$ , 1H); 5.45 (m, NH, 1H); 7.46 (m,  $H_{Ar}$  ortho, para, 6H); 7.62 (m,  $H_{Ar}$  meta, 4H);  $^{19}F$  NMR (282 MHz,  $CD_2Cl_2$ , 300K):  $\delta$ (ppm): -79.79 (s);  $^{13}C$  NMR (75 MHz,  $C_6D_6$ , 300K):  $\delta$ (ppm): 11.8 ( $CH_2-CH_3$ ); 17.3 (d,  $^2J_{CP} = 4.5$  Hz,  $CH_3$   $iPr$  b); 18.2 (d,  $^2J_{CP} = 2.0$  Hz,  $CH_3$   $iPr$  a); 19.0 (d,  $^2J_{CP} = 5.0$  Hz,  $CH_3$   $iPr$  a); 20.6 (d,  $^2J_{CP} = 4.0$  Hz,  $CH_3$   $iPr$  a); 22.9 ( $CH_2$   $COD$ ); 25.0 (d,  $^3J_{CP} = 8.7$  Hz,  $\underline{CH_2-CH_3}$ ); 27.3 (d,  $J_{CP} = 4.2$  Hz,  $CH_2$   $COD$ ); 28.1 (d,  $J_{CP} = 4.7$  Hz,  $CH_2$   $COD$ ); 29.4 (d,  $^1J_{CP} = 22.7$  Hz, CH  $iPr$  a); 29.9 (d,  $^3J_{CP} = 1.9$  Hz,  $CH_2$   $COD$ ); 31.5 (d,  $^1J_{CP} = 17.4$  Hz, CH  $iPr$  b); 31.7 ( $CH_2$   $COD$ ); 45.5 (d,  $^2J_{CP} = 12.3$  Hz,  $CH_2-N$ ); 72.3 (dd,  $^2J_{CP} = 19.2$  Hz,  $^2J_{CP} = 5.6$  Hz, CH  $COD$  allyl  $\beta$ ); 82.7 (dd,  $^2J_{CP} = 18.3$  Hz,  $^2J_{CP} = 4.0$  Hz, CH  $COD$  allyl  $\beta$ ); 110.9 (CH  $COD$  allyl  $\alpha$ ); 120.98 (qd,  $J_{CF} = 322.4$  Hz,  $^3J_{CP} = 4.2$  Hz); 128.6 (m, CH  $Ar$  ortho, 4C); 130.5 (d,  $^4J_{CP} = 1.8$  Hz, CH  $Ar$  para); 130.9 (d,  $^4J_{CP} = 1.9$  Hz, CH  $Ar$  para); 132.6 (d,  $^3J_{CP} = 10.8$  Hz, CH  $Ar$  meta, 2C); 133.3 (d,  $^3J_{CP} = 13.1$  Hz, CH  $Ar$  meta, 2C); 134.6 (d,  $^1J_{CP} = 55.6$  Hz,  $C^{IV}_{PPh_2}$  ipso); 134.9 (d,  $^1J_{CP} = 36.9$  Hz,  $C^{IV}_{PPh_2}$  ipso). EA (th): C : 53.45 (53.35) ; H : 6.61 (6.72) ; N : 3.86 (4.15). Crystals suitable for diffraction obtained from a cold saturated solution of the complex **14** in toluene.

## Crystal data

$C_{30}H_{45}F_3N_2NiO_2P_2S$	$F(000) = 5696$
$M_r = 675.38$	$D_x = 1.225$ Mg $m^{-3}$
Orthorhombic, $Fdd2$	Mo $K\alpha$ radiation, $\lambda = 0.7107$ Å
Hall symbol: F 2 -2d	Cell parameters from 5994 reflections
$a = 37.938$ (3) Å	$\theta = 4.4-28.5^\circ$
$b = 37.593$ (6) Å	$\mu = 0.72$ mm $^{-1}$
$c = 10.2721$ (8) Å	$T = 150$ K
$V = 14650$ (3) Å $^3$	Needle, yellow
$Z = 16$	$0.58 \times 0.21 \times 0.18$ mm

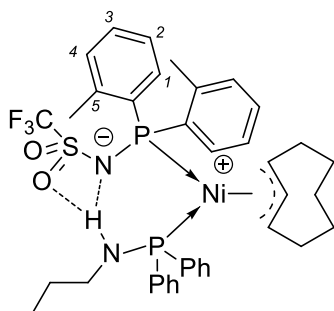
## Data collection

Xcalibur, Atlas, Gemini ultra diffractometer	8782 independent reflections
Radiation source: Enhance (Mo) X-ray Source	7121 reflections with $I > 2.0\sigma(I)$
graphite	$R_{\text{int}} = 0.000$
Detector resolution: 10.4685 pixels $\text{mm}^{-1}$	$\theta_{\text{max}} = 29.8^\circ$ , $\theta_{\text{min}} = 3.0^\circ$
$\omega$ scans	$h = 0 \rightarrow 51$
Absorption correction: analytical <i>CrysAlis PRO</i> , Agilent Technologies, Version 1.171.36.28 (release 01-02-2013 CrysAlis171.NET) (compiled Feb 1 2013, 16:14:44) Analytical numeric absorption correction using a multifaceted crystal model based on expressions derived by R.C. Clark & J.S. Reid. (Clark, R. C. & Reid, J. S. (1995). <i>Acta Cryst.</i> A51, 887-897)	$k = 0 \rightarrow 51$
$T_{\text{min}} = 0.728$ , $T_{\text{max}} = 0.899$	$l = -13 \rightarrow 14$
46638 measured reflections	

## Refinement

Refinement on $F^2$	Hydrogen site location: difference Fourier map
Least-squares matrix: full	H-atom parameters constrained
$R[F^2 > 2\sigma(F^2)] = 0.074$	Method = Modified Sheldrick $w = 1/[\sigma^2(F^2) + (0.1P)^2 + ****P]$ , where $P = (\max(F_o^2, 0) + 2F_c^2)/3$
$wR(F^2) = 0.218$	$(\Delta/\sigma)_{\text{max}} = 0.001$
$S = 1.00$	$\Delta_{\text{max}} = 0.94 \text{ e } \text{\AA}^{-3}$
8770 reflections	$\Delta_{\text{min}} = -1.34 \text{ e } \text{\AA}^{-3}$
380 parameters	Absolute structure: Flack (1983), 3773 Friedel-pairs
15 restraints	Flack parameter: 0.01 (2)
Primary atom site location: structure-invariant direct methods	

## Complex 15



METAMORPhos ligand **5**,  $\text{F}_3\text{C-SO}_2\text{-NH-P(o-tolyl)}_2$ ,  $\text{NEt}_3$  (462 mg, 1.00 mmol, 1.00 eq.) was placed in a Schlenk and dissolved in chlorobenzene (5 mL). In another Schlenk,  $\text{Ni(COD)}_2$  (275 mg, 1.00 mmol, 1.00 eq.), and propyl-1,1-diphenylphosphinamine (244 mg, 1.00 mmol, 1.00 eq.) and some 1,5-cyclooctadiene (0.5 mL) were dissolved in chlorobenzene (10 mL) in an ice bath. Both solutions were cooled to  $0^\circ\text{C}$  and the solution of METAMORPhos ligand was added dropwise to the other Schlenk. The mixture was left to stir for 4 h at room temperature leading to a dark brown solution. The solvents were evaporated under vacuum to give an oily solid. This residue was triturated

with pentane (2 x 10 mL) to give a powder which was washed with pentane (5 x 5 mL) giving a dark yellow powder. This solid was washed with cold diethylether ( $0^\circ\text{C}$ , 3 x 10 mL) resulting in a yellow powder. In order to remove traces of diethylether, the powder was suspended in toluene (3 mL) and the toluene was evaporated under vacuum (co-evaporation). This operation was repeated 3 times to give the expected product as a bright yellow powder (isolate yield: 280 mg, 36%). The product was not very soluble in aromatic hydrocarbons and the NMR was recorded in  $\text{CD}_2\text{Cl}_2$ .  $^{31}\text{P}\{^1\text{H}\}$  NMR (121 MHz,  $\text{CD}_2\text{Cl}_2$ , 300K):  $\delta$ (ppm): 52.33 (d,  $^2J_{\text{PP}} = 24.7$  Hz); 65.09 (d,  $^2J_{\text{PP}} = 24.5$  Hz).  $^1\text{H}$  NMR (300 MHz,  $\text{CD}_2\text{Cl}_2$ , 300K):  $\delta$ (ppm):



0.45 (t,  ${}^3J_{HH} = 7.4$  Hz, CH<sub>3</sub><sub>propyl</sub>, 3H); 0.4-0.65 (m, CH<sub>2</sub><sub>COD</sub>, 1H); 1.02 (sext, CH<sub>2</sub>-CH<sub>3</sub>, 2H); 1.00-1.95 (m, CH<sub>2</sub><sub>COD</sub>, 9H); 1.99 (s, CH<sub>3</sub><sub>tolyl b</sub>, 3H); 2.34 (s, CH<sub>3</sub><sub>tolyl a</sub>, 3H); 2.38 (m, CH<sub>2</sub>-NH, 1H); 2.60 (m, CH<sub>2</sub>-NH, 1H); 3.68 (m,  ${}^3J_{HH} = 5.9$  Hz,  ${}^2J_{HP} = ?$ , CH<sub>COD allyl β</sub>, 1H); 4.16 (m,  ${}^3J_{HH} = 7.0$  Hz,  ${}^2J_{HP} = 8.3$  Hz, CH<sub>COD allyl β</sub>, 1H); 5.38 (t,  ${}^3J_{HH} = 8.3$  Hz, CH<sub>COD allyl α</sub>, 1H); 6.59 (m, CH<sub>tolyl 2a</sub>, 1H); 7.01 (m, CH<sub>tolyl 4a</sub> and CH<sub>tolyl 4b</sub>, 2H); 7.12 (m, CH<sub>tolyl 3a</sub>, 1H); 7.29 (m, CH<sub>tolyl 3b</sub> and CH<sub>tolyl 2b</sub>, 2H); 7.41 (m, CH<sub>PPh2</sub>, 3H); 7.58 (m, CH<sub>PPh2</sub>, 5H); 7.70 (m, CH<sub>tolyl 1a</sub>, 1H); 7.73 (m, CH<sub>PPh2</sub>, 2H); 8.20 (m, CH<sub>tolyl 1b</sub>, 1H). <sup>13</sup>C NMR (75 MHz, C<sub>6</sub>D<sub>6</sub>, 300K): δ(ppm): 11.1 (CH<sub>3</sub><sub>nBu</sub>); 21.4 (CH<sub>3</sub><sub>tolyl a</sub>); 22.3 (d,  ${}^3J_{CP} = 9.1$  Hz, CH<sub>3</sub><sub>tolyl b</sub>); 23.0 (CH<sub>2</sub><sub>COD</sub>); 24.7 (d,  ${}^3J_{CP} = 5.8$  Hz, CH<sub>2</sub>-CH<sub>3</sub>); 26.8 (m, CH<sub>2</sub><sub>COD</sub>, 2C); 29.4 (CH<sub>2</sub><sub>COD</sub>); 46.5 (d,  ${}^2J_{CP} = 11.3$  Hz, CH<sub>2</sub>-NH); 80.1 (d,  ${}^2J_{CP} = 17.5$  Hz, CH<sub>COD allyl β</sub>); 86.6 (d,  ${}^2J_{CP} = 18.6$  Hz, CH<sub>COD allyl β</sub>); 111.5 (CH<sub>COD allyl α</sub>); 121.2 (qd,  ${}^1J_{CF} = 322$  Hz,  ${}^3J_{CP} = 6.5$  Hz, -CF<sub>3</sub>); 124.0 (d,  $J_{CP} = 15.7$  Hz, CH<sub>2a</sub>); 125.5 (d,  $J_{CP} = 8.1$  Hz, CH<sub>3b</sub>); 128.5 (d,  $J_{CP} = 9.5$  Hz, CH<sub>PPh2</sub>, 2C); 129.0 (d,  $J_{CP} = 9.9$  Hz, CH<sub>PPh2</sub>, 2C); 129.9 (s, CH<sub>2b</sub>); 130.2 (s, CH<sub>PPh2</sub>); 130.7 (CH<sub>3a</sub>); 131.2 (m, CH<sub>1b,4b,PPh2</sub>, 3C); 131.9 (d,  $J_{CP} = 5.9$  Hz, CH<sub>4a</sub>); 132.8 (d,  $J_{CP} = 11.2$  Hz, CH<sub>PPh2</sub>, 2C); 133.5 (d,  $J_{CP} = 13.0$  Hz, CH<sub>PPh2</sub>, 2C); 134.7 (d,  ${}^1J_{CP} = 47.5$  Hz, C<sup>IV</sup><sub>tolyl a CP</sub>); 135.4 (d,  $J_{CP} = 52.4$  Hz, C<sup>IV</sup><sub>PPh2, CP</sub>); 136.0 (d,  ${}^1J_{CP} = 40.7$  Hz, C<sup>IV</sup><sub>PPh2, CP</sub>); 138.9 (m, C<sup>IV</sup><sub>tolyl b, C-Me</sub>, C<sup>IV</sup><sub>tolyl b, C-P</sub>, 2C); 142.9 (m, C<sup>IV</sup><sub>tolyl a, C-Me</sub>). EA (th): C : 50.49 (59.16) ; H : 7.41 (5.88) ; N : 3.65 (3.63).

C <sub>38</sub> H <sub>45</sub> F <sub>3</sub> N <sub>2</sub> NiO <sub>2</sub> P <sub>2</sub> S	$F(000) = 1616$
$M_r = 771.50$	$D_x = 1.422$ Mg m <sup>-3</sup>
Monoclinic, $P2_1/n$	Mo $K\alpha$ radiation, $\lambda = 0.7107$ Å
Hall symbol: -P 2yn	Cell parameters from 36314 reflections
$a = 11.2995$ (5) Å	$\theta = 3.9\text{--}29.4^\circ$
$b = 19.119$ (1) Å	$\mu = 0.74$ mm <sup>-1</sup>
$c = 16.8177$ (9) Å	$T = 150$ K
$\beta = 97.401$ (5)°	Block, yellow
$V = 3602.9$ (3) Å <sup>3</sup>	$0.53 \times 0.38 \times 0.28$ mm
$Z = 4$	

## Data collection

Xcalibur, Atlas, Gemini ultra diffractometer	9847 independent reflections
Radiation source: Enhance (Mo) X-ray Source	7468 reflections with $I > 2.0\sigma(I)$
graphite	$R_{int} = 0.098$
Detector resolution: 10.4685 pixels mm <sup>-1</sup>	$\theta_{max} = 29.8^\circ$ , $\theta_{min} = 3.0^\circ$
$\omega$ scans	$h = -15 \rightarrow 15$
Absorption correction: analytical CrysAlis PRO, Agilent Technologies, Version 1.171.36.28 (release 01-02-2013 CrysAlis171.NET) (compiled Feb 1 2013, 16:14:44) Analytical numeric absorption correction using a multifaceted crystal model based on expressions derived by R.C. Clark & J.S. Reid. (Clark, R. C. & Reid, J. S. (1995). Acta Cryst. A51, 887-897)	$k = -26 \rightarrow 26$
$T_{min} = 0.969$ , $T_{max} = 0.982$	$l = -23 \rightarrow 22$
138950 measured reflections	

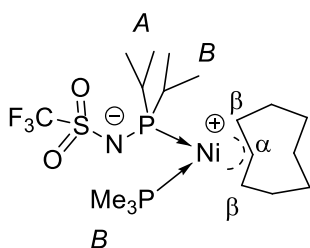
## Refinement

Refinement on $F^2$	Primary atom site location: structure-invariant direct methods
Least-squares matrix: full	Hydrogen site location: difference Fourier map
$R[F^2 > 2\sigma(F^2)] = 0.051$	H-atom parameters constrained
$wR(F^2) = 0.118$	Method, part 1, Chebyshev polynomial, (Watkin, 1994, Prince, 1982) [weight] = $1.0/[A_0 * T_0(x) + A_1 * T_1(x) + \dots + A_{n-1} * T_{n-1}(x)]$

	where $A_i$ are the Chebychev coefficients listed below and $x = F / F_{\max}$ Method = Robust Weighting (Prince, 1982) $W = [\text{weight}] * [1 - (\Delta F / 6 * \sigma F)^2]^2$ $A_i$ are: 0.178E + 04 0.261E + 04 0.144E + 04 413.
$S = 1.01$	$(\Delta/\sigma)_{\max} = 0.001$
9826 reflections	$\Delta_{\max} = 0.97 \text{ e } \text{\AA}^{-3}$
442 parameters	$\Delta_{\min} = -1.12 \text{ e } \text{\AA}^{-3}$
0 restraints	

## 5.5 Synthesis and characterisation of phosphine-based zwitterionic complexes

### Complex 16



METAMORPhos ligand **3** (212 mg, 0.80 mmol, 1.00 eq.) and trimethylphosphine (1M toluene solution, 1.00 mL, 1.00 mmol, 1.25 eq.) were placed in a Schlenk with toluene (30 mL). In another Schlenk  $\text{Ni}(\text{COD})_2$  (2200 mg, 0.80 mmol, 1.00 eq) was dissolved in toluene (20 mL). Both solutions were cooled in an ice bath and the solution containing phosphines was added *via* a cannula to the  $\text{Ni}(\text{COD})_2$  solution at  $0^\circ\text{C}$ . The mixture was left to stir overnight. The solvent was then evaporated to give a yellowish powder.

This crude product was co-evaporated with 5 mL of pentane and washed with  $3 \times 10$  mL of pentane to give a yellow powder (isolated yield: 245 mg, 60%).  $^{31}\text{P}\{^1\text{H}\}$  NMR (121 MHz,  $\text{C}_6\text{D}_6$ , 300K):  $\delta$ (ppm): 86.8 ppm (d,  $\text{P}(\text{iPr})_2$ ,  $^2J_{\text{PP}} = 31.05$  Hz); -11.4 ppm (d,  $\text{PMe}_3$ ,  $^2J_{\text{PP}} = 31.45$  Hz).  $^{19}\text{F}$  NMR (128 MHz,  $\text{C}_6\text{D}_6$ , 300K):  $\delta$ (ppm): -78.23 (s).  $^1\text{H}$  NMR (300 MHz,  $\text{C}_6\text{D}_6$ , 300K):  $\delta$ (ppm): 0.85 (dd,  $^3J_{\text{HH}} = 7.2$  Hz,  $\text{CH}_3_{\text{iPrA}}$ , 3H); 1.22 (d,  $^2J_{\text{HP}} = 8.9$  Hz,  $\text{CH}_3_{\text{PMe}_3\text{C}_3}$ , 9H); 1.28 (dd,  $^3J_{\text{HH}} = 6.3$  Hz,  $^3J_{\text{HP}} = 16.9$  Hz,  $\text{CH}_3_{\text{iPrA}}$ , 3H); 1.35 (m,  $\text{CH}_3_{\text{iPrB}}$ , 3H); 1.52 (dd,  $^3J_{\text{HH}} = 6.7$  Hz,  $^3J_{\text{HP}} = 13.3$  Hz,  $\text{CH}_3_{\text{iPrB}}$ , 3H); 1.0-1.8 (several m,  $\text{CH}_2_{\text{COD}}$ , 10H), 2.02 (m,  $\text{CH}_{\text{iPrB}}$ , 1H); 2.91 (sept,  $^3J_{\text{HH}} = 6.7$  Hz,  $\text{CH}_{\text{iPrA}}$ , 1H); 3.64 (m,  $\text{CH}_{\text{COD allyl } \beta}$ , 1H); 4.21 (m,  $\text{CH}_{\text{COD allyl } \beta'}$ , 1H); 4.39 (m,  $\text{CH}_{\text{COD allyl } \alpha}$ , 1H);  $^{13}\text{C}$  NMR ( $\text{C}_6\text{D}_6$ ):  $\delta$ (ppm): 15.86 (d,  $^1J_{\text{CP}} = 28.6$  Hz,  $\text{CH}_3_{\text{PMe}_3\text{C}_3}$ ); 17.46 (d,  $^2J_{\text{CP}} = 4.3$  Hz,  $\text{CH}_3_{\text{iPrB}}$ ); 18.61 (d,  $^2J_{\text{CP}} = 3.6$  Hz,  $\text{CH}_3_{\text{iPrA}}$ ); 19.59 (d,  $^2J_{\text{CP}} = 2.6$  Hz,  $\text{CH}_3_{\text{iPrB}}$ ); 19.91 (d,  $^2J_{\text{CP}} = 3.9$  Hz,  $\text{CH}_3_{\text{iPrA}}$ ); 22.85 (s,  $\text{CH}_2_{\text{COD}}$ ); 27.36 (d,  $J_{\text{CP}} = 4.6$  Hz,  $\text{CH}_2_{\text{COD}}$ ); 28.11 (d,  $J_{\text{CP}} = 3.4$  Hz,  $\text{CH}_2_{\text{COD}}$ ); 30.56 ( $\text{CH}_2_{\text{COD}}$ ); 31.00 ( $\text{CH}_2_{\text{COD}}$ ); 31.18 (d,  $^2J_{\text{CP}} = 22.1$  Hz,  $\text{CH}_{\text{iPrA}}$ ); 32.4 (d,  $^2J_{\text{CP}} = 22.0$  Hz,  $\text{CH}_{\text{iPrB}}$ ); 73.68 (dd,  $^2J_{\text{CP}} = 7.5$  &  $^2J_{\text{CP}} = 17.6$  Hz,  $\text{CH}_{\text{COD allyl } \beta}$ ); 75.90 (dd,  $^2J_{\text{CP}} = 3.9$  &  $^2J_{\text{CP}} = 20.2$  Hz,  $\text{CH}_{\text{COD allyl } \beta'}$ ); 109.98 ( $\text{CH}_{\text{COD allyl } \alpha}$ ); 121.92 (q,  $^1J_{\text{CF}} = 323.2$  Hz,  $\text{C}^{\text{IV}}_{\text{CF}_3}$ ). EA found (th): C 42.39 (42.54); H: 7.26 (7.14); N: 2.68 (2.76). Crystals suitable for X-ray diffraction are gotten from slow pentane diffusion in a toluene solution of the compound.

#### Crystal data

$\text{C}_{18}\text{H}_{36}\text{F}_3\text{NNiO}_2\text{P}_2\text{S}$	$F(000) = 1072$
$M_r = 508.21$	$D_x = 1.425 \text{ Mg m}^{-3}$
Monoclinic, $P2_1/n$	Mo $K\alpha$ radiation, $\lambda = 0.7107 \text{ \AA}$
Hall symbol: -P 2yn	Cell parameters from 18745 reflections
$a = 12.2161 (5) \text{ \AA}$	$\theta = 4.2\text{--}29.3^\circ$

$b = 15.2866$ (7) Å	$\mu = 1.08$ mm <sup>-1</sup>
$c = 12.7410$ (5) Å	$T = 150$ K
$\beta = 95.353$ (4)°	Block, yellow
$V = 2368.91$ (17) Å <sup>3</sup>	$0.38 \times 0.31 \times 0.28$ mm
$Z = 4$	

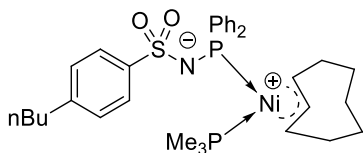
## Data collection

Xcalibur, Atlas, Gemini ultra diffractometer	6233 independent reflections
Radiation source: Enhance (Mo) X-ray Source	5551 reflections with $I > 2.0\sigma(I)$
graphite	$R_{\text{int}} = 0.046$
Detector resolution: 10.4678 pixels mm <sup>-1</sup>	$\theta_{\text{max}} = 29.7^\circ$ , $\theta_{\text{min}} = 3.1^\circ$
$\omega$ scans	$h = -16 \rightarrow 16$
Absorption correction: analytical <i>CrysAlis PRO</i> , Agilent Technologies, Version 1.171.36.28 (release 01-02-2013 CrysAlis171.NET) (compiled Feb 1 2013, 16:14:44) Analytical numeric absorption correction using a multifaceted crystal model based on expressions derived by R.C. Clark & J.S. Reid. (Clark, R. C. & Reid, J. S. (1995). <i>Acta Cryst. A</i> 51, 887-897)	$k = -21 \rightarrow 20$
$T_{\text{min}} = 0.752$ , $T_{\text{max}} = 0.800$	$l = -17 \rightarrow 17$
43569 measured reflections	

## Refinement

Refinement on $F^2$	Primary atom site location: structure-invariant direct methods
Least-squares matrix: full	Hydrogen site location: difference Fourier map
$R[F^2 > 2\sigma(F^2)] = 0.033$	H-atom parameters constrained
$wR(F^2) = 0.070$	Method, part 1, Chebyshev polynomial, (Watkin, 1994, <i>Prince</i> , 1982) [weight] = $1.0/[A_0 * T_0(x) + A_1 * T_1(x) + \dots + A_{n-1} * T_{n-1}(x)]$ where $A_i$ are the Chebyshev coefficients listed below and $x = F / F_{\text{max}}$ Method = Robust Weighting ( <i>Prince</i> , 1982) $W = [\text{weight}] * [1 - (\Delta F / 6 * \sigma F)^2]^2$ $A_i$ are: 300. 454. 232. 62.0
$S = 0.98$	$(\Delta/\sigma)_{\text{max}} = 0.001$
6220 reflections	$\Delta_{\text{max}} = 1.89 \text{ e } \text{Å}^{-3}$
253 parameters	$\Delta_{\text{min}} = -0.51 \text{ e } \text{Å}^{-3}$
0 restraints	

## Complex 17



METAMORPhos ligand **4** (390 mg, 1.00 mmol, 1.00 eq.) and trimethylphosphine (1 M toluene solution, 1.00 mL, 1.00 mmol, 1.00 eq.) were placed in a Schlenk with toluene (30 mL). In another Schlenk Ni(COD)<sub>2</sub> (270 mg, 1.00 mmol, 1.00 eq) was dissolved in toluene (20 mL). Both solutions were cooled in an ice bath and the

phosphine solution was added *via* a cannula to the Ni(COD)<sub>2</sub> solution at 0°C. After addition, the mixture was slowly brought to RT, stirred for 20 min and heated to 60°C for 1h to give a brownish mixture. The solvent was evaporated to give an orange powder (isolate yield: 39%). <sup>31</sup>P{<sup>1</sup>H} NMR (121 MHz, C<sub>6</sub>D<sub>6</sub>, 300K):  $\delta$ (ppm): 60.25 (d, <sup>2</sup>J<sub>PP-cis</sub> = 26.7 Hz); -0.11 (d, <sup>2</sup>J<sub>PP-cis</sub> = 26.7 Hz). <sup>1</sup>H NMR (300 MHz, C<sub>6</sub>D<sub>6</sub>, 300K):  $\delta$ (ppm): 0.81 (t, <sup>3</sup>J<sub>HH</sub> = 7.1 Hz 3H, CH<sub>2</sub>-CH<sub>3</sub>);

0.945 (d,  $^2J_{HP} = 8.8$  Hz, 9H, CH<sub>3</sub> PMe<sub>3</sub>); 1.18 (m, 2H, CH<sub>2</sub>-CH<sub>3</sub>); 1.20-1.35 (m, 4H, CH<sub>2</sub> COD); 1.40 (m, 2H, CH<sub>2</sub>-CH<sub>2</sub>-CH<sub>3</sub>); 1.45-1.95 (m, 4H, CH<sub>2</sub> COD); 2.07 (m, 2H, CH<sub>2</sub> COD); 2.38 (t,  $^3J_{HH} = 7.6$  Hz, 2H, Ar-CH<sub>2</sub>-CH<sub>2</sub>); 3.81 (m, 2H, CH COD allyl β); 4.98 (t,  $^3J_{HH} = 8.7$  Hz; 1H, CH COD allyl α); 7.03 (m, 5H, CH PPh<sub>2</sub>); 7.04 (d,  $^3J_{HH} = 8.05$  Hz, CH Ar-SO<sub>2</sub>, 2H); 7.91 (dd,  $J = 7.27$  & 9.62 Hz, CH PPh<sub>2</sub>, 5H); 8.47 (d,  $^3J_{HH} = 8.12$  Hz, CH Ar-SO<sub>2</sub>, 2H). <sup>13</sup>C NMR (75 MHz, C<sub>6</sub>D<sub>6</sub>, 300K): δ(ppm): 14.12 (CH<sub>2</sub>-CH<sub>3</sub>); 16.23 (dd,  $^1J_{CP} = 26.4$  Hz &  $^3J_{CP} = 1.6$  Hz, P-CH<sub>3</sub>, 3C); 22.57 (CH<sub>2</sub>-CH<sub>3</sub>); 23.46 (CH<sub>2</sub> COD); 27.71 (CH<sub>2</sub> COD); 27.94 (CH<sub>2</sub> COD); 29.48 (CH<sub>2</sub> COD); 31.06 (CH<sub>2</sub> COD); 33.69 (CH<sub>2</sub>-CH<sub>2</sub>-CH<sub>3</sub>); 35.70 (Ar-CH<sub>2</sub>); 76.73 (d,  $^2J_{CP} = 20$  Hz, CH COD allyl β) 81.67 (d,  $^2J_{CP} = 19$  Hz, CH COD allyl β); 109.57 (CH COD allyl α); 126.63 (CH Ar-SO<sub>2</sub>, 2C); 128.01 (d,  $^3J_{CP} = 8.6$  Hz, CH PPh<sub>2</sub> meta, 4C); 128.29 (CH Ar-SO<sub>2</sub>, 2C); 128.59 (CH PPh<sub>2</sub> para); 129.38 (CH PPh<sub>2</sub> para); 130.83 (d,  $^2J_{CP} = 43.8$  Hz, CH PPh<sub>2</sub> ortho, 2C); 130.99 (d,  $^2J_{CP} = 44.3$  Hz, CH PPh<sub>2</sub> ortho, 2C); 143.97 (d,  $^1J_{CP} = 118$  Hz, C<sup>IV</sup> PPh<sub>2</sub> ipso); 144.29 (C<sup>IV</sup> C-nBu); 144.64 (d,  $^1J_{CP} = 117$  Hz, C<sup>IV</sup> PPh<sub>2</sub> ipso); 147.38 (d,  $^3J_{CP} = 4.2$  Hz, C<sup>IV</sup> C-SO<sub>2</sub>). EA found (th): C 61.67 (61.69); H: 6.87 (7.08); N: 2.27 (2.19). Crystals suitable for diffraction were obtained from slow vapour diffusion of pentane in a toluene solution of the complex.

## Crystal data

2(C <sub>33</sub> H <sub>45</sub> NNiO <sub>2</sub> P <sub>2</sub> S)·C <sub>5</sub> H <sub>12</sub>	Z = 1
$M_r = 1352.95$	$F(000) = 722$
Triclinic, $P\bar{1}$	$D_x = 1.286$ Mg m <sup>-3</sup>
Hall symbol: -P 1	Mo K $\alpha$ radiation, $\lambda = 0.7107$ Å
$a = 8.6911$ (7) Å	Cell parameters from 13849 reflections
$b = 10.7717$ (7) Å	$\theta = 3.4\text{--}29.2^\circ$
$c = 18.951$ (1) Å	$\mu = 0.74$ mm <sup>-1</sup>
$\alpha = 92.304$ (5)°	$T = 150$ K
$\beta = 95.894$ (6)°	Block, yellow
$\gamma = 97.395$ (6)°	$0.47 \times 0.22 \times 0.16$ mm
$V = 1747.5$ (2) Å <sup>3</sup>	

## Data collection

Xcalibur, Atlas, Gemini ultra diffractometer	8989 independent reflections
Radiation source: Enhance (Mo) X-ray Source	6924 reflections with $I > 2.0\sigma(I)$
graphite	$R_{int} = 0.071$
Detector resolution: 10.4685 pixels mm <sup>-1</sup>	$\theta_{max} = 29.7^\circ$ , $\theta_{min} = 2.8^\circ$
$\omega$ scans	$h = -12 \rightarrow 11$
Absorption correction: analytical CrysAlis PRO, Agilent Technologies, Version 1.171.36.28 (release 01-02-2013 CrysAlis171.NET) (compiled Feb 1 2013, 16:14:44) Analytical numeric absorption correction using a multifaceted crystal, model based on expressions derived by R.C. Clark & J.S. Reid. (Clark, R. C. & Reid, J. S. (1995). Acta Cryst. A51, 887-897)	$k = -14 \rightarrow 14$
$T_{min} = 0.781$ , $T_{max} = 0.909$	$l = -25 \rightarrow 25$
47377 measured reflections	

## Refinement

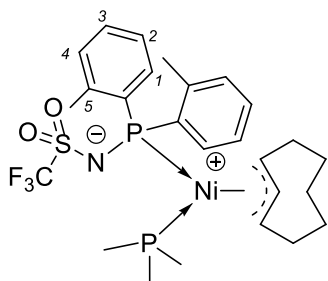
Refinement on $F^2$	Primary atom site location: structure-invariant direct methods
Least-squares matrix: full	Hydrogen site location: difference Fourier map
$R[F^2 > 2\sigma(F^2)] = 0.065$	H atoms treated by a mixture of independent and constrained refinement
$wR(F^2) = 0.138$	Method, part 1, Chebyshev polynomial, (Watkin, 1994, Prince, 1982) [weight] = $1.0/[A_0 * T_0(x) + A_1 * T_1(x) + \dots + A_{n-1} * T_{n-1}(x)]$ where $A_i$ are the Chebyshev coefficients listed below and $x = F / F_{max}$ Method = Robust Weighting (Prince, 1982) $W = [\text{weight}] * [1 - (\Delta F / 6 * \sigma F)^2]^2$ $A_i$ are: 0.145E + 04 0.214E + 04 0.114E + 04 306.
$S = 0.99$	$(\Delta/\sigma)_{max} = 0.013$
8971 reflections	$\Delta_{max} = 1.80 \text{ e } \text{Å}^{-3}$
397 parameters	$\Delta_{min} = -1.03 \text{ e } \text{Å}^{-3}$
32 restraints	

Symmetry code: (i)  $-x+1, -y, -z+1$ .Hydrogen-bond geometry ( $\text{Å}, ^\circ$ )

$D-H \cdots A$	$D-H$	$H \cdots A$	$D \cdots A$	$D-H \cdots A$
$C20-H201 \cdots O6^{\text{ii}}$	0.93	2.51	3.386 (8)	156 (1)

Symmetry code: (ii)  $x, y+1, z$ .

## Complex 18



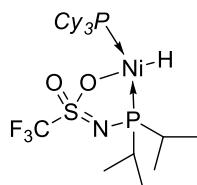
A mixture of solid METAMORPhos (o-tolyl) **5** (463 mg, 1.00 mmol, 1.00 eq.), Ni(COD)<sub>2</sub> (275 mg, 1.00 mmol, 1.00 eq.) was dissolved in chlorobenzene (20 mL). To this solution was rapidly added trimethylphosphine (1M in toluene, 1.00 mL, 1.00 mmol, 1.00 eq.). The mixture was left to stir for 15 min, leading to a very dark solution. The solvent was removed under reduced pressure leading to a dark solid. This solid was triturated in 20 mL of pentane leading to a powder and a solvent phase coloured in purple which was syringed out. This operation was repeated 5 times with 5 mL of pentane until a yellow solid was

obtained and the pentane phase was no longer purple. The powder was dried under vacuum to give a yellow solid (isolated: 320 mg, yield: 53%). <sup>31</sup>P{<sup>1</sup>H} NMR (121 MHz, C<sub>6</sub>D<sub>6</sub>, 300K):  $\delta$ (ppm): -15.10 (d, <sup>2</sup>J<sub>PP</sub> = 25.8 Hz); 54.75 (d, <sup>2</sup>J<sub>PP</sub> = 25.8 Hz); <sup>1</sup>H NMR (300 MHz, C<sub>6</sub>D<sub>6</sub>, 300K):  $\delta$ (ppm): 0.83-2.28 (signals of CH<sub>2</sub> of COD); 1.00 (d, <sup>2</sup>J<sub>HP</sub> = 8.5 Hz, CH<sub>3</sub> PMe<sub>3</sub>, 9H); 1.76 (s, CH<sub>3</sub> tolyl, 3H); 2.48 (s, CH<sub>3</sub> tolyl, 3H); 3.54 (qd, <sup>3</sup>J<sub>HH</sub> = 8.5 Hz & <sup>2</sup>J<sub>HP</sub> = 8.5 Hz, CH<sub>2</sub> COD allyl  $\alpha$ , 1H); 3.70 (qd, <sup>3</sup>J<sub>HH</sub> = 8.5 Hz & <sup>2</sup>J<sub>HP</sub> = 8.5 Hz, CH<sub>2</sub> COD allyl  $\beta$ , 1H); 4.78 (t, <sup>3</sup>J<sub>HH</sub> = 8.5 Hz, CH<sub>2</sub> COD allyl  $\alpha$ , 1H); 6.64-6.87 (m, CH<sub>Ar</sub> 4a,4b,3b, 3H); 6.96 (t, <sup>3</sup>J<sub>HH</sub> = 6.9 Hz, CH<sub>Ar</sub> 2b, 1H); 7.03 (t, <sup>3</sup>J<sub>HH</sub> = 7.0 Hz, CH<sub>Ar</sub> 2a, 1H); 7.25 (t, <sup>3</sup>J<sub>HH</sub> = 7.2 Hz, 1H, CH<sub>Ar</sub> 3a); 7.62 (dd, <sup>3</sup>J<sub>HH</sub> = 7.1 Hz & <sup>3</sup>J<sub>HP</sub> = 17.2 Hz, CH<sub>Ar</sub> 1a, 1H); 8.84 (d, <sup>3</sup>J<sub>HH</sub> = 7.6 Hz & <sup>3</sup>J<sub>HP</sub> = 12.0 Hz, 1H, CH<sub>Ar</sub> 1a); <sup>13</sup>C NMR (75 MHz, C<sub>6</sub>D<sub>6</sub>, 300K):  $\delta$ (ppm): 16.58 (dd, <sup>1</sup>J<sub>CP</sub> = 27.1 Hz, <sup>3</sup>J<sub>CP</sub> = 1.8 Hz, CH<sub>3</sub> PMe<sub>3</sub>, 3C); 21.15 (d, <sup>3</sup>J<sub>CP</sub> = 2.8 Hz, CH<sub>3</sub> tolyl, 1C); 22.55 (d, <sup>3</sup>J<sub>CP</sub> = 7.4 Hz, -CH<sub>3</sub> tolyl, 1C); 23.03 (s, CH<sub>2</sub> COD); 26.96 (d, <sup>2</sup>J<sub>CP</sub> = 4.6 Hz, CH<sub>2</sub> COD); 76.20 (dd, <sup>2</sup>J<sub>CP</sub> = 19.2 Hz & <sup>3</sup>J<sub>CP</sub> = 4.3 Hz, CH<sub>2</sub> COD allyl  $\alpha$ , 1H); 85.50 (d, <sup>2</sup>J<sub>CP</sub> = 17.2 Hz, CH<sub>2</sub> COD allyl  $\beta$ ); 109.67 (s, CH<sub>2</sub> COD allyl  $\alpha$ ); 121.78 (qd, <sup>1</sup>J<sub>CF</sub> = 322.2 Hz, <sup>3</sup>J<sub>CP</sub> = 6.5 Hz, C<sup>IV</sup><sub>CF3</sub>); 123.26 (d, <sup>4</sup>J<sub>CP</sub> = 16.9 Hz, CH<sub>Ar</sub> 3); 125.83 (d, <sup>4</sup>J<sub>CP</sub> = 8.4 Hz, CH<sub>Ar</sub> 3); 129.78 (s, CH<sub>Ar</sub> 2); 130.62 (CH<sub>Ar</sub> 2); 131.13 (d, <sup>3</sup>J<sub>CP</sub> = 8.8 Hz, CH<sub>Ar</sub> 4); 132.18 (d, <sup>2</sup>J<sub>CP</sub> = 6.5 Hz, CH<sub>Ar</sub> 1); 132.71 (d, <sup>3</sup>J<sub>CP</sub> = 5.8 Hz, CH<sub>Ar</sub> 4); 135.73 (d, <sup>1</sup>J<sub>PP</sub> = 50 Hz, C<sup>IV</sup><sub>ipso</sub>);

136.60 (d,  $^2J_{CP} = 37.5$  Hz, CH<sup>Ar</sup>); 137.98 (d,  $^2J_{CP} = 16.4$  Hz, C<sup>IV</sup><sub>CAR-CH3</sub>); 139.50 (d,  $^1J_{CP} = 52$  Hz, C<sup>IV</sup><sub>ipso</sub>); 143.97 (s, C<sup>IV</sup><sub>CAR-CH3</sub>). EA : C : 51.57 (51.68); H : 5.89 (6.00); N : 2.47 (2.33).

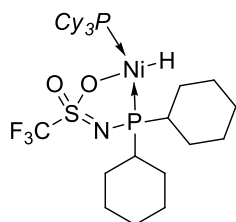
## 5.6 Synthesis and characterisation of hydride complexes 23, 26

### Complex 23



METAMORPhos ligand **3**: F<sub>3</sub>C-SO<sub>2</sub>N=P(*i*Pr)<sub>2</sub>H (796 mg, 3.00 mmol, 1.00 eq.), tricyclohexylphosphine (825 mg, 3.00 mmol, 1.00 eq.) and Ni(COD)<sub>2</sub> (840 mg, 3.00 mmol 1.00 eq.) were placed in a Schlenk and dissolved in toluene (20 mL). The mixture was stirred at 60°C for 16 h leading to an orange solution. Then the solvents were evaporated under reduced pressure to give a solid that was washed with pentane (3 x 10 mL) and dried under vacuum to give a yellow powder (isolated yield: 694 mg, yield: 38 %). Crystals suitable for diffraction were obtained from slow vapour diffusion of pentane in a toluene solution of the complex. <sup>31</sup>P NMR (121 MHz, C<sub>6</sub>D<sub>6</sub>, 300K): δ(ppm): 36.1 (dd,  $^2J_{PP} = 236$  Hz,  $^2J_{PH} = 64$  Hz); 103.4 (dd,  $^2J_{PP} = 236$  Hz,  $^2J_{PH} = 77$  Hz); <sup>1</sup>H NMR (300 MHz, C<sub>6</sub>D<sub>6</sub>, 300K): δ(ppm): -26.87 (dd,  $^2J_{PH} = 63.9$  Hz,  $^2J_{PH} = 77.9$  Hz, Ni-H, 1H); 0.50-2.50 m, signals of Cy and *i*Pr, 47 H). <sup>19</sup>F NMR (282 MHz, C<sub>6</sub>D<sub>6</sub>, 300K): δ(ppm): -76.34. E.A. (th) : C: 43.10 (50.21); H 6.00 (8.43); N 1.11 (3.66). The product holds inorganic material probably Ni(0).

### Complex 26



METAMORPhos ligand **7** (F<sub>3</sub>C-SO<sub>2</sub>N=PCy<sub>2</sub>H) (518 mg, 1.50 mmol, 1.00 eq.), tricyclohexylphosphine (420 mg, 1.50 mmol, 1.00 eq.) and Ni(COD)<sub>2</sub> (412 mg, 1.50 mmol 1.00 eq.) were placed in a Schlenk and dissolved in toluene (20 mL). The mixture was stirred and heated at 60°C for 16 h. Then the solvents were evaporated under reduced pressure to give a solid that was washed with pentane (3 x 10 mL) and dried under vacuum to give a yellow powder (isolated yield: 465 mg, yield: 45%). <sup>31</sup>P NMR (121 MHz, C<sub>6</sub>D<sub>6</sub>, 300K): δ(ppm): 36.6 (dd,  $^2J_{PP} = 236$  Hz,  $^2J_{PH} = 67$  Hz); 78.6 (dd,  $^2J_{PP} = 237$  Hz &  $^2J_{PH} = 82$  Hz); <sup>1</sup>H NMR (300 MHz, C<sub>6</sub>D<sub>6</sub>, 300K): δ(ppm): -26.91 (dd,  $^2J_{PH} = 77.4$  Hz,  $^2J_{PH} = 62.9$  Hz, Ni-H, 1H); 0.50-2.50 (m, signals of Cy, 55H); <sup>19</sup>F NMR (282 MHz, C<sub>6</sub>D<sub>6</sub>, 300K): δ(ppm): -76.21; E.A. (% th): C: 54.50 (54.40); H: 8.38 (8.25); N: 2.14 (2.05).

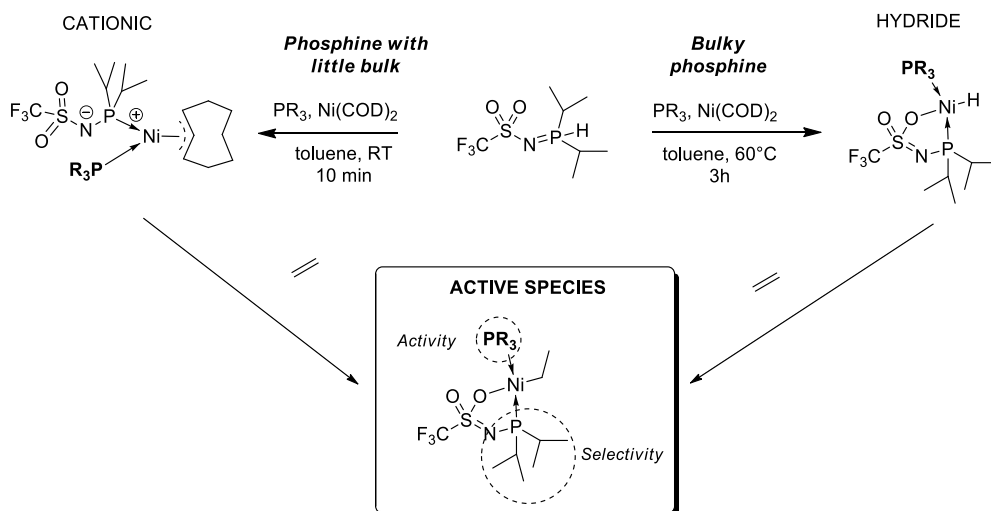
## 6 References

- [1] R. S. Bauer, H. Chung, P. W. Glockner, W. Keim, *Ethylene Oligomerization*, **1972**, U.S. Patent US3644563.
- [2] S. R. Bauer, H. Chung, P. Glockner, W. Keim, H. van Zwet, *Ethylene Polymerization*, **1972**, U.S. Patent US3635937.
- [3] S. R. Bauer, P. W. Glockner, W. Keim, R. F. Mason, *Ethylene Oligomerization*, **1972**, U.S. Patent US3647915.
- [4] R. F. Mason, *Alpha-Olefin Production*, **1972**, U.S. Patent US3686351.
- [5] W. Keim, F. H. Kowaldt, R. Goddard, C. Krüger, *Angew. Chem., Int. Ed.* **1978**, *17*, 466–467.
- [6] P. Kuhn, D. Sémeril, D. Matt, M. J. Chetcuti, P. Lutz, *Dalt. Trans.* **2007**, 515–528.
- [7] P. Kuhn, D. Sémeril, C. Jeunesse, D. Matt, M. Neuburger, A. Mota, *Chem. Eur. J.* **2006**, *12*, 5210–5219.

- [8] A. Kermagoret, P. Braunstein, *Dalt. Trans.* **2008**, 33, 822–831.
- [9] P. W. Jolly, G. Wilke, *The Organometallic Chemistry of Nickel, Volume I*, Academic Press, **1974**.
- [10] U. Müller, W. Keim, C. Krüger, P. Betz, *Angew. Chem., Int. Ed.* **1989**, 28, 1011–1013.
- [11] J. C. Jenkins, M. Brookhart, *J. Am. Chem. Soc.* **2004**, 126, 5827–5842.
- [12] D. Adhikari, M. Pink, D. J. Mindiola, *Organometallics* **2009**, 28, 2072–2077.
- [13] H.-W. Suh, L. M. Guard, N. Hazari, *Polyhedron* **2014**, 1–7.
- [14] C. J. Moulton, B. L. Shaw, *Dalt. Trans.* **1975**, 1020–1024.
- [15] B. J. Boro, E. N. Duesler, K. I. Goldberg, R. a Kemp, *Inorg. Chem.* **2009**, 48, 5081–5087.
- [16] S. Lin, M. W. Day, T. Agapie, *J. Am. Chem. Soc.* **2011**, 133, 3828–31.
- [17] R. Cariou, T. W. Graham, D. W. Stephan, *Dalt. Trans.* **2013**, 42, 4237–4239.
- [18] L. P. Bheeter, M. Henrion, L. Brelot, C. Darcel, M. J. Chetcuti, J.-B. Sortais, V. Ritleng, *Adv. Synth. Catal.* **2012**, 354, 2619–2624.
- [19] D. Vacic, W. Jones, *J. Am. Chem. Soc.* **1997**, 85, 10855–10856.
- [20] K. Jonas, G. Wilke, *Angew. Chem., Int. Ed.* **1969**, 8, 519–520.
- [21] Q. Dong, Y. Zhao, Y. Su, J.-H. Su, B. Wu, X.-J. Yang, *Inorg. Chem.* **2012**, 51, 13162–13170.
- [22] A. Miedaner, D. L. DuBois, C. J. Curtis, R. C. Haltiwanger, *Organometallics* **1993**, 12, 299–303.
- [23] M. Green, *J. Chem. Soc. A* **1971**, 152–154.
- [24] C. A. Tolman, *Chem. Rev.* **1976**, 77, 313–348.
- [25] M. Peuckert, W. Keim, *Organometallics* **1983**, 2, 594–597.
- [26] W. Keim, B. Hoffmann, R. Lodewick, M. Peuckert, G. Schmitt, J. Fleischhauer, U. Meier, *J. Mol. Catal.* **1979**, 6, 79–97.
- [27] H. Maciejewski, A. Sydor, B. Marciniak, M. Kubicki, P. B. Hitchcock, *Inorganica Chim. Acta* **2006**, 359, 2989–2997.
- [28] M. P. Lanci, D. W. Brinkley, K. L. Stone, V. V. Smirnov, J. P. Roth, *Angew. Chem., Int. Ed.* **2005**, 117, 7439–7442.
- [29] R. Mynott, A. Mollbach, G. Wilke, *J. Organomet. Chem.* **1980**, 199, 107–109.
- [30] W. Keim, A. Behr, B. Gruber, B. Hoffmann, F. H. Kowaldt, U. Kürschner, B. Limbacher, F. P. Sisti, *Organometallics* **1986**, 5, 2356–2359.
- [31] M. B. Smith, A. M. Z. Slawin, J. D. Woollins, *Polyhedron* **1996**, 15, 1579–1583.

# Chapter 6

## Zwitterionic and Nickel Hydride Complexes: Reactivity for Ethylene Oligomerisation





## 1 Introduction

In Chapters 4 and 5, we disclosed and developed a new class of single component nickel catalysts. A simple change in phosphorus substituents at the ligands of these complexes, leads to a dramatic shift in selectivity from a broad LAO distribution (comparable to SHOP) to selective 1-butene formation. Such a change in selectivity is unusual considering that a change in the chelate phosphine of the SHOP system has only little influence on the product distribution, leading in all cases to a broad (unselective) LAO distribution.<sup>[1]</sup> We wondered if the various zwitterionic nickel catalysts operate *via* one unique mechanism or *via* two different mechanisms explaining the difference in product distribution.

In order to discriminate between the two pathways, we evaluated the performances of a small set of zwitterionic cationic and related hydride complexes (from Chapter 5) as catalysts in the reaction of ethylene oligomerisation. Based on the product distribution displayed by various catalysts as well as high pressure (ethylene) NMR experiments, detailed insight was obtained on the different structural elements that are relevant for selectivity. A catalytic pathway is proposed accordingly.

## 2 Catalytic experiments with isolated complexes

The catalytic activity of the complexes **1-10** and **Ref** depicted in Figure 1 was evaluated in a 250 mL steel autoclave under an ethylene atmosphere at constant pressure (30 bars) at 40°C and 80°C for 90 minutes. The ethylene uptake was quantified by measuring the mass reduction inside the ethylene supply cylinder.

The results are presented in Table 1. An initial exothermic reaction was observed in all experiments. The mass balance for all experiments was greater than 80%. In all cases the oligomers that formed were linear alpha olefins (LAO) as shown by the 1-C<sub>4</sub> and 1-C<sub>6</sub> fractions presented in Table 1.

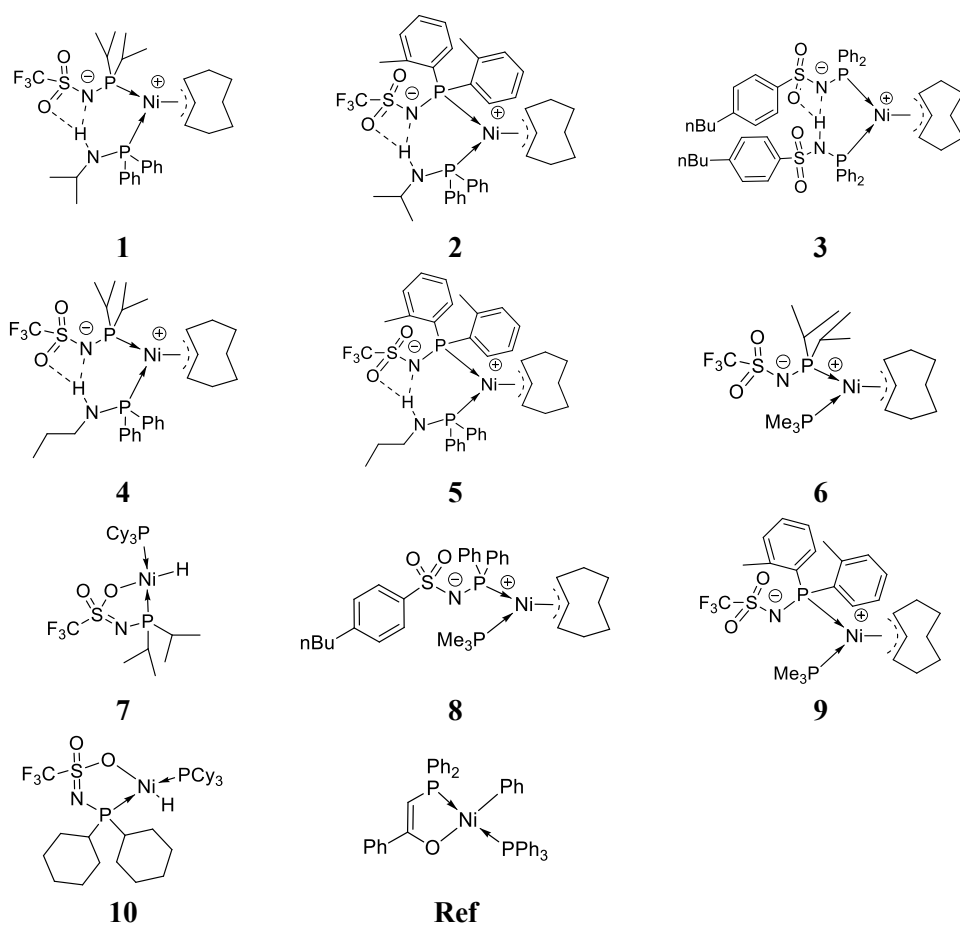


**Figure 1.** Nickel complexes evaluated in ethylene oligomerisation.

**Table 1.** Catalytic reactions for isolated complexes at 40 and 80°C

Entry	Complex	$n_{\text{Ni}}$ ( $\mu\text{mol}$ )	T	Mass of oligomers (g)	TOF <sup>[a]</sup>	Product distribution <sup>[b]</sup>			1- C <sub>4</sub> <sup>[b,c]</sup>	1- C <sub>6</sub> <sup>[b,c]</sup>	K <sub>SF</sub>
						C <sub>4</sub>	C <sub>6</sub>	C <sub>8</sub> <sup>+</sup>			
1	<b>1</b>	10	40°C	10.2	12	35	28	37	99.7	98.8	K=0.45
2	<b>2</b>	10	40°C	21.0	24	85	13	2	99.0	87.8	-
3	<b>3</b>	10	40°C	4.4	5	93	6	1	99.7	95.5	-
4	<b>3</b>	10	80°C	5.8	7	86	12	2	99.4	91.9	-
5	<b>4</b>	10	40°C	18.1	21	36	28	36	99.5	98.0	K=0.44
6	<b>5</b>	10	40°C	9.2	11	88	11	1	99.0	91.4	-
7	<b>6</b>	10	40°C	5.8	7	37	29	34	99.7	99.0	K=0.42
8	<b>7</b>	50	40°C	4.0	<1	39	27	34	99.8	99.1	K=0.43
9	<b>8</b>	50	40°C	1.7	<1	94	5	1	99.4	96.9	-
10	<b>8</b>	10	80°C	7.6	9	86	12	2	98.3	90.5	-
11	<b>9</b>	10	40°C	1.1	1	89	9	2	99.2	95.2	-
12	<b>9</b>	10	80°C	9.0	10	81	16	3	95.8	86.6	-
13	<b>10</b>	50	40°C	6.6	1	21	22	57	99.7	99.2	K=0.57
14	<b>Ref</b>	50	50°C	33.2	5	1	2	97	77.2	96.4	K=0.83

Reaction conditions: 30 bar C<sub>2</sub>H<sub>4</sub>, 40°C, solvent: toluene (55 mL), 90 min, <sup>[a]</sup> in kg<sub>oligo</sub>/(g<sub>Ni-h</sub>), calculated on the basis of the products formed within 90 min <sup>[b]</sup> determined by GC within all products formed, <sup>[c]</sup> 1-C<sub>4</sub> determined within C<sub>4</sub>, 1-C<sub>6</sub> determined within C<sub>6</sub>.

The group of supramolecular complexes **1-5** with an amino(aryl)phosphine co-ligand displayed the best activity of all the tested complexes, reaching up to 24 kg<sub>oligo</sub>/(g<sub>Ni-h</sub>) for **2**. A regular ethylene uptake was observed indicating the stability of the complex under the catalytic reaction conditions. Within this group, some differences in activity were observed. Complex **2** was twice as active as complex **1** and also had a linear ethylene uptake. In comparison, complex **3** was approximately 1/4 as active as **2** and the ethylene consumption was not linear as the uptake reached a plateau after 60-70 min (see Figure 2). This low consumption was probably due to the electron withdrawing character of the sulphonamide, which destabilised the complex and led to decomposition in solution. Complexes **4** and **5** displayed activity in the range of **1** and **2**, with **5** being twice as active as **4**.

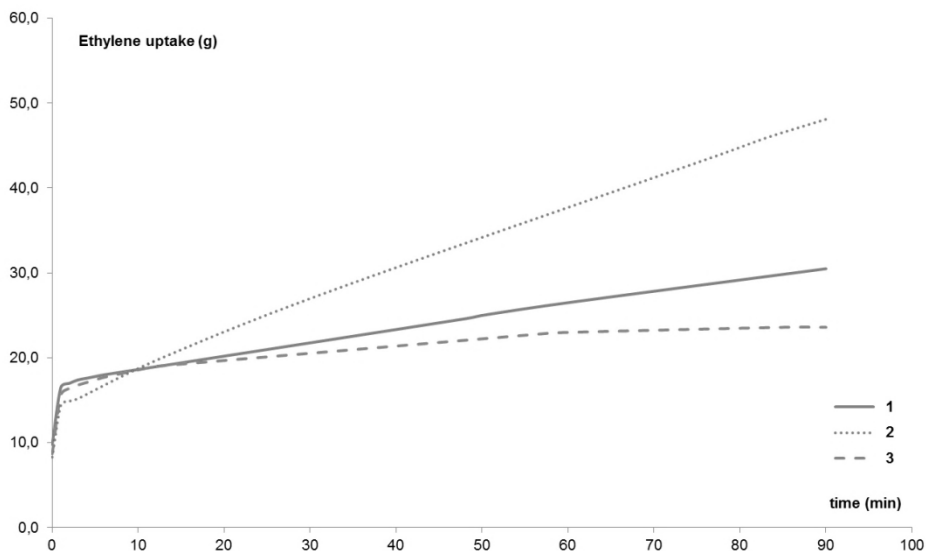


**Figure 2.** Ethylene uptake (g) in function of time for catalysts **1**, **2**, **3** at 40°C.

Although the reactions were reproducible, we observed in a series of subsequent reactions that the catalytic activities slowly increased. This tendency could be due to the deposition of small amounts of catalysts at the reactor steel surface. This phenomenon is critical for the reproducibility of catalytic oligomerisation systems and is generally addressed by the passivation of the reactor with an alkylaluminum or MAO solution prior to catalysis.<sup>[2]</sup> These activators react with traces of reactive species such as water and create a thin protective layer inside the reactor. Also performing the catalysis in a continuous reactor would most likely increase the catalytic activity (after an induction delay). For these reasons the productivity values presented here are probably underestimated.

Changing the aminophosphine co-ligand for trimethylphosphine in complexes **6**, **8**, **9** resulted in a drop of activity by a factor 2-3 compared to the analogous supramolecular complexes. The complexes **8** and **9** were almost inactive at 40°C ( $0.3 \text{ kg}_{\text{oligo}}/(\text{g}_{\text{Ni}}\cdot\text{h})$  and  $1.1 \text{ kg}_{\text{oligo}}/(\text{g}_{\text{Ni}}\cdot\text{h})$ ) but increasing the temperature to 80°C triggered their activation. This effect of temperature was particularly visible for complex **9** for which activity at 40°C was  $0.3 \text{ kg}_{\text{oligo}}/(\text{g}_{\text{Ni}}\cdot\text{h})$  while it increased to  $9 \text{ kg}_{\text{oligo}}/(\text{g}_{\text{Ni}}\cdot\text{h})$  (see the monitoring of ethylene uptake for **9** in Figure 3).

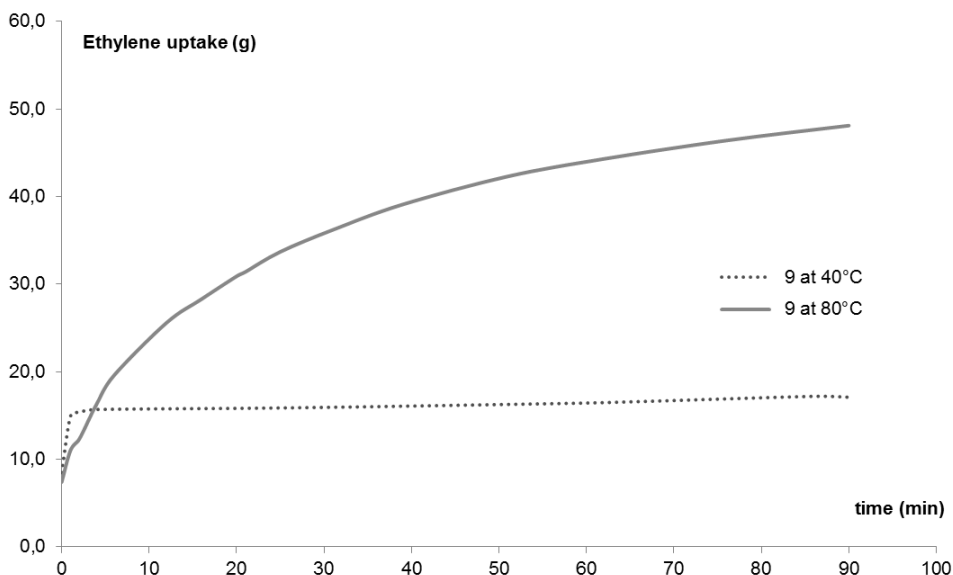


**Figure 3.** Ethylene uptake (g) as function of time for catalyst **9** at 40°C and 80°C.

At 80°C, **8** and **9** displayed similar consumption profile as **6** (around  $8 \text{ kg}_{\text{oligo}}/(\text{g}_{\text{Ni}} \cdot \text{h})$ ) which is representative for this class of  $\text{PMe}_3$  complexes and also corresponds to the activity of the complex **Ref**. Changing  $\text{PMe}_3$  for the more bulky  $\text{PCy}_3$  resulted in the nickel hydride complexes **7** and **10** (see Chapter 5), which at 40°C displayed catalytic activity similar to those of  $\text{PMe}_3$  complexes, with **10** being slightly more active than **9**. The activity of all these METAMORPhos-based complexes is higher than their carbonyl equivalent (SHOP complexes). Indeed, supramolecular catalysts **1**, **2**, **4**, **5** are more active than SHOP-type catalysts. In addition,  $\text{PMe}_3$  and  $\text{PCy}_3$  based complexes **6**, **7**, **8**, **9** and **10** produce oligomers whereas the carbonyl equivalents (SHOP-type) have been described as inactive under the same conditions.<sup>[1]</sup> This suggests that the sulphonyl group has a positive influence on the oligomerisation activity of the nickel complexes.

Regarding their selectivity in the oligomerisation reaction, the complexes can be divided into two categories: 1) selective 1-butene formation, 2) non-selective systems that form a Schulz-Flory distribution of LAO. Complexes **1**, **4**, **6**, **7**, **10** led to linear alpha olefins with a wide Schulz-Flory distribution of oligomers. Complex **1** (consisting of aminophosphine and METAMORPhos  $\text{F}_3\text{C-SO}_2\text{-N=PH}(i\text{Pr})_2$ ), produced a broad oligomer distribution ( $\text{C}_4 = 35\%$ ,  $\text{C}_6 = 28\%$ ,  $\text{C}_8^+ = 37\%$ ,  $\text{K}_{\text{SF}} = 0.45$ ). Changing the co-ligand (**4**) only slightly affect selectivity ( $\text{C}_4 = 36\%$ ,  $\text{C}_6 = 28\%$ ,  $\text{C}_8^+ = 36\%$ ,  $\text{K}_{\text{SF}} = 0.44$ ). Similarly, the selectivity was the same for a series of complexes with the same METAMORPhos and using co-ligands  $\text{PMe}_3$  (**6**) or  $\text{PCy}_3$

(7), suggesting that neither the geometry (hydride *vs.* zwitterionic) nor the co-ligand has much effect on selectivity, as long as the METAMORPhos ligand is not changed. However, a change of the METAMORPhos ligand does have a significant effect on the reaction; ethylene oligomerisation by hydride complexes **7** and **10**, which have the same PCy<sub>3</sub> co-ligand but a different METAMORPhos ligand, led to products with a significantly different Schulz-Flory constant ( $K_{SF}$  (**7**) = 0.42 *vs.*  $K_{SF}$  (**10**) = 0.57) showing that the product distribution is significantly shifted to higher molecular weight when **10** was employed as catalyst.

Complexes **2**, **3**, **5**, **8**, **9** produce very short oligomers, that consisted mostly of butenes and smaller fractions of hexenes and octenes. Supramolecular complexes **2** and **5** based on METAMORPhos F<sub>3</sub>C-SO<sub>2</sub>-NH-P(*o*-tolyl)<sub>2</sub> produced 85% and 88% of butenes respectively, of which 99% was 1-butene. Changing the aminophosphine for PMe<sub>3</sub> (**2** *vs.* **9**) did not have an effect on the selectivity at 40°C. However, the reaction carried out of heating to 80°C (entry 14) led to a sharp decrease of the butenes content as well as the alpha-selectivity. Complexes **3** and **8**, based on the same aryl METAMORPhos 4-*n*BuPh-SO<sub>2</sub>-NH-PPh<sub>2</sub>, produced high fractions of butenes (> 93%) compared to **2** and **5**. While catalyst **4** was catalytically active at 40°C, ethylene oligomerisation with **8** only proceeded upon heating the autoclave to 80°C. Increasing the temperature for **3**, **8**, **9** also led to an activity increase but a decrease in the selectivity for butenes and the alpha-selectivity. This decrease is likely caused by co-dimerisation of ethylene and 1-butene to ethyl-2-butene-1, as mentioned in Chapters 1 and 3.

## 3 Mechanistic aspects of the oligomerisation reaction

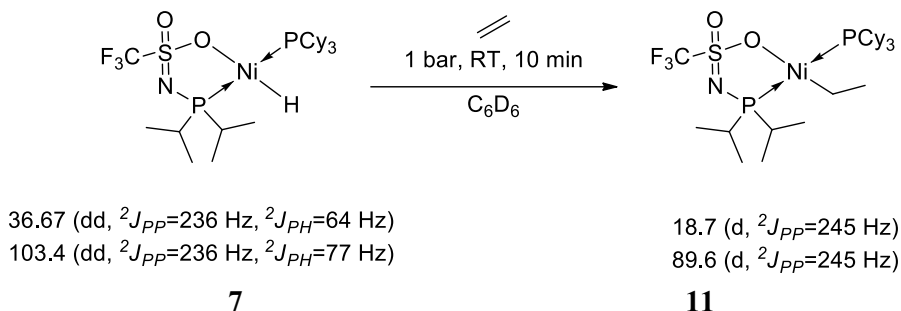
### 3.1 Reactivity of the complexes under an ethylene atmosphere

In order to understand the result of catalytic reactions at a molecular level, we determined the behaviour of the complexes under an ethylene atmosphere. The reactivity of nickel hydride and nickel zwitterionic complexes was studied. A mechanism for the ethylene oligomerisation with these new complexes is proposed on the basis of these experiments.

#### 3.1.1 Reactivity of nickel hydride complexes

Keim *et al.* demonstrated through low temperature NMR spectroscopy that the active species for ethylene oligomerisation is a nickel-hydride.<sup>[3]</sup> Based on this, we investigated by <sup>31</sup>P NMR spectroscopy the reactivity of METAMORPhos-based hydride complexes **7** and **10** with ethylene. When ethylene gas was bubbled through a solution of complex **7** (see Scheme 1), we observed within 10 min, full conversion

(see Figure 4) of **7** to a new complex that shows two resonances in the  $^{31}\text{P}$  NMR spectrum at  $\delta(\text{C}_6\text{D}_6, \text{ppm})$ : 18.7 (d,  $^2J_{\text{PP}} = 245$  Hz) and 89.6 (d,  $^2J_{\text{PP}} = 245$  Hz).



**Scheme 1.** Reaction of complex **7** in  $\text{C}_6\text{D}_6$  with ethylene to form complex **11**.

The large coupling constant  $^2J_{\text{PP}} = 245$  Hz observed for the new complex (close to that of **7**) indicates that the phosphorus atoms are in *trans* position. Moreover, the hydride signal initially observed in  $^1\text{H}$  NMR (300MHz,  $\text{C}_6\text{D}_6$ , 300K) at  $\delta(\text{ppm})$  -26.8 (dd,  $^2J_{\text{PH}} = 64$  Hz,  $^2J_{\text{PH}} = 78$  Hz), disappeared and two new signals at  $\delta(\text{C}_6\text{D}_6, \text{ppm})$ : 0.35 (br m); 0.75 (t) appeared, as depicted in Figure 5. These new signals are consistent with a Ni-CH<sub>2</sub>-CH<sub>3</sub> group according to literature, indicating that the hydride reacted with ethylene to form a nickel ethyl complex.<sup>[3-5]</sup> Upon closer inspection of the phosphorus NMR spectrum of **11**, a second doublet system with low intensity, close to the main one is observed (same coupling constants and a very similar value of chemical shifts). Interestingly 1-hexene reacted with the nickel hydride complex **7** leading to signals at  $\delta(\text{C}_6\text{D}_6, \text{ppm})$ : 18.4 (d,  $^2J_{\text{PP}}=246$  Hz); 89.8 (d,  $^2J_{\text{PP}}=246$  Hz) which are very similar to those of complex **11**. Given the relative proximity, the small doublet system signals observed in the spectrum in Figure 4(b) certainly correspond to a Ni-CH<sub>2</sub>-CH<sub>2</sub>-CH<sub>2</sub>-CH<sub>3</sub> chain.

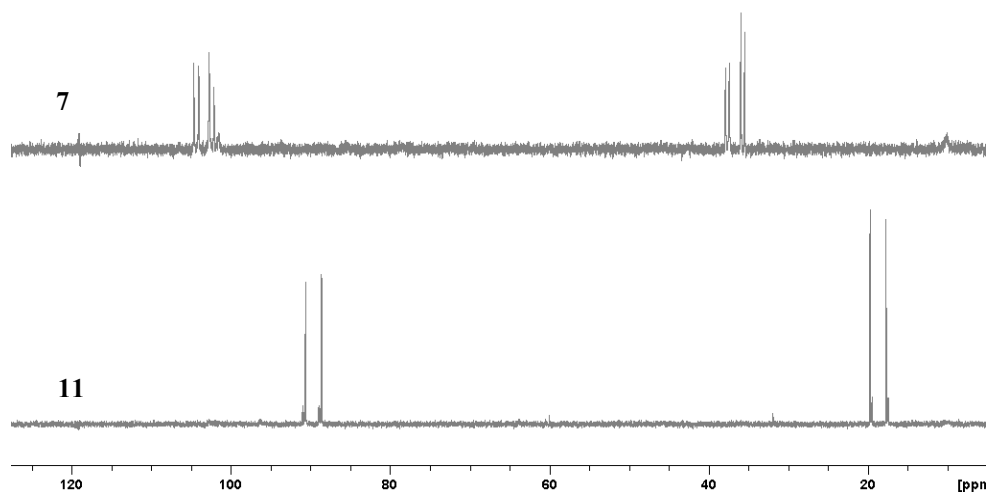


**Figure 4.**  $^{31}\text{P}$  NMR (121 MHz,  $\text{C}_6\text{D}_6$ , 300K) spectrum of complex **7** and same complex upon bubbling ethylene for 10 min at RT: **11**.

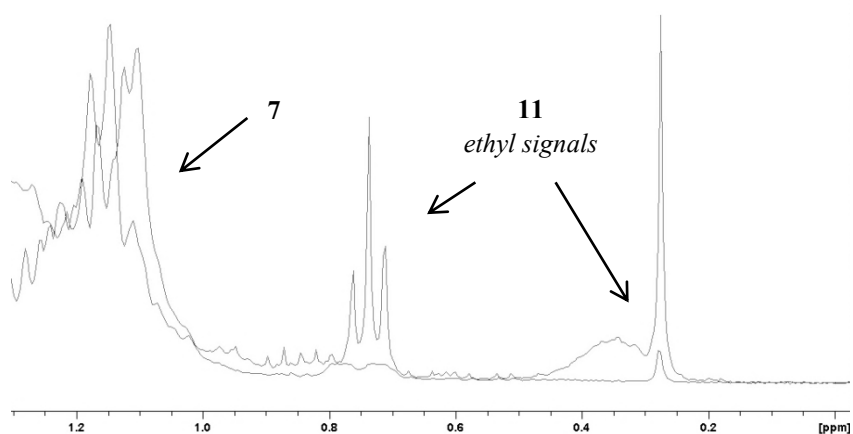


**Figure 5.**  $^1\text{H}$  NMR (300 MHz,  $\text{C}_6\text{D}_6$ , 300K) upfield part of spectrum of complex **7** and same complex upon bubbling ethylene for 10 min at RT: **11**: new signals: triplet at 0.75 ppm and broad multiplet at 0.35 ppm.

Given the significant change observed in the  $^{31}\text{P}$  NMR spectrum (as depicted in Figure 4) upon bubbling ethylene through a solution of complex **7**, which reveals the transformation of the nickel hydride to the nickel-ethyl, we thought that the chemical shift assigned to METAMORPhos phosphine of the newly formed complex could be a good system descriptor. To validate this hypothesis we gathered different complexes with the same METAMORPhos ligand and reported the corresponding  $^{31}\text{P}$  chemical shifts of METAMORPhos ligands in Table 2.



Zwitterionic complexes **1** and **6** display very close chemical shifts for  $P_{\text{MET}}$  at  $\delta(\text{C}_6\text{D}_6)$ : 85.8 ppm and 87.1 ppm respectively, showing that the nature of the co-ligand in *cis* position with respect to METAMORPhos has not much influence on the chemical shift of  $P_{\text{MET}}$ . The chemical shift difference between a zwitterionic and a nickel ethyl complex is not significant either as there is only a difference of 2.8 ppm between  $P_{\text{MET}}$  of **6** and **11**. Yet, there is a larger difference between zwitterionic and hydride complexes (difference of 16.3 ppm between **6** and **7**) and as a consequence also between nickel ethyl complexes and nickel hydride complexes. The same trend was observed upon comparing properties of the complexes **2**, **9** and **12** with different METAMORPhos ligands. The notable difference in the  $^{31}\text{P}$  NMR spectra between nickel hydride and nickel ethyl complexes could be used as a quick determination tool for the (*in situ*) identification of species in solution by  $^{31}\text{P}$  NMR spectroscopy.

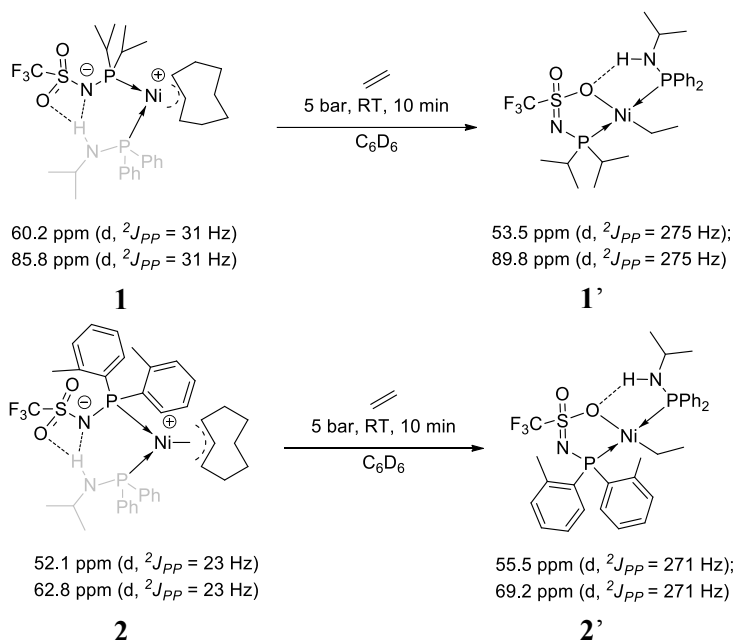
**Table 2.** Series of nickel complexes (isolated and *in situ*) based on the METAMORPhos scaffold and corresponding  $^{31}\text{P}$  NMR signal of the METAMORPhos ligand phosphines.

<b>1</b>	<b>6</b>	<b>7</b>	<b>11</b>
85.8 ppm	87.1 ppm	103.4 ppm	89.6 ppm
<b>2</b>	<b>9</b>	<b>12</b>	
52.1 ppm	54.8 ppm	63.3 ppm (tol-d <sub>8</sub> )	

### 3.1.2 Reactivity of zwitterionic nickel complexes

#### 3.1.2.1 Zwitterionic supramolecular complexes:

At room temperature and under 5 bar of ethylene pressure, we showed in Chapter 4 that the supramolecular zwitterionic complexes **1** and **2** rearranged to *trans* complexes **1'** and **2'**, with characteristic signals in the  $^{31}\text{P}$  NMR spectra. The presence of vinylcyclooctene was also observed, leading to a proposed conversion into the *trans*-(PO,P)Ni-ethyl complexes according to Scheme 2.



**Scheme 2.** Reaction of zwitterionic and supramolecular complex **1** and **2** (in solution in  $C_6D_6$ ) with ethylene to form *trans*-(PO,P)Ni-ethyl complexes **1'** and **2'**.

Interestingly, the  $^{31}P$  NMR signal of complex **1'** at 89.8 ppm fits relatively well with the signal of the *trans*-(PO,P)Ni-ethyl complex **11** ( $\delta(C_6D_6)$ : 89.6 ppm see Table 2), which suggests that **1'** adopts also the structure of a *trans*-(PO, P) chelated Ni-ethyl complex.

### 3.1.2.2 Zwitterionic $PR_3$ complexes:

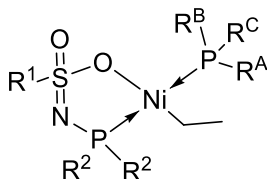
The rearrangement of zwitterionic complexes under an ethylene atmosphere is not specific to supramolecular complexes **1** and **2**, since phosphine-based complex **8** also converts to a new species according to  $^{31}P$  NMR spectroscopy. Indeed, new broad signals form at  $\delta(C_6D_6)$ : -17.8 and 89.7 ppm when this complex is reacted with ethylene, which suggests that **8** also rearranges to a *trans*-(PO,P) Ni-ethyl complex. Moreover, this transformation was also visible by the decrease in the intensity of the allylic protons of the original zwitterionic complex. After 1 h, under an ethylene atmosphere of 5 bar, the system had also formed oligomers according to NMR. This rearrangement should also be possible in other zwitterionic complexes.

We have seen that both hydride and zwitterionic complexes rearranged in presence of ethylene to a *trans*-(PO,P)Ni-ethyl complex and that this intermediate is likely the active species for ethylene oligomerisation. The very high selectivity for LAO obtained for all the catalysts described is a strong evidence for the active species

consisting of an anionic PO chelated nickel complex such as **11**. According to Jensen *et al.* this type of complexes, having an alkyl chain in *trans* position relative to the oxygen, are energetically favourable.<sup>[6]</sup> All these arguments seem to indicate that the Ni-ethyl complex **11** is the typical structure of the active species for both the zwitterionic and nickel hydride complexes described in this Chapter.

### 3.2 Mechanistic and parameter study, influence of groups

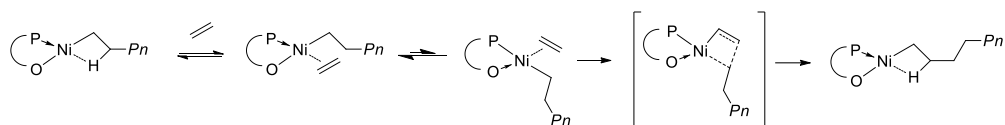
Considering that the active catalytic species was similar to the simplified structure **13** (see Figure 6), we set out to investigate the influence of each R-group to understand from which part the selectivity of this type of complexes originated and particularly to understand what governed the switch between selective and non-selective systems.



**13**

**Figure 6.** Postulated general active species for ethylene oligomerisation of METAMORPhos based complexes.

Starting from the active species **13**, two mechanisms of olefin oligomerisation can be considered: either a metallacyclic mechanism or a Cossee-Arlman mechanism (presented in Chapter 1). The first one is known to produce one olefin with high selectivity and has been largely reviewed for chromium and titanium.<sup>[7-9]</sup> However, the high linearity observed within all the oligomers fractions (1-C<sub>4</sub> in C<sub>4</sub>, 1-C<sub>6</sub> in C<sub>6</sub> and 1-C<sub>8</sub> in C<sub>8</sub>) and the fact that the starting complex must be a Ni(0) to perform oxidative coupling, excludes the metallacyclic mechanism for the current class of complexes. The very high linearity and alpha selectivity for linear olefins observed for all catalysts supports a Cossee-Arlman mechanism in which ethylene coordinates to the metal and then inserts in the metal-alkyl chain.<sup>[10-12]</sup> This mechanism was confirmed by Brookhart *et al.* who, in addition, observed by NMR spectroscopy the existence of a Ni-ethyl  $\beta$ -agostic bond in the elementary steps of chain growth.<sup>[13-16]</sup> Also computational studies on Ni diimine or PO chelated complexes established that this interaction is crucial as it facilitates the 1,2-insertion of ethylene into the Ni-C bond as shown in Scheme 3.<sup>[6,17-22]</sup>



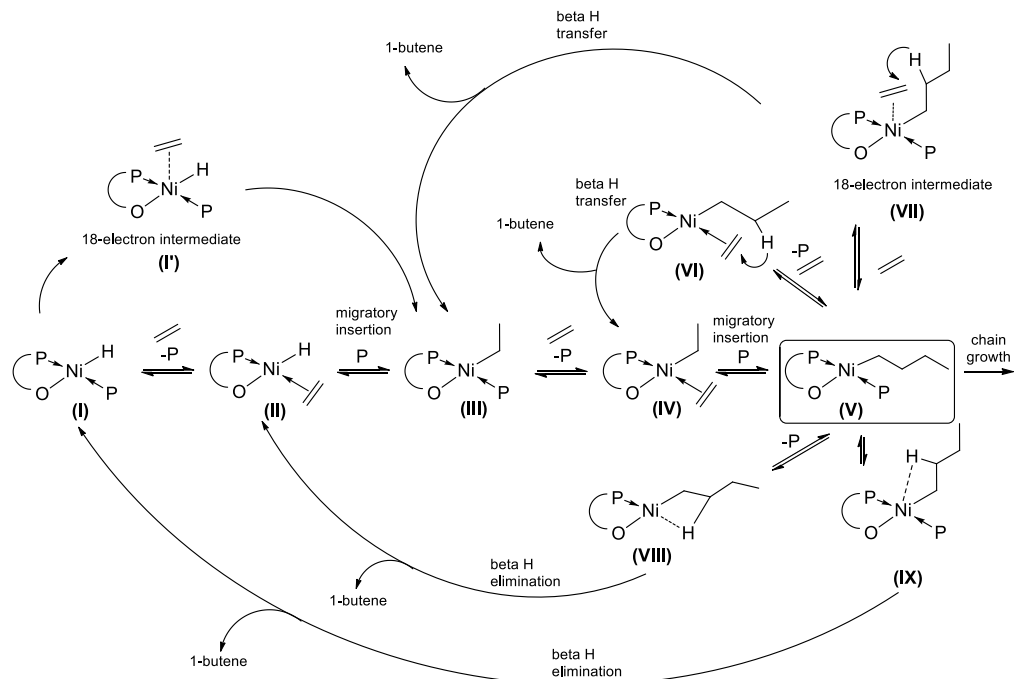
**Scheme 3.** Cossee-Arlman chain growth mechanism taking in account the Ni-ethyl  $\beta$ -agostic bond.

Based on these arguments, the METAMORPhos-based catalysts that we describe most likely follow this mechanism. We considered in this approach both  $\beta$ -H elimination and  $\beta$ -H transfer as the two possible termination steps as they are hard to distinguish experimentally. Moreover, although a dissociative pathway seems like the most obvious route for chain termination, joint kinetic and mechanistic studies by the groups of Monteiro and Matt on closely related structures, indicated that  $\beta$ -H elimination can also proceed by an associative pathway in which intermediates with 18 valence electrons would form.<sup>[23,24]</sup> A mechanism accounting for all those possible chain propagation and termination pathways with key intermediates is proposed in Scheme 4. We could experimentally confirm the first steps as the hydride intermediate (**I**) was isolated as complexes **7** and **10** with PCy<sub>3</sub>. We also confirmed the formation of intermediate (**III**) from (**I**) in the presence of ethylene by NMR studies (see **11** in Scheme 1).

The formation of intermediate (**III**) from (**I**) has often been described *via* intermediate (**II**), which is a *cis* (ethylene, hydride) nickel complex. The equilibrium between (**I**) and (**II**) depends on the concentrations of both ethylene and the co-ligand. Indeed, Keim *et al.* showed by low temperature NMR experiments (according to couplings and signals width) that the co-ligand is involved in a fast equilibrium between coordinated state and the free ligand. However, we did not observe this when hydride complex **7** was reacted with ethylene at room temperature.<sup>[25]</sup> Another possible pathway to get (**III**) from (**I**) could be through the extra coordination of ethylene to complex (**I**) leading to 18 valence electron species (**I'**). Indeed this type of coordination has already been observed in the crystal structure of a (PO,PMe<sub>3</sub>,PMe<sub>3</sub>)NiMe complex obtained by the group of Keim.<sup>[25]</sup> This shows that these two pathways can account for ethylene insertion.

Once intermediate (**III**) is formed, it can incorporate ethylene within the Ni-C bond *via* coordination / insertion until the chain terminates. Possible termination pathways include associative or dissociative  $\beta$ -H elimination or transfer that releases an olefin and regenerates the catalyst (either Ni-H or Ni-Et). From the catalytic experiments, the differences in selectivity (1-butene *vs.* broad Schulz-Flory oligomers distribution) indicates that intermediate (**V**) was discriminating between both pathways. We believe that the pathway from (**V**) is strongly dependent on the structural parameters

of the complex (electron density, steric bulk) and cannot be predicted without calculations.



**Scheme 4.** Catalytic pathway involved in 1-butene formation with (PO,P)Ni complexes

Having proposed these different possible catalytic pathways, we set out to understand the effect of each group of the generic structure **13**, on the activity and selectivity of the catalytic reaction.

### 3.2.1 Influence of the sulphonyl moiety

The sulphonyl group was not responsible for the clear change in selectivity for complexes **4** and **5** as reported in Table 1. Two complexes based on the same sulphonamide ( $F_3C-SO_2-NH_2$ ) gave (for **4**) a broad range of olefins or an excellent selectivity for 1-butene (for **5**).

Although the sulphonyl group was not the determining factor for the selectivity switch, it did increase the activity of the catalytic systems compared to the (PO) carboxyl based catalyst. The difference in activity certainly stems from a stronger ability of the sulphonamide (discussed in Chapter 2) to remove electron density from the nickel centre, which renders the nickel more electrophilic, which in turn increases the reaction rate. A similar behaviour on the effect of the sulphonyl group was noted by DuPont *et al.*. They compared complexes **14** and **15** and observed that a

sulphonate based complex (**15**) led to an increased polymerisation activity as depicted in Scheme 5.<sup>[26]</sup> The sulphonyl group does not seem to have a beneficial influence on the selectivity for short oligomers. Indeed complex **15** with a sulphonyl group produced significantly longer chains than the carbonyl complex **14**.

	<b>14</b>	<b>15</b>
TON	13900	20940
activity max.*	0.7	1.2
M <sub>w</sub> (g/mol)	4495	254356
M <sub>w</sub> /M <sub>n</sub>	4.9	106.4
* in kg <sub>C<sub>2</sub>H<sub>4</sub></sub> /(g <sub>Ni</sub> ·h) calculated from values of TON (reaction time 18h)		
Conditions 1,2,4-trichlorobenzene 10 mL, RT, 18 h, 69 bar C <sub>2</sub> H <sub>4</sub> , 10 eq. of B(C <sub>6</sub> F <sub>5</sub> ) <sub>3</sub>		

**Scheme 5.** PO chelated zwitterionic complexes, effect of the sulphonyl group reported by DuPont *et al.*<sup>[26]</sup>

### 3.2.2 Influence of the co-ligand and the H-bond on the catalyst properties

Similar to the sulphonyl group, the labile phosphine (aminophosphine or phosphine) also has a strong influence on complex activity. This is clear if complexes are compared that have the same METAMORPhos ligand. For example, complex **4** with a mildly coordinating aminophosphine produced 20.5 kg<sub>oligo</sub>/(g<sub>Ni</sub>·h). This value dropped significantly with the basic and strongly coordinating PMe<sub>3</sub> in **6** to 6.8 kg<sub>oligo</sub>/(g<sub>Ni</sub>·h), and catalyst **7** with PCy<sub>3</sub> (0.6 kg<sub>oligo</sub>/(g<sub>Ni</sub>·h)) is almost inactive. This strong influence suggests that the labile ligand is in competition with ethylene for coordination to the metal, which corresponds to the equilibria (I)-(II) and (III)-(IV) of Scheme 4. Electron-rich phosphines, which exert a strong binding to the metal, push the equilibrium to the left with (I) or (III) as the resting state, thereby preventing ethylene coordination. Less basic phosphines favour ethylene coordination, pushing the equilibrium towards (II), which can in a second step favour chain growth by migratory insertion of ethylene in the ethyl chain. These observations are in line with previous studies on PO nickel oligomerisation catalysts that established co-ligand competition with ethylene.<sup>[23,25,27]</sup> PMe<sub>3</sub> has been reported as ligand that leads to inactive systems due to strong binding.<sup>[1,28]</sup>

As we could not isolate a non H-bonded complex with similar electronic and steric properties (due to instability) we cannot draw firm conclusions about the effect of the

hydrogen bond on the catalytic performance. The H-bond is not the discriminating parameter for narrow product distributions (as non-H bonded complex **8**, **9** also produced selectively 1-butene). However, it was clear that this non-covalent interaction results in the stabilisation of the catalytic species while using mildly coordinating phosphines, giving the most reactive stable catalytic systems. The additional phosphine had little influence on the selectivity, as can be concluded from the results with complexes **1**, **4**, **6**, **7**, which are based on the same METAMORPhos ligand. In contrast, this co-ligand has a much greater effect in the case of SHOP systems as  $\text{PMe}_3$  could shift to a greater extent the oligomer distribution.<sup>[29]</sup> The rationale behind this observation is that the labile phosphine is involved in the catalytic cycle and potentially in the chain termination step as suggested by Monteiro *et al.*. A possible termination pathway involves the formation of a 18-electron species as suggested by Kuhn *et al.*, which corresponds to intermediates (**VII**) or (**IX**) of Scheme 4.<sup>[1,23]</sup>

### 3.2.3 Influence of the chelate phosphine

Complexes **1**, **4**, **6**, **7**, **10** generated oligomers with a Schulz-Flory product distribution ( $K_{\text{SF}} = 0.44$  for **1**, **4**, **6**, **7** and  $0.57$  for **10**). Although in the literature it has not been reported the Cossee mechanism ever leads to selective 1-butene formation, it is in theory possible that short product distributions, centred on 1-C<sub>4</sub>, could be obtained. The  $K_{\text{SF}}$  constants should be very small or close to zero (see Chapter 1 and experimental part).

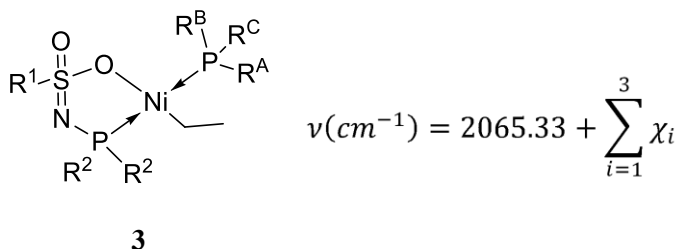
As Schulz-Flory constants could not be calculated from the C<sub>8</sub>-C<sub>16</sub> oligomers for short oligomers distributions, they were modelled on the basis of C<sub>4</sub> and C<sub>6</sub> content and the results are presented in Table 3 ( $K_{\text{SF}} = 0.04$  for **3** and **8** and  $K_{\text{SF}} = 0.08$  for **2**, **4**, **5**). It appears that the determining parameter for the selectivity is the METAMORPhos chelate as this is the only part in the complex that is different. Differences in selectivity cannot be related to phosphine bulk, as bulky phosphines **9** and **10** generated opposite values for  $K_{\text{SF}}$ .

It is very likely that the dependence on the chelate is due to electronic parameters (basicity) of the phosphine in the METAMORPhos ligand. As we did not have in hands the experimental values of Tolman electronic parameters for METAMORPhos ligand, they were estimated. For a given P(X<sub>1</sub>X<sub>2</sub>X<sub>3</sub>) phosphine the value of the electronic parameter is given by the formula in Figure 7 where  $\chi_i$  corresponds to the electronic contribution of the substituent X<sub>i</sub> (in cm<sup>-1</sup>). These substituent contributions were established from tabulated PX<sub>3</sub> phosphines by  $\chi_i = (\nu_{\text{PX}_3} - 2065.33)/3$  (See SI for more information and values). Considering the chelate phosphine in **13** the value of the electronic parameter is the following:

$$\begin{aligned}
 \nu_{\text{METAMORPhos}} &= 2065.33 + (\chi_{R^2} + \chi_{R^2} + \chi_{N=\text{SO}_2R^1}) \\
 &= 2065.33 + 2*(\nu_{P(R^2)_3})/3 + \chi_{N=\text{SO}_2R^1} \\
 &= 2065.33/3 + (2/3)(\nu_{P(R^2)_3}) + \chi_{N=\text{SO}_2R^1}
 \end{aligned}$$

$$\boxed{\nu_{\text{METAMORPhos}} = (2/3) \cdot \nu_{P(R^2)_3} + [688.44 + \chi_{N=\text{SO}_2R^1}]}$$

Neglecting the influence of  $R^1$ , the contribution of substituent  $\chi_{N=\text{SO}_2R^1}$  can be considered as constant for all METAMORPhos ligands. This leads to a linear relation between the electronic parameter of METAMORPhos and the electronic parameter of the corresponding  $P(R^2)_3$  phosphine.

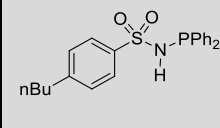
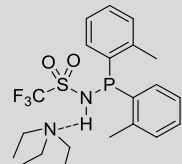
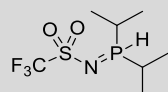
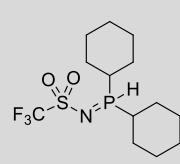


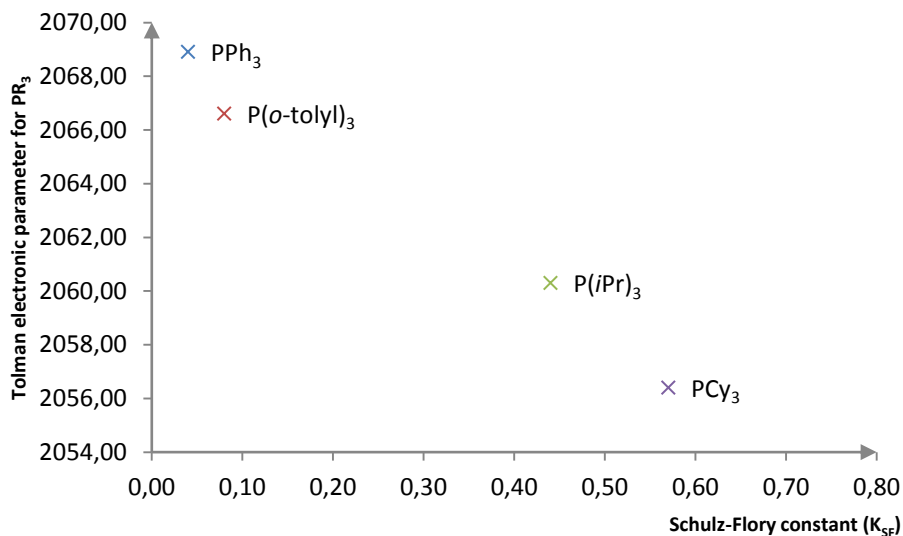
**Figure 7.** Calculation of the electronic parameter  $\nu_{\text{METAMORPhos}}$  for METAMORPhos ligand in the proposed active species.

There is another interesting relation between the basicity of the related  $P(R^2)_3$  phosphines with the Schulz-Flory constant ( $K_{\text{SF}}$ ) as is clear from Figure 8. The Tolman electronic parameter for the phosphines correlates with the value of  $K_{\text{SF}}$ . Less electron donating phosphines lead to very low values of  $K_{\text{SF}}$  (corresponding to selective systems). Indeed a good linear fit, given by the equation:  $\nu_{\text{CO } P(R^2)_3} = -21,626 K_{\text{SF}} + 2069,2$  ( $R^2 = 0,98$ ) is obtained showing that the phosphine basicity is the main ligand parameter that determines the selectivity. Provided that the relation is linear within  $K_{\text{SF}}$  [0-1], the best selectivity should be reached, in theory, for a  $P(R^2)_3$  phosphine with  $\nu_{\text{CO}} = 2069.2 \text{ cm}^{-1}$  which correspond to  $\text{PPh}_3$ . We argue that other phosphines with weaker electron donating abilities ( $\nu_{\text{CO}} > 2060 \text{ cm}^{-1}$  such as:  $\text{P}(\text{CH}=\text{CH}_2)_3$ ,  $\text{P}(p\text{-F-C}_6\text{H}_4)_3$ ,  $\text{P}(p\text{-Cl-C}_6\text{H}_4)_3$ ,  $\text{P}(m\text{-Cl-C}_6\text{H}_4)_3$ ,  $\text{P}(\text{CH}_2\text{-CH}_2\text{-CN})_3$  or even phosphites?) should outperform  $\text{PPh}_3$ , (for accessible METAMORPhos see Chapter 2).



**Table 3.** Values of Schulz-Flory constants, based on the oligomers distribution from the oligomerisation of ethylene with complexes **1**, **2**, **3**, **4**, **5**, **6**, **7**, **8**, **9** and **10**.

Ligand				
Complexes	<b>3, 8</b>	<b>2, 5, 9</b>	<b>1, 4, 6, 7</b>	<b>10</b>
Mean $K_{SF}$	0.04	0.08	0.44	0.57
$\nu_{CO}$ ( $\text{cm}^{-1}$ ) for $\text{PR}_3$	2068.9	2066.6	2060.3	2056.4

**Figure 8.** Correlation between Tolman electronic parameter for  $\text{Ni}(\text{CO})_3\text{PR}_3$  (phosphine basicity of  $\text{P}(\text{R}^2)_3$ ) and the Schulz-Flory constant ( $K_{SF}$ ) presented in Table 3.

These results show that the METAMORPhos chelate and the basicity of its phosphine are the main parameters determining the selectivity of the ethylene oligomerisation reaction. This linear relation strongly supports that there is only one mechanism that leads to a broad oligomers distribution and in optimised cases to selective 1-butene formation.

The very low degree of branching observed with our catalysts is fairly comparable to SHOP type catalysts, which can also display linearity up to 99%.<sup>[27]</sup> Recent calculations on SHOP systems showed that the easiest termination pathway is the

stepwise beta-hydrogen transfer through an axial agostic interaction (intermediates **(VI)** and **(VII)** of Scheme 4) and not *via* beta-H elimination (intermediates **(VIII)** and **(IX)** of Scheme 4).<sup>[6,21]</sup> Also, the branching is prevented by a strong difference of the  $\sigma$  donating capacity of the two P and O atoms, which disfavours hydride formation, the complex that is responsible of branching and isomerisation. Moreover, we expect that the energy barrier between propagation and termination (possibly modelled by the Gibbs free energy difference) would be close to zero, a typical feature of oligomerisation systems producing short oligomers. Further insight in the detailed mechanism should come from molecular modelling.

We speculate that the the very high selectivity for short oligomers obtained with METAMORPhos-based systems (compared to the SHOP system), originates from the electronics of the N-P bond. Surprisingly, SHOP type complexes with O-C=N-P chelates received less attention than the O-C=C-P chelates. Two literature references by Keim *et al.* propose the synthesis of **16** and claim “catalytic activity” of this class of complexes with no further detail on selectivity.<sup>[30,31]</sup> However, more recently Peulecke *et al.* described the catalytic system based on **17 (a)** in combination with Ni(COD)<sub>2</sub>, which at 100°C and 50 bar of C<sub>2</sub>H<sub>4</sub> produced predominantly 1-butene and a smaller quantity of linear hexenes and octenes (75% 1-C<sub>4</sub><sup>-</sup>, 20 % C<sub>6</sub><sup>-</sup>, 5% C<sub>8</sub><sup>-</sup>, activity of 2.9 kg<sub>C<sub>2</sub>H<sub>4</sub></sub>/(g<sub>Ni</sub>.h). In comparison, the system based on **17 (b)** + Ni(COD)<sub>2</sub> was more active, affording mainly branched hexenes, probably due to co-dimerisation.<sup>[32]</sup> We argue that these systems rearranged to O-C=N-P chelates and that such rearrangement is responsible for the high selectivity for short olefins when used in combination with aryl substituents.

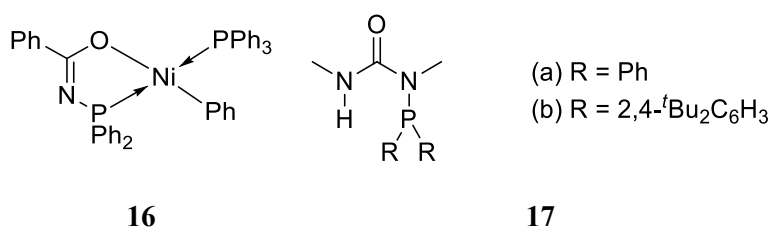


**Figure 9.** Examples of PNCO-based chelated nickel complexes from literature.<sup>[30–32]</sup>

## 4 Extension to *in situ* catalyst screening: preliminary results.

*In situ* formation of catalyst prior to the catalytic reactions can yield a significant amount of information in a short period of time because isolation of the catalytic species and product is no longer necessary. This strategy has already been employed for rapid screening of ligands in nickel catalysed oligomerisation of ethylene.<sup>[33]</sup> As

the zwitterionic complexes formed quickly and quantitatively in solution, according to NMR spectroscopy, this approach is also applicable for the METAMORPhos based complexes. The catalysts were preformed *ex situ* in Schlenks and after the incubation time to reach quantitative complex formation, the crude mixtures were injected in the reactor (see Table 4).

Catalysts **3** and **8** were selected for their ability to generate 1-butene with high selectivity. For these reactions the catalyst loading was increased (20 or 100  $\mu\text{mol}$ ). The formation of catalyst **3** *in situ* was carried out in a 4 mM solution of toluene and complete after 30 min at 45°C, while **8** was formed in toluene at room temperature after 10 min. The catalytic reactions were performed in similar conditions complexes **3** (at 40°C) and **8** (at 80°C). Complex **3** formed *in situ*, was as selective as the isolated catalyst with, however, reduced activity. Surprisingly, at a loading of 100  $\mu\text{mol}$  the activity dropped to 2.6  $\text{kg}_{\text{oligo}}/(\text{g}_{\text{Ni}}\cdot\text{h})$  though the alpha selectivity remained above 99%. The activity of complex **8** was lowered by a factor of 5 when catalyst was formed *in situ* and the alpha selectivity dropped from 98.3 to 95.0 %. These observations could be explained by the presence of a limitation on the diffusion of ethylene into the solution that was not a limiting factor for the lower catalyst loading with the isolated catalyst. Alternatively, the 1,5-COD (or 1,3-COD) present in the catalytic mixture and originating from  $\text{Ni}(\text{COD})_2$  may have interfered with the active species. Also high temperatures generally lead to less reproducible results, as a result of catalyst decomposition.

**Table 4.** Catalytic oligomerisation of ethylene with complexes **3** and **8** formed *in situ*

Complex	Loading ( $\mu\text{mol}$ )	Temperature	mass of oligomers (g)	Productivity <sup>[a]</sup>	Product distribution <sup>[b]</sup>			1-C <sub>4</sub> <sup>[b]</sup>	1-C <sub>6</sub> <sup>[b]</sup>
					C <sub>4</sub>	C <sub>6</sub>	C <sub>8</sub> <sup>+</sup>		
<b>3</b>	10	40°C	4.4	5.0	93	6	1	99.7	95.5
<b>3</b> <i>in situ</i>	20	40°C	7.6	4.3	92	7	1	99.6	93.6
<b>3</b> <i>in situ</i> <sup>[c]</sup>	100	40°C	22.5	2.6	94	6	0	99.2	86.7
<b>8</b>	10	80°C	7.6	8.6	86	12	2	98.3	90.5
<b>8</b> <i>in situ</i>	20	80°C	3.3	1.9	91	8	1	95.0	89.0

Reaction conditions : 30 bar C<sub>2</sub>H<sub>4</sub>, 40-80°C, solvent : toluene (55 mL), 90 min, <sup>[a]</sup> productivity in  $\text{kg}_{\text{oligo}}/(\text{g}_{\text{Ni}}\cdot\text{h})$ , <sup>[b]</sup> determined by GC, <sup>[c]</sup> Reaction started at 30°C to avoid exotherm.

## 5 Conclusion

The evaluation of a larger and diverse set of zwitterionic and nickel hydride complexes have been explored in the ethylene oligomerisation reaction. These complexes gave catalytically active systems producing LAO with a Schulz-Flory

type product distribution with activity up to  $24 \text{ kg}_{\text{oligo}}/(\text{g}_{\text{Ni}}\cdot\text{h})$ . The single-component complexes react with ethylene to form a *trans*-(PO,P) nickel-ethyl complex, when starting from a nickel hydride or a zwitterionic nickel complex. This species probably corresponds to the active species in ethylene oligomerisation.

The difference in catalytic properties, allowed to determine a clear relation between the catalyst structure and their performances. The chelate phosphine of the METAMORPhos has a strong influence on the selectivity of the reaction: strongly donating alkylphosphines produced large Schulz-Flory distributions ( $K_{\text{SF}} = 0.44$  or  $0.57$ ) while less donating aryl phosphines led to selective systems for 1-butene production ( $K_{\text{SF}} = 0.04$  or  $0.08$ ). Moreover there was a linear correlation between the basicity of this phosphine and the Schulz-Flory constant, which suggests that all these new class of catalysts produce LAO *via* the same mechanism.

The co-ligands have no influence on the selectivity of the catalytic reaction. However, they affect the catalytic activity. Electron rich co-ligands ( $\text{PMe}_3$  or  $\text{PCy}_3$ ) led to poorly active systems due to strong binding to the metal, preventing ethylene coordination. Aryl P-substituted aminophosphine ligands, that are weaker coordinating, lead to very active systems that outperform SHOP catalysts. Furthermore, the hydrogen bond between the two moieties in the supramolecular complexes increases the stability of the complexes. Especially arylphosphine-based co-ligands which could be isolated and which constitute the most active complexes in this study demonstrated to give active and stable catalysts.

The possibility to break down a complex catalytic system into smaller elemental contributions constitutes a major contribution to the comprehension of ethylene oligomerisation systems. Until now, with PO chelated complexes, it was only possible to increase the 1-butene fraction by using strongly coordinating phosphines ( $\text{PMe}_3$ ,  $\text{PEt}_3$ ), which consequently also decreased the catalytic activity.<sup>[1]</sup> The catalytic system based on supramolecular ligands that we describe has advantageously separated contributions: the chelate rules the selectivity while the labile phosphine is responsible for high activity. This system offers the possibility to construct tailor-made catalysts for the selective production of olefins.

## 6 Experimental part

### 6.1 General

The benchmark complex **Ref** was prepared according to known literature procedure and NMR analysis was in accordance with literature.<sup>[34]</sup> Toluene from the SPS (Solvent Purification System MBraun) was used. NMR solvents were degassed by freeze-pump-thaw cycling under argon and stored over activated 3 Å molecular sieves. NMR spectra ( $^1\text{H}$ ,  $^{31}\text{P}\{^1\text{H}\}$ ) were measured on a BRUKER 300 MHz spectrometer. Analyses of liquid phases were performed on a GC Agilent 6850 Series II equipped with a PONA column. The gas phase for ethylene oligomerisation were analysed by gas GC on HP 6890.

### 6.2 High pressure ethylene NMR experiments

For NMR experiments, ca. 20 mg of complex were charged in a high pressure NMR tube in the glove box under argon and dissolved in 0.6 mL of dry, degassed  $\text{C}_6\text{D}_6$ . The tube was closed and connected outside of the glove box to ethylene supply by the screw cap. The ethylene pressure was set at 5 bars and the line was purged 5 times (vacuum / ethylene) to get rid of residual oxygen. Then the screw cap was opened to pressurise the tube, which was then closed, disconnected and vigorously shaken. All these operation were repeated twice to ensure saturation of ethylene in the tube.

### 6.3 Procedure for the oligomerisation of ethylene

The reactor of 250 mL was dried under vacuum at 100°C for 2 hours and then pressurised to 5 bar of ethylene. The ethylene supply was closed and the reactor was cooled down at room temperature. Ethylene inside the reactor was evacuated, maintaining however a slight over pressure inside the reactor (0.4 bar). The solvent used for catalysis (toluene, 50 mL) was injected and then heated to 40°C (or 50°C) under magnetic stirring (1000 rpm). When the temperature inside the reactor was stabilised, stirring was stopped and the catalyst solution (10 or 50  $\mu\text{mol}$  in toluene: 5 mL) was injected. Then the reactor was pressurised to 30 bar of ethylene and the pressure maintained by connection to a an ethylene supply cylinder (80 bar) positioned on a balance (semi-batch). The reaction started ( $t=0$ ) with magnetic stirring (1000 rpm) and the reaction ran for 90 min with a regular monitoring the ethylene uptake by the mass reduction of the ethylene supply cylinder. The reaction was stopped by closing the ethylene supply and cooling the reactor to 25°C (250 rpm). The gas phase was evacuated, quantified through a flowmeter and collected in a 30L plastic drum by water displacement (stirring the liquid phase to 1000 rpm was necessary to degas completely the liquid phase). The plastic drum containing the gas phase was shaken with residual water to homogenise the gas and a portion of this gas phase was collected in a glass ampulla and injected in GC. After all the gas fraction had been evacuated, stirring was stopped and the reactor was carefully opened. The liquid phase was transferred with a plastic pipette to a glass bottle cooled to 0°C (to minimise butene losses). The liquid phase was quantified by mass and a cold sample injected directly in GC.

Catalytic experiments were duplicated and carried out to have oligomers formed in sufficient quantity so the mass balance between ethylene consumption and product formation is representative.



**Figure 10.** Oligomerisation unit T095 used for this study (on the left, ethylene ballast on a balance, on the right: reactor)

#### 6.4 Determination of Schulz-Flory constant ( $K_{SF}$ )

The Schulz-Flory constant  $K_{SF}$  (also called growing factor), was calculated from the oligomers product distribution (% weight) determined by GC. For large product distributions, the value of the constant was averaged on the  $C_8$ - $C_{18}$  oligomers. The general formula is given by:

$$\log\left(\frac{\%weight\ of\ p}{p}\right) = (\log K_{SF\ p})(p - 1) + Cte$$

In which  $p$  corresponds to the number of monomer units (for ethylene  $p$  = number of carbons / 2) and  $Cte$  is a constant. In practice, the determination of the constant at the degree  $p$  is realized between  $p$  and the consecutive oligomer  $p + 1$  and it gives:

$$K_{SF(p)} = \left(\frac{\%weight\ C_{p+1}}{\%weight\ C_p}\right) \cdot \left(\frac{p}{p + 1}\right)$$

The individual  $K_{SF}$  constants between  $C_8$  and  $C_{18}$  are then averaged and correspond to the  $K_{SF}$  presented in this chapter. The value of  $K_{SF}$  is between 0 and 1. Values of  $K_{SF}$  close to 1

correspond to large product distributions centered on high molecular weight oligomers while values close to 0 correspond to short distributions and ultimately selectivity for  $C_4$  as seen in Figure 11 and Table 5. For very short oligomer distributions, the constant  $K_{SF}$  was determined from the  $C_4$  and  $C_6$  fractions. Some values of  $K_{SF}$  and the resulting oligomer distribution are reported in Table 6 for  $K_{SF}$  between 0.01 and 0.09.

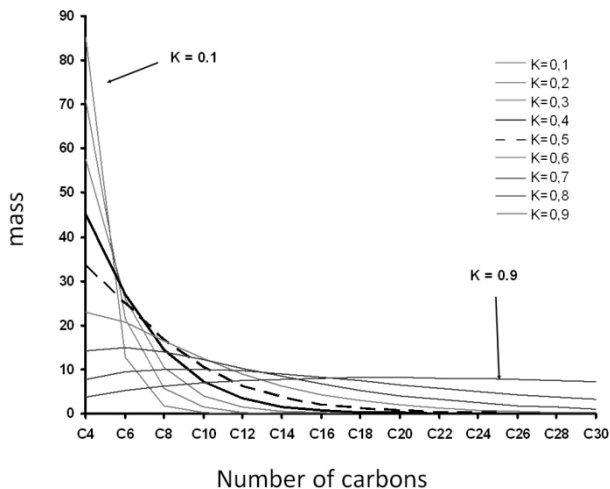


**Figure 11.** Ethylene oligomers wt.% distribution  $C_4$ - $C_{30}$  for values of the Schulz-Flory constant ( $K_{SF}$ ) between 0 and 1.

**Table 5.** Ethylene oligomers wt.% distribution  $C_4$ - $C_{30}$  for values of Schulz-Flory constant ( $K_{SF}$ ) between 0 and 1

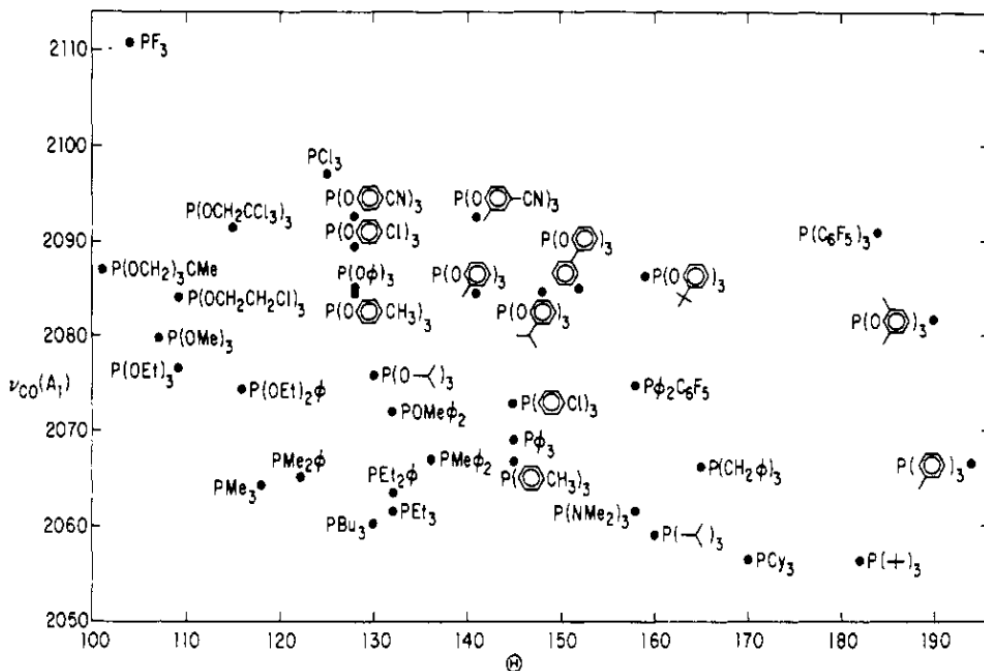
wt. %	Monomer units (p)	$K = 0,1$	$K = 0,2$	$K = 0,3$	$K = 0,4$	$K = 0,5$	$K = 0,6$	$K = 0,7$	$K = 0,8$	$K = 0,9$
$C_4$	2	85,26	71,11	57,65	45,00	33,34	22,95	14,26	7,81	3,79
$C_6$	3	12,79	21,33	25,94	27,00	25,01	20,65	14,97	9,37	5,11
$C_8$	4	1,71	5,69	10,38	14,40	16,67	16,52	13,97	10,00	6,14
$C_{10}$	5	0,21	1,42	3,89	7,20	10,42	12,39	12,22	10,00	6,90
$C_{12}$	6	0,03	0,34	1,40	3,46	6,25	8,92	10,27	9,60	7,45
$C_{14}$	7	0,00	0,08	0,49	1,61	3,65	6,25	8,39	8,96	7,83
$C_{16}$	8	0,00	0,02	0,17	0,74	2,08	4,28	6,71	8,19	8,05
$C_{18}$	9	0,00	0,00	0,06	0,33	1,17	2,89	5,28	7,37	8,15
$C_{20}$	10	0,00	0,00	0,02	0,15	0,65	1,93	4,11	6,55	8,15
$C_{22}$	11	0,00	0,00	0,01	0,06	0,36	1,27	3,16	5,77	8,07
$C_{24}$	12	0,00	0,00	0,00	0,03	0,20	0,83	2,42	5,03	7,92
$C_{26}$	13	0,00	0,00	0,00	0,01	0,11	0,54	1,83	4,36	7,73
$C_{28}$	14	0,00	0,00	0,00	0,01	0,06	0,35	1,38	3,76	7,49
$C_{30}$	15	0,00	0,00	0,00	0,00	0,03	0,22	1,04	3,22	7,22
$C_{14}^+$	-	0,00	0,10	0,74	2,94	8,30	18,57	34,31	53,22	70,61

**Table 6.** Ethylene oligomers wt.% distribution C<sub>4</sub>-C<sub>12</sub> for values of Schulz-Flory constant (K<sub>SF</sub>) between 0.01 and 0.09

wt. %	Monomer units (p)	K = 0,01	K = 0,02	K = 0,03	K = 0,04	K = 0,05	K = 0,06	K = 0,07	K = 0,08	K = 0,09
C <sub>4</sub>	2	98,50	97,01	95,52	94,04	92,56	91,09	89,63	88,17	86,71
C <sub>6</sub>	3	1,48	2,91	4,30	5,64	6,94	8,20	9,41	10,58	11,71
C <sub>8</sub>	4	0,02	0,08	0,17	0,30	0,46	0,66	0,88	1,13	1,40
C <sub>10</sub>	5	0,00	0,00	0,01	0,02	0,03	0,05	0,08	0,11	0,16
C <sub>12</sub>	6	0,00	0,00	0,00	0,00	0,00	0,00	0,01	0,01	0,02

## 6.5 Tolman cone angle and electronic parameter predication

The electronic and steric contributions of common phosphines can be evaluated with Tolman cone angle and Tolman electronic parameter. The two-dimensional representation of these properties is called the Tolman plot and is presented in Figure 12. It is possible to discriminate the electronic and the steric properties. For example P(*n*Bu)<sub>3</sub> and P(*i*Pr)<sub>3</sub> have similar electronic but different steric properties.

**Figure 12.** Tolman plot for common phosphines (Tolman electronic parameter vs. Tolman cone angle), extracted from Tolman *et al.*<sup>[35]</sup>

The value of cone angle for a phosphine in the case of symmetrical and dissymmetrical ligands is given by the following equation where  $\theta_i/2$  is the value of half-angle for substituent *i*. The values of  $\theta_i$  for one substituent correspond to the tabulated cone angle values for PR<sub>3</sub> ligand.



$$\theta = \frac{2}{3} \sum_{i=1}^3 \frac{\theta_i}{2}$$

More simply, it is the average value of all the cone angle of each homo-substituted phosphine. Considering a hetero-substituted phosphine  $PX_1X_2X_3$  and knowing the cone angle values of the trisubstituted phosphines  $P(X_1)_3$ ,  $P(X_2)_3$ ,  $P(X_3)_3$ , the cone angle value for  $PX_1X_2X_3$  is  $\theta_{PX_1X_2X_3} = 1/3 (\theta_{P(X_1)_3} + \theta_{P(X_2)_3} + \theta_{P(X_3)_3})$ . For example, considering that,  $\theta_{PH_3} = 87^\circ$  and  $\theta_{PCy_3} = 170^\circ$ , the phosphine  $PCy_2H$  has a cone angle value of:  $1/3 (170 + 170 + 87)$  so  $\theta_{PCy_2H} = 142^\circ$ . Some values of Tolman cone angle for common phosphines are provided in Table 7.

**Table 7.** Tolman experimental cone angle for several common phosphines

Phosphine	$\Theta$ ( $^\circ$ )	Phosphine	$\Theta$ ( $^\circ$ )
$PH_3$	87	$PPh_2(OEt)$	133
$PPhH_2 P(OCH_2)_3$	101	$PEt_2Ph, PMePh_2$	136
$PF_3$	104	$P(CF_3)_3$	137
$Me_2PCH_2CH_2PMe_2 P(OMe)_3$	107	$PEtPh_2$	140
$P(OEt)_3$	109	$Cy_2PCH_2CH_2PCy_2$	142
$P(CH_2O)_3$	114	$PPh_3$	145
$Et_2PCH_2CH_2PEt_2$	115	$PPh_2(i-Pr)$	150
$P(OMe)_2Ph$ or $Et$	115	$PPh_2(t-Bu)$	157
$PPh(OEt)_2$	116	$PPh_2(C_6F_5)$	158
$PMe_3$	118	$P(i-Pr)_3$	160
$Ph_2PCH_2PPh_2$	121	$PBz_3$	165
$PMe_2Ph$	122	$PCy_3, PPh(t-Bu)_2$	170
$PMe_2CF_3, PCl_3$	124	$P(O-t-Bu)_3$	175
$Ph_2PCH_2CH_2PPh_2$	125	$P(t-Bu)_3$	182
$PPh_2H, P(OPh)_3$	128	$P(C_6F_5)_3$	184
$P(O-i-Pr)_3$	130	$P(o-Tol)_3$	194
$PBr_3$	131	$P(mesityl)_3$	212
$PEt_3 PPr_3, PBu_3, PPh_2(OMe)$	132		

The value of Tolman Electronic Parameter for a phosphine corresponds to the highest vibrational value of the carbonyl observed in infrared spectroscopy for the mono phosphine complexes  $Ni(CO)_3(PX_1X_2X_3)$  in  $cm^{-1}$ . The reference for the scale is the very electron rich  $P(tBu)_3$  with a frequency of  $2065.33 cm^{-1}$ . Many values for symmetrical phosphines have been determined experimentally. For a given  $PX_1X_2X_3$  phosphine the value of the electronic parameter is given by the formula:

$$\nu(cm^{-1}) = 2065.33 + \sum_{i=1}^3 \chi_i$$

$\chi_i$  corresponds to the electronic contribution of the substituent  $X_i$  (in  $\text{cm}^{-1}$ ). These substituent contributions are established from tabulated  $\text{PX}_3$  phosphines by  $\chi_i = (\nu_{\text{PX}_3} - 2065.33)/3$ . For a dissymmetrical phosphine such as  $\text{PCy}_2\text{H}$ , the electronic parameter is calculated as follows. With  $\nu_{\text{PCy}_3} = 2056.4 \text{ cm}^{-1}$  and  $\nu_{\text{PH}_3} = 2083.2 \text{ cm}^{-1}$ , the substituent contributions are  $\chi_{\text{Cy}} = 0.1 \text{ cm}^{-1}$  and  $\chi_{\text{H}} = 9.03 \text{ cm}^{-1}$ . Therefore  $\nu_{\text{PCy}_2\text{H}} = 2065.33 \text{ cm}^{-1}$ . Some values of Tolman electronic parameter for common phosphines are provided in Table 8. Due to the high toxicity of  $\text{Ni}(\text{CO})_4$  some correlations with other metals have been established and linked to the original displacement observed for nickel they are presented on Table 9.<sup>[36,37]</sup>

**Table 8.** Tolman electronic parameter  $\nu_{\text{CO}}$  ( $\text{cm}^{-1}$ ) for common phosphines

Phosphine	$\nu_{\text{CO}}$ ( $\text{cm}^{-1}$ )		
P(t-Bu) <sub>3</sub>	2056.1	PPh <sub>2</sub> (OMe)	2072.0
PCy <sub>3</sub>	2056.4	PPh(O-i-Pr) <sub>2</sub>	2072.2
P(o-OMe-C <sub>6</sub> H <sub>4</sub> ) <sub>3</sub>	2058.3	P( <i>p</i> -Cl-C <sub>6</sub> H <sub>4</sub> ) <sub>3</sub>	2072.8
P(i-Pr) <sub>3</sub>	2059.2	PPh <sub>2</sub> H	2073.3
PBu <sub>3</sub>	2060.3	PPh(OBu) <sub>2</sub>	2073.4
PEt <sub>3</sub>	2061.7	P( <i>m</i> -F-C <sub>6</sub> H <sub>4</sub> ) <sub>3</sub>	2074.1
PEt <sub>2</sub> Ph	2063.7	PPh(OEt) <sub>2</sub>	2074.2
PMe <sub>3</sub>	2064.1	PPh <sub>2</sub> (OPh)	2074.6
PMe <sub>2</sub> Ph	2065.3	PPh <sub>2</sub> (C <sub>6</sub> F <sub>5</sub> )	2074.8
P( <i>p</i> -OMe-C <sub>6</sub> H <sub>4</sub> ) <sub>3</sub> , PPh <sub>2</sub> (o-OMe-C <sub>6</sub> H <sub>4</sub> )	2066.1	P(O- <i>i</i> -Pr) <sub>3</sub>	2075.9
PBz <sub>3</sub>	2066.4	P(OEt) <sub>3</sub>	2076.3
P(o-Tol) <sub>3</sub>	2066.6	PPhH <sub>2</sub>	2077.0
P( <i>p</i> -Tol) <sub>3</sub> , PEtPh <sub>2</sub>	2066.7	P(CH <sub>2</sub> CH <sub>2</sub> CN) <sub>3</sub>	2077.9
PMePh <sub>2</sub>	2067.0	P(OCH <sub>2</sub> CH <sub>2</sub> OMe) <sub>3</sub>	2079.3
P( <i>m</i> -Tol) <sub>3</sub>	2067.2	P(OMe) <sub>3</sub>	2079.5
PPh <sub>2</sub> (NMe <sub>2</sub> )	2067.3	PPh(OPh) <sub>2</sub>	2079.8
PPh <sub>2</sub> (2,4,6-Me-C <sub>6</sub> H <sub>2</sub> )	2067.4	PPh <sub>2</sub> Cl	2080.7
PPhBz <sub>2</sub>	2067.6	PMe <sub>2</sub> CF <sub>3</sub>	2080.9
PPh <sub>2</sub> ( <i>p</i> -OMe-C <sub>6</sub> H <sub>4</sub> )	2068.2	P(O-2,4-Me-C <sub>6</sub> H <sub>3</sub> ) <sub>3</sub> , PH <sub>3</sub>	2083.2
PPh <sub>2</sub> Bz	2068.4	P(OCH <sub>2</sub> CH <sub>2</sub> Cl) <sub>3</sub>	2084.0
PPh <sub>3</sub>	2068.9	P(O-Tol) <sub>3</sub>	2084.1
PPh <sub>2</sub> (CH=CH <sub>2</sub> )	2069.3	P(OPh) <sub>3</sub>	2085.3
P(CH=CH <sub>2</sub> ) <sub>3</sub> , PPh <sub>2</sub> ( <i>p</i> -F-C <sub>6</sub> H <sub>4</sub> )	2069.5	P(OCH <sub>2</sub> ) <sub>3</sub> CR	2086.8
PPh( <i>p</i> -F-C <sub>6</sub> H <sub>4</sub> ) <sub>2</sub>	2070.0	P(OCH <sub>2</sub> CH <sub>2</sub> CN) <sub>3</sub>	2087.6
P( <i>p</i> -F-C <sub>6</sub> H <sub>4</sub> ) <sub>3</sub>	2071.3	P(C <sub>6</sub> F <sub>5</sub> ) <sub>3</sub>	2090.9
PPh <sub>2</sub> (OEt)	2071.6	PCl <sub>3</sub>	2097.0
		PF <sub>3</sub>	2110.8

**Table 9.** Indirect ways to determine experimentally Tolman Electronic Parameter.

Starting precursor	Complex formed	Relation with Tolman Electronic Parameter.
Ni(CO) <sub>4</sub>	Ni(CO) <sub>3</sub> P	TEP
Se	Se=P	TEP = 0.159 <sup>l</sup> J <sub>PSe</sub> + 1952.3 (cm <sup>-1</sup> )
Mo(CO) <sub>6</sub>	Mo(CO) <sub>5</sub> P	TEP = 1.116 ν <sub>CO(Mo)</sub> - 243 (cm <sup>-1</sup> )
Rh(CO) <sub>3</sub> Cl	Rh(CO)CIP <sub>2</sub>	TEP = 0.226 ν <sub>CO(Rh)</sub> + 1621 (cm <sup>-1</sup> )

## 7 References

- [1] P. Kuhn, D. Sémeril, D. Matt, M. J. Chetcuti, P. Lutz, *Dalt. Trans.* **2007**, 515–528.
- [2] C. Carlini, M. Marchionna, A. Raspolli Galletti, *J. Mol. Catal. A* **2001**, *169*, 79–88.
- [3] U. Müller, W. Keim, C. Krüger, P. Betz, *Angew. Chem., Int. Ed.* **1989**, *28*, 1011–1013.
- [4] T. Adam, M. Robert, *J. Am. Chem. Soc.* **1971**, *95*, 4073–4074.
- [5] P. W. Jolly, K. Jonas, C. Krüger, *J. Organomet. Chem.* **1971**, *33*, 109–122.
- [6] W. Heyndrickx, G. Occhipinti, V. R. Jensen, *Chem. Eur. J.* **2014**, 7962–7978.
- [7] D. S. McGuinness, *Chem. Rev.* **2011**, *111*, 2321–2341.
- [8] T. Agapie, *Coord. Chem. Rev.* **2011**, *255*, 861–880.
- [9] P. W. N. M. van Leeuwen, N. D. Clément, M. J.-L. Tschan, *Coord. Chem. Rev.* **2011**, *255*, 1499–1517.
- [10] P. Cossee, *J. Catal.* **1964**, *38*, 80–88.
- [11] J. Arlman, P. Cossee, *J. Catal.* **1964**, *104*, 99–104.
- [12] J. Arlman, *J. Catal.* **1964**, *98*, 89–98.
- [13] M. Brookhart, M. L. H. Green, *J. Organomet. Chem.* **1983**, *250*, 395–408.
- [14] L. K. Johnson, C. M. Killian, M. Brookhart, *J. Am. Chem. Soc.* **1995**, *117*, 6414–6415.
- [15] S. A. Svejda, L. K. Johnson, M. Brookhart, C. Hill, N. Carolina, R. V June, *J. Am. Chem. Soc.* **1999**, 10634–10635.
- [16] M. D. Leatherman, S. a Svejda, L. K. Johnson, M. Brookhart, *J. Am. Chem. Soc.* **2003**, *125*, 3068–3081.
- [17] L. Deng, P. Margl, T. Ziegler, *J. Am. Chem. Soc.* **1997**, *119*, 1094–1100.
- [18] S. Strömberg, K. Zetterberg, P. E. M. Siegbahn, *Dalt. Trans.* **1997**, 4147–4152.
- [19] D. G. Musaev, R. D. J. Froese, K. Morokuma, *Organometallics* **1998**, 1850–1860.
- [20] T. K. Woo, T. Ziegler, *J. Organomet. Chem.* **1999**, *591*, 204–213.
- [21] W. Heyndrickx, G. Occhipinti, Y. Minenkov, V. R. Jensen, *Chem. Eur. J.* **2011**, *17*, 14628–14642.
- [22] F. Hasanayn, P. Achord, P. Braunstein, *Organometallics* **2012**, *31*, 4680–4692.
- [23] A. Lisboa Monteiro, M. O. de Souza, R. F. de Souza, *Polym. Bull.* **1996**, *36*, 331–336.
- [24] P. Kuhn, D. Sémeril, C. Jeunesse, D. Matt, M. Neuburger, A. Mota, *Chem. Eur. J.* **2006**, *12*, 5210–5219.

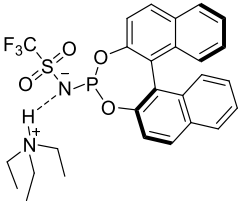
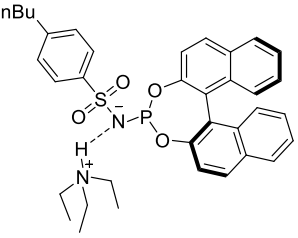
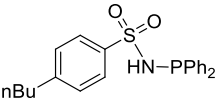
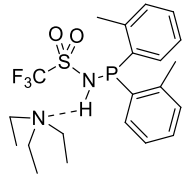
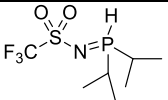
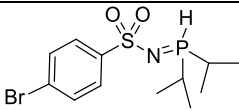
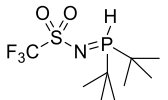
- [25] J. Heinicke, M. He, A. Dal, H.-F. Klein, O. Hetche, W. Keim, U. Flörke, H.-J. Haupt, *Eur. J. Inorg. Chem* **2000**, 2000, 431–440.
- [26] L. Wang, E. M. Hauptman, L. Kaye, E. F. Mccord, S. J. McLain, Y. Wang, *Catalysts for Olefin Polymerization*, **2010**, U.S. Patent US 2010/0029469 A1.
- [27] M. Peuckert, W. Keim, *Organometallics* **1983**, 2, 594–597.
- [28] J. Pietsch, P. Braunstein, Y. Chauvin, *New J. Chem.* **1998**, 22, 467–472.
- [29] J. Heinicke, M. Köhler, N. Peulecke, W. Keim, *J. Catal.* **2004**, 225, 16–23.
- [30] W. Keim, A. Behr, B. Gruber, B. Hoffmann, F. H. Kowaldt, U. Kürschner, B. Limbacher, F. P. Sistic, *Organometallics* **1986**, 5, 2356–2359.
- [31] A. Behr, W. Keim, G. Thelen, *J. Organomet. Chem.* **1983**, C38–C40.
- [32] O. Kühl, P. Lobitz, N. Peulecke, *Phosphorus, Sulfur, Silicon Relat. Elem.* **2011**, 37–41.
- [33] S. D. Ittel, L. K. Johnson, M. Brookhart, *Chem. Rev.* **2000**, 100, 1169–204.
- [34] W. Keim, F. H. Kowaldt, R. Goddard, C. Krüger, *Angew. Chem., Int. Ed.* **1978**, 17, 466–467.
- [35] C. A. Tolman, *Chem. Rev.* **1977**, 77, 313–348.
- [36] K. K. Banger, A. K. Brisdon, C. J. Herbert, H. A. Ghaba, I. S. Tidmarsh, *J. Fluor. Chem.* **2009**, 130, 1117–1129.
- [37] A. M. Ejgandi, Measuring the Electronic and Steric Effect of Some Phosphine Ligands, University of Manchester, **2010**.



# Appendix

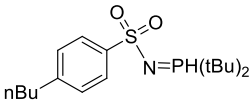
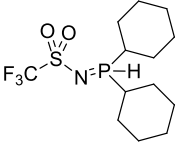
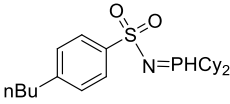
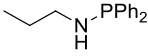
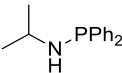
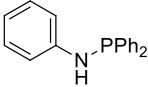
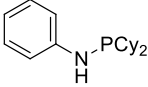
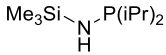
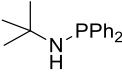
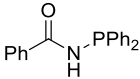
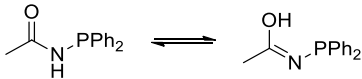
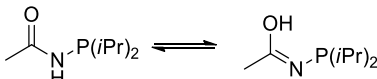
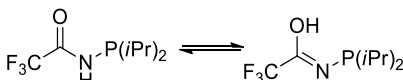
# 1 Isolated ligands and complexes

## 1.1 METAMORPhos, aminophosphine and amidophosphine ligands

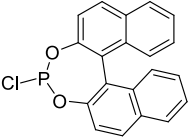
Molecule	tautomer	Reference thesis	Reference (external) <sup>7</sup>	Indicative <sup>31</sup> P chemical shift (ppm)
	NH.NEt <sub>3</sub>	Ch2, <b>1</b>	PB101 (118188)	165.2 (CD <sub>2</sub> Cl <sub>2</sub> )
	NH.NEt <sub>3</sub>	Ch2, <b>2</b>	PB97 (118180)	171.07 (CD <sub>2</sub> Cl <sub>2</sub> )
	PH, NH	Ch2, <b>3</b>	PB03 PB28 (118122)	2.82(PH, C <sub>6</sub> D <sub>6</sub> ) 32.8(NH, C <sub>6</sub> D <sub>6</sub> )
	NH.NEt <sub>3</sub>	Ch2, <b>8</b> Ch5, <b>1</b>	PB418 (125087)	15.77 (PH) 22.62(NH.NEt <sub>3</sub> ) C <sub>6</sub> D <sub>6</sub>
	PH	Ch2, <b>11</b> Ch5, <b>2</b>	PB54 (118128)	40.54 (C <sub>6</sub> D <sub>6</sub> ) 42.32 (CDCl <sub>3</sub> )
	PH	Ch2, <b>12</b>	PB93 (132682)	36.5 (PH, CD <sub>2</sub> Cl <sub>2</sub> )
	PH	Ch2, <b>15</b>	PB15 PB235 (118132)	49.07 (CDCl <sub>3</sub> ) 50.61 (CD <sub>2</sub> Cl <sub>2</sub> )

<sup>7</sup> References to lab journal and CataSepa. CataSepa is an intranet catalyst database of IFPEN gathering all the ligands and complexes synthesised as well as the catalytic reactions. The characterisation of ligands of this thesis is available using the reference number into parenthesis.

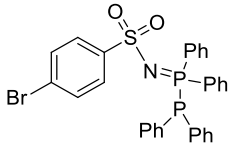
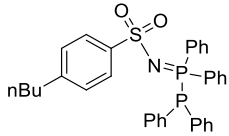
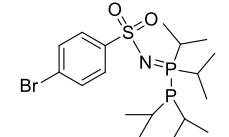
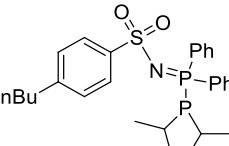
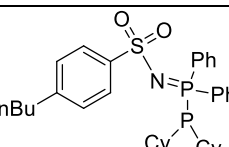
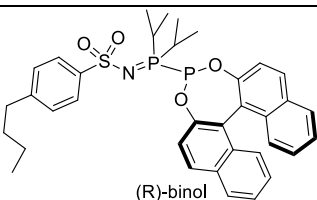
## Appendix

	PH	Ch2, <b>17</b>	PB236 (118202)	44.76 (CD <sub>2</sub> Cl <sub>2</sub> ) 42.23 (tol- <i>d</i> <sub>8</sub> )
	PH	Ch2, <b>19</b>	PB144 PB223 (118191)	35.3 (CD <sub>2</sub> Cl <sub>2</sub> )
	PH	Ch2, <b>20</b>	PB146 (118197)	28.84 (CD <sub>2</sub> Cl <sub>2</sub> )
	NH	Ch5, <b>A</b>	PB397 (oil) (125093)	41.05 (CDCl <sub>3</sub> )
	NH	Ch4, <i>experimental part</i> Ch5, <b>B</b>	PB204 (120483) PB281 (120499) PB459	33.75 (CD <sub>2</sub> Cl <sub>2</sub> ) 34.7 (C <sub>6</sub> D <sub>6</sub> )
	NH	Ch5, <b>C</b>	PB230 PB490 (120489)	27.45 (CD <sub>2</sub> Cl <sub>2</sub> )
	NH	Ch5, <b>D</b>	PB246 (125085)	41.01 (C <sub>6</sub> D <sub>6</sub> )
	NH	Ch5, <b>E</b>	PB377 (125088)	48.36 (C <sub>6</sub> D <sub>6</sub> )
	NH	Ch5, <b>F</b>	PB245 (oil) (120498)	22.5 (C <sub>6</sub> D <sub>6</sub> )
	NH	Ch2, <b>21</b>	PB349 (120901)	24.7 (NH, CD <sub>2</sub> Cl <sub>2</sub> )
	NH, OH	Ch2, <b>22</b>	PB332 (123145)	30.3 (OH, CD <sub>2</sub> Cl <sub>2</sub> ) 22.8 (NH, CD <sub>2</sub> Cl <sub>2</sub> )
	NH, OH	Ch2, <b>23</b>	PB352 (oil) (125091)	49.7 (NH, CD <sub>2</sub> Cl <sub>2</sub> ) 56.14 (OH, CD <sub>2</sub> Cl <sub>2</sub> )
	NH, PH	Ch2, <b>24</b>	PB354 (125092)	40.1 (PH, CD <sub>2</sub> Cl <sub>2</sub> ) 56.9 (NH, CD <sub>2</sub> Cl <sub>2</sub> )



	/	Ch2 <i>experimental part</i>	PB173	177 (C <sub>6</sub> D <sub>6</sub> )
---	---	---------------------------------	-------	--------------------------------------

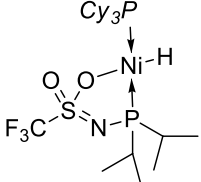
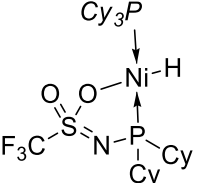
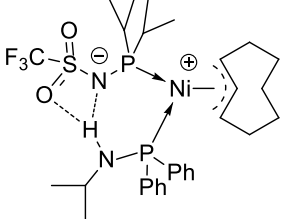
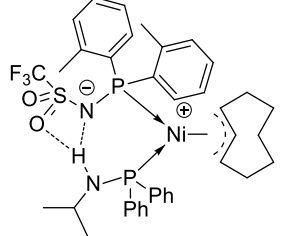
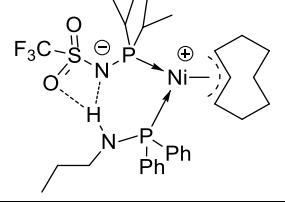
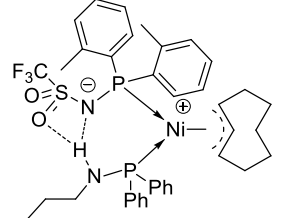
## 1.2 Iminobisphosphine ligands

Molecule	Reference thesis	Reference (external)	Chemical shift <sup>31</sup> P (ppm)
	Ch3, 1	PB78 PB09 (118550)	19.72 & -18.74 (J=281.1 Hz) (CD <sub>2</sub> Cl <sub>2</sub> )
	Ch3, 2	PB116 (118210)	19.& -17.90 (J= 278.0 Hz) (CD <sub>2</sub> Cl <sub>2</sub> )
	Ch3, 3	PB92 (118212)	50.39 & -6.30 (J = 329.8 Hz) (CD <sub>2</sub> Cl <sub>2</sub> )
	Ch3, 4	PB68 PB177 (118217)	20.13 & 2.80 (J = 311.6 Hz) (CD <sub>2</sub> Cl <sub>2</sub> )
	Ch3, 5	PB179 PB422 (118216)	20.44 & -4.98 (J = 314.4 Hz) (CD <sub>2</sub> Cl <sub>2</sub> )
 (R)-binol	Ch3 <i>experimental part</i>	PB174 (118177)	-2.77 & 49.89 (J = 350.2 Hz) (CD <sub>2</sub> Cl <sub>2</sub> )

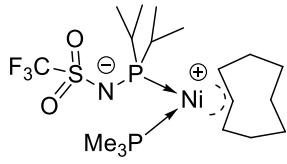
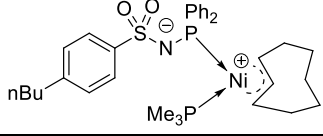
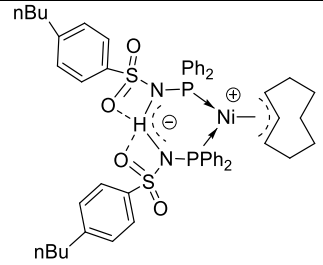
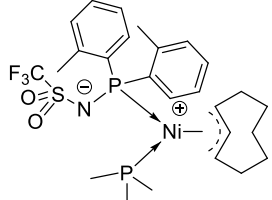
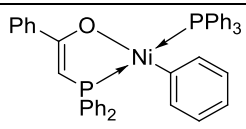
## 1.3 Nickel complexes

Molecule	Reference thesis	Reference external	Chemical shift $^{31}\text{P}$ (ppm)
	Ch2, <b>25</b>	PB29 PB43 (132667)	/
	Ch2, <b>26</b>	PB40 PB106 (132668)	/
	Ch3, <b>6</b>	PB98 (118620)	65.52 (CD <sub>2</sub> Cl <sub>2</sub> )
	Ch3, <b>8</b>	PB99 (118622)	111.26 (CD <sub>2</sub> Cl <sub>2</sub> )
	Ch3, <b>7</b>	PB124 (118633)	64.07 (CD <sub>2</sub> Cl <sub>2</sub> )
	Ch3, <b>9</b>	PB68 (118634)	117.10 & 61.16 ( $^2J_{PP} = 121.4$ Hz)
	Ch3, <b>10</b>	PB181 PB422 (118636)	108.15 & 60.28 ( $^2J_{PP} = 119.2$ Hz)

Appendix

	<p>Ch5, <b>17</b></p>	<p>PB253, PB184, PB127, PB125 (121961)</p>	<p>36.1 (dd, <math>^2J_{PP} = 236</math> Hz, <math>^2J_{PH} = 64</math> Hz); 103.4 (dd, <math>^2J_{PP} = 236</math> Hz, <math>^2J_{PH} = 77</math> Hz) (C<sub>6</sub>D<sub>6</sub>)</p>
	<p>Ch5, <b>34</b></p>	<p>PB225 (122218)</p>	<p>36.6 (dd, <math>^2J_{PP} = 236</math> Hz, <math>^2J_{PH} = 67</math> Hz); 78.6 (dd, <math>^2J_{PP} = 237</math> Hz &amp; <math>^2J_{PH} = 82</math> Hz) (C<sub>6</sub>D<sub>6</sub>)</p>
	<p>Ch4, <b>4</b> Ch5, <b>11</b></p>	<p>PB222 PB224 PB415 (121850)</p>	<p>85.76 &amp; 60.22 (<math>J_{PP} = 31</math> Hz) (C<sub>6</sub>D<sub>6</sub>)</p>
	<p>Ch4, <b>3</b> Ch5, <b>12</b></p>	<p>PB455 (126060)</p>	<p>52.13 &amp; 62.82 (<math>^2J_{PP} = 23.3</math> Hz) (C<sub>6</sub>D<sub>6</sub>)</p>
	<p>Ch5, <b>14</b></p>	<p>PB488 (132681)</p>	<p>64.55 &amp; 92.16 (<math>^2J_{PP} = 31.6</math> Hz) (CD<sub>2</sub>Cl<sub>2</sub>)</p>
	<p>Ch5, <b>15</b></p>	<p>PB483 (132671)</p>	<p>52. &amp; 65.09 (<math>^2J_{PP} = 24.5</math> Hz) (CD<sub>2</sub>Cl<sub>2</sub>)</p>

Appendix

 <p>Chemical structure showing a nickel atom coordinated to a sulfonamide phosphine ligand (with a trifluoromethyl group, <math>\text{F}_3\text{C}</math>) and a cyclopentadienyl anion. The phosphorus atom is also coordinated to a methyl group (<math>\text{Me}_3\text{P}</math>).</p>	Ch5, <b>16</b>	PB300 PB416 (120500)	86.8 & -11.4 ( $^2J_{PP} = 31.45 \text{ Hz}$ ) ( $\text{C}_6\text{D}_6$ )
 <p>Chemical structure showing a nickel atom coordinated to a sulfonamide phosphine ligand (with an n-butyl group, <math>\text{nBu}</math>) and a cyclopentadienyl anion. The phosphorus atom is also coordinated to a methyl group (<math>\text{Me}_3\text{P}</math>).</p>	Ch5, <b>28</b>	PB307, PB424 (120501)	60.25 & -0.11 ( $^2J_{PP-cis} = 26.7 \text{ Hz}$ ) ( $\text{C}_6\text{D}_6$ )
 <p>Chemical structure showing a nickel atom coordinated to a sulfonamide phosphine ligand (with an n-butyl group, <math>\text{nBu}</math>) and a cyclopentadienyl anion. The phosphorus atom is also coordinated to a methyl group (<math>\text{Me}_3\text{P}</math>) and a diphenylamino group (<math>\text{N-Ph}_2</math>).</p>	Ch5, <b>13</b>	PB389, PB386, PB435, PB436 (125084)	54.06 ( $\text{C}_6\text{D}_6$ )
 <p>Chemical structure showing a nickel atom coordinated to a sulfonamide phosphine ligand (with a trifluoromethyl group, <math>\text{F}_3\text{C}</math>) and a cyclopentadienyl anion. The phosphorus atom is also coordinated to a methyl group (<math>\text{Me}_3\text{P}</math>).</p>	Ch5, <b>29</b>	PB470 (127004)	-15.10 & 54.75 ( $^2J_{PP} = 25.8 \text{ Hz}$ ) ( $\text{C}_6\text{D}_6$ )
 <p>Chemical structure showing a nickel atom coordinated to a phosphine ligand (with a phenyl group, <math>\text{Ph}</math>) and a cyclopentadienyl anion. The phosphorus atom is also coordinated to a methyl group (<math>\text{PPh}_3</math>).</p>	Ch 4 and Ch5 <b>Ref</b>	PB308 (120502)	19.5 & 22.4 ( $^2J_{PP} = 284 \text{ Hz}$ ) ( $\text{C}_6\text{D}_6$ )
$\text{NiCl}_2(\text{DPPE})$	Ch3 <i>experimental part</i>	DP631 (101163)	57.55 ( $\text{CD}_2\text{Cl}_2$ )
$\text{NiBr}_2(\text{DPCyE})$	Ch3 <i>experimental part</i>	PB449 (125082)	95.37 ( $\text{CD}_2\text{Cl}_2$ )
$\text{NiBr}_2(\text{DPiPrE})$	Ch3 <i>experimental part</i>	PB450 (121849)	88.84 ( $\text{CD}_2\text{Cl}_2$ )

## 2 Publications and patents

### 2.1 Publication:

- **Iminobisphosphines to (non-) symmetrical di(phosphino)amine ligands: Metal-induced synthesis of diphosphorus nickel complexes and application in ethylene oligomerisation reactions.**  
P. Boulens, M. Lutz, E. Jeanneau, H. Olivier-Bourbigou, J. N. H. Reek, P. – A. R. Breuil *Eur. J. Inorg. Chem.* **2014**, 3754–3762
- **Self-assembled organometallic nickel complexes as catalysts for selective oligomerisation of ethylene into 1-butene**  
P. Boulens, E. Jeanneau, J. N. H. Reek, H. Olivier-Bourbigou, P.-A. R. Breuil,  
(submitted)

### 2.2 Patents:

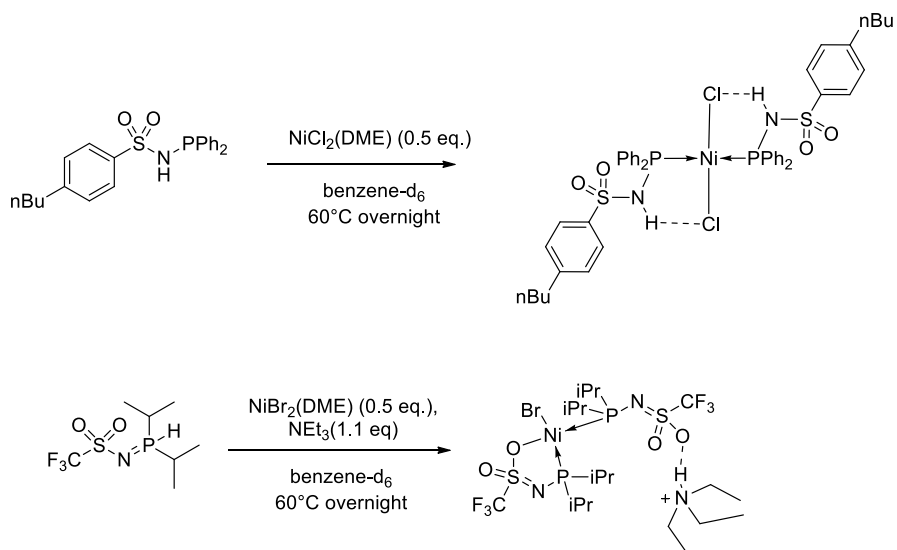
Inventors: P. Boulens, P.A. Breuil, H. Olivier-Bourbigou, J. N. H. Reek.

- **Patent INPI n° 13/62.239** (06/12/2013) : Nouvelle composition catalytique à base de nickel et son utilisation dans un procédé d'oligomérisation des oléfines
- **Patent INPI n° 13/56.269** (28/06/2013) : Nouvelle composition catalytique à base de nickel et son utilisation dans un procédé d'oligomérisation des oléfines.
- **Patent INPI n° 13/56.271** (28/06/2013) : Nouveau complexe à base de nickel et son utilisation dans un procédé d'oligomérisation des oléfines
- **Patent INPI n° 14/53.816** (28/04/2014) : Nouvelle composition catalytique à base de nickel et son utilisation dans un procédé d'oligomérisation des oléfines
- **Patent INPI n° 14/53.817** (28/04/2014) : Nouveaux complexes à base de nickel et leur utilisation dans un procédé de transformation des oléfines.
- **Patent INPI n° 14/53.818** (28/04/2014) : Nouveaux complexes cycliques à base de nickel et leur utilisation dans un procédé de transformation des oléfines.

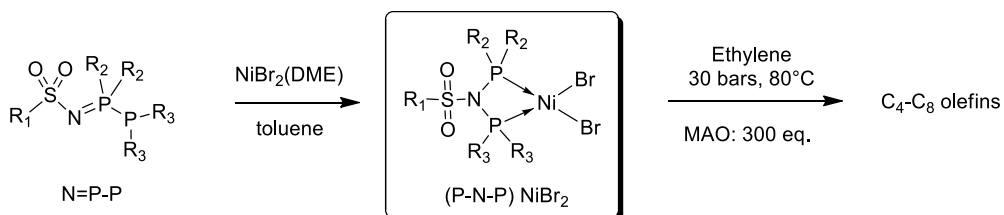
# Summary

The demand for short Linear Alpha Olefins (LAO) is constantly increasing in the industry, which motivates the search for robust catalysts affording one LAO (1-butene, 1-hexene or 1-octene) selectively. Among the different metals used for ethylene oligomerisation, nickel has certainly the richest history of coordination and organometallic chemistry, documented for over one century now. Phosphine ligands in combination with nickel have shown a strong ability in changing the selectivity of this nickel catalysed reaction. Their robustness permitted their use industrially in the SHOP and Phillips processes for the production of LAOs with broad distribution (Schulz-Flory) or 2-butene. So far, it is still a challenge to find proper nickel complexes to oligomerise selectively ethylene in 1-butene, 1-hexene or 1-octene. For this purpose, we investigated dissymmetric ligands and supramolecular concepts based on sulphonamido-phosphorus ligands aiming for novel, selective nickel catalysts.

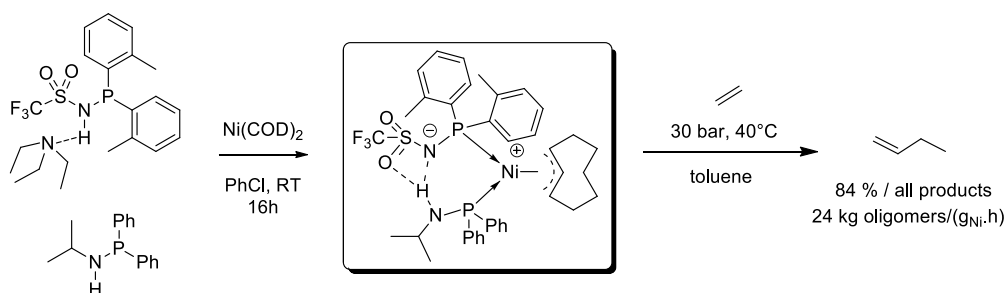
In the first part of this thesis, we describe the synthesis of ligand building blocks that facilitate the formation of supramolecular systems based on hydrogen-bonds. A one-step synthesis was developed that allowed the preparation of small libraries of aminophosphines  $R^1\text{-NH-P}(R^2)_2$ , amidophosphines  $R^1\text{-CO-NH-P}(R^2)_2$ , and sulphonamido phosphines ( $R^1\text{-SO}_2\text{-NH-P}(R^2)_2$ , known as METAMORPhos). Next to this, we also reported a side reaction that produces iminobisphosphines of formula:  $R^1\text{-N=P}(R^2)_2\text{-P}(R^2)_2$ . The occurrence of this side reaction strongly depends on the steric parameters at the ligand. Sulphonamido phosphine ligands exist in two different tautomers (NH or PH) while for the amidophosphines three tautomers were observed (NH, PH, OH), a sign of rich electronic variety brought within the ligand library. Coordination chemistry studies of METAMORPhos ligands with Ni(II) revealed the potential of these ligands as at least three different coordination modes with the same type of ligand were observed.



The evaluation of the use of bidentate diphosphine ligands in nickel (II) catalysed oligomerisation has so far been limited to symmetrical ligands, mainly because the synthesis to dissymmetrical ligands is more tedious. We anticipated that dissymmetrical diphosphine ligands with two different phosphine contributions could control elementary steps in the catalysis and favour termination over propagation. We found that iminobisphosphines, in the presence of a nickel (II) precursor, rearranged to form dissymmetrical diphosphine chelated nickel complex of structure  $((\text{R}^2)_2\text{P}-\text{N}(\text{R}^1)-\text{P}(\text{R}^3)_2)\text{NiBr}_2$  that were isolated and characterised. The rearrangement involves the cleavage of the P-P bond mediated by the nickel complex. Nickel complexes with both symmetrical and dissymmetrical, bidentate ligands were explored in ethylene oligomerisation and when activated with MAO they were active producing short oligomers. The complexes were also active in propylene oligomerisation for which the dissymmetrical nature of the complexes had a direct impact on outcome of the reaction: arylphosphines favoured high selectivity for the dimer while basic phosphines gave high yields of 2,3-dimethylbutenes, a valuable chemical intermediate. The same strategy transposed to chromium did not lead to selective ethylene transformation.

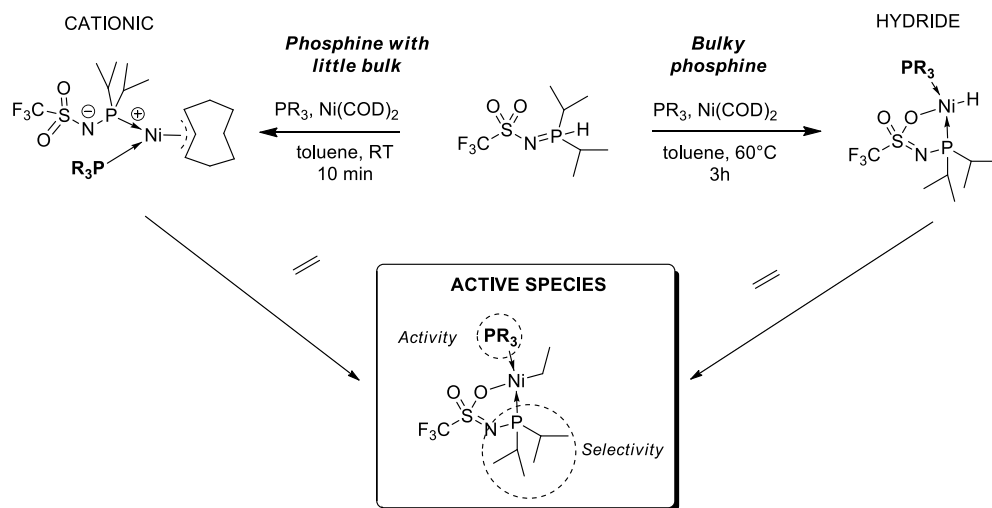


Based on coordination studies of METAMORPhos ligand with nickel, we disclosed a new synthetic approach, based on Ni(0) to generate supramolecular nickel (II) complexes based on the interaction between a sulphonamido phosphine and an additional aminophosphine. The presence of an intramolecular hydrogen-bond in this assembly was unambiguously proven by crystal structures and in solution by NMR analysis of the complexes. This new class of zwitterionic organometallic and supramolecular nickel complexes showed good chemical and thermal stability. Most importantly, these complexes oligomerised ethylene, even in the absence of any co-catalysts, and displayed high activity (up to 24 kg<sub>oligo</sub>/(g<sub>Ni</sub>.h)). In addition, complexes based on aryl P-substituted METAMORPhos ligands displayed exceptional selectivity for 1-butene, which is currently a highly demanded olefin for polyethylene industry.

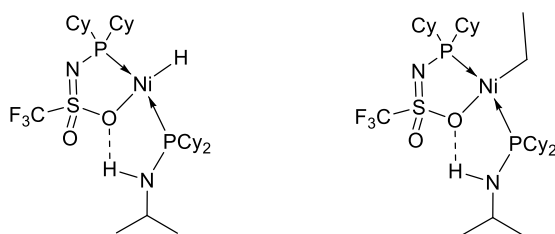


To have a better understanding of this system, we extended this concept to diverse combinations of METAMORPhos ligands with different co-ligands. The formation of a relatively large set of complexes was confirmed by unlocked <sup>31</sup>P NMR. We found that bulky co-ligands such as PCy<sub>3</sub> could transform a zwitterionic diphosphine nickel complex to a neutral PO chelated nickel hydride complex. A few nickel hydride complexes were thus isolated using bulky phosphines (PCy<sub>3</sub>, P(*t*Bu)<sub>3</sub>, P(*i*Pr)<sub>3</sub>). Under high-pressure of ethylene, both complexes (zwitterionic and hydride) led to *trans*-(PO,P)Ni-ethyl complex, assigned as the active species. Isolated zwitterionic and hydride catalysts were both active in ethylene oligomerisation, and some complexes gave high selectivity in the formation of 1-butene. By a careful analysis of the structural parameters, we also established that METAMORPhos was responsible for selectivity while the co-ligand regulated activity. We also identified a strong supramolecular control of the stability of the complex. While aminophosphines with a proton donor moiety in combination with the hydrogen acceptor properties of the METAMORPhos ligands generated zwitterionic complexes that were very stable, complexes with co-ligands with identical electronic and steric parameter that did not have a H-donor, led only to complex decomposition.



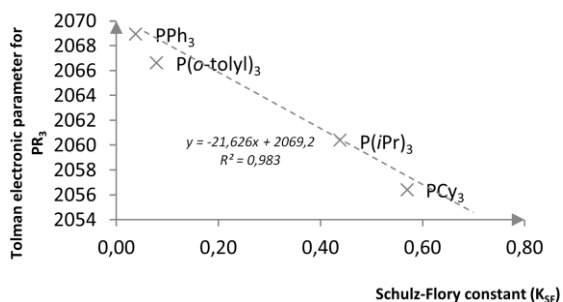
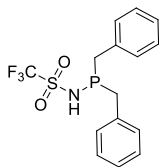
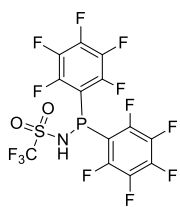


A first perspective for the work described in this thesis is about the mechanism. What is exact role of the hydrogen-bond during the mechanism, and how does the *cis* to *trans* rearrangement under ethylene play a role? Proving that there is a H-bond cannot be easily established by NMR *via in situ* spectroscopy. Isolating the active species or using a characterisation “*in operando*” (IR, NMR ...) in combination with DFT calculations could bring new information. Maybe using very basic and bulky aminophosphine co-ligands (in presence of ethylene) could lead to supramolecular hydride complexes with two phosphines in *trans* (or to the corresponding ethyl complex). The nature of the binding of the oxygen atom to the nickel should also be further explored to know what type of interaction exist during catalysis.



A second perspective is about tuning and simplifying the catalyst. We have shown in this thesis that by an efficient ligand tailoring, including the application of hydrogen bonds, we could shift the selectivity in the nickel-catalysed ethylene oligomerisation to produce a distribution of LAO with controlled length ( $K_{\text{SF}}$ ), or even 1-butene selectively. Preliminary insights in the role of each fragment of the nickel complex has been obtained, which highlighted the importance of the METAMORPhos ligand as the key of achieve high selectivity. Also, a tentative correlation was established between the Tolman electronic parameter of the phosphine ligands used and the

oligomer distribution modelled by the Schulz-Flory constant ( $K_{SF}$ ). This approach should be confirmed by using more experimental data points, i.e. by developing METAMORPhos ligands substituted on phosphorus by benzyl groups or by pentafluorophenyl groups. The latter has a value of Tolman electronic parameter of  $2090.9 \text{ cm}^{-1}$  and therefore is on the edge of the current experimental graph, suggesting that nickel complexes based on this ligand should lead to a complete control of selectivity.

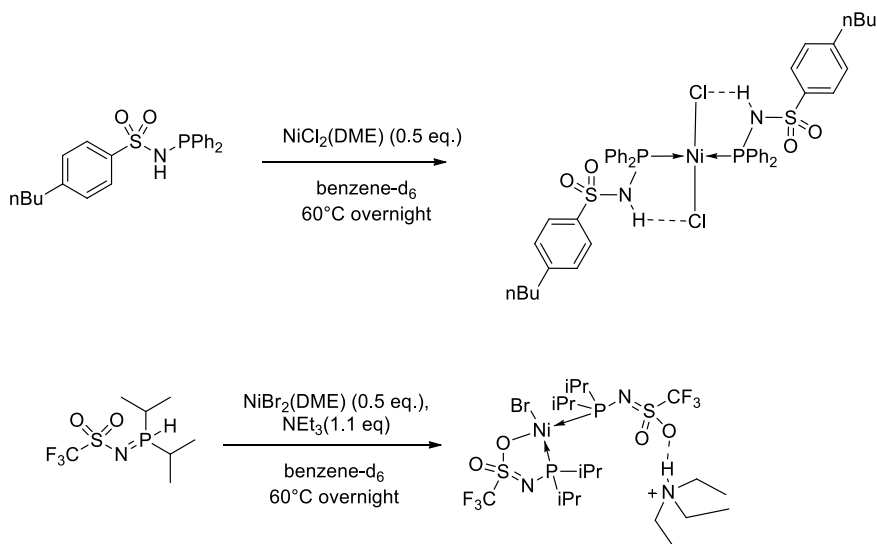




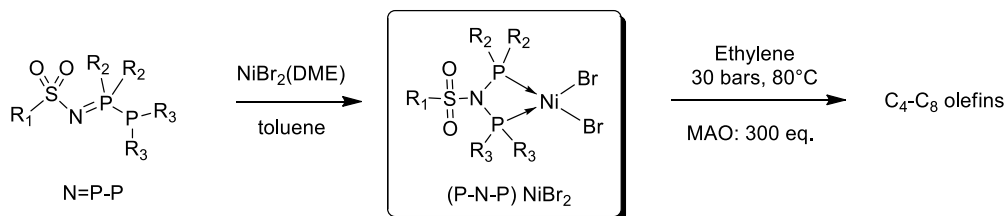
# Résumé

La demande en Alpha Oléfines Linéaires (LAO) courtes est en constante augmentation dans l'industrie. Elle motive la découverte de systèmes catalytiques robustes pouvant produire des oléfines de manière sélective tels que le butène-1, l'hexène-1 ou l'octène-1. Parmi les différents métaux utilisés comme catalyseurs de cette réaction, le nickel a très certainement un des passifs les plus riches. Il a fait l'objet d'importants travaux notamment en chimie organométallique et de coordination depuis maintenant plus d'un siècle. Plusieurs procédés industriels comme SHOP et Phillips, encore en fonctionnement actuellement, permettent la production contrôlée de LAO ou bien la production sélective de butène-2. Un des défis actuels, consiste à transformer sélectivement l'éthylène en butène-1, hexène-1 ou octène-1. Pour tenter d'y parvenir, nous nous sommes intéressés à l'utilisation de ligands phosphorés fonctionnalisés permettant d'accéder à différents modes de coordination et de générer divers complexes symétriques et dissymétriques par des stratégies covalentes ou supramoléculaires.

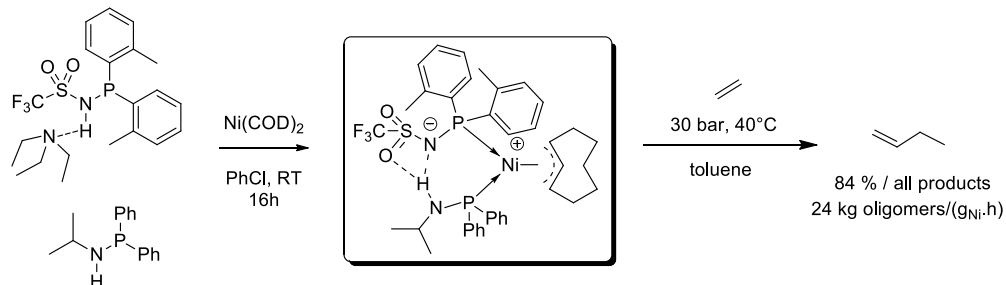
Dans une première partie, nous avons exploré la synthèse de ligands phosphorés pouvant établir entre eux des liaisons hydrogènes. Par une approche synthétique rapide, nous avons préparé plusieurs ligands aminophosphines  $R^1\text{-NH-P}(R^2)_2$ , amidophosphines  $R^1\text{-CO-NH-P}(R^2)_2$  et sulphonamido phosphines  $R^1\text{-SO}_2\text{-NH-P}(R^2)_2$ , ces derniers connus comme les ligands METAMORPhos. Lors de la synthèse de ces ligands, nous avons observé une réaction secondaire produisant des iminobisphosphines de formule  $R^1\text{-N=P}(R^2)_2\text{-P}(R^2)_2$  dont la formation a pu être réduite par l'introduction de groupements encombrés sur le phosphore. A l'instar des oxydes de phosphines secondaires (SPO) qui existent sous deux formes tautomères, les ligands sulphonamido phosphines et les amidophosphines présentent également plusieurs formes tautomères. Leur existence dépend des effets électroniques des substituants. Les tautomères NH ou PH sont observés avec les ligands METAMORPhos alors que les amidophosphines peuvent stabiliser les tautomères NH, PH et OH. Des expériences de chimie de coordination des ligands METAMORPhos à des précurseurs de Ni(II) ont montré qu'un ligand pouvait à lui seul générer jusqu'à 3 modes de coordination différents.



L'évaluation des ligands diphosphines bidentates pour l'oligomérisation de l'éthylène a été jusqu'à présent limitée aux ligands symétriques. Cependant l'introduction de ligands diphosphines dissymétriques pourrait permettre de contrôler les étapes déterminantes en catalyse (propagation et rupture de chaîne) par l'apport de deux contributions électroniques différentes au niveau du métal. Les iminobisphosphines obtenues précédemment en tant que sous produit ont pu être obtenues sélectivement et permettent notamment de générer des structures symétriques ou dissymétriques. En effet les iminobisphosphines subissent un réarrangement en présence de précurseurs de Ni(II) pour donner des complexes de nickel dissymétriques de formule générale  $((\text{R}^2)_2\text{P}-\text{N}(\text{R}^1)-\text{P}(\text{R}^3)_2)\text{NiBr}_2$ . La formation de ces complexes est due à la rupture de la liaison P-P de l'imino-bisphosphine par le nickel. Les complexes de nickel ainsi produits (symétriques ou dissymétriques), fournissent, après activation par du MAO, des systèmes très actifs pour l'oligomérisation de l'éthylène, produisant des oléfines courtes. Ces complexes sont également actifs pour l'oligomérisation du propylène où la nature dissymétrique des complexes a un impact fort sur les produits formés. Les arylphosphines favorisent la formation de dimères tandis que les phosphines basiques conduisent à de fortes proportions en 2,3-diméthylbutènes, utilisés notamment en chimie fine. La même stratégie transposée au chrome ne s'est pas révélée être adaptée pour l'oligomérisation sélective de l'éthylène.

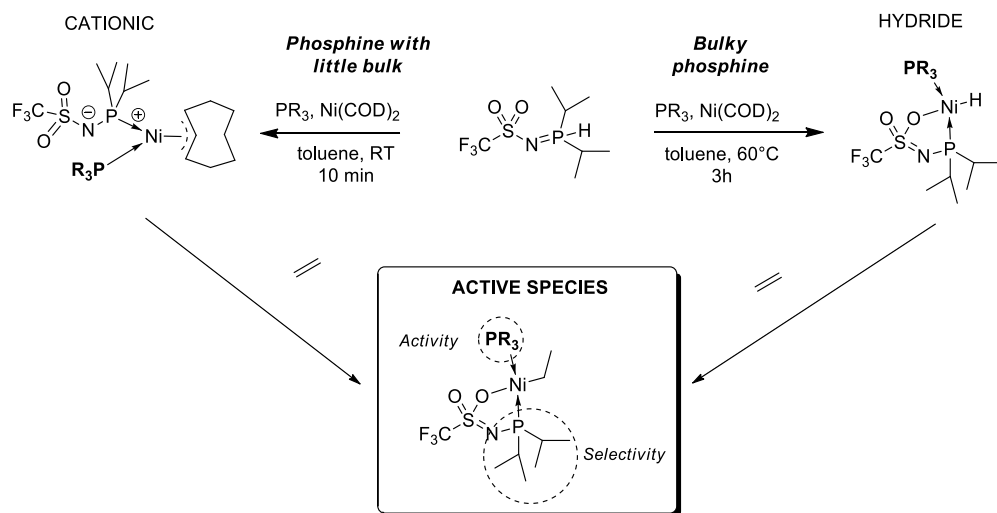


Sur la base des études de coordination du ligand METAMORPhos, nous décrivons une nouvelle approche synthétique à base de Ni(0), pour générer des complexes supramoléculaires de nickel (II) basés sur l'interaction entre une sulphonamido-phosphine et une aminophosphine. La présence d'une liaison hydrogène intramoléculaire dans cet assemblage a été confirmée par RMN mais aussi par l'obtention de DRX sur des monocristaux. Cette nouvelle classe de complexes zwitterioniques, organométalliques et supramoléculaires permet de réaliser l'oligomérisation de l'éthylène sans co-catalyseurs et avec une activité considérable jusqu'à  $24 \text{ kg}_{\text{oligo}}/(\text{g}_{\text{Ni}} \cdot \text{h})$ . De plus, les complexes possédant des phosphines substituées par des groupements aryles sur le ligand METAMORPhos présentent une sélectivité exceptionnelle en butène-1, une oléfine très demandée dans l'industrie des plastiques.

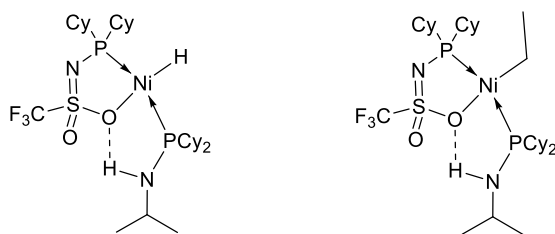


Pour mieux comprendre ce système catalytique, nous avons étendu ce concept à différentes combinaisons de METAMORPhos et de co-ligands fonctionnalisés ou non. La formation d'un large panel de complexes supramoléculaires a pu être établie par RMN du phosphore. L'utilisation de co-ligands avec un fort encombrement stérique ( $PCy_3$ ,  $P(tBu)_3$ ,  $P(iPr)_3$ ) conduit à des complexes hydrures chélatés par un ligand PO dont certains ont été isolés et caractérisés. Ces complexes subissent un réarrangement sous pression d'éthylène et conduisent à des composés du type *trans*-(PO,P)Ni-éthyle qui correspondent très probablement à l'espèce active. Les complexes zwitterioniques et hydrures sont d'excellents catalyseurs dans la réaction d'oligomérisation de l'éthylène et conduisent à de fortes sélectivités en butène-1 dans certains cas. Une analyse des différents paramètres structuraux a permis d'établir le rôle de chaque groupement dans le contrôle de l'activité et de la sélectivité du

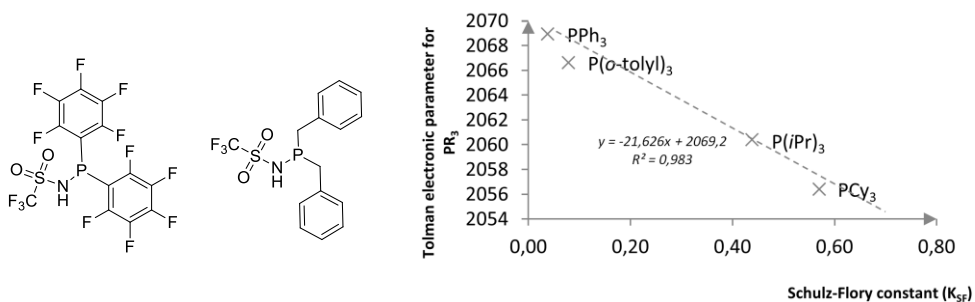
complexe. Alors que le co-ligand régule l'activité du système catalytique, la sélectivité dépend exclusivement du ligand METAMORPhos et en particulier des propriétés électroniques de sa phosphine. Il apparait également que la liaison hydrogène permet de stabiliser et d'isoler des complexes zwitterioniques très réactifs. En effet, des ligands aux propriétés électroniques et stériques similaires mais dépourvus de caractère donneur d'hydrogène forment des systèmes instables ne permettant pas d'isoler le complexe.



Une première perspective consiste à mieux comprendre le mécanisme d'activation de ces complexes. Quel est le devenir de la liaison hydrogène sous éthylène après le réarrangement du complexe *cis* vers *trans* ? Des études RMN préliminaires menées pour tenter de répondre à la question n'ont pas été concluantes, cependant, l'isolation de l'espèce active et sa caractérisation par DRX ou des études *in operando* (IR, RMN) jointes à des calculs théoriques pourraient fournir davantage d'informations sur la géométrie de cette espèce. Par ailleurs, il serait possible d'atteindre un complexe ayant une géométrie proche de l'espèce active en synthétisant des complexes de type nickel hydrure supramoléculaire par l'action d'aminophosphines très encombrées en tant que co-ligands. Cela permettrait de mieux comprendre la nature de la liaison Ni-O et son rôle en catalyse.



Une autre perspective est le contrôle de la sélectivité par les paramètres structuraux, avec pour but de simplifier le catalyseur. Nous avons montré qu'il était possible de moduler la sélectivité du catalyseur par des paramètres structuraux pour aller soit vers une distribution de LAO de longueur contrôlée soit vers du butène-1 sélectivement. Une tentative de corrélation a été établie entre la distribution des oligomères (modélisée par la constante de Schulz-Flory :  $K_{SF}$ ) et le paramètre électronique de Tolman de la phosphine. Cette approche doit cependant être confortée avec davantage de points expérimentaux dans le domaine d'application mais aussi aux extrémités. Cette approche linéaire permettrait d'avoir un contrôle complet sur la sélectivité de la réaction d'oligomérisation.



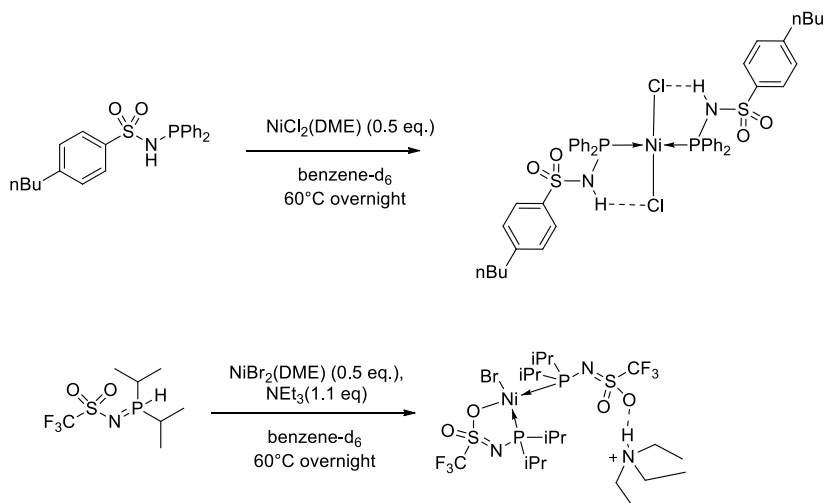




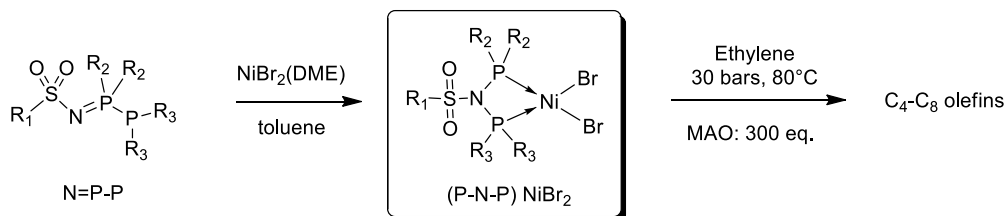
# Samenvatting

De industriële vraag naar korte lineaire alfa-alkenen neemt nog steeds toe waardoor de zoektocht naar robuuste katalysatoren voor het selectief verkrijgen van bepaalde alfa-alkenen (1-buteen, 1-hexeen of 1-octeen) nog steeds relevant is. Van alle verschillende metalen gebruikt voor de oligomerisatie van etheen heeft Nikkel de meest rijke geschiedenis in de coördinatie- en organometaal-chemie waar al sinds een eeuw over wordt geschreven. Nikkel complexen op basis van fosfine liganden kunnen deze reactie met hoge selectiviteit katalyseren afhankelijk van de eigenschappen van het ligand. Vanwege hun robuustheid kunnen ze industrieel worden toegepast in SHOP of Phillips processen waarbij een grote verscheidenheid aan lineaire alfa-alkenen (Schulz-Flory) of 2-buteen geproduceerd kunnen worden. Tot dusver blijft één uitdaging bestaan, namelijk het gebruik van Nikkel complexen voor het selectief oligomeriseren van etheen om 1-buteen, 1-hexeen of 1-octeen te maken. Voor dit doel hebben wij het gebruik van disymmetrische en supramoleculaire liganden, beide gebaseerd op sulfoamido-fosfor liganden, onderzocht met als doel de ontwikkeling van nieuwe en selectieve katalysatoren.

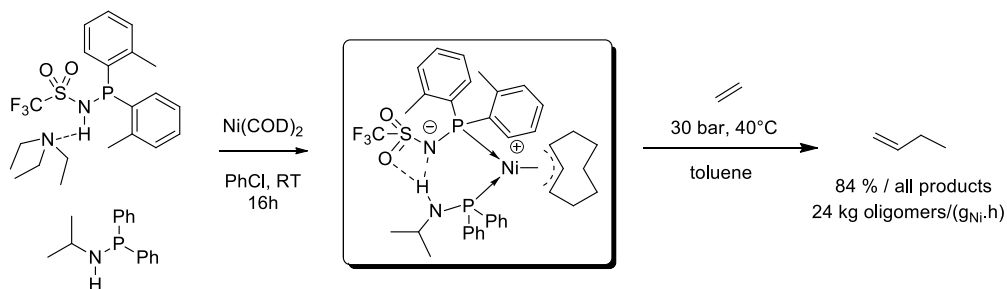
In het eerste deel van dit werk hebben we de synthese van ligandbouwstenen ontwikkeld om supramoleculaire ligand systemen gebaseerd op waterstofbruggen te maken. *Via* een éénstaps synthese kunnen deze bouwstenen gemaakt worden, en zo zijn kleine bibliotheken verkregen van aminofosfines  $R^1\text{-NH-P(R}^2\text{)}_2$ , amidofosfines  $R^1\text{-CO-NH-P(R}^2\text{)}_2$  en sulfoamido fosfines  $(R^1\text{-SO}_2\text{-NH-P(R}^2\text{)}_2)$ , bekend onder de naam METAMORPhos). Naast deze bibliotheken, beschrijven we ook de vorming van een bijproduct; *via* een zijreactie worden iminodifosfines geproduceerd met de formule:  $R^1\text{-N=P(R}^2\text{)}_2\text{-P(R}^2\text{)}_2$ , wiens voorkomen wordt bepaald door sterische parameters op het ligand. Sulfoamidofosfine liganden bestaan in twee verschillende tautomeren (NH of PH) die met elkaar in evenwicht zijn, terwijl amidofosfine liganden als drie tautomeren kunnen bestaan (NH, PH, OH). Uit onderzoek naar de coördinatiechemie van METAMORPhos liganden met Ni(II) blijkt de potentie van dit type liganden. Er zijn drie verschillende coördinatie mogelijkheden met hetzelfde type ligand gevonden, waarbij de effecten van het ligand significant verschillend zijn.



De toepassing van bidentaat difosfine liganden op Nikkel (II) gekatalyseerde oligomerisaties is tot dusver beperkt tot symmetrische liganden omdat synthese (en dus het gebruik) van disymmetrische liganden minder toegankelijk is. Wij verwachtten dat disymmetrische difosfine liganden met twee verschillende fosfordonor atomen kunnen bijdragen aan het sturen van de selectiviteit in de katalytische reactie. Deze liganden kunnen bepaalde elementaire stappen versnellen ten op zichte van anderen de katalytische cyclus en daarmee bijvoorbeeld de voorkeur geven aan terminatie boven propagatie. In het tweede deel van het proefschrift is de omlegging van iminobisfosfines naar disymmetrische difosfine-liganden bestudeerd, hetgeen in aanwezigheid van een Nikkel (II) precursor efficiënt verloopt en nikkel complexen met de structuur  $((R^2)_2P-N(R^1)-P(R^3)_2)NiBr_2$  geeft. Voor de omlegging is de nikkel precursor essentieel om de P-P binding te splitsen. Deze complexen zijn vervolgens gebruikt als katalysator, na activatie met methylaluminoxane (MAO), in etheen oligomerisatie reacties en de symmetrische en disymmetrische Nikkel complexen waren zeer actief. in de productie van korte oligomeren. De complexen waren ook actief in propeen oligomerisaties. In deze reactie hadden liganden een duidelijk effect op de reactiviteit: arylfosfines gaven de voorkeur aan een hoge selectiviteit voor dimeren terwijl basische fosfines leidden tot hoge opbrengsten 2,3-dimethylbuteen, een waardevol chemisch intermediair. Wanneer dezelfde strategie werd toegepast op op chroom complexen leidde dit niet tot selectieve omzetting van etheen.

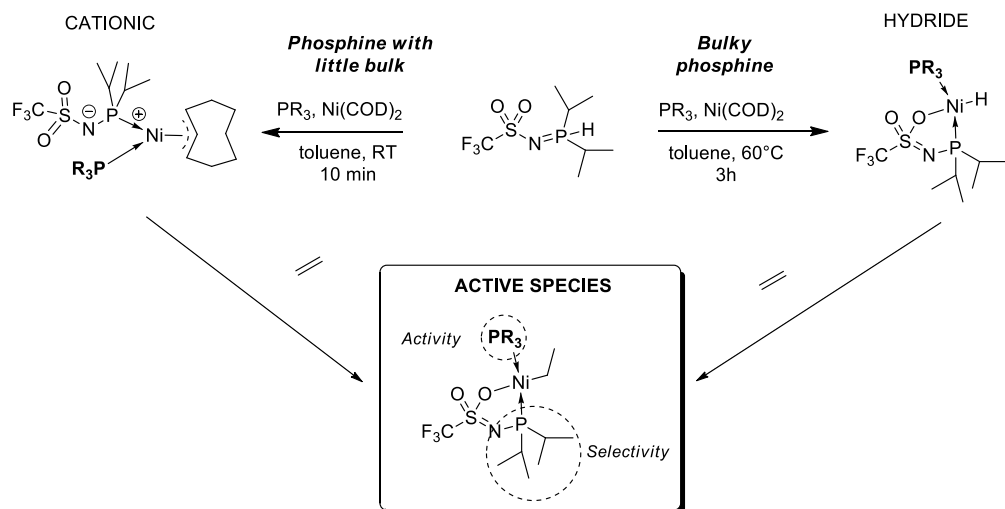


Vervolgens hebben we Coördinatie studies uitgevoerd met nikkel en METAMORPhos liganden hetgeen heeft geleid tot een nieuwe synthese route voor het genereren van supramoleculair Ni(II) complexen. Deze complexen hebben een sulfoamido fosfine en een aminofosfine ligand, en tussen beide liganden wordt een waterstofbrug gevormd. De aanwezigheid van een intramoleculaire waterstofbrug in dit complex was onomstotelijk bewezen door de kristalstructuren die zijn opgehelderd en NMR spectroscopie uitgevoerd in oplossing. Deze nieuwe klasse van zwitterionische, supramoleculaire nikkel complexen hebben een goede chemische en thermische stabiliteit. Ze zijn actief in de oligomerisatie van etheen, ook in afwezigheid van een co-katalysator, en een hoge activiteit is waargenomen (tot  $24 \text{ kg}_{\text{oligo}}/(\text{g}_{\text{Ni}} \cdot \text{h})$ ). Bovendien, geven de complexen gebaseerd op aryl P-gesubstitueerde METAMORPhos liganden buitengewoon hoge selectiviteit voor de vorming van 1-buteen, een verbinding waarvan de vraag hoog is in de polyethen industrie.

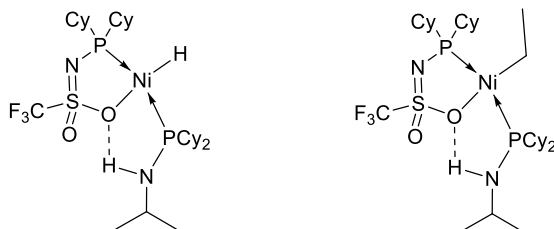


Om dit systeem beter te kunnen begrijpen is het concept uitgebreid door een uiteenlopende combinaties van METAMORPhos en verschillende co-liganden te gebruiken. Om snel inzicht te krijgen in welke complexen er *in situ* gevormd zijn is NMR spectroscopie gebruikt. Wij zijn erachter gekomen dat bulky co-liganden zoals  $\text{PCy}_3$  geen zwitterionisch difosfine Nikkel complexen maar neutrale PO chelerende nikkel hydride complexen geven. Een aantal nikkel hydride complexen zijn geïsoleerd door gebruik te maken van grote fosfines ( $\text{PCy}_3$ ,  $\text{P}(\text{tBu})_3$ ,  $\text{P}(\text{iPr})_3$ ). *In situ* experimenten onder een hoge druk van etheen gas laten zien dat beide complexen (zwitterionisch en hydride) omgezet worden tot het *trans*-(PO,P)Ni-ethyl complex, het voorgestelde actieve deeltje in de katalytische oligomerisatie reactie. Geïsoleerde zwitterionische en hydride katalysatoren zijn beiden actief in de

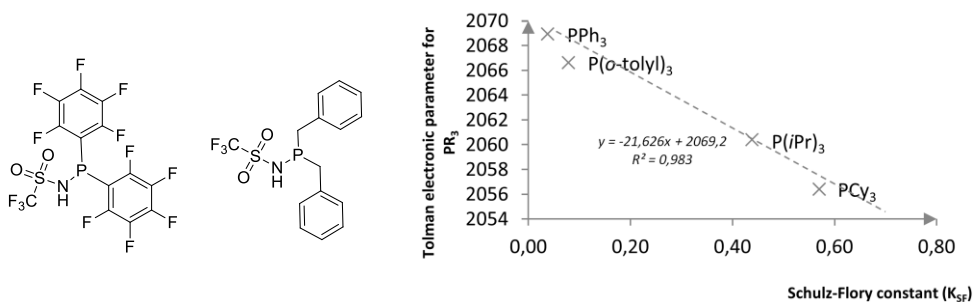
oligomerisatie van etheen, bepaalde complexen geven een hoge selectiviteit voor de vorming van 1-buteen. Door zorgvuldige analyse van de structurele parameters hebben wij ook vastgesteld dat METAMORPhos verantwoordelijk is voor de selectiviteit terwijl het co-ligand de bepalend is voor de activiteit. Ook is vastgesteld dat de waterstofbrug tussen de twee liganden aan het nikkel een belangrijke rol speelt: complexen gebaseerd op aminofosfines (welke een waterstofbrug vormen met METAMORPhos) geven stabiele, edoch actieve, zwitterionische complexen, terwijl analogen co-liganden die deze waterstofbrug niet kunnen vormen tot snelle decompositie leiden.



De nieuwe complexen beschreven in dit proefschrift geven interessante selectiviteit en activiteit, en reeds een klein beetje inzicht in het mechanisme. Er blijven echter nog een aantal vragen over. Is de de waterstofbrug binding tijdens de katalytische cyclus intact, bv ook na de *cis* tot *trans* isomerisatie onder etheen gas? Het bewijs hiervoor is niet eenvoudig met NMR spectroscopie vaste stellen. Het isoleren van het actieve complex of het gebruik van een "*in operando*" karakterisatie techniek (IR, NMR ...) tezamen met DFT berekeningen zouden nieuwe informatie kunnen opleveren. Misschien dat het gebruik van zeer basische en grote aminofosfine co-liganden (in de nabijheid van etheen) zouden kunnen leiden tot supramoleculaire hydride complexen met twee fosfines in *trans* positie (of ten opzichte van het bijbehorende ethyl complex). Ook zou de aard van de binding van het zuurstof atoom aan Nikkel verder moeten worden uitgezocht om te weten te komen welk type interactie van belang is tijdens katalyse.



Een tweede uitdaging voor verder onderzoek is het afstemmen en versimpelen van de katalysator. In dit proefschrift hebben wij laten zien dat door middel van het aanpassen van het ligand systeem, inclusief de waterstofbrug tussen de twee ligand bouwstenen, wij de selectiviteit van de Nikkel gekatalyseerde oligomerisaties van etheen kunnen controleren: een verdeling van alfa-alkenen met gecontroleerde lengte ( $K_{SF}$ ) of de selectieve vorming van 1-buteen kan worden verkregen. Voorlopige inzichten in de rol van elk fragment zijn verkregen door intensieve studies. Het bleek dat het METAMORPhos fosfine ligand dominant was in de bepaling van de selectiviteit. Een voorzichtige correlatie is vastgesteld tussen de Tolman elektronische parameters van het fosfine en de Schulz-Flory constante ( $K_{SF}$ ) die de oligomeer verdeling bepaald. Deze aanpak zal moeten worden bevestigd door meer experimenten door METAMORPhos ligande met verschillende substituenten te bestuderen, bv met pentafluorofenyl groepen. Deze groepen hebben een Tolman elektronische parameter waarde van  $2090.0 \text{ cm}^{-1}$  en daardoor is de voorspelling dat deze systemen tot de hoogste selectiviteit zullen leiden.





# Acknowledgements

In this final part, I would like to thank all those who contributed directly or indirectly to the realisation of this thesis. Besides being an enriching scientific experience it is also a real human adventure. During these three years spent between the group of Amsterdam and the group of Lyon, I was very lucky to get to know fantastic and passionate people, share moment of excitement or sadness when getting nice crystal structures or selective catalyst. I enjoyed the friendly and warm atmosphere of the Homkat group such as in the cooking course or the Sinterklass borrels! Besides the labwork it was also a pleasure to meet people again outside of the lab and share good times together. You made my stay in the Netherlands unforgettable!

First of all, I would really like to thank my supervisors, Denis Guillaume, H el ene Olivier-Bourbigou (at IFPEN Solaize, France) and Joost Reek (Universiteit van Amsterdam) for accepting me as a PhD student after a first work experience at IFP. Joost, thank you for welcoming me in your team in Amsterdam, but also for your commitment to my subject. I really enjoyed your enthusiasm for scientific discussion and your sense of humour! Many thanks for your patience and your help to correct the manuscript. Thank you H el ene for your input on my thesis and our neverending discussions about chemical process but also your availability to answer my scientific questions even during your holidays! I would like to thank the members of the committee who kindly accepted to read my thesis: Prof. Bas de Bruin (also for fruitful discussions), Jr. Prof. Fr ed eric Patureau (also for nice discussions on METAMORPhos and chemistry), Prof. Sander Woutersen, Prof. C. J. (Kees) Elsevier, Dr. Elsje Alessandra Quadrelli and Prof. Gadi Rothenberg (also for the Write it Right course in Leiden). Thank you also Jarl Ivar van der Vlugt for your interesting discussions on chemistry.

Thank you to Pierre-Alain Breuil, the direct supervisor of my thesis for your unconditional daily support, your motivation and strong perseverance on this exciting research subject. Thank you also for your advice and your regular availability. I count on you to keep the story of METAMORPhos going at IFPEN, also our roads will surely meet again. Please drop by and say hello if you come to Normandy!

Next, I would like to thank my brave paranimphs, Stefan Leenders and Yann Gloaguen for their unconditional support and for accepting this job. Stephan, we started the same day at HomKat! I wish you a lot of success with your cages! Thank you also for your permanent good mood that made the entire lab an amazing place to



work, also for the “disco Fridays afternoons” and the neverending Backstreet Boys songs at our fumehoods plus the nice times outside of the lab. Please feel free to come back to Lyon but this time when the weather is better! Yann (aka Yannou), we have been roommates for a while on the remote island of IJburg in Ben van Meerendonkstraat (remember?). Although you sometimes steal my food in the fridge and particularly my awesome “Gratin aux poireaux et au jambon” I spent very funny times with you and your friends, thanks also for helping me moving downtown and for good drinks and pleasant moments at the beach or NCCC! I hope that we will keep in touch and I wish you the best with Sofia Derossi, (aka Zof, a really amazing girl !!! wish to meet you soon again) in your new flat in Insulindeweg!

Fredéric Terrade (aka Fred), the French successor of Frédéric Patureau who taught me everything on METAMORPhos ligands and also on phosphorus chemistry. The lab leader of E1.18. I’m afraid that the CDs of Muse and Placebo went dusty when you left! Thanks a lot also for your enthusiasm and your crazy ideas on chemistry and catalysis, also for helping me on the catalytic hydrogenation tests with NPP ligands and rhodium. I will also remember the nice parties in Javastraat also with Pawel Dydio (the greatest polish cook and maybe heavy drinker...:). Congratulations again Fred for your thesis and I wish you the best for your Postdoc in Leiden and also with Jacques. Thank you also to Tatiana Besset (aka Tati), a toughworker in the lab, for good times and your permanent happiness. I’m really happy for your job position in Caen and within less than 1 hour drive, I have no excuse to pay you a visit soon. Rafa Gramage Doria, I wish you the best in Japan, come back quickly! Last member of the “French team” but not least: Julien Daubignard (aka Juju), a passionate singer but also guitar and keyboard player. I will keep in good memory the concert of Sébastien Tellier in Amsterdam we went together but also nice runs in Amsterdam Noord. Take time to enjoy life and remember: ”l’alliance bleue” will guide you. I wish you the best for the end of your thesis and also to Brit. Thank you Alma Itzel Olivos Suárez and Ivo for your outstanding Kaas fondue but also for your lovely (especial) accent!

A huge thank to Rosalba Bellini, especially for your very first kind words to me when I arrived in the lab: “Don’t talk to me like this”. That was really a pleasure to have you back in France and make you discover Lyon together with Henri. You are a champion at learning languages (especially French!) maybe you should reconsider a career in literature? Thanks a lot for your humour at the 3<sup>rd</sup> degree and also for giving me a lift to IFPEN so many times.

Thank you Sander Oldenhof for our scientific discussions on METAMORPhos and cooperation, I wish we could publish something together on MM! I would also like

to thank people from InCatT: Sander Kluwer, Remko Detz and Lidy van der Burg (#1 grade extra-dry triethylamine), for their regular input and for sharing knowledge about ligand synthesis. Thank you also Zohar Abiri for your shaman recipes when I got cold and your help in the lab.

Thank you to Martin Koelewijn (koffie tijd !!! also for your precious help with the thesis and the Samenvatting), Vincent Vreeken, Linda Jongbloed, my deskmates for advice but also for running together at the Dam to Dam loop or the Amsterdam half-marathon. I wish you the best for the end of your thesis.

Thank you also to Yasemin Gumrukcu, my fumehood and flat neighbour for discussions and good times. Thanks to my other neighbours: Andrei Chirila, Tatu Kumpulainen and Deniz Gunbas, Tendai Gadzikwa in Fokke Simonzstraat but also to Pietra and Jibo Jiang in Ijburg.

Jurjen Meeuwissen, that was nice talking to you we will certainly meet again soon at Total some day!

Thank you also to Annemarie Walters (great singer!), Leszek Rupnicki (ex-flatmate and labmate), Bart van den Bosch, Monalisa Goswami, Fenna van de Watering, Matthias Otte (officemate, for german humour and translations), Arnaud Perrier, Volodymyr Lyaskovskyy (aka Vova), Gennady Oshovsky, Gianluca Ciancaleoni (for your kindness and knowledge on NMR), Avi Schultz (the wikipedia man! I surely have to get a movie culture somehow), Danny Broere (for your enthusiasm and great parties), René Becker, Esther Vleugel, Eleonora Russotto, Dennis Hetterscheid, Sandra de Boer, Nicole Franssen, Jelmer Otten, Paul Kuijpers, Christophe Rebreyend, Ricardo Zaffaroni, Marten Ploeger, Zhou Tang, Ping Li, Nanda Paul, Ruben Drost, Soraya Sluijter, Vlien Jansen, Stanimir Popovic, Lianne Jongens, Hocine Alliche, Zea Strassberger ...

I would like to thank the technicians who made sure that everything was working Erik Duin-Berteling, Taasje Mahabiersing, Lidy van der Burg and Fatna Ait El Maate. Thank you for helping me to build the steel reactor for high pressure catalytic reactions and also when I moved back to France. I want also to express my gratitude to Jan Meine Ernsting, Jan Genevasen, and Els Engelen-Goris for their help and assistance with NMR experiments. Many thanks also to Martin Lutz for the crystal structure determinations, Han Peeters for the high resolution mass analysis and Gertjan Bon for apparatus glassblowing. Thanks to Petra Hagen for her help in housing, Hippert Renate, Paul Collignon and finally HIMS for the financial participation in the costs related to the printing of the manuscript.

Thank you also to my friends in Amsterdam for nice moments: Reinier, Alfred, Jeroen, Sergey, Paul, Robert (also for helping me a lot with the thesis).

La deuxième partie de la thèse fut aussi très enrichissante et passionnante au sein d'IFPEN. Je souhaite tout d'abord remercier Fabien Grasset, Alexandre Nasr et Adrien Boudier les ex-doctorants du département Catalyse Moléculaire (R062) qui m'ont motivé à faire une thèse à l'issue de mon stage ingénieur. Merci pour les bons moments passés avec vous !

Merci Lionel Magna pour ta disponibilité, ton expertise et ta pédagogie pour me briefer sur les procédés catalytiques et l'oligo de l'éthylène. Merci également pour le suivi de ma thèse et les différentes idées échangées. Bon courage pour le P-T-F-L (il paraît que ça marche plutôt pas mal !) Merci Didier Bernard pour tes anecdotes de chimie des temps reculés et tes connaissances en chimie organique et en recherche bibliographiques approfondies. Merci aussi de m'avoir conseillé pour plusieurs entretiens professionnels. Merci aussi Christophe Vallée et Damien Delcroix pour vos différentes contributions à ma thèse et nos discussions sportives. Un grand merci également à Nicolas Dellus et Florie Lavigne pour votre passion pour la chimie organométallique et nos discussions fondamentales de paillasse et autres.

Merci aux techniciens de l'équipe. Merci Sébastien Drochon, pour tous tes conseils en particulier sur les réacteurs et pour m'avoir formé aux manipulations haute pression et à la bonne utilisation de la GC et de l'IR ! Merci de m'avoir facilité le travail sur la calibration des instruments et les méthodes pour que tout soit prêt à mon retour d'Amsterdam. J'ai beaucoup appris grâce à toi et en particulier développé un sens de la rigueur accru ;). Un grand merci à David Proriol qui m'a pris en charge au tout début, pendant mon stage et m'a appris comment manipuler avec dextérité de façon inerte. C'est en partie grâce à toi que j'ai pu isoler les composés décrits dans cette thèse. Merci aussi pour ta disponibilité à toute épreuve et ta gentillesse et pour m'avoir formé sur les différentes techniques analytiques de la RMN. Merci à toi Manu Pellier pour ta bonne humeur et ton charentais ! J'attends ma revanche pour le triathlon de Vienne... Je te souhaite plein de bonheur avec ta famille en espérant surtout que tes enfants ne deviennent jamais comme toi ! Prends soin de « Maman ». Merci Séverine Forget pour ton aide au labo et en particulier la GC/MS et les boîtes à gants et également pour ta recherche active de sosies à IFPEN. Merci Sandrine Bérard pour ta bonne humeur et les délicieux macarons à la pause-café. Merci également pour la gestion des produits et de la base de données. Un grand merci pour Olivia Chaumet-Martin, la « maman » du groupe qui fait tout pour maintenir une super ambiance. Tu es géniale ! Stéphane Harry, courage ça fonctionnera en continu un jour ! ... ou peut être en Sibérie. Aurélie Camarata, je te souhaite plein de

bonheur, merci pour ta joie de vivre ! Alexandre Rebaud, toujours motivé et dynamique, tu feras un excellent technicien, bon courage à toi dans ta recherche d'emploi. Merci à Daniel Andry pour le travail de verrerie, Erwann Jeanneau pour les structures DRX. Je tiens également à remercier vivement les secrétaires Sylvie Montagne, Sandrine Leblond, Nathalie Farenq et Estelle Carton pour leur travail formidable (feuille de temps, rapports, organisation, déplacements,...).

Merci à Alban Chappaz, qui a commencé et terminé en même temps que moi, pour nos échanges sur la transformation de la biomasse. Bravo pour ta performance musicale au Gills'. Un immense merci pour ta disponibilité et pour le covoiturage régulier Lyon-IFPEN. Je te souhaite de trouver un postdoc qui te plaise au Brésil ou aux States. Merci, Hugo Audoin pour ton humour sarcastique et ta tchatche de dingue! Bon courage pour la dernière ligne droite ! Merci Benjamin Burcher, nouvelle recrue pour m'avoir fait découvrir des musiques dont je suis fan. Merci aussi pour ta gentillesse et ta simplicité (ça doit venir de Haute Savoie ?) et de m'avoir covoituré plusieurs fois. Je suis certain que tu vas trouver THE catalyseur, je te souhaite plein de courage. J'aimerais remercier aussi les autres thésards avec qui j'ai passé des bons moments à IFPEN, Lyon, Londres ou Amsterdam. Merci Camille Gouedard, mon co-bureau pour ton humour et les anecdotes et potins croustillants. Merci pour ton soutien en fin de thèse, je te souhaite de trouver un super poste, tu le mérites. Merci Déborah Staub, pour ton dynamisme et ta joie de vivre, ce fut un plaisir de te faire visiter Amsterdam avec Camille. Merci aux autres thésards Régis Koerin (bon courage dans ton nouveau job en process), Camille Morin, Ferdaous Dorai, Caroline Besson-Blondel, Louis Corbel-Demilly, Cécile Guin, Manu Bernard (pour notre compétition de natation en eau glacée !), Sofia Da Silva Rodrigues, Marius Silaghi, Ferdaous Dorai, Mathias Dodin (tu étais ma prochaine victime du killer), Agnès Gorczyca (j'espère que tu te plairais à l'IUT !), Matthieu Lagache, Svetan Kolitcheff, Robin Lafficher, Matthieu Ozagac, Anna Brisou... Un grand merci également à mes amis de Lyon et des quatre coins de la France, Fabrice Marcellini, ainsi qu'à Gilles Rautureau, Gerald Bettridge pour m'avoir boosté quand j'en avais besoin, pour votre support logistique et votre contribution au manuscrit. A tous, je vous souhaite une excellente carrière et une vie personnelle pleine de satisfactions.

Finalement je tiens à remercier toute ma famille de Lyon, de Haute-Savoie et de l'Ain pour leur soutien sans faille et leur aide dans mon parcours scolaire et professionnel.

Pierre, Lyon, France 08/201

